University of Glasgow

Lewis, Natasha Shanti (2018) Development of a three-dimensional haematopoietic stem cell-permissive bone marrow niche model using magnetic levitation. PhD thesis.

DEVELOPMENT OF A THREE-DIMENSIONAL HAEMATOPOIETIC STEM CELL-PERMISSIVE BONE MARROW NICHE MODEL USING MAGNETIC LEVITATION

Natasha Shanti Lewis

(BA)

Submitted in fulfilment of requirements for the degree of Doctor of Philosophy (PhD)

**Centre for Cell Engineering
College of Medical, Veterinary and Life Sciences
Institute of Molecular, Cell and Systems Biology
University of Glasgow
Glasgow, G12 8QQ**

April 2018

Abstract

Haematopoietic stem cells (HSCs) have a huge clinical relevance as they are regularly used in bone marrow transplants worldwide. This therapy has profound potential to alleviate diseases of the blood and immune system, where others are ineffective. However, HSCs cannot currently be cultured long term *ex vivo*, as they rapidly differentiate or senesce. Hence, genetically matched donors must often be found for transplant and studies of HSCs require costly animal models.

Mimicking the microenvironment of the bone marrow, in which they reside, by incorporating supportive stromal cells including mesenchymal stem cells (MSCs), has the potential to overcome these limitations. This project aimed to create an HSC-permissive MSC spheroid culture system using magnetic nanoparticles and a collagen gel. An existing spheroid system was optimised for HSC-MSC co-culture and then characterised to assess the potential for HSC support. MSC spheroids were more quiescent, and expressed higher levels of HSC-supportive genes such as nestin and CXCL12.

Subsequently, additional bone marrow cell types were introduced to the model to mimic vascular and endosteal areas of the bone marrow niche. HSC behaviour within these models was investigated. MSCs, endothelial cells, and osteoblasts exhibited gene expression changes in line with those predicted from examination of the physiology of endosteal and vascular regions of the bone marrow: i.e. higher activity at the vascular niche (model including endothelial cells), and lower activity at the endosteum (model including osteoblasts). However, gene transcription and phenotypic analyses of HSCs following culture within the bone marrow models produced more inconclusive results. Hence, further optimisation of the conditions of the model and repetition of results presented here are required to develop the system so that it truly mimics physiological bone marrow.

The development of such a model has many applications, including in drug discovery, modelling disease states, and probing haematopoietic functions.

Table of Contents

List of Tables

List of Figures

Publications

Publications authored by the candidate on research relating to this thesis.

Lewis, N., Lewis, E.E.L., Mullin, M., Wheadon, H., Dalby, M.J., Berry, C.C. Magnetically levitated mesenchymal stem cell spheroids cultured with a collagen gel maintain phenotype and quiescence. *Journal of Tissue Engineering,* 2017, *8,* 1-11.

Lewis, E.E.L., Wheadon, H., **Lewis, N.**, Yang, J., Mullin, M., Hursthouse, A., Stirling, D., Dalby, M.J., Berry, C.C. A quiescent, regeneration-responsive tissue engineered mesenchymal stem cell bone marrow niche model via magnetic levitation. *ACS Nano,* 2016, *10* (9), 8346-8354.

Conference proceedings

2017 FEBS Workshop: Biological Surfaces and Interfaces "Co-culture within endosteal and perivascular bone marrow niche models influences cell behaviour." St Feliu, Spain (poster presentation).

2017 European Nanomedicine "Co-culture within endosteal and perivascular bone marrow niche models influences cell behaviour." King's College London, UK (poster presentation).

2016 Microenvironments for Medicine "Magnetically levitated spheroids as a model of the stem cell niche." Beatson Institute, Glasgow, UK (flash poster presentation).

2016 10th UK Mesenchymal Stem Cell meeting "Modelling the bone marrow using magnetically levitated mesenchymal stem cell spheroids." York, UK (poster presentation).

2016 British Orthopaedic Research Society "The magnetic labelling of stem cells to develop a functional haematopoietic stem cell niche *in vitro.*" Glasgow, UK (oral presentation).

2016 British Society of Nanomedicine "Magnetically levitated spheroids as a model of the stem cell niche." Swansea, UK (oral presentation).

2015 9th UK Mesenchymal Stem Cell Meeting "The magnetic labelling of stem cells to develop a functional haematopoietic stem cell niche *in vitro*." Manchester, UK (oral presentation).

2015 British Society of Nanomedicine "Mesenchymal stem cell spheroids as a model of the stem cell niche" Swansea, UK (oral presentation).

2015 Tissue and Cell Engineering Society "Magnetic labelling of stem cells to develop a haematopoietic stem cell" Southampton, UK (poster presentation).

Awards

Poster Prize, European Nanomedicine Meeting, King's College London, April 2017.

Group Prize Winner, Impact in 60 Seconds Competition, University of Glasgow, December 2016.

2nd Poster Prize, Institute of Molecular, Cell and Systems Biology Postgraduate Symposium, March 2016.

Young Researcher of the Month, Institute of Molecular, Cell and Systems Biology, January 2016.

Best Oral Presentation, 9th UK Mesenchymal Stem Cell Conference, Manchester, December 2015.

Runner-up, Impact in 60 Seconds Competition, University of Glasgow, November 2015.

Acknowledgements

Firstly, I would like to thank my supervisor Dr Catherine Berry for the support and guidance she has provided throughout my PhD training and the preparation of this thesis. Above and beyond scientific support, her encouragement to take part in many extra-curricular activities has made my experience much richer and has helped me develop into a scientist. Thank you also to Professor Matthew Dalby who has given advice on both the project and on general matters. Professor Jo Mountford also gave valuable guidance on HSC culture, contacts, and use of her equipment.

Many people have given their valuable time and expertise to support me during my PhD. I would like to thank Dr Helen Wheadon, Michaela Kolokouri, and Jennifer Cassels from the Paul O'Gorman Leukaemia Research Centre for providing use of their equipment and technical advice for flow cytometry. Thanks to Margaret Mullin for her assistance with electron microscopy. Towards the end of the project Ewan Ross and Caroline Busch have been invaluable in helping my last experiment to finally be successful. Huge thanks to everyone else in CCE who has provided time and advice, particularly Carol-Anne Smith for assisting in countless stressful situations! Thanks to everyone in CCE and MiMe for making my PhD so enjoyable, in particular Hilary Anderson, Paula Sweeten, and Hannah Donnelly for helping me to not be scientifically shady.

Lastly, I would like to thank my family who have supported me throughout the four years I have spent in Glasgow, Hanna Buist who is now basically my family, Beth Parrott for answering my invitation to visit, and to Matthew Lowdon who has believed in me more than I believe in myself.

Author's Declaration

I hereby declare that the research reported within this thesis is my own work, unless otherwise stated, and that at the time of submission is not being considered elsewhere for any other academic qualification.

Natasha Lewis

21st September 2017

Abbreviations

ALCAM	Activated leukocyte-cell adhesion molecule, also known as CD166
ALP	Alkaline phosphatase
Ang-1	Angiopoietin 1
BIT	BSA, insulin, and transferrin
BM	Bone marrow
BMI1	B lymphoma Mo-MLV insertion region 1 homolog
BrdU	Bromodeoxyuridine
BSA	Bovine serum albumin
c-Kit	Also known as CD117
CaR	Calcium sensing receptor
CAR	CXCL-12 abundant reticular cells
CD	Cluster of differentiation
CDK	Cyclin dependent kinase
CLP	Common lymphoid progenitor
CMP	Common myeloid progenitor
CXCL12	C-X-C motif chemokine 12 (also known as SDF1)
CXCR4	C-X-C chemokine receptor type 4
DAPI	4',6-diamidino-2-phenylindole
DMEM	Dulbecco's modified Eagle's medium
DMSO	Dimethyl suphoxide
DNA	Deoxyribose nucleic acid
EC	Endothelial cell
EDTA	Ethylenediaminetetraacetic acid
ELISA	Enzyme-linked immunosorbent assay
FACS	Fluorescence-activated cell sorting
FBS	Fetal bovine serum
FBXW7	F-box and WD40 repeat domain-containing 7
FITC	Fluorescein isothiocyanate
G-CSF	Granulocyte colony stimulating factor
GMP	Granulocyte-monocyte progenitor
GvHD	Graft-versus-host disease
HA	Hyaluronic acid
HEPES	4-(2-hydroxyethyl)-1-piperazineethanesulfonic acid
HH	Hedgehog
HHIP	Human hedgehog-interacting protein
HIF1-α	Hypoxia-inducible transcription factor 1 alpha
HPSC	Haematopoietic stem or progenitor cell
HS	Human serum
HSC	Haematopoietic stem cell
hTERT	Human telomerase reverse transcriptase
HUVECs	Human umbilical vein endothelial cells
ICAM-1	Intercellular adhesion molecule 1
Ig	Immunoglobulin
IMDM	Isocove's modified Dulbecco's medium
ISCT	International Society for Cellular Therapy
Jag-1	Jagged 1
JAK	Janus kinase
LDL	Low density lipoprotein
LFA-1	Lymphocyte function-associated antigen 1
LSC	Leukaemic stem cell

LTR	Long-term reconstitution
MAPK	Mitogen-activated protein kinase
MCM	Mini-chromosome maintenance protein
MEP	Megakaryocyte-erythroid progenitor
MEP	Megakaryocyte/erythrocyte progenitor
MG63	Human osteosarcoma cell line
MLP	Multi-lymphoid progenitor
MMP	Matrix metalloprotease
MNC	Mononuclear cells
MPL	Myeloproliferative leukemia protein, also known as CD110
MPP	Multipotent progenitor
MSC	Mesenchymal stem cell
MTT	4,5-dimethylthiazol-2-yl)-2,5-diphenyltetrazolium bromide
NICD	Notch intracellular domain
NSC	Neural stem cell
OB	Osteoblasts
OPN	Osteopontin
PBS	Phosphate buffered saline
PCR	Polymerase chain reaction
PI3K	Phosphoinositide 3-kinase
RM	Recommended medium
RNA	Ribose nucleic acid
ROS	Reactive oxygen species
RUNX1/2	Runt-related transcription factor 1 or 2
SCF	Stem cell factor
SDF1	Stromal derived factor, also known as CXCL12
SEM	Scanning electron microscopy
SHH	Sonic hedgehog
SMO	Smoothened, part of the Hedgehog pathway
SNS	Sympathetic nervous system
STAT3	Signal-transducer and activator of transcription 3
TCP	Tissue culture plastic
TEM	Transmission electron microscopy
Tie-2	Tyrosine kinase with immunoglobulin-like and EGF-like domains 2
TPO	Thrombopoietin
TRITC	Tetramethylrhodamine
VCAM-1	Vascular cell adhesion molecule 1
VLA-4	Very late antigen-4, also known as integrin $\alpha 4\beta 1$
VLA-5	Very late antigen-5, also known as integrin $\alpha 5\beta 1$

CHAPTER 1

Chapter 1   Introduction

The bone marrow (BM) is a unique organ with multiple vital functions in red blood cell production (haematopoiesis) and the lymphatic system (white blood cell production) in tetrapods (Sanchez et al. 2014). As the site of haematopoiesis, study of the BM and its resident cells has been an area of intensive investigation. To this end, recapitulating the BM architecture to allow studies *in vitro* has huge clinical significance, both in terms of supporting artificial haematopoiesis, and as a platform for drug discovery and testing in the pharmaceutical industry. This chapter will give an overview of the BM, its resident cell types and their clinical significance, interactions between the cell types, and the physical and chemical characteristics that are fundamental to its function. It will then explore current *ex vivo* BM models, and describe the aims for this project.

1.1 Bone marrow architecture

The BM is located in the hollow interior of bones. Initially thought to be a diffuse structure in which cells relating to haematopoiesis were randomly distributed, in the 1990s structural analysis revealed a highly-ordered architecture, which has functional significance for haematopoiesis (Lord 1990), as depicted in Figure 1.1. BM with a predominant haematopoietic role is called 'red marrow' and is mainly located in trabecular bone, in small thin bones, and in the epiphysis of long bones. Red marrow is highly vascularised and has a large surface area, mainly due to the honeycomb network of trabecular plates.

Aside from haematopoiesis, an additional function of the BM is fat storage, wherein the marrow mainly consists of adipocytic inactive haematopoietic tissue termed 'yellow marrow'. This is found only in the medullary cavities of cortical bone (Figure 1.1) and has a poor vascular supply. The proportion of yellow BM increases during adulthood and aging to around 50%. In cases of blood cell type imbalance or blood loss, yellow marrow can be converted to red to increase blood production (Clarke 2008).

The trabecular region comprises several anatomical features which have an influence on haematopoiesis. One of these, the endosteum, is described as a "membranous structure covering the inner surface of cortical bone, trabecular

bone, and the blood vessel canals present in bone" (Clarke 2008). The endosteum is in contact with both the bone marrow and trabecular bone, lining the hollow medullary cavity, and has a protective role (Figure 1.1). The endosteum itself is comprised of a flattened, quiescent osteoblast (OB) subset (Clarke 2008) and is a proposed site for haematopoiesis.
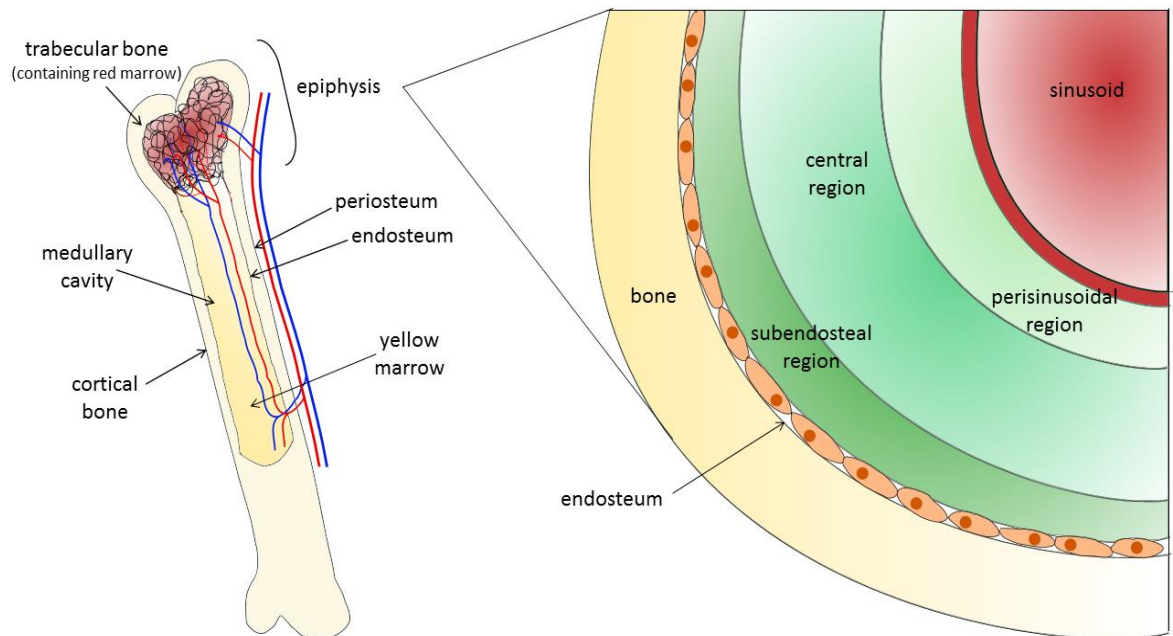
Figure 1.1 Schematic of bone architecture.
Trabecular bone containing red marrow is located in the bone epiphysis, and yellow marrow is situated in the medullary cavity. The endosteum comprises a layer of quiescent osteoblasts (orange), with a network of sinusoids located within the epiphysis lined with endothelial cells. Original image.

The BM is also highly vascularised. Internal vessels are connected to the exterior *via* hollow tubes in cortical bone termed 'Haversian canals' and 'Volkman's canals', which are orientated perpendicularly to each other and form a branching network. These vessels play a large role in cellular turnover in the marrow. They are highly permeable and made up of endothelial cells which also produce regulatory factors that influence the production of blood cells (Itkin et al. 2016).

As early as 1990, the radial organisation of the BM had been described, indicating an organised and distinct architecture (Lord 1990). Colony-forming unit (CFU) capacity, a proxy for self-renewal capacity, is greatest in HSCs located in the endosteal region and commitment to erythropoiesis triggers movement of cells to the centre of the marrow and the sinusoid: showing that these locations are related to haematopoietic stem cell (HSC) state and behaviour.

1.2 Bone marrow resident cells

The BM comprises several key cell types that contribute to the process of haematopoiesis by interacting directly and indirectly with HSCs. These interactions maintain HSCs and trigger haematopoietic events.

1.2.1 Mesenchymal stem cells

Mesenchymal stem cells (MSCs) are adult stem cells that reside in many organs of the body, including the BM. MSCs are multipotent and produce mesenchymal lineage cells, including chondrocytes, adipocytes, OBs, and myoblasts. They are important in the healing and regeneration process, have immunomodulatory capacity, and are a key support of HSCs (as described later in the text).

The identification of MSCs is complex as they can be obtained from multiple tissue sources, and several subsets exist with subtly different biological activities. A position statement from the International Society for Cellular Therapy defined the minimal criteria for MSCs as: (1) cells must be plastic adherent under standard culture conditions; (2) they must be positive for CD105, CD73, and CD90; negative for CD45, CD34, CD14 or CD11b, CD79α or CD19, and HLA-DR surface molecules; and (3) they must have the ability to differentiate into osteoblasts, adipocytes, and chondroblasts *in vitro* (Dominici et al. 2006). These properties can be validated by quantitative RNA analysis, flow cytometric analysis of functionally relevant surface markers, and protein analysis of the secretome (Galipeau et al. 2015). However, no single marker associated with MSC 'stemness' has been agreed upon and many 'proxy' identifiers for subsets of MSCs with differing functions have also been identified (Table 1.1). Markers are often used for identification and/or isolation of MSC subsets.

Many subsets of BM-resident cells with MSC-like properties have been implicated in haematopoietic function. For example, CXCL12-abundant reticular cells (CaR) cells are located adjacent to sinusoids in the BM, and have been found to have a role in haematopoiesis, particularly in the support of B cells (Eltoukhy et al. 2016). Similarly, nestin-expressing cells occupy a similar location, are involved in HSC support, and have mesenchymal lineage potential (Méndez-Ferrer et al. 2010). Although evidence suggests that these cells are not the same cell type, they may

overlap with each other and with alarger MSC population. Furthermore, it has been suggested that CAR cells may in fact be MSC progenitors.

MSC subpopulation	Source	Biological properties	Reference
STRO-1[+]	BM	Promote angiogenesis. May not support HSC engraftment. Also expressed by erythroid cells, so STRO-1 may not be a suitable marker for multipotent MSCs.	Mo et al. 2016; Lv et al. 2014
CD271^{+}	BM Adipose tissue	Express higher levels of differentiation-related genes than cells isolated by plastic adherence. Enhanced chondral repair. Express higher levels of immunosuppressive cytokines. Enhance HSC engraftment ability.	Álvarez-Viejo 2015; Mo et al. 2016; Lv et al. 2014
CD105^{+}	BM Umbilical cord blood Wharton's jelly	Enhanced myogenic differentiation.	Mo et al. 2016
CD146^{+}	BM Skeletal muscle pericytes	Enhanced osteogenic differentiation. Produce cardiomyocytes and pro-angiogenic factors. Marker is downregulated in differentiated cells.	Mo et al. 2016
CD44^{+}	BM	Increased proliferation and homing capacity.	Mo et al. 2016
Nestin^{+}	BM	Involved in HSC niche and cellular support.	Mo et al. 2016
CXCR4^{+}	BM	Enhanced migration and engraftment.	Mo et al. 2016
PDGFRα^{+}	Fetal BM	HSC supportive. Express nestin.	Pinho et al. 2013
CD51^{+}	Fetal BM	HSC supportive. Express nestin.	Pinho et al. 2013
CD49f^{+}	BM	Multipotent, CFU-Fs. Knock-down causes HSC differentiation.	Lv et al. 2014

Table 1.1 Subpopulations of human mesenchymal stem cells (MSCs), with markers used for identification.
Details of the cell subsets defined by these markers are given. BM, bone marrow, CD, cluster of differentiation; PDGFR, platelet derived growth factor receptor.

1.2.2 Haematopoietic stem cells

HSCs are able to differentiate into all cellular components of the blood: erythrocytes, lymphocytes, and myelocytes, *via* a process termed haematopoiesis (Wang & Wagers 2011) (Figure 1.2). Their regenerative potential gives them great clinical relevance in haematologic diseases, such as leukaemias, anaemias, and autoimmune disorders. HSCs are multipotent (they can differentiate into multiple but limited cell types) and give rise to oligopotent progenitor cells (which can differentiate into just a few cell types). These oligopotent cells subsequently have gradually restricted differentiation potentials, resulting in the production of the mature cells of the blood system. The term HSPC (haematopoietic stem and progenitor cell) collectively describes HSCs and these multipotent and oligopotent progenitors. These comprise megakaryocyte-erythrocyte progenitors (MEPs),

common myeloid progenitors (CMPs), common lymphoid progenitors (CLPs); and granulocyte-monocyte progenitors (GMPs). Except for a subset of HSCs, long-term reconstituting HSCs, these progenitors all present the cluster of differentiation 34 (CD34) glycoprotein on their cell surface.
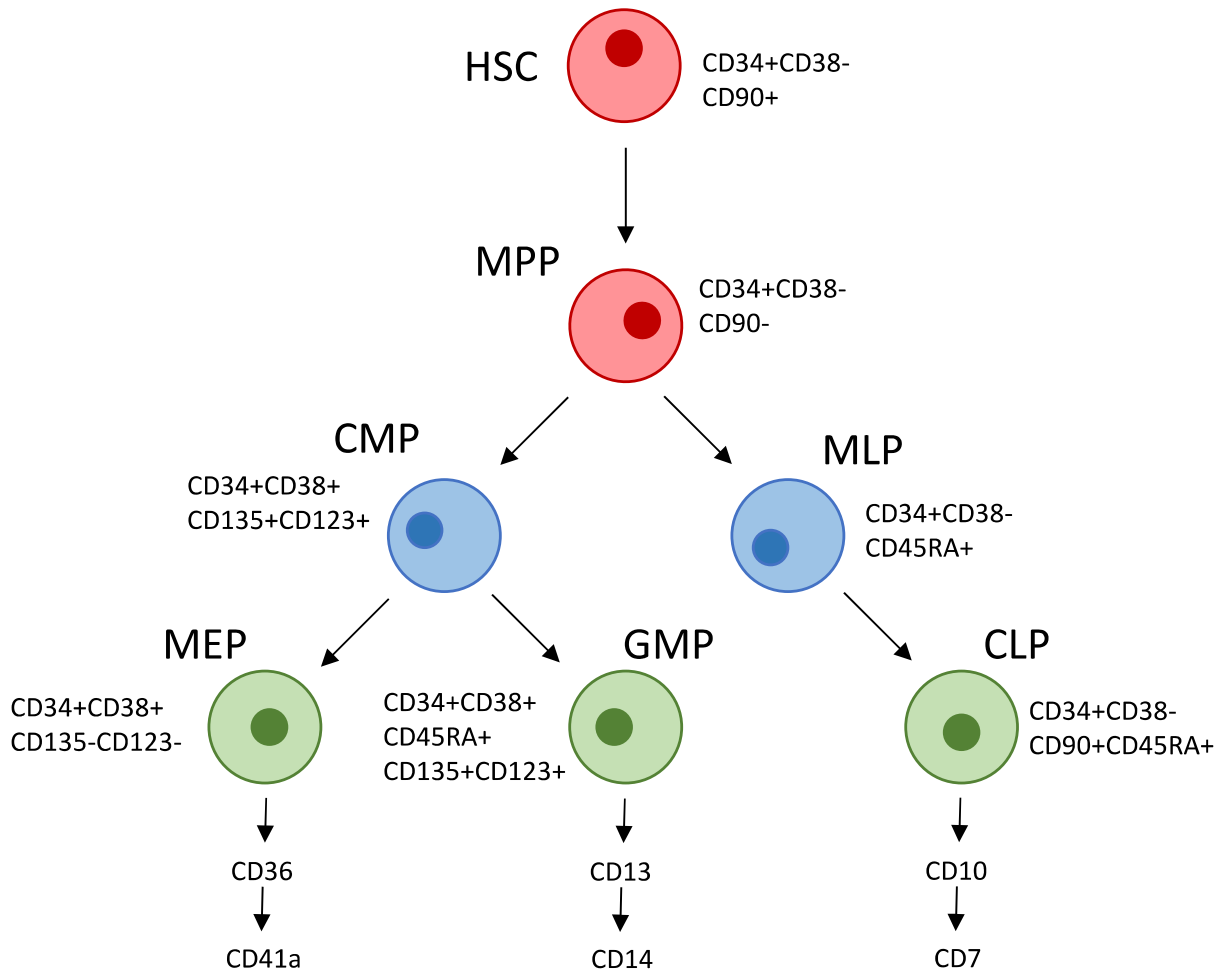
Figure 1.2 Schematic of haematopoietic development, including emergence of identifying cell surface markers.
HSC, haematopoietic stem cell; MPP, multipotent progenitor; MLP, multipotent lymphoid progenitor; CMP, common myeloid progenitor; MEP, megakaryocyte-erythroid progenitor; GMP, granulocyte-macrophage progenitor; CLP, common lymphoid progenitor.

Isolating and distinguishing subsets of HSPCs can be performed using a selection of cell surface markers. The basic phenotype used for isolating progenitors is CD34+CD38-, however, more specific progenitors can be identified using a more comprehensive panel of markers, as described in **Error! Reference source not found..** The progenitors do not express markers indicating the various haematopoietic lineages: these only appear during terminal differentiation. The CD34 marker does remain expressed on progenitors lower in the hierarchy, whereas expression of CD38 tends to increase in most of the lineage progenitors.

Clinically, purification of BM or mobilised peripheral blood samples is performed, normally limited to removal of plasma, removal of donor T lymphocytes, and purification of a CD34+ population, which is sufficient for clinical purposes (Antin & Raley 2013). However, for detailed investigation of progenitor function and location within the BM (the 'niches'), identification of other progenitor subsets is required using the unique combinations of cell surface markers.

1.2.3 Osteoblasts

Osteoblasts (OBs) are bone forming cells, responsible for synthesis and mineralisation of bone during formation and remodelling. They secrete vesicles which concentrate calcium and phosphate, and degrade mineralisation inhibitors. OBs arise from MSCs as a result of Wnt/ß-catenin signalling, accompanied by a morphological shift from spindle shaped to large cuboidal cells with large nuclei, extensive endoplasmic reticulum, and enlarged Golgi apparatus. Active OBs secrete type I collagen and other matrix proteins towards bone formation. Following bone formation activity OBs either apoptose (50-70%), become osteocytes, or become flattened bone lining cells that form the endosteum, which are thought to be quiescent OBs (Clarke 2008).

1.2.4 Endothelial cells

Endothelial cells (ECs) form the lining of all blood vessels, in a sheet termed the endothelium. In capillaries and sinusoids, which are abundant in the BM vascular system, the vessels consist entirely of endothelial cells, basal lamina, and pericytes. As such, they are a major constituent of the BM microenvironment (Alberts et al. 2002). Sinusoids are highly fenestrated venous vessels, and are hence the main conduit for HSC egress from the BM. Also present are arterioles, small vessels that link arteries with capillary networks. These vessels also have muscular walls (Crane et al. 2017). BM ECs are phenotypically distinct from those found in the microvasculature of other organs, as they constitutively express cytokines and adhesion molecules. They also exhibit specific binding affinity for CD34+ progenitors and megakaryocytes, indicating a role in regulating haematopoiesis (Rafii et al. 1995; Almeida-Porada & Ascensao 1996; Whoriskey et al. 1994).

1.2.5 Megakaryocytes

Megakaryocytes represent 1 in 10,000 cells of the BM. They have large nuclei and are responsible for platelet production. Mature megakaryocytes are polyploid as a result of serial endomitosis. They localise to ECs of sinusoids in the BM, with EC-megakaryocyte adhesion enhancing survival, maturation, and platelet production. Other stromal cell types are inhibitory, so their specific localisation may also protect them from such signals (Avecilla et al. 2004).

1.2.6 Nerve cells

The sympathetic nervous system (SNS), consisting of various types of nerve fibres, is involved in BM structure and function. The SNS controls HSC egress from the BM, bone remodelling, and transduction of circadian oscillation signals from the suprachiasmatic nucleus (SCN) (Méndez-Ferrer et al. 2009). Large nerve bundles enter the BM along with the major arteries at various locations. Nerve terminal contact with other BM cells is limited: signal transduction is non-synaptic and involves intercellular junctions (Elefteriou et al. 2014). The ubiquity of the SNS means that it is present and active in every area of the BM.

1.3 Bone marrow stem cell transplants

1.3.1 Summary of stem cell transplants to date

BM transplants are the original and remain the main stem cell therapy in clinical use today. Over 50,000 people are treated with a BM transplant each year and over 1,000,000 people had received one by December 2012. The classical treatments are for blood disorders such as leukemia, thalassemia, and anaemia. Increased knowledge of human leukocyte antigen (HLA) typing and matching patients in the 1960s encouraged the development of multiple registries of donors, which have expanded in the subsequent decades. However, less than 30% of patients have an HLA-identical donor (Copelan 2006), and many patients still cannot find a match, due to complex multiple ethnicities. In fact, 40% of patients need to be matched by someone in another country (WHO 2013). Fifty percent of these patients can find a donor through international databases, but the three-month duration of this process means that less than half of plausible donors are actually used (Copelan 2006).

Mobilised peripheral blood is an alternative HSC source to direct BM transplants. BM transplants are expensive and as such are limited to wealthy nations. Although peripheral blood stem cells (PBSCs) engraft quickly and can be obtained without specialist staff and hospitalisation, the rate of graft versus host disease (GvHD) is higher and survival is lower. The donor is treated with the mobilisation inducer granulocyte colony stimulating factor (G-CSF); Mozobil (pleraxifor hydrochloride), a C-X-C chemokine receptor type 4 (CXCR4) agonist; or chemotherapy regimens against lymphoma. The blood is collected and processed to remove red cells, plasma, and T lymphocytes, and isolate CD34+ cells, before being infused into the patient (Antin & Raley 2013). This process has widened the availability of BM transplants beyond the Western world (Yoshimi et al. 2016).

Autologous transplants are a more recent development that has been used to treat aggressive cancers, for which there is no other option. A patient's cells can be removed prior to treatment and replaced after myeloablative therapy (high dose chemotherapy that kills BM cells), hence eliminating GvHD. However, these transplants can be less effective against cancer, with increased relapse rates; as there is a graft-versus-tumour effect against tumour stem cells, wherein an allogeneic BM transplant immunologically attacks remaining tumour cells. This effect is lacking in autologous transplants (Copelan 2006). Cord blood as an alternative stem cell source is also promising, as the HLA requirement is less stringent and appropriate samples can often be found quickly. However, the volume available is limited and slower engraftment increases the probability of infection. Combining stem cell sources and expanding CD34+ cells from cord blood *ex vivo* to increase cell number are active areas of research.

Although HSC transplants are performed routinely, MSCs are also an emerging cell therapy for tissue repair and immune disorders. In particular, they can be applied alongside HSCs in BM transplants to enhance engraftment and reduce GvHD due to their immunomodulatory properties. They do not require HLA matching as they do not induce *in vivo* lymphocyte proliferation, and are hence a much more easily obtainable therapy. Prochymal® was the world's first stem cell 'drug' to be approved by the Food and Drug Administration (FDA) in 2012 (Wei et al. 2013). Investigation into use of these cells for other indications is ongoing.

As described above, despite decades of research, there remain several issues associated with BM transplants. The ability to sustain and expand an HSC population *ex vivo* has the potential to overcome therapy limitations. Furthermore, creating an HSC supportive environment would also allow detailed study of the control mechanisms therein, using an *in vitro* system that is more representative of the *in vivo* situation.

1.3.2 HSC clinical trials

Clinical research into HSC therapies is very active. A search on www.clinicaltrials.gov for 'haematopoietic stem cells' identified 2635 studies with the search term, of which 783 are currently active (accessed 22/02/2017, Figure 1.3). Although the majority of these studies focus on evaluating the outcomes of current practice, improving graft versus host disease (GvHD) and infection complications, augmenting transplants with new drugs, and treating multiple types of leukemias, the repertoire of HSC-treatable diseases is expanding. There are active clinical trials using HSCs to treat kidney disease, Crohn's disease, and other autoimmune diseases.

Source:https://ClinicalTrials.gov
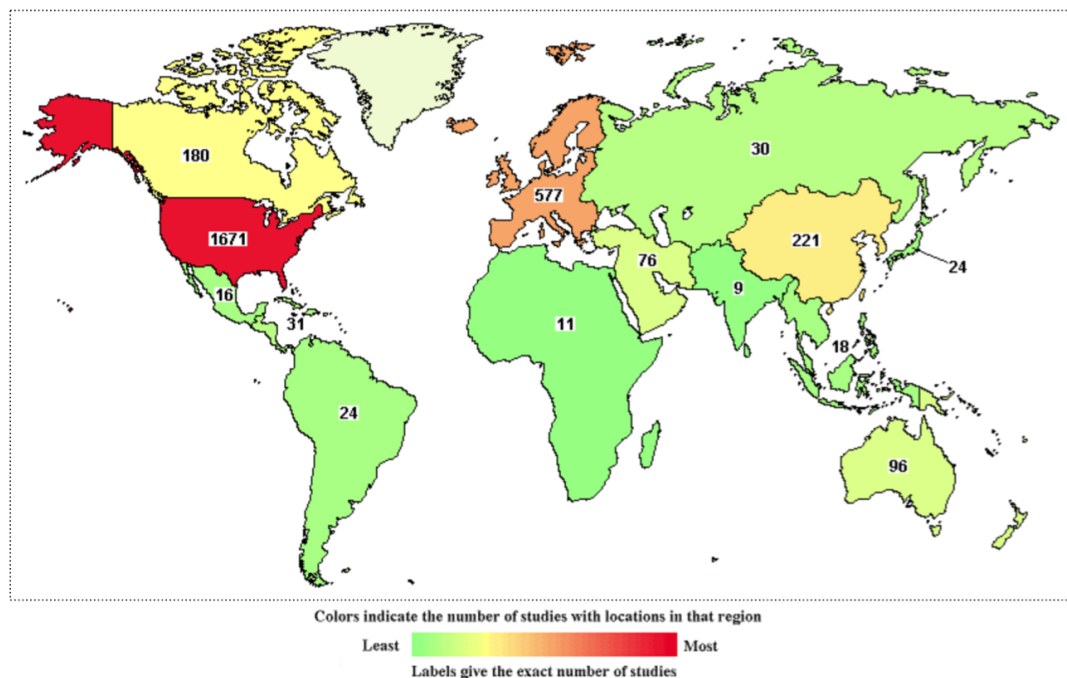
Figure 1.3 World map illustrating past and current clinical trials involving haematopoietic stem cells (HSCs). From www.clinicaltrials.gov.

There is also a huge potential for HSCs in gene therapies. The gene editing clustered regularly interspaced short palindromic repeats (CRISPR)/Cas9[1] system is a relatively new technique that has only recently gained regulatory approval in embryos (Callaway 2016). Given the fact that blood/mobilised peripheral blood transplants are an established procedure with extensive infrastructure, one of the obvious first targets for CRISPR gene therapies is the blood, using both HSCs and terminally differentiated cells. This is in contrast to bulk tissues, where delivery of edited cells or the editing machinery itself may be more difficult. Edited HSCs could be used to treat patients with disorders such as β thalassemia, Wiskott-Aldrich syndrome, and adenosine deaminase deficiency (leading to severe combined immunodeficiency (SCID). Creating a culture system in which HSCs could be maintained and processed for gene editing techniques could accelerate this process. The limitations of traditional tissue culture mean that a new system could extend the available timeframe for editing whilst a patient is waiting for a transplant. It also means that a patient's own cells can be edited with lower risk of GvHD and other complications, compared to obtaining an allogeneic donor. Furthermore, editing of HLA markers themselves could circumvent the need for identifying a donor. Some proof-of concept studies have begun to investigate the feasibility of this technology, although it is still in the early stages (Torikai et al. 2016; Gundry et al. 2016; Genovese et al. 2014).

A high-profile use of stem cell transplants that has been recently reported widely in the media is the trial for patients with multiple sclerosis. This involved autologous HSC transplants given to patients for whom other treatments had failed. There was a 2.8% mortality rate in the 100 days following transplant, but almost half of the recipients remained free from neurological progression for 5 years following the procedure (Muraro et al. 2017).

It is evident that, although a long-established technique, there are several aspects of BM stem cell transplants that can be developed. Many improvements have been made over the years; for example, stem cell transplants are now often performed

---

[1] CRISPR/Cas9 is a prokaryotic adaptive immune system component that recognises foreign (viral) DNA and allows it to be destroyed. CRISPR passes on the details of the viral DNA it has encountered to its progeny, as a 'genetic vaccination card'. CRISPR refers to the DNA sequence. In targeting gene editing, Cas9 is a nuclease that complexes with synthetic guide RNA (gRNA), complementary to the desired cut site in the genome.

from mobilised peripheral blood, rather than BM itself, which does not require invasive surgery, reducing risks and costs. However, increasing the success of autologous transplants, by increasing yields or expanding the HSC population, has the potential to widen the treatment to many individuals who do not currently have the option of a donor. A platform for gene editing could enhance effectiveness and negate the need for matched donors. A deeper understanding of HSC biology, and of the environment in which they reside, is fundamental for this goal.

1.3.3 MSC clinical trials

MSCs, as adult stem cells, have lower regenerative capacity than the alternative embryonic stem cells (ESCs) and induced pluripotent stem cells (iPSCs), however, ethical issues and the potential to form teratomas during clinical use respectively limit these alternatives. MSCs are therefore of key clinical interest as a cell therapy and are the most commonly used non-HSC stem cells in clinic. Their usefulness as a treatment is due to their regenerative capacity, production of growth factors in damaged tissues, and their immunosuppressive properties. Furthermore, due to innate tumour homing capabilities, MSCs can be engineered to deliver anti-tumour drugs and nanoparticles. Although they have been in clinical use since the early 2000s, optimisations including MSC source and route of administration need to be addressed (Baldari et al. 2017).

A similar search on www.clinicaltrials.gov for 'mesenchymal stem cells' retrieved 696 clinical trial studies, of which 243 are currently open (accessed 22/02/2017, Figure 1.4). The immunomodulatory capacity of these cells, as well as their regenerative potential in multiple organs of the body, means that they are being trialled for orthopaedic applications as well as multiple organ diseases such as pulmonary fibrosis, Limbus Corneae Insufficiency Syndrome, and polycystic kidney disease (Wei et al. 2013).

Colors indicate the number of studies with locations in that region

Least ———— Most

Labels give the exact number of studies

Source:https://ClinicalTrials.gov
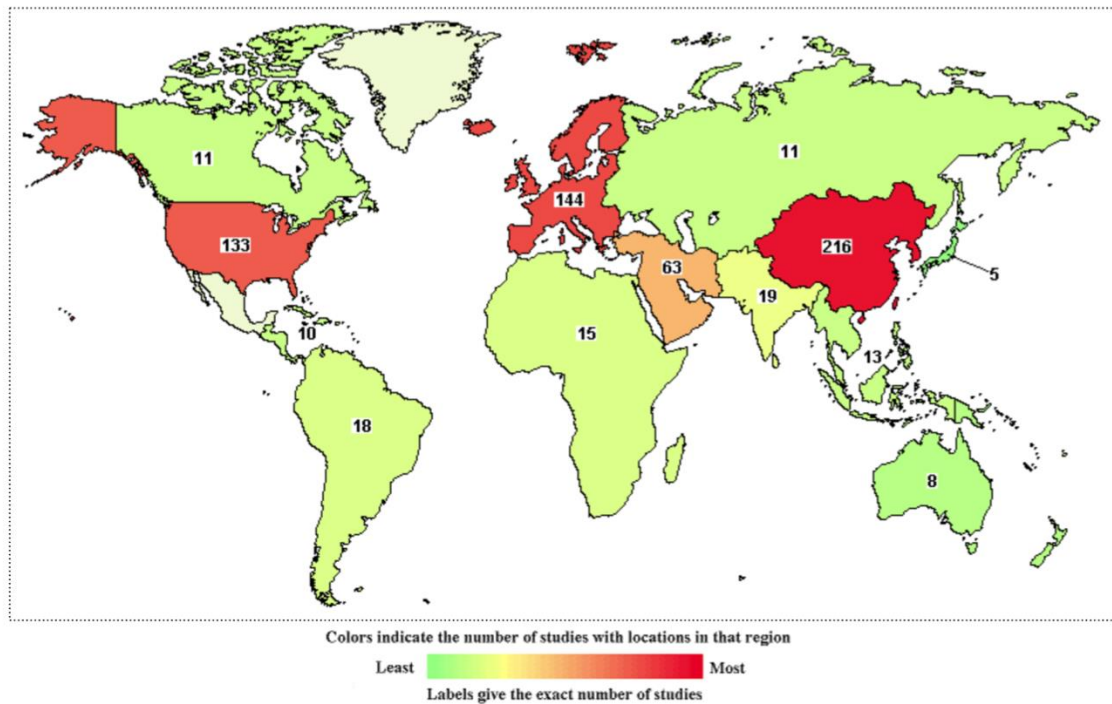
Figure 1.4 World map illustrating past and current clinical trials involving mesenchymal stem cells (MSCs). From www.clinicaltrials.gov.

1.4 The HSC microenvironment within the bone marrow

The concept of a specialised HSC microenvironment within BM, termed a niche, is long established (Schofield 1978) and is the subject of ongoing investigation. The niche functions to maintain a quiescent pool of HSCs, which are nevertheless able to self-renew, differentiate, and mobilise in the event of haematopoietic injury. The niche also protects the cells from overstimulation and prevents inappropriate differentiation. Cell-cell interactions, the SNS, and hormonal inputs have all been identified as playing a role in the regulation of haematopoiesis. Cell-extracellular matrix (ECM) interactions, oxygen tension, and calcium ion concentration are also fundamental physical features of the niche (Wang & Wagers 2011). The HSC niche is clearly a very complex environment and many features are not yet fully understood.

Examining this niche is necessary in order to recapitulate a suitable HSC culture environment *ex vivo*. In adults, HSCs reside in the BM, predominantly in the trabecular rich metaphysis (Ellis et al. 2011). Here, HSCs have been observed in contact with the endosteum (the surface of the bone), and localised around sinusoids (capillaries which supply the marrow), as shown earlier in Figure 1.1

(Kiel et al. 2005). This has given rise to a 'zoned model' of the haematopoietic niche (Figure 1.5, Suárez-Álvarez et al. 2012). It is hypothesised that the endosteum houses quiescent HSCs, with the more active cycling HSCs located around the sinusoid (Ehninger & Trumpp 2011). However, with the recent use of advanced techniques for imaging HSCs *in situ* or in large areas of tissue, it has been suggested that this model is over-simplified: that in the trabecular bone the endosteum and vasculature are in close contact and so HSCs may be interacting with both suggested niche components simultaneously (Ugarte & Forsberg 2013; Nombela-Arrieta et al. 2013; Ellis et al. 2011). Kunisaki et al. 2013 imaged BM from both long bones and the sternum, finding evidence for the sinusoid being a proliferative niche, but also identifying a putative arteriolar niche. Arterioles, exhibiting characteristic smooth muscle, nerves, and matrix, were associated with highly nestin^{+} perivascular cells, which were also more quiescent and produced more HSC-supportive factors than those localised to sinusoids. Quiescent HSCs localised to these arterioles.
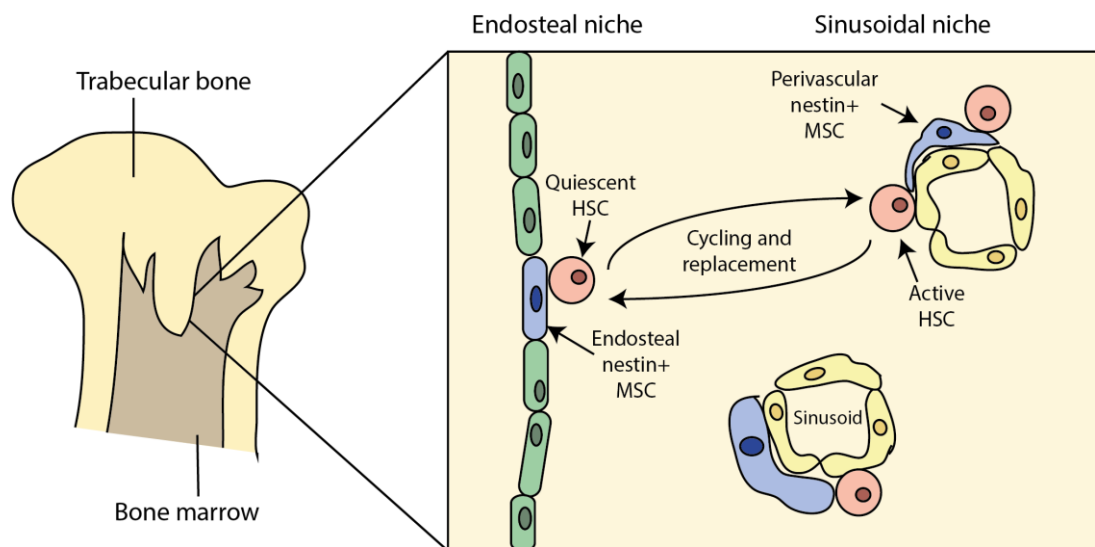
Figure 1.5 The 'zoned model' of the HSC niche.
HSCs are hypothesised to reside in two separate zones in the bone marrow: the sinusoidal niche and the endosteal niche, migrating between the two. Nestin[+] MSCs are important for HSC support in both zones. Adapted from Ehninger & Trumpp 2011.

The precise location of HSCs relative to endosteum or elements of the vasculature (sinusoids and arterioles), and thus the nature of cellular signals they receive, may determine whether the cells proliferate or are quiescent. Different areas of the BM or cellular components may serve distinct functions depending on the stage of

haematopoiesis, with each lineage progenitor residing in its own specific microenvironment (Wang & Wagers 2011; Ding & Morrison 2013).

1.4.1 Cellular support of HSCs

Several different cell types have a proposed role in HSC regulation; including MSCs, pericytes, ECs, and OBs. The observation that most HSCs are located adjacent to bone in the endosteum initially placed osteoblasts as the main supporting cell. However, later genetic evidence called this into question, concluding that any effect of osteoblasts is indirect (Morrison & Scadden 2014) as the endosteum is in such close proximity to the vasculature. Other cell types have also been implicated, including C-X-C motif chemokine 12 (CXCL12)-abundant reticular (CaR) cells, which functionally overlap in part with MSCs and are located both perivascularly and endosteally (Sugiyama et al. 2006). However, the extent to which stromal cell subsets are distinct has not yet been established (Wang & Wagers 2011).

More recently, the emphasis has been on nestin$^+$ MSCs, a subset of CaR cells, as the main HSC support. They are enriched in several important HSC maintenance factors, localise to perivascular regions, and are closely associated with the SNS. As osteoprogenitors they have features of both the osteoblastic and the endothelial niches, replacing the idea of osteoblasts themselves maintaining HSCs, and giving a 'master' role to the MSC which can coordinate many other cell types (Méndez-Ferrer et al. 2010). These cells are themselves maintained as quiescent by the niche and establish gradients of secreted cell products to control HSCs (Bianco 2011).

Although OBs may not be direct regulators of HSCs, they do have several unique functions. Firstly, they produce the matrix protein osteopontin (OPN) at the endosteum, to which HSCs can bind to via β1 integrins, an interaction which promotes HSC quiescence (Janeczek et al. 2015). They also produce thrombopoietin (TPO), and angiopoietin-1 (Ang-1) which are both important for HSC regulation. However, deletion of the adhesion protein N-cadherin has no effect on proliferation or differentiation of HSCs, showing that direct cell-cell interactions are not necessary for the role of OBs in the niche (Janeczek et al. 2015). A further complication arises from the fact that identification of cells of

the osteoblastic lineage is not straightforward due to a lack of available cell-surface markers. Furthermore, the endosteal lining of the marrow is made up of active osteoblasts and quiescent bone lining cells, the latter outnumbering the former. The positions of these cells in the osteoblastic hierarchy remains to be distinguished, and they may have different roles in the HSC niche. In fact, the main member of the OB lineage in HSC regulation may be an immature skeletal stem cell or pre-osteoblast, which have both been shown to produce HSC-relevant cytokines and can be found in perivascular locations (Askmyr et al. 2009).

ECs form the network of vasculature in the trabeculum. Although this is mostly comprised of sinusoids (Kunisaki et al. 2013), several other vessel types are also present. As well as providing a mechanical barrier for blood cells and platelets, ECs release angiocrine signals that participate in HSC development and regulation, and contribute to the sinusoidal HSC niche. In particular, HSCs require stem cell factor (SCF) expressed by ECs, but not SCF expressed by OBs or nestin$^+$ cells (Ding et al. 2012). Regenerated sinusoidal ECs are required for successful engraftment of HSCs following myeloablative therapy (Hooper et al. 2009). Furthermore, the integrity of blood vessels may have an effect on HSCs: HSCs close to sinusoids have higher ROS levels than arteriolar HSCs, and retention is higher at arterioles. Homing and endothelial transmigration are exclusive to sinusoids as they are highly permeable (Itkin et al. 2016). Hence, differences between ECs may contribute to the heterogeneity of HSC niches.

1.5 HSC homing, lodgement, and engraftment in the bone marrow

There are three processes that occur to establish HSCs in the niche from the circulation, either after recovery or during foetal-to-adult niche transition (Figure 1.6). The first process is termed 'homing', where HSCs enter the BM from the circulation and migrate through the endothelium of the vasculature. HSCs are chemoattracted to the BM through several mechanisms. The most important of these is the CXCR4/CXCL12 interaction. Other chemoattractants include SCF/c-Kit and prostaglandin E2, whilst CD48 also plays an important role (Heazlewood et al. 2014)). The migration of HSCs through the vasculature is similar to that of lymphocytes: weak initial adhesion and rolling is mediated by endothelial selectins binding to oligosaccharides on the migrating cell. Lymphocyte function-associated

antigen 1 (LFA-1) activation in the mobile cell then initiates stronger binding and allows the cell to migrate through the endothelium (Papayannopoulou 2003).
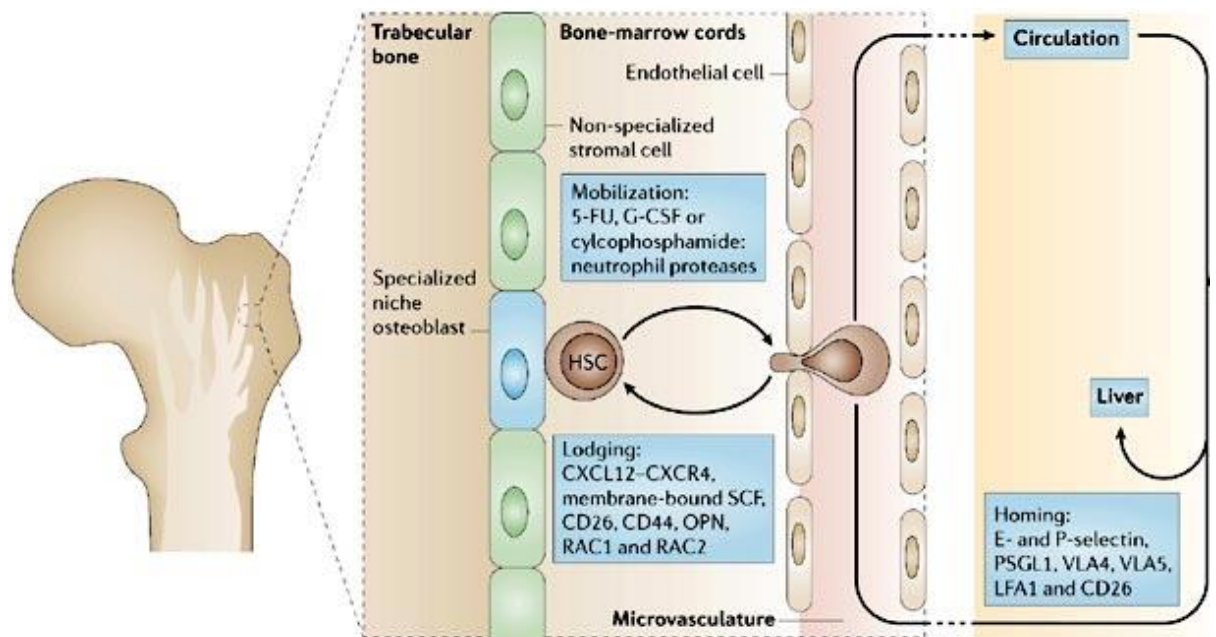
Figure 1.6 HSC homing to and migration from the BM niche.
Multiple signalling molecules are involved in homing, lodgement, and engraftment. Taken from Wilson & Trumpp 2006. Permission to reproduce this figure has been granted by Springer Nature.

The second process, lodgement, occurs in the BM and involves the migration of HSCs to specific niches within the BM. The membrane bound form of SCF and hyaluronic acid (HA) are critical in HSC lodgement. OPN, localised to the endosteal surface, is also important for HSC retention in the niche (Heazlewood et al. 2014).

Finally, engraftment is the ability of the migrated HSCs to respond to the signals within the niche to encourage retention (Heazlewood et al. 2014). Megakaryocytes release cytokines including insulin-like growth factor 1 (IGF-1), which enhance HSC proliferation post-transplant. These cells are important for engraftment in the endosteal region (Heazlewood et al. 2013). Cells which are in gap 1 (G_1) or G_0 stages of the cell cycle are also better at engrafting than dividing cells (Fleming et al. 1993).

Conversely, HSC mobilisation from the niche is initiated by reduction in adhesion and desensitisation to cytokine signalling. Elastase and cathepsin G cleave CXCR4, CXCL12, VCAM-1, and very late antigen-4 (VLA-4). Matrix metalloproteases (MMPs) cleave c-Kit and degrade OPN. The action of osteoclasts also degrades OPN and encourages HSC egress from the BM (Janeczek et al. 2015). Collectively, the action

of these enzymes decreases HSC affinity for the niche, provoking migration into the blood. Granulocyte colony stimulating factor (G-CSF) and granulocyte macrophage colony stimulating factor (GM-CSF) are cytokines that negatively regulate the CXCR4/CXCL12 axis and are clinically exploited to mobilise HSCs to the blood for transplant (Suárez-Álvarez et al. 2012).

1.6 Molecular interactions within the HSC niche

There are many interactions that occur in the niche between HSCs and the supporting cells (Figure 1.7). These exchanges act in two ways, which are not mutually exclusive. Some facilitate direct attachment, retaining the HSCs in a supportive environment. Secondly, they initiate further downstream pathways to influence cell behaviour and fate. Changes in these signals can influence HSCs, for example causing them to move into the bloodstream or to differentiate. The molecules involved can be split into two categories: membrane bound receptors (direct adhesion) and cytokines (interaction *via* secreted factors). The key interactions are summarised in Table 1.2.
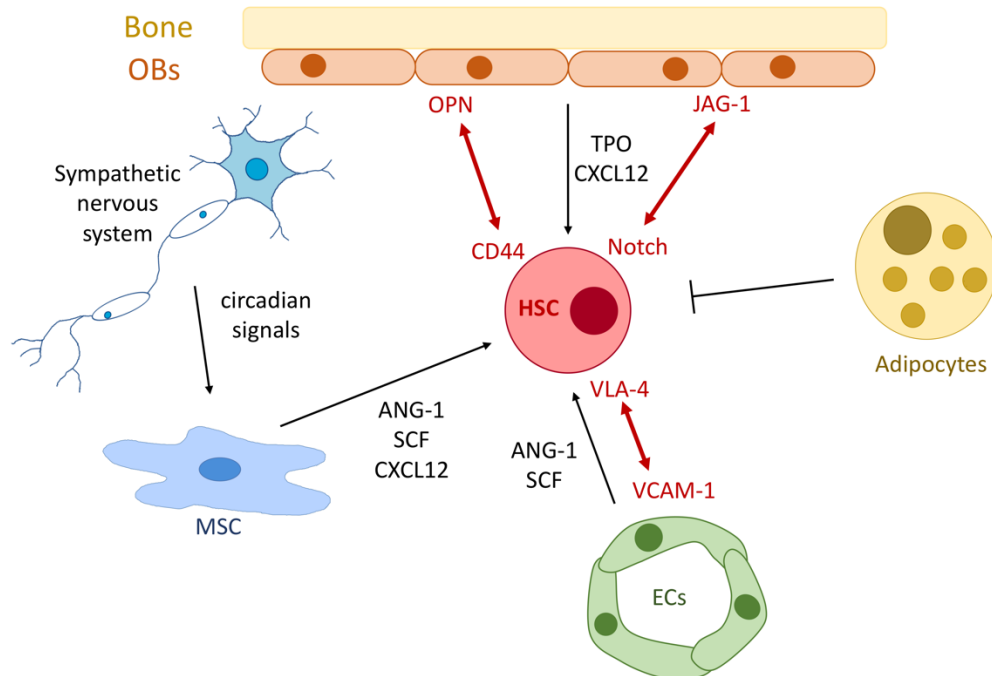
**Figure 1.7 Schematic of the key established interactions between BM niche cells and HSCs.
Red arrows indicate direct interactions between membrane-bound molecules; black arrows
indicate interactions *via* secretion of soluble factors. OBs, osteoblasts; ECs, endothelial
cells.**

1.6.1 Membrane bound receptors

Several classes of membrane bound receptors play a role in HSC homing and adhesion in the niche. These include integrins, cadherins, and selectins. They recognise counterpart ligands on the opposing cell type and are intimately connected to cytoskeleton components (usually actin) *via* linkage proteins. They can also feed in to other signalling pathways through these linkers.

Integrins are predominantly involved in cell adhesion to the ECM, although they are involved in cell-cell adhesion. They are linked to the cell cytoskeleton *via* actin filaments, and initiate intracellular signalling when bound, thus acting as an environmental sensing mechanism. Integrins are composed of two transmembrane glycoprotein subunits; α and β. In humans, there are 8 varieties of β subunit, and 18 types of α subunit, reflecting the diversity of integrin heterodimers (Brizzi et al. 2012). They also have functional overlap, with several varieties able to bind to the same ECM components. The ligands for β_2 subunits are immunoglobulin (Ig) superfamily counter-receptors, and so are involved in cell-cell binding. They are exclusively expressed on haematopoietic cells and include HSC integrin LFA-1, which binds to Ig superfamily molecule intercellular adhesion molecule 1 (ICAM-1) on MSCs (Simmons et al. 1992; Teixido et al. 1992). Alternatively, VLA-4 is a $\beta 1$ integrin, which binds to VCAM-1. Blocking $\beta 1$ using an antibody has been found to reduce adhesion of haematopoietic progenitor cells (HPSCs) to a feeder layer of MSCs (Jing et al. 2010). Higher expression of fibronectin, cadherin-11, VCAM-1, and integrins is associated with greater adhesion (Wagner, Wein, et al. 2007).

Whether cadherins are involved in HSC adhesion to the niche is controversial. Cadherins operate through homophilic adhesion. Some groups have asserted that HSCs and niche cells do not express N-cadherin (Kiel et al. 2007; Kiel et al. 2009), and deletion studies did not have any effect on cell number and function. However, other studies have observed expression of N-cadherin and cadherin-11, and found them to mediate HSC-MSC interaction, with a vital role in adhesion to the niche (Wein et al. 2010; Hosokawa et al. 2010). This discrepancy may be due in part to differences in experimental techniques. It is likely that N-cadherin is expressed only at very low levels in a small subset of HSCs, and that its function is not essential for HSC maintenance. There may however be redundancy with other cadherins (Li & Zon 2010).

E-selectin is expressed by the vascular endothelium. The absence of E-selectin slows the cycling of HSCs, supporting the hypothesis that sinusoidal HSCs are more active than endosteal HSCs (Moore 2012; Winkler et al. 2012). Conversely, the OPN negatively regulates HSC proliferation. OPN expression is restricted to the endosteum, further supporting the zoned niche model (Nilsson et al. 2005).

1.6.2 Cytokines

Cytokines are small proteins that are active in cell signalling, and are produced by a broad range of cells. Recognition of cytokines by receptors on the surface of cells triggers intracellular signalling cascades, which then induce changes in cell behaviour. Cytokines have fundamental roles in immune responses and in development, as well as inter-cell communication in the BM niche. Several cytokine interactions are important for attracting and retaining HSCs into the niche, as explained in section 1.5. These interactions have a combinatorial role: both in increasing HSC adherence to cells and ECM, and activating downstream pathways that promote quiescence, an immature phenotype, and self-renewal. Gradients of these factors can facilitate attraction of HSCs to the niche.

As described earlier, the CXCR4/CXCL12 axis is vital to HSC communication within the BM. The receptor CXCR4 is expressed by HSCs, which recognises the ligand CXCL12 that is secreted by CAR cells in the niche. Deletion of the receptor results in severe reduction of the HSC population (Sugiyama et al. 2006) and blocking the CXCR4 receptor by drugs or antibodies has been shown to mobilise HSCs from the niche: a fact that is exploited to harvest HSCs from donors for transplant (Petit et al. 2002).

The c-Kit ligand is expressed by HSCs at all stages of development. The ligand, SCF, is expressed in both soluble and membrane bound forms by perivascular niche cells, with the membrane bound form facilitating attachment directly, and activating c-Kit for a prolonged period. The interaction may also contribute to upregulation of the ß1 integrins VLA-4 and VLA-5, increasing affinity for fibronectin and thus adhesion to the niche (Ashman 1999).

Angiopoietin-1 (Ang-1)/Tie-2 tyrosine kinase receptor signalling also upregulates β1 integrins on HSCs. Activation of the Tie-2 receptor on HSCs *via* the binding of

Ang-1 feeds into the phosphoinositide 3-kinase (PI3K)-AKT signalling cascade. Downstream effects of this pathway include cell cycle regulation, leading to quiescence and preventing apoptosis. Ang-1 exposure maintains an immature HSC phenotype by retaining the expression of c-Kit and Tie-2 cell surface markers, which are characteristic of the immature state (Arai et al. 2004).

Quiescent HSCs express myeloproliferative leukemia protein (MPL), the receptor for thrombopoietin (TPO), which is secreted by osteoblastic cells. MPL expression in HSCs is closely correlated with cell cycle status, and TPO application affects levels of c-Myc, cyclin dependent kinase inhibitors p57, p21, and p27, and Tie2. In turn, three major signalling pathways are activated after MPL activation: p42/44 MAPK, PI3K-Akt, and Janus kinase (JAK)-signal transducer and activator of transcription (STAT) 3 and STAT5 (Yoshihara et al. 2007).

Interaction type	HSC molecule	Niche molecule	Description	Effects	Reference
Membrane bound	VLA-4 LFA-1	VCAM-1 ICAM-1	Integrin-Ig superfamily interactions.	Physically anchors HSCs to the niche.	Wagner et al. 2007; Simmons et al. 1992; Teixido et al. 1992
	N-cadherin	N-cadherin	Homotypic adhesion.	Physically anchors HSCs to the niche (under controversy).	Li & Zon 2010b
	Not yet identified	E-selectin	E-selectin is expressed on vascular endothelium.	Enhances HSC cycling.	Winkler et al. 2012, Moore 2012
	CD44, multiple integrins	OPN	OPN is expressed at the endosteum.	Negatively regulates HSC proliferation.	Nilsson et al. 2005
	HA	CD44	HSCs synthesise a membrane bound form of HA.	Inhibits HSC proliferation and differentiation.	Nilsson et al. 2003
Cytokine	CXCR4	CXCL12 (SDF1)	CXCL12 is secreted by the niche cell and recognised by the CXCR4 receptor on HSCs.	Direct adhesion. Upregulation of VCAM-1. Inhibition of HSC cycling.	Sugiyama et al. 2006; Suárez-Álvarez et al. 2012
	c-Kit	SCF	SCF is expressed in both soluble and membrane bound forms.	Membrane bound SCF: direct attachment. VLA-4 and VLA-5 upregulation, increasing adhesion to fibronectin.	Ashman 1999
	Tie-2	Ang-1	Niche cells secrete Ang-1. Tyrosine kinase signalling feeds into downstream pathways.	Upregulates β1 integrins. Cell cycle regulation leads to quiescence, apoptosis	Arai et al. 2004

				prevention, and increased self-renewal. Maintenance of immature phenotype.	
	MPL	TPO	TPO is secreted by MSCs.	Upregulation of ß1 integrins. Feeds into cell cycle regulation affecting levels of c-Myc, p57, p21, and p27. Affects levels of Tie-2 and activates other signalling pathways.	Yoshihara et al. 2007

Table 1.2 Key molecular interactions established between HSCs and supportive niche cells within the bone marrow.
VLA-4, very late antigen 4; LFA-1, lymphocyte function-associated antigen 1; VCAM-1, vascular cell adhesion molecule 1; ICAM-1, intercellular adhesion molecule 1; CXCR4, C-X-C chemokine receptor type 4; SCF, stem cell factor; OPN; osteopontin, HA, hyaluronan, CXCL-12, C-X-C motif chemokine 12; MPL, myeloproliferative leukaemia protein; TPO, thrombopoietin.

1.6.3 Signalling pathways in the niche

Multiple intracellular signalling pathways act in the niche to facilitate cell-cell communication and alter cell behaviour. These can be triggered by adhesive interactions, or cytokine signals as described in section 1.6. These pathways include Hedgehog, Notch, Wnt, and tissue growth factor ß (TGF-ß) pathways.

1.6.3.1 Notch signalling

The Notch signalling pathway (Figure 1.8) acts during cell-cell communication and has multiple functions in development. In particular, during bone development it is involved in HSC expansion and participates in osteoblastic lineage commitment. As both Notch receptors and ligands are transmembrane proteins, direct cell-cell contact is required for activation of the pathway. Notch was initially identified as being involved in haematopoiesis as aberrations in Notch can lead to leukaemias (Gu et al. 2016). It appears to have a role in both lymphoid and myeloid lineages, although there is more evidence from malignancies of the former.
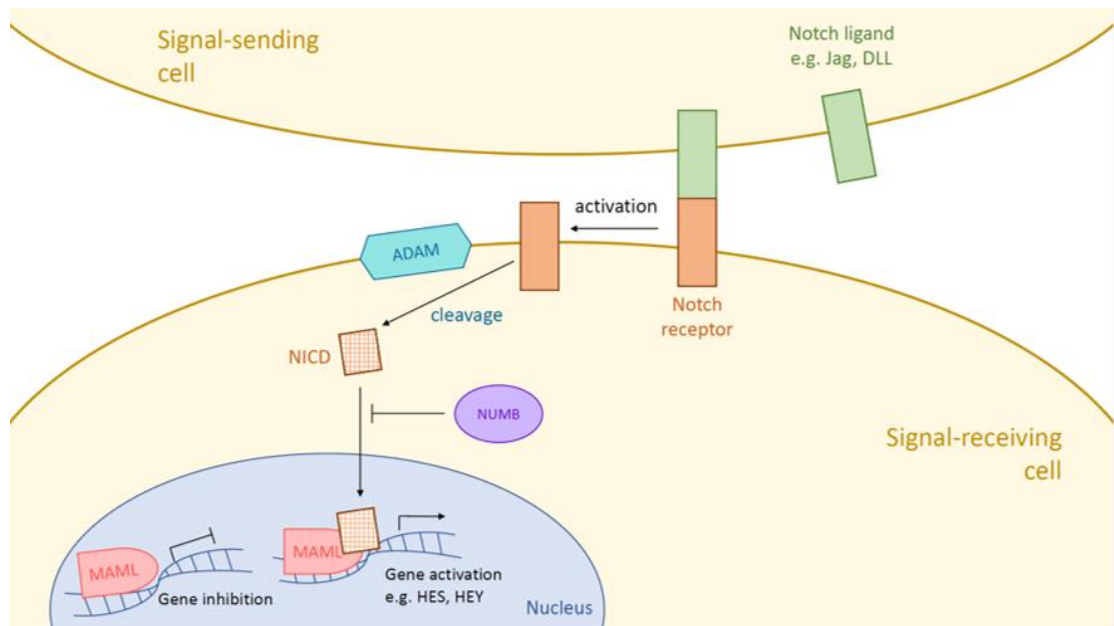
Figure 1.8 Schematic of the Notch signalling pathway.
Interaction of a Notch ligand presented by a signal-sending cell with a Notch receptor
expressed by a signal-receiving cell initiates cleavage of the recptor by an ADAM family
member to produce a Notch intracellular domain (NICD) This NICD then translocates to the
nucleus and complexes with proteins such as MAML to activate transcription of downstream
target genes such as HES and HEY. NICD, Notch intracellular domain; ADAM, a disintegrin
and metalloproteinase; MAML, Mastermind-like protein; HES, hairy and enhancer of split;
HEY, hairy/enhancer-of-split related with YRPW motif.

Notch 1-4 are transmembrane receptors that require direct cell contact for activation, whilst JAG1, JAG2, DLL1, and DLL4 are Notch ligands. Ligand interaction induces Notch cleavage, and hence release of activated Notch intracellular domain (NICD), which translocates into the nucleus. Binding of NICD to CBF1 alters its activity from repressor to an activator, by recruiting coactivators such as Mastermind-like (MAML). HEY1 and HES1 are downstream genes, which can indicate Notch activation, and induce changes in the expression of other genes.

Notch activation increases HSC self-renewal. The levels of Notch also direct HSC fate in binary decisions throughout all stages of differentiation. The proposed mechanism for this influence is *via* interaction of notch with CBP/p300, a complex that is necessary for activity of specific transcription factors, some of which are involved in lineage specification (Krause 2002).

Notch signalling has also been implicated as an intermediary in the interaction between HSCs and the endosteal niche. Notch signalling has a role in other stem cell niches, giving a precedent for its activity in the BM niche. Although there is some contradictory evidence, notch signalling does seem to play a part in HSC

maintenance by stromal niche cells (Weber & Calvi 2010). Notch ligands are expressed by OBs and CD146^{+}, nestin^{+} MSCs, which express a high level of Jag-1, the ligand for the Notch receptor expressed by HSCs (Corselli et al. 2013). Notch signalling pathways are important in embryonic haematopoiesis (Bigas et al. 2010), and inhibition of notch decreased the yield of HSPCs from co-cultures of MSCs with HSCs, implicating an important role in the BM niche. Although many other pathways are important to overall niche function, the requirement for direct cell interaction for Notch activation may explain the lack of success for replicating the effects of a 'feeder layer' in HSC culture. The Notch pathway is spontaneously activated in feeder layer systems with direct cell contact, but requires application of synthetic Notch ligands when support cells are not present in other models.

The effects of Notch signalling on MSC differentiation, particularly osteogenesis, are ambiguous. Removal of Notch from MSCs induces a short term dramatic increase in bone (Hilton et al. 2008). Hence, Notch signalling may maintain a pool of MSC progenitors by suppressing osteogenesis. This is supported by evidence from Dong et al. (2010), showing that Notch is a general repressor of MSC differentiation, without lineage bias. Notch signalling from mature OBs may induce further self-renewal through feedback signals. Reduced Notch signalling increases CXCR4 expression, hence increasing MSC migratory activity towards CXCL12 (Xie et al. 2013).

1.6.3.2 Hedgehog signalling

Although the most studied role of HH signalling (Figure 1.9) is in embryonic development, there is emerging evidence that HH is active in the adult, implicated in the regeneration of tissues from adult stem cells, and metastasis. In particular, MSCs constitutively express a high level of HH pathway components (Fontaine et al. 2008), and reduction in signalling has been associated with differentiation. Hedgehog (HH) ligands bind to the Patched (PTCH) receptor, which, when unbound, inhibits Smoothened (SMO). Following binding of Sonic hedgehog (SHH) or a homologue, inhibition of SMO is terminated. In turn, SMO activates the transcription factors GLI1-3. GLI3 is a repressor, whilst the other two are activators. Hedgehog signalling is dependent on the presence of primary cilia, an organelle where PTCH and SMO reside.
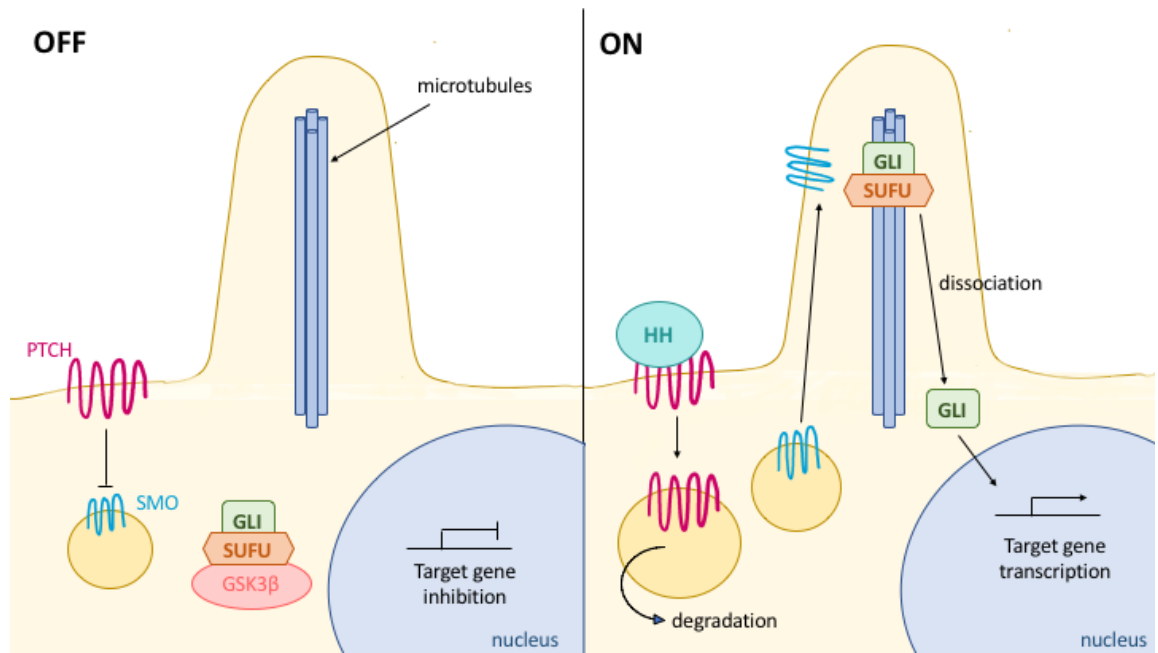
Figure 1.9 Schematic of the Hedgehog signalling pathway.
Binding of the HH ligand triggers degradation of the PTCH receptor, which in turn alleviates inhibition of SMO, allowing it to interact with microtubules in the adjacent primary cilium. SMO interaction with microtubules causes dissociation of the GL!/SUFU complex, allowing translocation of GLI to the nucleus, where it activates transcription of target genes. HH, Hedgehog; PTCH, Patched; SMO, Smoothened; SUFU, Suppressor of Fused; GLI, Glioma associated oncogene; GSK3β, glycogen synthase kinase 3 β.

Evidence for HH signalling involvement in haematopoiesis is contradictory. On one hand, loss- and gain-of-function studies have identified no role for HH in maintenance and self-renewal of HSCs (Gao et al. 2009), whereas previous reports had found a role for the pathway in cell cycle regulation (Trowbridge et al. 2006). More certain is the evidence that HH signalling is involved in later stages of haematopoiesis and development of some haematological malignancies (Gao et al. 2009; Bai et al. 2008).

1.6.3.3 Wnt signalling

The Wnt pathway is a highly conserved signalling pathway that acts to promote HSC self-renewal and prevent differentiation (Figure 1.10, Reya et al. 2003) through both canonical and non-canonical pathways. However, the exact target genes of the pathway have not yet been identified. There are 19 distinct Wnt proteins in the human genome with speculated functional overlap: these are glycoproteins that are secreted from cells and bind to the Frizzled family receptor. The canonical Wnt pathway induces changes in gene expression. Two non-canonical pathways, the planar cell polarity (PCP) and the Wnt-Ca^{2+} pathway

influence the cell cytoskeleton and regulate internal calcium levels, respectively. Activation of the receptor by binding of Wnt ligands allows ß-catenin to escape degradation and form complexes with downstream transcription factors. These include TCF1, TCF4, TCF3, and LEF1 (Staal & Luis 2010).
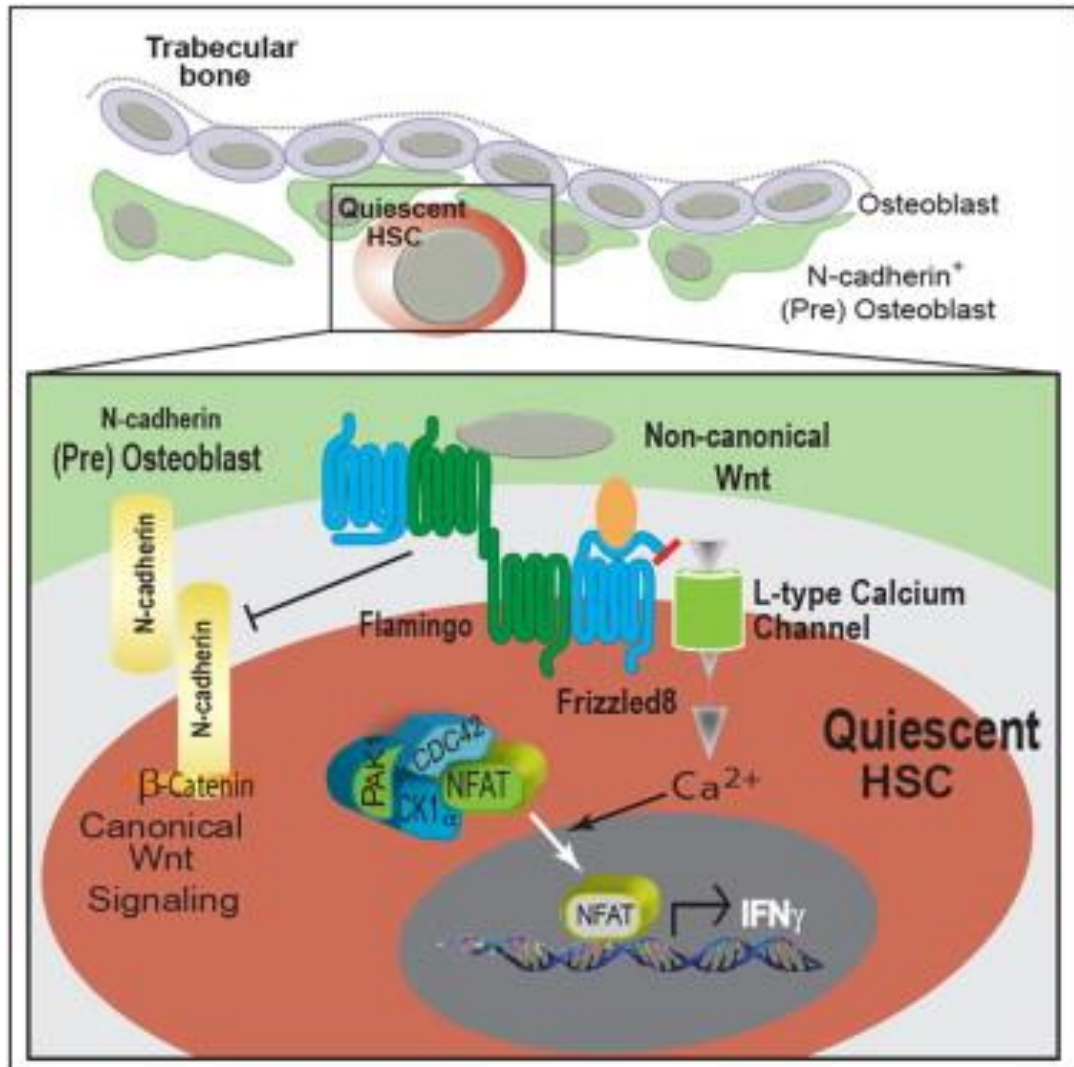
Figure 1.10 Schematic of the Wnt signalling pathway in the HSC niche.
OBs express non-canonical Wnt ligands that are recognised by the Frizzled receptor expressed by haematopoietic cells. This then influences Ca²⁺ levels within the cell, in turn triggering changes in gene expression. The canonical pathway involves β-catenin interacting with transcription factors that also cause gene expression changes. Taken from Sugimura et al. 2012. Permission to reproduce this figure has been granted by Elsevier.

Overexpression of Wnt signalling components could enhance HSC self-renewal, although may alternatively lead to HSC exhaustion (decline in functionality) (Staal & Luis 2010). Canonical Wnt signalling has the potential to activate the cell cycle to a greater extent (Sugimura et al. 2012). The supply of cell-extrinsic Wnt signals to HSCs originates from niche cells, although the relative contributions of different stromal cell types is unknown. Non-canonical Wnt ligands are expressed by OBs,

which can also suppress canonical Wnt signalling (Sugimura et al. 2012). A putative role for Wnt signalling in homing to endosteal niche cells has also been identified. Perturbation of the pathway may have an influence on development of LSCs and vice-versa (Lane et al. 2011).

1.6.3.4 Transforming growth factor beta signalling

TGF-ß family members are cytokines, the binding of which to its receptor initiates a signalling cascade, most commonly the Smad signalling pathway. They regulate a broad spectrum of cell behaviours, including proliferation, differentiation, survival, migration, and ECM production. (Vaidya & Kale 2015).

In terms of haematopoietic progenitors, multiple studies have shown that TGF-ß potently inhibits proliferation of early progenitors. Downstream Smad4 appears to be essential for HSC self-renewal, and preserves immaturity by increasing expression of CD34. The possible mechanism for preserving stem cell functions is *via* inhibition of lipid raft clustering, which is required for HSCs to augment cytokine signalling and re-enter the cell cycle (Yamazaki et al. 2009). TGF-ß signalling may act in concert with CXCL12 signals *via* PI3 and Smad pathways, to achieve a balance between quiescence and activation caused by each of the cytokines respectively in the niche. However, effects on more mature lineage progenitors are dependent of differentiation stage and activation states of other cytokines (Vaidya & Kale 2015).

TGF-ß molecules are produced by many niche cell types, including OBs and macrophages. However, TGF-ß exists with its prodomain in the ECM, requiring activation by ECM-modulator enzymes such as plasmin, MMPs, and thrombin to interact with receptors (Vaidya & Kale 2015). The niche environment may be a facilitative site for latent TGFß activation, and hence HSC quiescence (Yamazaki et al. 2009).

1.7 Additional factors regulating the niche

In addition to cellular interactions, the physical and chemical characteristics of the BM feed into SC regulation. Some of these, including hypoxia, calcium levels, and shear force are examined below.

1.7.1 Hypoxia

Despite being highly vascularised, the pO_2 levels in the BM are lower than in other organs. The extravascular environment, the site of haematopoiesis and maintenance, is defined as hypoxic (< 1% O_2 (Imanirad & Dzierzak 2013)). These hypoxic conditions have implications in haematopoiesis as they induce changes in proliferation, survival, and metabolism genes *via* the action of hypoxia-inducible factors (HIFs). Characteristics of physiologically hypoxic cells include low reactive oxygen species (ROS) levels, lower oxygen consumption and ATP content, high HIF levels, low mitochondrial potential, and reliance on glycolysis rather than oxidative respiration, all characteristics observed in long term (LT)-HSCs (Imanirad & Dzierzak 2013). A recent study showed that HSC hypoxic status is independent of location within the marrow: HIF-1α was stably expressed on a cell-specific rather than location specific basis, and is even retained in circulating HSCs. Cell-autonomous factors rather than environmental conditions may determine a hypoxic phenotype (Nombela-Arrieta et al. 2013).

Hypoxic conditions may also facilitate homing and retention in the niche as CXCR4 expression is regulated by HIF-1α. Similarly, vascular endothelilal growth factor (VEGF) expression is hypoxia-inducible, and its expression by HSCs is related to engraftment, survival, and colony formation. HIF-1α also has a role in maintaining MSC quiescence, prevents RUNX2 expression (inhibiting osteogenesis), and enhances expression of niche factors (Morikawa & Takubo 2016). Studies involving HSC support cells clearly indicate that hypoxia is a factor in HSC fate. For example, silencing of HIF in murine MSCs favours early expansion of co-cultured HSCs, followed by increased differentiation (Guarnerio et al. 2014). In OBs, HIF-1α expression can affect the progression to MPPs and regulate erythropoiesis by increased erythropoietin expression, and in ECs upregulate niche factors. Furthermore, oxygen concentration affects the maturation of megakaryocytes, which occurs faster in higher oxygen environments. Thus, O_2 concentration can determine the size of the megakaryocyte population and hence the concentration of niche factors (Morikawa & Takubo 2016). Hence, hypoxia acts to augment niche functionality *via* both HSCs themselves and influencing niche constituents.

There is some evidence to suggest that high levels of O_2 lead to deregulation of the stem cell niche. The putative mechanism for hypoxia enhancing 'stemness' is

through HIF-1α, which influences expression of quiescence genes. For example, CXCL12 is constitutively expressed in the BM but requires activation of HIF-1α for expression in other tissues (Suárez-Álvarez et al. 2012). This mechanism could act to attract HSCs to sites of vascular injury, which are generally hypoxic. Furthermore, there is evidence to suggest that MSCs grown in 3D hydrogels *in vitro* exhibit a hypoxic phenotype, in concordance with an increase in HSC-supportive capacity (Sharma et al. 2012). Hence, these systems allow a degree of hypoxia to be maintained.

1.7.2 Calcium

HSCs deficient in the calcium sensing receptor (CaR) are able to home to the niche but exhibit impaired lodgment. This is due to a reduced ability to adhere to collagen I (Drüeke 2006). Artificial stimulation of the receptor enhances CXCR4 signalling and cell migration toward CXCL12. A proposed model suggests that HSCs sense Ca^{2+} ions released during bone remodelling by osteoclasts when they initially enter the endosteal niche. Activation of CaR in turn activates CXCR4 and direct adhesion to the niche (Lam et al. 2010). Selectins, integrins, and cadherins are all dependent on calcium for their adhesive properties, and so calcium concentration in the niche may affect adhesion.

1.7.3 Shear force

CD44 (which is expressed on HSCs) attachment to hyaluronan (HA) in the ECM has an important role in HSC homing and engraftment. This interaction has been shown to be stimulated by flow rate (Christophis et al. 2011). The shear stress generated by fluid flow can also affect MSC phenotype, inducing osteoblastic or endothelial differentiation (Dong et al. 2009; Yourek et al. 2010).

1.8 Cellular interactions with extracellular matrix within the bone marrow

In the BM, the extracellular matrix (ECM) is secreted by stromal cells and is mainly composed of collagen type I, particularly around the trabecular region. Fibronectin is also located both perivascularly and endosteally (Nilsson et al. 1998; Leisten et al. 2012), and several other proteins such as laminin, heparin, and proteoglycans are present, although only 10-15% of total bone protein is non-

collagenous (Clarke 2008). The ECM provides a surface for secreted cytokines and growth factors and cells to adhere to, enabling gradients to be established. Hence, the complex 3D architecture of the BM has fundamental importance for control of cell behaviour. Any attempt at physiological replication of the BM must incorporate this structure.

1.8.1 HSC-ECM interactions

The ECM is an important part of the BM niche, although it has been largely neglected in the literature due to HSCs being thought of as non-adherent cells. Recently, however, numerous studies have emphasised the importance of cell-ECM interactions in HSC regulation. HSC-ECM interactions occur *via* HSC integrins; VLA-4 and VLA-5 are specific to fibronectin, α6ß1 to laminin, and α2ß1 to collagen (Celebi et al. 2011). Integrins are intimately linked to the cytoskeleton, and so attachments can mediate cell growth, differentiation, and self-renewal. For example, myosin asymmetry, mediated by adhesion, regulates asymmetric division in hematopoiesis (Shin et al. 2014). The ECM has an influence on cell cycle progression; the interaction of integrins with fibronectin and collagen *in vitro* imposed a block on S phase in $CD34^+$ cells (Jiang et al. 2000; Oswald et al. 2006). ECM properties such as stiffness may therefore be an important consideration for influencing HSC quiescence.

HA is an abundant ECM polysaccharide that is important for HSC homing as it binds to the CD44 receptor on HSCs (Lapidot & Petit 2002). Cytoskeletal linker proteins connect CD44 to the actin cytoskeleton, feeding into transduction pathways, consequences of which include activation of further adhesion molecules. There is also some evidence for cross-talk between CD44 and the CXCR4/CXCL12 axis. CD44 has several additional ligands such as collagen, laminin, and fibronectin as well as integrins. CD44 also stimulates osteopontin secretion, which is chemotactic for HSCs (Zöller 2011).

Cultivating HSCs in an artificial ECM has obvious potential for *in vitro* control. HSCs cultivated in a fibrillar collagen I matrix show reduced expansion but greater colony forming unit (CFU-C) potential. RNA analysis has identified many genes which were upregulated in the 3D environment compared to control, among which were a large number of cytokines and growth factors implicated in HSC regulation,

as well as genes involved in the cell cycle (Oswald et al. 2006). Growing cells in an artificial ECM made up of more than one constituent may give greater growth advantages, as the molecules may have a synergistic effect on HSCs through formation of heterotertiary structures (Celebi et al. 2011).

1.8.2 MSC-ECM interactions

Several recent studies have shown that MSCs are finely tuned to the BM ECM microenvironment. Matrix stiffness, surface mobility, and topography are among factors which have been shown to influence the differentiation state of MSCs (Kilian et al. 2010; Dalby et al. 2007; Engler et al. 2006; McBeath et al. 2004). Exploitation of these parameters could enable MSCs to be maintained in a multipotent state in which they can support HSCs. For example, Leisten *et al.* (2012) found that using a collagenous matrix supported clonal proliferation to a greater extent than standard liquid culture. Culturing MSCs in a 3D environment may also induce nestin expression and hence generate the rare subset of MSCs that support HSCs (Lewis et al. 2016). MSCs also secrete collagen type I, osteopontin, and fibronectin, thus influencing the BM ECM.

1.9 *In vitro* models of the bone marrow microenvironment

Recapitulating the BM niche microenvironment *ex vivo* requires combination of the components described above to preserve functionality. The BM has a complex architecture, comprising organ structures such as the endosteum, ECM components such as collagen, and vascular structures including sinusoids. Furthermore, multiple cell types are involved in maintenance of HSCs and control of haematopoiesis. MSCs are critical for support, with cells in various areas of the niche (OBs at the endosteum, and ECs in the vasculature), fine-tuning the activity of progenitors in these areas. Creating a niche model that is able to replicate all of these aspects is a challenging task, and requires a move from traditional 2D tissue culture methods to 3D environments that are able to mimic physiology.

1.9.1 3D MSC culture

There have been many studies into developing 3D culture techniques for MSCs to recapitulate the *in vivo* state. Requiring a combination of biology, materials

science, and engineering, these commonly involve a matrix or scaffold to support various cell behaviours. These can be either synthetic, such as polycaprolactone and polyethylene glycol, or natural, using constituents of the ECM such as collagen, gelatin, or hyaluronan. Alternatively, inorganic materials such as nanoparticles and graphene have been investigated. MSCs grown in 3D constructs generally demonstrate enhanced differentiation capacities and self-renewal, and have potential for scalability (Kyu Hong et al. 2015), clear advantages over traditional 2D culture.

More recently, 3D MSC culture techniques have involved creating aggregates of cells termed 'spheroids'. Spheroids facilitate inter-cell interactions, replicate gradients of nutrients and oxygen that would be observed *in vivo*, and can generate their own ECM (Cesarz & Tamama 2016). Traditional methods of spheroid generation include hanging drops and culture in non-adherent conditions, but with the increase in interest, additional techniques are also being investigated, such as formation *via* magnetic levitation. Table 1.3 summarises results from recent studies that have used spheroid systems for MSC culture, and how culture affects MSC behaviour and phenotype. A study published from the Centre for Cell Engineering used magnetically levitated MSC spheroids, which were subsequently cultured within a collagen gel. The MSCs became quiescent and maintained expression of nestin and STRO-1, indicating a strong MSC phenotype. In addition, MSCs were also capable of injury response, migrating towards co-cultured scratch assays and differentiating appropriately to regenerate the injured cell type (Lewis et al. 2016).

Materials/ Technique	Cells	Application	Remarks	References
Hanging drop	Rat MSCs	Brain injury	Comparison of MSCs derived from monolayer and 3D spheroids	Guo, Ge, et al. 2014
	hBM-MSCs	Apoptosis	Model included fibrin hydrogel. Resistance to apoptosis and enhanced proangiogenic potential	Murphy et al. 2014
	mBM-MSCs	Cytotoxicity and differentiation studies	Cells retained differentiation and clonogenic capacity	Banerjee & Bhonde 2006
	hUC-MSCs	Elucidate pluripotent mechanisms	Relaxation of cytoskeletal tension Is associated with pluripotency	Zhou et al. 2017
	hBM-MSCs	Investigate therapeutic potential	Spheroids enhance anti-inflammatory properties	Bartosh et al. 2010
	hUC-MSCs	Evaluate efficiency for transplantation	Spheroids have enhanced engraftment and vascularization	Bhang et al. 2012
	hBM-MSCs	Examine cellular anti-inflammatory effects	Conditioned medium from spheroids stimulates macrophages to become anti-inflammatory	Ylöstalo et al. 2012
	hUC-MSCs	Probe epigenetic changes	Passage 6 MSCs regained clonogenic and differentiation capacity	Guo, Zhou, et al. 2014
Low adherence or forced aggregation	MSCs	MSC expansion (scale up)	Serum free media optimised	Alimperti et al. 2014
	hBM-MSCs	Investigate role of the cytoskeleton	3D aggregation alters mitochondrial function, and induces functional activation, and cellular stress response	Tsai et al. 2015
	hMSCs	Investigated the effects of preserving ECM produced by spheroids	Endogenous ECM enhanced proliferation, differentiation and survival	Kim & Ma 2013
	mBM-MSCs	Enhance utility of MSCs for therapies	No necrosis, enhanced multilineage potential	Baraniak & McDevitt 2012

	Rabbit MSCs	Characterise spheroids	Micropatterned wells. Superior neovessel formation and wound healing	Rettinger et al. 2014
Liquid overlay	Adipose tissue MSCs	Evaluate as a vascularisation strategy	Implanted spheroids induced strong angiogenic host response	Laschke et al. 2013
Chitosan	hUC-MSCs	Cell-matrix interaction	Calcium signalling inside spheroid	Yeh et al. 2014
	hMSCs/ endothelial progenitors	Angiogenesis	Sphere morphology influenced by cell-substrate interaction	(Hsu et al. 2014)
	Adipose tissue MSCs	Maintain stemness	Upregulation of pluripotency genes, enhanced differentiation	Cheng et al. 2012
Microfluidics, 'micromasses'	hBM-MSCs	'Developmental engineering' for skeletal tissue regeneration	Exposure to morphogens identified chondrogenic concentrations	Occhetta et al. 2015
Micropatterned substrates	hMSCs	Assess potential for tissue engineering	Greater differentiation capacity: downregulation of self-renewal genes	Wang et al. 2009
Chambered slides	Synovial CD105+ MSCs	Chondrogenesis	Chondrocytes were produced by spheroids	Arufe et al. 2009
Magnetic levitation, collagen I gel	hBM-MSCs	Probe wound healing response	MSCs migrate from spheroid in response to co-culture wounding	Lewis et al. 2016
	hBM-MSCs	Characterise MSCs in magnetically levitated spheroids	MSCs are more quiescent in spheroids	Lewis et al. 2017

Table 1.3 Summary of several studies using 3D spheroid systems to culture MSCs.
Adapted from Kyu Hong et al. 2015. hBM-MSCs, human BM-MSCs; mBM-MSCs, murine BM-MSCs; hUC-MSCs, human umbilical cord MSCs.

1.9.2 MSC and HSC co-cultures

It is well established that MSCs are required to support a successful HSC population *in vitro*, indeed, such cultures have been considerably more successful than attempts using HSC maintenance factors in the media, such as cytokines, for support (Table 1.4). HSCs co-cultured with stromal support cells demonstrate higher expansion (McNiece et al. 2004; Salati et al. 2013), improved clonogenic capacity (Salati et al. 2013; Wagner et al. 2008), and enhanced engraftment (Wagner et al. 2008; Perdomo-Arciniegas & Vernot 2011). Other studies have shown that stromal cells influence differentiation (Salati et al. 2013; Cheng et al. 2000; Perucca et al. 2017), that HSCs also have an effect on MSCs (Perucca et al. 2017), and allowed preliminary studies into niche structure (Jing et al. 2010). The importance of the rare subset of nestin[+] MSCs, mentioned previously, was demonstrated by Corselli et al. (2013): they cultured nestin[+] MSCs together with HSCs and showed that a larger self-renewing population of the latter was maintained without differentiation, compared to culture with unfractionated MSCs. This support occurred through cell-cell contacts and through activation of the cell membrane bound Notch protein by direct cell contact, leading to downstream signalling (Figure 1.11, Corselli et al. 2013).
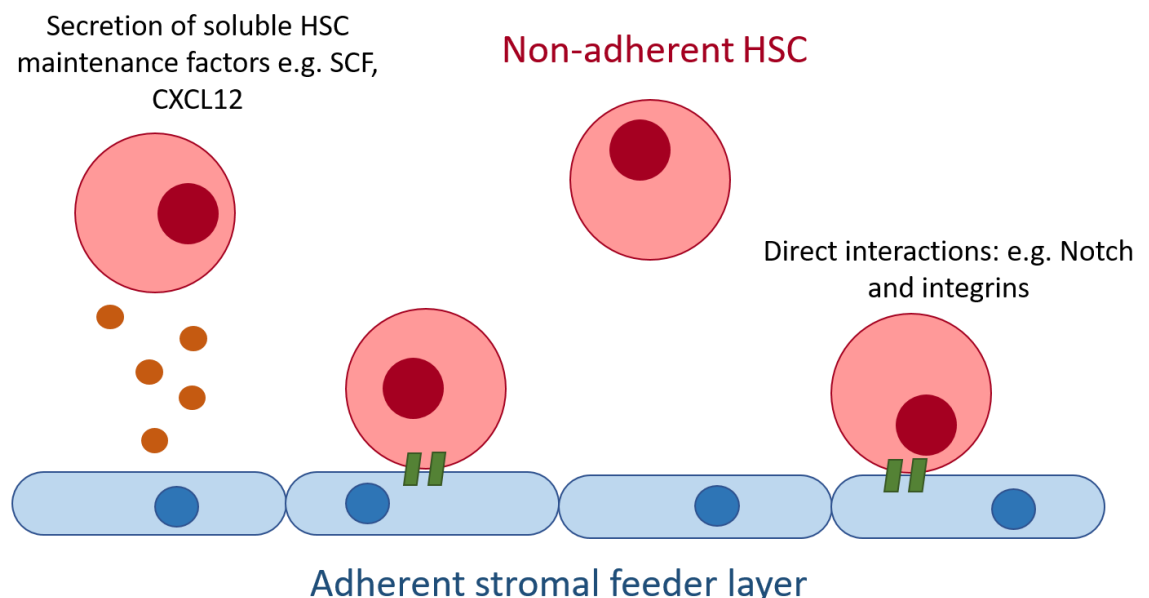
Figure 1.11 Schematic of HSC-stromal co-culture systems and mechanisms.
Typical 'feeder layer' culture systems provide a stromal cell sheet over which is overlaid haematopoietic lineage cells in suspension. Cytokines (such as CXCL12 and SCF) released by the stromal cells encourage migration of the suspension cells to the layer, resulting in direct interactions via membrane bound proteins such as integrins and Notch receptors.

More recently, attempts have been made to move away from traditional monolayer cell culture techniques employed in these co-culture studies. MSCs within their niche in the bone marrow exist as discrete cell populations in a 3D environment; therefore, it is believed that mimicking such culture conditions *in vitro* may enhance MSC properties, and in turn enhance HSC support. Culturing MSCs as adherent cells will impair their ability to secrete vital HSC maintenance factors, favouring a move towards 3D culture (Isern et al. 2013). However, MSCs cultured as 3D cell aggregates (spheroids or 'mesenspheres') are known to enhance the self-renewal of MSCs, and indeed have been shown to sustain HSC self-renewal and expansion without direct cell contact (Isern et al. 2013).

Bearing this in mind, there have been several co-culture studies utilising 3D scaffolds (Leisten et al. 2012; Sharma et al. 2012; Ferreira et al. 2012). These models have been shown to preserve HSC quiescence, expression of stem cell markers, and HSC functionality. Microchip systems have produced similar results, with the added parameter of fluid flow (Torisawa et al. 2014; Wuchter et al. 2016). Some of these studies are documented in (Table 1.4). In general, these co-culture systems replicate the physiological ratios of haematopoietic progenitors more closely than culture in isolation.

Despite these successes, the complexity of the bone marrow niche must not be underestimated. Nestin[+] MSCs may be the 'keystone of the niche' (Frenette et al. 2013), but the BM environment houses multiple cell types that feed into HSC regulation, directly and indirectly. Hormonal and neuronal inputs will also play a role. Therefore, co-culture with multiple cell types may be necessary to retain niche functionality *ex vivo*. Some recent studies have begun to develop 3D models with more than two niche types, such as in Huang et al. (2016), which included ECs in an attempt to model the endothelial niche.

System	Material	Cell types	Remarks	Reference
Co-culture of non-adherent cells with feeder layer	None	Adipose and fetal BM MSCs, hUC-CD34+	Identification of a specific subset of HSC-supportive MSCs.	Corselli et al. 2013
		hBM-MSCs, hUC-CD34+	CD34+ population increased in culture with MSCs.	McNiece et al. 2004
		hUC-CD34+, BM OBs	23-fold expansion of HSPC population and increase in clonogenic capacity. OBs favoured mono/macrophage lineage at the expense of erythroid.	Salati et al. 2013
		hBM-MSCs, hUC-CD34+/CD38-	HSCs with higher self-renewal capacities also exhibited higher adherence to MSCs.	Wagner et al. 2008
		hUC-CD34+, BM adherent cells.	HSCs cultured with MSCs exhibited higher LFA-1 expression, enhanced VCAM-1 dependent migration, and improved capacity for engraftment.	Perdomo-Arciniegas & Vernot 2011
		hBM-MSCs, hBM-CD34+	MSCs induced megakaryocytic differentiation of CD34+ cells, and subsequently platelet formation.	Cheng et al. 2003
		Mobilised peripheral blood CD34+, hBM-MSCs	Distinct microenvironments observed in the model: HSC proliferation at the MSC surface, and maintenance of quiescent cells beneath the layer.	Jing et al. 2010
		hUC-CD34+, hBM-MSCs	MSCs prime HSCs for erythroid differentiation. HSCs direct the BM niche towards the vascular compartment, enhancing hypoxia and angiogenesis related pathways.	Perucca et al. 2017
Co-culture within a gel	Puramatrix gel	Human CD34+, marrow or placenta MSCs	3D MSCs fostered a large pool of quiescent MSCs, combined with robust multi-lineage haematopoiesis: only a few stem cell clones activated to produce daughters to avoid exhaustion.	Sharma et al. 2012

Co-culture in collagen scaffold	Collagen I/III gel	hBM-MSC or hUC-MSC, umbilical cord CD34+	hUB-MSCs are unsuitable for HSC maintenance long-term. Collagen promotes HSC migration and MSCs enhance CD34+CD38- phenotype. MSC-derived fibronectin may contribute to increased HSC migration compared to cell-free collagen.	Leisten et al. 2012
Bone marrow-on-a-chip	PDMS; collagen I containing demineralised bone powder, BMP2, and BMP4.	Populated with host cells following implantation, extracted whole engineered bone for analysis	Complex niche physiology and architecture reconstituted, HSCs present in similar proportions to *in vivo*. Also integrates effects of flow force.	Torisawa et al. 2014
Microcavity arrays: perfused microchip with microwell cavities for high-density 3D cell culture.	Collagen I	hBM-MSCs, hUC-CD34+	3D co-culture compared to 2D: MSCs formed a network with integrated HSCs. Higher expression of stem cell markers observed.	Wuchter et al. 2016
3D co-culture comprising matrix and bioceramic scaffold	3D β-tricalcium phosphate, Matrigel or collagen I/III gels.	hBM-MSCs, hUC-CD34+	CD34+CD38- HSPCs were maintained in β-TCP scaffold containing collagen I/III and Matrigel, including haematopoietic recruitment, proliferation and differentiation, and ECM remodelling.	Ferreira et al. 2012
Spheroids, termed 'mesenspheres'	None	hUC-CD34+, hBM-MSCs	Mesenshperes enhanced HSC expansion.	Isern et al. 2013
Bio-derived bone scaffolds, multiple cell types	Decellularised bone scaffold, collagen I and fibronectin gel	hBM-MSCs, HUVECs, hUC-CD34+	The system supported HSC expansion, and maintained quiescence. HUVECs improved osteogenic differentiation of MSCs. Both adherent cell types together were more effective that co-culture alone.	Huang et al. 2016

Table 1.4 Summary of co-culture studies to support HSCs *ex vivo.*
hBM, human bone marrow; hUC, human umbilical cord

1.10 Conclusion

From reviewing the literature in this chapter, it is evident that (1) there is an obvious clinical need for HSC culture *ex vivo*, (2) in order to do this, a better understanding of HSC biology is required to improve the approach in developing models, and (3) the optimal model will include all the major components of the HSC BM niche. The HSC niche is an incredibly complex environment, which is only beginning to be understood. The many varied facets described in this chapter including the supportive cells, 3D architecture, and ECM proteins, as well as maintenance factors (cytokines etc.) need to be taken into consideration when developing a successful *in vitro* culture HSC model. This project aims to develop a functional, supportive HSC niche environment by co-culturing them with MSC spheroids (generated *via* magnetic levitation), with a type I collagen gel. The model will then be extended to include ECs and OBs, to mimic the vascular and endosteal niche zones, respectively. During the course of this project the interactions between the co-cultured cells will be examined and compared to the *in vivo* interactions.

1.10.1   Hypothesis and objectives

The hypothesis of this study is that culture within a *in vitro* bone marrow niche model influences cell phenotype and behaviour in such a way as to more accurately represent *in vivo* cell phenotype and behaviour compared to traditional tissue culture. To test this hypothesis, the aims of this project are as follows:

- Optimisation of various cell culture techniques to allow effective co-culture of primary HSCs and MSCs, using an existing magnetically levitated MSC spheroid model (Lewis et al. 2016). These include cell isolation and cell culture medium. Subsequently, optimisation of techniques for isolation of cell populations for downstream analysis. This part of the project is described in Chapter 3.

- Characterisation of the MSC spheroid model in terms of its capacity to support HSCs and hence mimic the BM microenvironment. These include structural characterisation, evaluation of cell viability, and expression of

niche-related genes. The findings from this part of the project can be found in Chapter 4.

- Extension of the MSC spheroid model to include additional BM-resident cell types that play a role in different areas of the niche: ECs and OBs to replicate the vascular and endosteal niches respectively. This is followed by analysis of gene expression by the different cell types and flow cytometric analysis of HSCs to determine the influence these environments have on the cells. This part of the project is detailed in Chapter 5.

CHAPTER 2

Chapter 2   Materials and methods

This chapter describes the materials and methods used to carry out the studies detailed in later chapters.

2.1 Cell Culture

A variety of cell types were employed throughout the project, including mesenchymal stem cells (MSCs), human umbilical vein endothelial cells (HUVECs), osteoblasts (OBs), human osteosarcoma MG63 cells (MG63s), immortalized mouse myoblasts (C2C12s), immortalised human dermal fibroblasts (hTERTS), mononuclear cells isolated from bone marrow (MNCs), and HSPCs defined as expressing the cell surface marker CD34. The details of cell sources and culture conditions are given in Table 2.1. Adherent cells were passaged when confluent using trypsin according to standard methods. All cells were grown in an incubator at 37 °C, 5% CO_2. MSCs were used between passage 1-4, HUVECs between passage 1-6, OBs between 1-10, and CD34+ cells were used up to a week after isolation.

Cell type	Source	Basal medium	Supplements
MSCs	Promocell	DMEM	10% FBS with 2% antibiotic mixture, 1% Non-Essential Amino Acids (NEAA, Sigma), and 1% Sodium Pyruvate (Sigma). 2% FBS in PBS (recommended medium, RM) used for enrichment.
MG63s	Sigma-Aldrich		
hTERTs	Clontech Laboratories		
MNCs	Primary human tissue		
C2C12s	Sigma-Aldrich		
OBs	Promocell		10% FBS with 2% antibiotic mixture, 1% NEAA, and 1% Sodium Pyruvate, or osteogenic media (DMEM containing 0.1 μM dexamethasone and 350 μM ascorbate-2-phosphate).
HUVECs	Promocell	EBM	SingleQuots^{TM} endothelial growth supplement (Lonza)
CD34+ HSPCs	Primary human tissue	IMDM	20% BIT 9500 Serum Substitute (StemCell Technologies), 0.02% antibiotic mixture, 20 ng ml^{-1} IL-3, 20 ng ml^{-1} IL-6, 20 ng ml^{-1} G-CSF, 100 ng ml^{-1} Flt3L, and 100 ng ml^{-1} SCF. All

			growth factors were obtained from Peprotech. 2% FBS in PBS (recommended medium, RM) used for enrichment.

Table 2.1 Cell types, sources, and culture conditions used for experiments.
MSCs, mesenchymal stem cells; HUVECs, human umbilical vein endothelial cells; OBs, osteoblasts; MG63s, human bone osteosarcoma cells; hTERTs, immortalised human dermal fibroblasts; MNCs, mononuclear cells; HSPCs, haematopoietic stem and progenitor cells; C2C12s, mouse myoblast cell line; DMEM, Dulbecco's Modified Eagle's Medium (Sigma); IMDM, Isocove's Modified Dulbecco's Medium (Sigma); EBM, Endothelial basal medium (Lonza); FBS, fetal bovine serum; BIT, bovine serum albumin, insulin, transferrin.

2.1.1 Isolation of human serum and mononuclear cells from clinical samples

Mononuclear cells (MNCs) were obtained from clinical samples kindly provided by Mr Dominic Meek from patients undergoing routine hip replacement surgery. Samples were extracted from femoral heads, transferred into transport media (1% phosphate buffered saline (PBS), EDTA), resuspended in 10 ml of PBS, and spun for 10 min at 445 × g. The supernatant containing human serum was removed and frozen for downstream processing. The pellet was resuspended in cell culture medium, and spun once more at the same parameters. Supernatant was discarded, the pellet was resuspended in 10 ml of DMEM and then layered onto 7.5 ml of Ficoll-Paque PLUS (GE Healthcare), which was spun for 45 min at 445 × g. After the spin, the mononuclear cell fraction was removed using a Pasteur pipette. This was washed twice in cell culture medium for 10 min at 445 × g. The final cell pellet containing MNCs was either: resuspended in cell culture media and transferred to a flask for culture; resuspended in PBS, 2% FBS, 1 mM EDTA for enrichment; or resuspended in freezing buffer for storage at -80 °C.

2.1.2 Enrichment of mononuclear cell fraction for the CD34 marker

Desired cell types were extracted from the MNC fraction using the EasySep™ system (STEMCELL Technologies, Vancouver, Canada). The HSPC population was taken to be defined by the presence of the CD34 cell surface marker.

Immediately after processing, MNCs (obtained as described in section 2.1.1) were resuspended in 1 ml of RM. Enrichment was performed using an EasySep™ Human CD34 Positive Selection Kit (STEMCELL Technologies), according to the manufacturer's instructions. Cells were incubated with 100 µl CD34 positive

selection cocktail for 10 min at room temperature. Fifty microlitres of magnetic nanoparticles were added for a second 10 min incubation. RM was added to a total volume of 2.5 ml, and the tube was placed into the EasySep™ magnet without the lid. After 5 min, the excess was transferred to a fresh universal. Two and a half millilitres of RM were added and this process was repeated a further 3 times. After the last incubation, the remaining cells were resuspended in 4 ml IMDM and transferred to a new vented culture flask.

2.1.3 Freezing cells for storage

MNCs (obtained as described in section 2.1.1) were frozen and stored at -80 °C in FBS containing 20% DMEM and 10% DMSO. Post-enrichment, CD34+ cells were frozen in PBS containing 1% human serum albumin (HSA) and 10% DMSO.

2.1.4 Thawing cells from storage

Cells were revived by rapidly thawing in a 37 °C water bath. They were then transferred into 10 ml of warmed culture media, spun for 5 min at 445 × g, and transferred to a flask containing warmed medium.

2.2   Magnetic cell levitation and spheroid formation

The 3D model used throughout this project was based upon MSC spheroids (aggregates of cells) cultured within a type I collagen gel. The following describes the method used for spheroid generation and subsequent culture conditions. Adherent cells (Promocell MSCs, MG63s, C2C12s, or hTERTs) were seeded into 24 well plates at a density of 1 x 10^4 cells ml^{-1}, with 1 ml suspension in each well. After 24 hours, either unlabelled, green, or red fluorescently labelled magnetic iron oxide (FeO_3) 200 nm diameter nanoparticles (Chemicell) were added to the adhered cells at a concentration of 0.1 mg ml^{-1}, and subsequently incubated for 30 min over a magnetic plate to enhance cellular uptake. Samples were then washed with HEPES saline three times to remove excess nanoparticles and detached *via* trypsin. The resulting cell suspension was centrifuged (4 min, 445 × g), the supernatant was removed and the cells were re-suspended in fresh medium. This suspension was then transferred to 6-well plates at a concentration of 2.22 x 10^3 cells ml^{-1}, with 4.5 ml medium per well, with magnets fixed to the

culture plate lid to attract the magnetically labelled cells together. Spheroids formed after 24 hours.

2.2.1 Implanting spheroids into collagen type I gel

After 24 hours, the cell spheroids were transferred from media into a 24 well plate, to each of which 1 ml of fresh collagen gel solution was added. Approximately 6 ml of collagen gel solution was generated by addition of 2.5 ml 2.05 mg ml^{-1} rat tail collagen (FirstLink, Wolverhampton, UK) to 0.5 ml FBS, 0.5 ml IMDM/DMEM, and 0.5 ml 10x DMEM (FirstLink), adjusted to pH 8.2 with 0.1 M NaOH and prepared on ice. The plate was then returned to the incubator to allow gelation to occur. A magnet was placed over each well for the first 24 hours of culture.
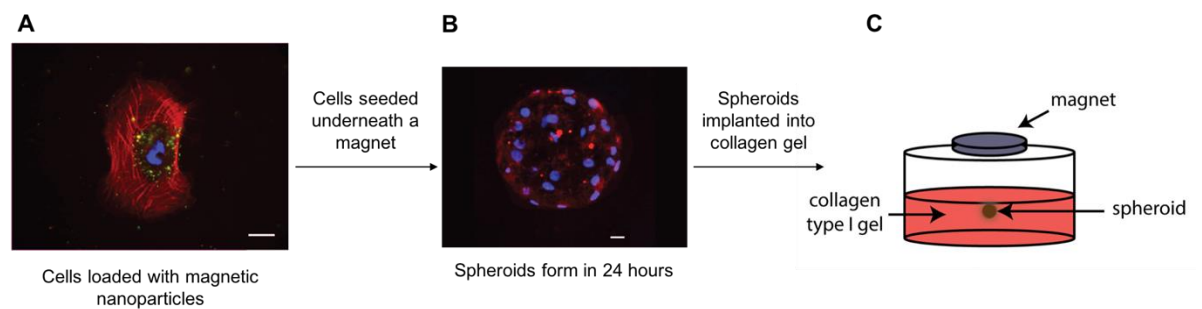
Figure 2.1 Spheroid formation procedure.
A: MSC loaded with magnetic nanoparticles. Red, actin; blue, nucleus; green, nanoparticles.
B: MSC spheroid forms after 24 hours of culture in medium underneath a magnet. Red, STRO-1; blue, nuclei. C: Schematic of spheroid implanted into collagen gel.

2.3 Viability staining

Cell viability was determined using an ethidium homodimer/calcein AM (Life Technologies) stain. Medium containing 1 µl ml^{-1} mix of both stains was added to live cells. After 1 hour, the cells were washed, the medium was exchanged for fresh, warm medium, and the cells were imaged using a fluorescence microscope. Cells fluorescing in the TRITC channel were deemed 'dead' and those fluorescing in the FITC channel were deemed 'alive'. Images were processed in ImageJ and binomial statistical tests were performed on the live/dead cell counts.

2.4 Coomassie blue cell morphology staining

Cultures were initiated, and cells were grown for a set period of time before being fixed for 15 min at 37 °C with 4% formaldehyde, 2% sucrose in PBS. Samples were then washed twice in PBS. One millilitre of filtered Coomassie blue solution was added to each sample, and incubated for 2 min at room temperature. Samples were washed twice more in PBS and then imaged on a light microscope.

2.5 Immunostaining

Cultures were initiated, and cells were grown for a set period of time before being fixed for 15 min at 37 °C with 4% formaldehyde, 2% sucrose in PBS. If appropriate, they were incubated in permeabilising buffer (10.3 g sucrose, 0.292 g NaCl, 0.06 g MgCl2 (hexahydrate), 0.476 g HEPES, 0.5 ml Triton X in 100 ml PBS, pH 7.2) for 5 min at 4 °C. Samples were blocked in PBS/BSA and stained with primary antibody (Table 2.2) diluted with 1% BSA/PBS for 1 hour at 37 °C. After the incubation, they were washed three times in PBS/0.5% Tween 20. They were then incubated with biotin conjugated secondary antibody (1:200 in 1% BSA/PBS, Vector Laboratories, mouse or rabbit) for 1 hour at 37 °C. After 3 washes in PBS/0.5% Tween 20, streptavidin-FITC (1:50 in 1% BSA/PBS, Vector Laboratories) was added, and incubated for 30 min at 37 °C. The samples were then washed three more times in PBS/0.5% Tween 20 and mounted in DAPI. An Axiovert 200 fluorescence microscope was used to image the samples.

Phalloidin was used to stain actin filaments on fixed samples for fluorescence microscopy if appropriate. At the primary antibody incubation stage, phalloidin diluted 1:500 in 1% PBS/BSA was added.

Primary antibody	Manufacturer	Dilution	Secondary antibody
BrdU	GE Healthcare, Chicago, IL, USA	1:100	Mouse
Nestin	Santa Cruz Biotechnologies, Dallas, TX, USA	1:100	Mouse
STRO-1	Santa Cruz Biotechnologies	1:50	Mouse
CXCL12	Abcam, Cambridge, UK	1:200	Rabbit

Table 2.2 Antibodies used for immunohistochemistry.

2.6 BrdU proliferation assay

BrdU is a synthetic thymine analogue which can be incorporated into the DNA of dividing cells in lieu of thymidine as it is being synthesised. This incorporation can be visualised using immunostaining. One millimolar BrdU solution in medium was added to cells in culture. After a 6-hour incubation cells were washed in 1x PBS, fixed in 4% formaldehyde and permeabilised. The immunostaining procedure described in section 2.5 was then applied, using a BrdU antibody (1:100 in DNase). Image analysis was performed in ImageJ to assess the percentage of cells undergoing S-phase, indicated by nuclear co-localisation of BrdU antibody signal and DAPI signal.

2.7 MTT metabolic activity assay

3-(4,5-dimethylthiazol-2-yl)-2,5-diphenyltetrazolium bromide (MTT) is a yellow tetrazolium dye which is reduced to insoluble purple formazan by oxidoreductase enzymes involved in metabolic processes in cells. An MTT assay is used to evaluate the metabolic activity of cells and can be used as a proxy for viability or proliferation tests. After a set period of growth, 20 µl of MTT dye solution (5 mg ml^{-1} MTT (Sigma-Aldrich) in PBS, pH 7.4) was added to each well of a 96-well plate and incubated for 2.5 hours. After the incubation, formazan crystals were solubilised with 200 µl DMSO (dimethyl sulphoxide). The absorbance of each well at 550 nm was read on a Dynatech MR7000 microplate reader. A blank sample (culture medium with no cells) was used to calibrate the spectrophotometer to zero absorbance.

2.8 ELISA assays

Enzyme-linked immunosorbent assays (ELISAs) were performed to measure the amounts of particular cytokines secreted by MSCs. A Human CXCL12 Quantikine ELISA (R & D Systems, Minneapolis, USA) was performed according to the manufacturer's instructions. Cell culture supernates were collected at the specified time points and stored at 4 °C until required. One hundred microlitres of Assay Diluent RD1-55 were added to each microplate well, followed by 100 µl of standard, sample, or control. The microplate was incubated at 4 °C overnight. Wells were washed four times in 400 µl wash buffer (provided), then 200 µl of Human SDF-1α Conjugate was added to each well. After another incubation at 4 °C overnight, washing was repeated as before. Two hundred microlitres of Substrate Solution were added and the plate was incubated for 30 min at room temperature in the dark. Fifty microlitres of Stop Solution were added to terminate the reaction and the absorbance at 450 nm was measured.

2.9 Electron microscopy

Samples were prepared for visualisation *via* Scanning Electron Microscopy (SEM) and Transmission Electron Microscopy (TEM) with the assistance of Margaret Mullin, the electron microscopy technician. In brief, samples were fixed in 2.5% glutaraldehyde in 0.1 M sodium cacodylate buffer (SC) for 1 hour. Cells were washed 3 times in 0.1 M SC, then incubated for 1 h in 1% osmium tetroxide. Samples were rinsed 3 times in distilled water before a 1 h incubation in 0.5% aqueous uranyl acetate in the dark. They were washed a further two times in distilled water, then subjected to dehydration through an alcohol series before critical point drying.

SEM samples were then mounted onto stubs, coated in gold and imaged on a scanning electron microscope. TEM samples were embedded in resin and sectioned prior to imaging on a transmission electron microscope.

2.10 RNA extraction and isolation

RNA extractions from cell pellets were performed using a QIAGEN RNeasy mini kit, according to the manufacturer's protocol. All centrifuge runs were at 8000 × *g* for

15 seconds unless otherwise stated. Pellets were either used immediately after cell harvest or after storage at -80 °C. Three hundred and fifty microlitres of buffer RLT were added to each pellet, and the sample was homogenised by vigorous pipetting. Three hundred and fifty microlitres of 70% ethanol were added to the lysate, and mixed by pipetting. The sample was immediately transferred to an Rneasy MinElute spin column in a 2-ml collection tube, and centrifuged. The flow-through was discarded from the collection tube. Three hundred and fifty microlitres of buffer RW1 were added to the spin column and centrifuged. Eighty microlitres of DNase I in buffer RDD were added directly to the spin column membrane, and incubated at 20-30 °C for 15 min. Three hundred and fifty microlitres of buffer RW1 were added, and the column was centrifuged. The collection tube was discarded and replaced, 500 µl buffer RPE was added, and the column was centrifuged again. Five hundred microlitres of 80% ethanol was added, and the column was centrifuged at 8000 × g for 2 min, after which the collection tube was discarded. The spin column was placed into a new collection tube and centrifuged at 16,000 × g for 5 min to dry the membrane. The flow-through and collection tube were discarded. The column was then placed into a 1.5 ml collection tube. Fourteen microlitres of RNase-free water were added to the centre of the spin column membrane, and the RNA was eluted by centrifuging at 16,000 × g for 1 min.

For samples with low cell numbers, RNA extraction was performed using an ARCTURUS PicoPure RNA Isolation Kit (Applied Biosystems), according to the manufacturer's protocol. Cells were pelleted by centrifugation at 3,000 × g for 10 min. The supernatant was discarded and the pellet was resuspended in 1 ml of cell suspension medium (0.9 ml PBS/10% BSA; 0.1 ml 0.5 M EDTA). The sample was then centrifuged at 3,000 × g for 5 min. One hundred microlitres of extraction buffer were added and the pellet was resuspended with a pipette. The sample was incubated at 42 °C for 30 min, then centrifuged at 3,000 × g for 2 min. The supernatant was transferred to a new microcentrifuge tube. The RNA purification column was preconditioned by adding 250 µl conditioning buffer to the column filter membrane and incubating for 5 min at room temperature. The column was then centrifuged in a collection tube for 1 min at 16,000 × g. One hundred microlitres of 70% ethanol was added to the cell extract, and it was mixed by pipetting. This mixture was then pipetted into the preconditioned purification

column. To bind RNA to the column, it was centrifuged for 2 min at $100 \times g$, immediately followed by centrifugation at $16,000 \times g$ for 30 seconds to remove flowthrough. One hundred microlitres of wash buffer was added and the column was centrifuged for 1 min at $8,000 \times g$. One hundred microlitres of wash buffer 2 was added and the column was centrifuged at $16,000 \times g$ for 2 min. The purification column was then transferred to a new 0.5 ml microcentrifuge kit, and 11 µl elution buffer was pipetted directly onto the membrane. The column was incubated for 1 min at room temperature, then centrifuged for 1 min at $1,000 \times g$ to distribute the elution buffer in the column, followed by a spin for 1 min at $16,000 \times g$ to elute the RNA. RNA content was quantified using a NanoDrop 2000 spectrophotometer (ThermoFisher Scientific, Waltham, MA, USA). The samples were either stored at -80 °C or used immediately.

2.11 Reverse transcription

Reverse transcription was performed using a QuantiTect® Reverse Transcription Kit according to the manufacturer's protocol. Template RNA samples were thawed on ice. The kit reagents (gDNA Wipeout Buffer, Quantiscript® Reverse Transcriptase, Quantiscript RT Buffer, RT Primer Mix, and RNasefree water) were thawed at room temperature (15–25 °C). The solutions were gently mixed and centrifuged to collect residual liquid from the sides of the tube. All subsequent reactions were prepared on ice. RNA content was normalised to 500 ng total in the reaction, if possible. If the total quantity in the sample, determined by Nanodrop quantification, was insufficient to yield this amount, the total volume of the RNA elute was used. The genomic DNA elimination reaction was set up with 2 µl of gDNA Wipeout Buffer and the appropriate amount of template RNA to yield a total amount of 500 ng, made up to 14 µl with RNase-free water. This reaction was incubated for 2 min at 42 °C, and then placed immediately on ice. The reverse transcription reaction was set up with 1 µl Quantiscript Reverse Transcriptase, 4 µl Quantiscript RT buffer, 1 µl RT primer mix, and 14 µl template RNA from the genomic DNA elimination reaction (total reaction volume 20 µl). This mix was incubated for 15 min at 42 °C, followed by an incubation for 3 min at 95 °C to inactivate the Quantiscript Reverse Transcriptase. The reverse transcription reactions were stored at -20 °C.

2.12 Fluidigm Real-Time PCR

2.12.1   Specific target amplification

Specific target amplification (STA) reactions were performed to increase the mRNA of the gene targets. Primers for the genes listed in Table 2.3 were designed using the Sigma online primer design tool. One microlitre aliquots of 100 µM forward and reverse primer sets were pooled and diluted in DNA suspension buffer to create a 500 nM (10x) primer mixture. Pre-mix solutions were made up for each cDNA sample: comprising 2.5 µl TaqMan PreAmp Master Mix (Applied Biosystems), 0.5 µl 500 nM pooled primer mix, and 0.75 µl water. One and a quarter microlitres of cDNA sample was added to this mixture, to a final volume of 5 µl, and the reaction was vortexed. The samples were then run on a thermocycler under the sequence outlined in Table 2.4.

Gene	Forward	Reverse
ENOX2	GAGCTGGAGGGAACCTGATTT	CACTGGCACTACCAAACTGCA
ALCAM	TCCAGAACACGATGAGG	GTAGACGACACCAGCAACAAGG
Vimentin	CATCAACACCGAGTTCAAG	ATCTTATTCTGCTGCTCCA
CD63	CCCTTGGAATTGCTTTTGTT	TATTCCACTCCCCCAGATGA
CD271	CCTCATTCCCTGTCTATTGCTCC	GTTGGCTCCTTGCTTGTTCTGC
CD34	CGGAGGAGGTAGAAGTAG	AGAGTAAGGATATGTTAGGT
CXCR4	TTACCATGGAGGGGATCAGT	GTAGATGGTGGGCAGGAAGA
RUNX2	AACAAGACCCTGCCCGTGG	CATTCAGCAGAGGCATTCCGG
Osterix	TTCTGCGGCAAGAGGTTCACTC	GTGTTTGCTCAGGTGGTCGCTT
BMP2	AGACCTGTATCGCAGGCACT	CCACTCGTTTCTGGTAGTTCTTCC
VLA4	GCATACAGGTGTCCAGCAGAGA	AGGACCAAGGTGGTAAGCAGCT
VCAM1	TTGGCTCACAATTAAGAAGTT	GCAGGTATTATTAAGGAGGATG
LFA1	CTGCTTTTGCCAGCCTCTCTGT	GCTCACAGGTATCTGGCTATGG
ICAM1	TCCTCAGTCAGATACAACAG	TCTTGCTCCTTCCTCTTG
N-cadherin	CTGCTTCAGGCGTCTGTAGA	GCCTGTCCTTCATGCACATC
E-selectin	CCTGCTACCTACCTGTGA	CGAAGCCAGAGGAGAAAT
B2M	TTGTCTTTCAGCAAGGACTGG	ATCCGGCATCTTCAAACCTCC
OPN	AGCTGGATGACCAGAGTGCT	TGAAATTCATGGCTGTGGAA
CXCL12	AGCATCTCAAAATTCTCAACA	GGTACTCCTGAATCCACTT
c-Kit	GCATTCAAGCACAATGGCAC	CCAATCAGCAAAGGAGTGAA
SCF	AGTGATTGTGTGGTTTCTTC	ACTGCTACTGCTGTCATT
Tie2	CCTCTTGTATCTGATGCTGAA	CCTGGTGCTGGTTCATTA
Ang1	AACATGAAGTCGGAGATGG	GCTTTCTGGTCTGCTCTG
MPL	ACTCAGCGAGTCCTCTTTGTGG	CATAGCGGAGTTCGTACCTCAG
TPO	AGGGATTCAGAGCCAAGATT	AGTCCACGAGTTCCATTCAA
NOTCH1	TCCACTGTGAGAACAACACGC	ACTCATTGACATCGTGCTGGC
NOTCH2	GCAAAGTGTATCGATCACCCGA	TGCAGGTGTAGGAATCAATACCATC
NOTCH3	TACTGGTAGCCACTGTGAGCAG	CAGTTATCACCATTGTAGCCAGG
NOTCH4	TTCCACTGTCCTCCTGCCAGAA	TGGCACAGGCTGCCTTGGAATC
JAG1	TGGGATTCCAGTAATGACACCG	GTAGTCATCACAGGTCACGC
JAG2	CAAAAACCTGATTGGCGGCT	CACACACTGGTACCCGTTCA

DLL1	GCCTGGATGTGATGAGCAGC	ACAGCCTGGATAGCGGATACAC
DLL3	CACTCAACAACCTAAGGACGCAG	GAGCGTAGATGGAAGGAGCAGA
DLL4	TCGCTCATCATCGAAGCTTGG	CAGTTCTGACCCACAGCTAGG
MAML	GCAACAGCAGTTCCTTCAGAGG	GTGAACTGTCCAACCTGCTGTG
UBE	CCATGGCTCTGAAGAGAATCC	GATAGGGACTGTCATTTGGCC
HEY1	CCGTGGATCACCTGAAAATGC	GGCATCTAGTCCTTCAATGATGC
HEY2	GAAGATGCTCCAGGCTACAGG	CCTTCCACTGAGCTTAGGTACC
FBXW7	CCTTCTCTGGAGAGAGAAATGC	CTGTCTGATGTATGCACTTTTCC
NUMB	CCAAACCAGTGACAGTGGTGGC	CCCAAGGGTTGGTTTCACGC
LFNG	GCCACAAGGAGATGACGTT	GAGCAGTTTGTGATGACCACG
MFNG	CTGGTACAGTTCTGGTTTGC	ATGTGTCCATGAAACGGGAGC
VEGF	AGAAGGAGGAGGGCAGAATCA	AGGGTACTCCTGGAAGATGTCC
TP53	TTCTTGCATTCTGGGACAGCC	GGGGGTGTGGAATCAACCC
MYC	GACTCTGAGGAGGAACAAGA	TTGGCAGCAGGATAGTCCTT
TCF3	TGACCTCCTGGACTTCAGC	ACCTGAACCTCCGAACTGC
TCF4	AATCAAAACAGCTCCTCCGATT	CCATCTTGCCTCTTGGCCG
TCF7	TCAACCAGATCCTGGGTCGC	CCTTTCCTTGCGGGCCAG
SMO	CTGACCGCTTCCCTGAAGG	CGTCCTCGTACCAGCTCTTGG
SMAD6	CTCCCTACTCTCGGCTGTCT	AGAATTCACCCGGAGCAGTG
SMAD7	CCATCACCTTAGCCGACTCT	CCAGGGGCCAGATAATTCGT
SHH	CGAGCGATTTAAGGAACTCACC	GCGTTCAACTTGTCCTTACACC
PTCH1	ACATTTGTGTTACAAATCAGGAGAGC	CTGTCCCAGACTGTAATTTCGC
PTCH2	TGTGGTGGGAGGCTATCTG	GCATGGTCACACAGGCATAG
ATP	TCCATCCTGTCAGGGACTATG	ATCAAACTGGACGTCCACCAC
p38	GAGCGTTACCAGAACCTGTCTC	AGTAACCGCAGTTCTCTGTAGGT
NFKB1	AGATGATCCATATTTGGGAAGGC	TTGCTCTAATATTTGAAGGTATGGGC
NFKB2	CTTCTCTGCCTTCCTTAG	GATCTCACTGCTGTCAT
MPO	GCATCATCGGTACCCAGTTC	GTGGTGATGCCTGTGTTGTC
MEIS1	AAGCAGTTGGCACAAGACACGG	CTGCTCGGTTGGACTGGTCTAT
LEF1	CACTGACAGTGACCTAATGC	CAACGACATTCGCTCTCATT
HIF1A	TACTCATCCATGTGACCATGAGG	TAGTTCTTCCTCGGCTAGTTAGG
HHIP	GCCATTCAGTAATGGTCCTTTGG	CCACTGCTTTGTCACAGGAC
GSK3B	CGACTAACACCACTGGAAGCT	GGATGGTAGCCAGAGGTGGAT
GLI1	AGCCAAGCACCAGAATCGG	TCTTGACATGTTTTCGCAGCG
GLI3	CTCCTATGGTCACTTATCTGCAAGT	TGAACCTAAGCTCTGTTGTCGG
GATA1	TATTCCTCTCCCAAGCTTCG	CATCTTGTGATAGAGGCCGCA
GATA2	GCGCAGCAAGGCTCGTT	AGCATTGCACAGGTAGTGGC
GATA3	CGAACTGTCAGACCACCACA	GGTTTCTGGTCTGGATGCCTT
FOS	AGGAGAATCCGAAGGGAAAGG	TAGTTGGTCTGTCTCCGCTTG
E2F1	GGACCTGGAAACTGACCATCAG	CAGTGAGGTCTCATAGCGTGAC
E2F2	CTCTCTGAGCTTCAAGCACCTG	CTTGACGGCAATCACTGTCTGC
E2F3	AGCGGTCATCAGTACCTCTCAG	TGGTGAGCAGACCAAGAGACGT
CYCLIN E1	GTCCTGGCTGAATGTATACATGC	CCCTATTTTGTTCAGACAACATGGC
CDKn1A	GTGGACCTGGAGACTCTCAG	CCTCTTGGAGAAGATCAGCCG
CD79	GAACGAGAAGCTCGGGTTG	TGCCCACATCCTGGTAGGT
RNF	GGTGTCTCTTCAACGGAGGAA	TAGTGAGGCATCATCAGTGGC
BMP10	ACCCACCAGAGTACATGTTGG	GCCCATTAAAACTGACCGGC
BMI1	GCATCGAACAACGAGAATCA	GCTGGTCTCCAGGTAACGAA
AKT1	TGGACTACCTGCACTCGGAGAA	GTGCCGCAAAAGGTCTTCATGG
AKT2	CCAACACCTTTGTCATACGCTGC	GCTTCAGACTGTTGGCGACCAT
ADAM17	CTTCTACAGATACATGGGCAGAG	CTCTATCTGTATTCCATAGCCTTTAA
ADAM10	ATGGCAAAGATGATAAAGAATTATGCC	AATCGTTGCAAGGGGATCC
SUFU	CTCCAGGTTACCGCTATCGTCA	TGCTCAGGGATGTTGGCAGAAG
STAT3	CCTAGATCGGCTAGAAAACTGG	GGGTCCCCTTTGTAGGAAAC
RUNX1	CACCTACCACAGAGCCATCAA	CTCGGAAAAGGACAAGCTCC

SPI1	GTGCCCTATGACACGGATCT	AAGCTCTCGAACTCGCTGTG
MCM4	TGACCGTTACCCTGACTCAA	GGGAATCAGCTGGGATGTCC
CYCLIND1	CAGAAGGAGATTGTGCCATCC	GAAGCGGTCCAGGTAGTTCA
CYCLIND2	CCACCGACTTTAAGTTTGCC	CACGTCTGTGTTGGTGATCT
CD44	GGCAAGAAACCTGGGATTGG	GCCTGCTGAGATGGTATTTGA
HES1	GGAGAAAAATTCCTCGTCCC	CGCGAGCTATCTTTCTTCAG
PML	CCGTCATAGGAAGTGAGGTCTTC	GTTTTCGGCATCTGAGTCTTCCG
Nestin	GCAGCGTTGGAACAGAGGT	GCGATCTGGCTCTGTAGGC
BMP7	CAGGCCTGTAAGAAGCACGA	TGGTTGGTGGCGTTCATGTA
CYC1	ACTGCGGGAAGGTCTCTACTT	GGGTGCCATCGTCAAACTCTA

Table 2.3 Primers used in Fluidigm analysis.
Shaded cells indicate genes used as housekeeping controls for normalisation.

Condition	Hold	10-14 cycles		Hold
Temperature	95 ℃	95 ℃	60 ℃	4 ℃
Time	10 min	15 sec	4 min	∞

Table 2.4 Thermal cycler protocol for pre-amplification of cDNA samples.

2.12.2   Exonuclease treatment

Exonuclease treatment was used to remove unincorporated primers. Exonuclease I was diluted to 4 U μl^{-1} to a volume of 2 μl per reaction (1.4 μl water, 0.2 μl Exonuclease I reaction buffer, 0.4 μl Exonuclease I at 20 U μl^{-1}). This 2 μl was added to the STA reactions, which were then vortexed, centrifuged, and run in a thermal cycler as described in Table 2.5.

Condition	Digest	Inactivate	Hold
Temperature	37 ℃	80 ℃	4 ℃
Time	30 min	15 min	∞

Table 2.5 Thermal cycler protocol for exonuclease treatment of cDNA samples.

The products were then diluted 5-fold in TE buffer (TEKnova, PN T0224), and stored at -20 ℃ or used immediately for on-chip PCR.

2.12.3   Sample pre-mix preparation

Two times (2X) SsoFast EvaGreen Supermix with low ORX (Bio-Rad, PN 172-5211) was mixed with 20X DNA Binding Dye Sample Loading Reagent (Fluidigm, PN 100-3738) in an 11:1 ratio. Two point seven five microlitres of this 'pre-mix' was added to 2.25 μl of the STA and exonuclease treated cDNA sample. This final mixture was vortexed for 20 seconds and centrifuged for 30 seconds. All reactions were kept on ice.

2.12.4   Assay mix preparation

One hundred micromolar stocks of forward and reverse primers for each assay were diluted to a final concentration of 5 µM (2.5 µl 2X Assay Loading Reagent, 2.25 µl 1X DNA Suspension Buffer, and 0.25 µl 100 µM mixed forward and reverse primers). The mixture was vortexed for 20 sec and centrifuged for 30 sec.

2.12.5   Chip priming and loading

The 96.96 Dynamic Array IFC was primed with control line fluid, which was injected into each accumulator on the chip. The chip was placed into the IFC controller MX, and the Prime (136x) script was run. Five microlitres of each assay and each sample were pipetted into each respective inlet in the chip. The chip was inserted into the IFC Controller and the Load Mix (136x) script was run to load the samples and assays into the chip. The chip was then run in the BioMark HD system using the protocol described in Table 2.6.

Segment	Type	Temperature (°C)	Duration (sec)	BioMark HD Ramp Rate (°C/s)
1	Thermal Mix	70	2400	5.5
		60	30	5.5
2	Hot Start	95	60	5.5
3	PCR (30 cycles)	96	5	5.5
		60	20	5.5
4	Melting Curve	60	3	1
		60-95	1	1

Table 2.6 Cycling parameters for the 96.96 Dynamic Array IFC.

Results from the chip analysis were analysed using the $2^{-\Delta\Delta CT}$ method (Schmittgen & Livak 2008).

2.13 Flow cytometry

Cells for flow cytometric analysis were harvested from culture models using collagenase and/or trypsin, and centrifuged at 400 × *g* for 10 min. They were resuspended in 800 µl 1% FBS in PBS containing 1 mM EDTA (FACS buffer). They were washed once more using the same parameters. If required, they were then stained with appropriate antibodies (100 µl, 10 µl ml^{-1}) for 30 min at 4 °C and protected from light. They were then centrifugally washed twice more and resuspended in 200 µl FACS buffer. They were then run on a BD FACSCantoII

analyser, or a BD FACSAria cell sorter. An unstained control sample was used to set the voltage for each channel, and an isotype control sample (with cells) was also included. Details of antibodies used are presented in Table 2.7.

Manufacturer	Marker	Fluorochrome	Organism and isotype
BD Biosciences	CD7	BV421	Mouse IgG1
BD Biosciences	CD41a	FITC	Mouse IgG1
BD Biosciences	CD36	APC	Mouse IgM
BD Biosciences	CD14	PE	Mouse IgG2b
BD Biosciences	CD45	APC-Cy7	Mouse IgG1
BioLegend	CD44	PE-Cy7	Rat IgG2b
BD Biosciences	CD45	BV421	Mouse IgG1
BD Biosciences	CD34	APC	Mouse IgG1
eBioscience	CD13	PE	Mouse IgG1
BD Biosciences	CD10	PE-Cy7	Mouse IgG1
BD Biosciences	CD38	V450	Mouse
BD Biosciences	Lineage	FITC	Mouse
BD Biosciences	CD123	APC	Mouse
BD Biosciences	CD135	PE	Mouse
BD Biosciences	CD45RA	APC-H7	Mouse
BD Biosciences	CD90	PE-Cy7	Mouse
BD Biosciences	CD34	PerCP	Mouse
R&D Biosystems	Osteopontin	APC	Mouse
Miltenyi	CD31	APC	Mouse IgG1
BD Biosciences	Mouse IgG1, κ Isotype control	V450	-
BD Biosciences	Mouse IgG1, κ Isotype control	PE-Cy7	-
BD Biosciences	Mouse IgG2b, κ (specific for dansyl) Isotype control	APC	-
BD Biosciences	Mouse IgG2a, κ (specific for TNP) Isotype control	APC-H7	-
BD Biosciences	Mouse IgG1, κ Isotype control	PE	-
BD Biosciences	Mouse IgG1, κ Isotype control	PerCP	-

Table 2.7 Antibodies used for flow cytometry.

2.13.1   Compensation

To correct for any spectral overlap, a process of fluorescence compensation was performed using UltraComp eBeads™ compensation beads (ThermoFisher Scientific). For each antibody used, 1 drop of beads in 100 μl FACS buffer was stained with 1 μl antibody for 10 min, 4 °C. The beads were then washed by

centrifuging at 600 × *g* for 5 min and resuspended in 200 μl FACS buffer. Each sample was run on the cytometer under the compensation set up, and the spectral overlap settings were set automatically.

2.13.2 Phenotyping panels

For phenotyping experiments described in Chapter 3 and Chapter 5, the antibody panels listed in Table 2.8 were used.

Panel 1		Panel 2		Panel 3	
Marker	**Label**	**Marker**	**Label**	**Marker**	**Label**
CD38	V450	CD7	BV421	CD45	BV421
Lin	FITC	CD41a	FITC	CD41a	FITC
CD123	APC	CD36	APC	CD34	APC
CD135	PE	CD14	PE	CD13	PE
CD45RA	APC-H7	CD45	APC-Cy7	free	APC-H7
CD90	PE –Cy7	CD44	PE-Cy7	CD10	PE-Cy7
CD34	PerCP	free	PerCP	free	PerCP

Table 2.8 Antibody panels used for phenotyping experiments.

2.13.3 Gating strategies

For each panel of antibodies listed in Table 2.8, specific gating strategies were used in the analysis of the data. These strategies are described below.

For all panels, firstly the viable cell population was identified using a forward scatter area (FSC-A) versus side scatter area (SSC-A) scatter diagram (Figure 2.2A). From within this population, doublets were excluded using an FSC-A versus FSC-H (height) scatter diagram (Figure 2.2B).

For panel 1, viable, single cell CD34+CD38+ and CD34+CD38- populations were then identified (Figure 2.2C). Within these subsets, progenitors as listed in Table 2.9 were identified using the remaining four markers (Figure 2.2D&E). A hierarchical overview of this process is show in (Figure 2.2F). The process for identifying subsets of progenitors using antibody panel 1 is depicted in Figure 2.2. Phenotypes of the progenitors investigated are listed in Table 2.9.
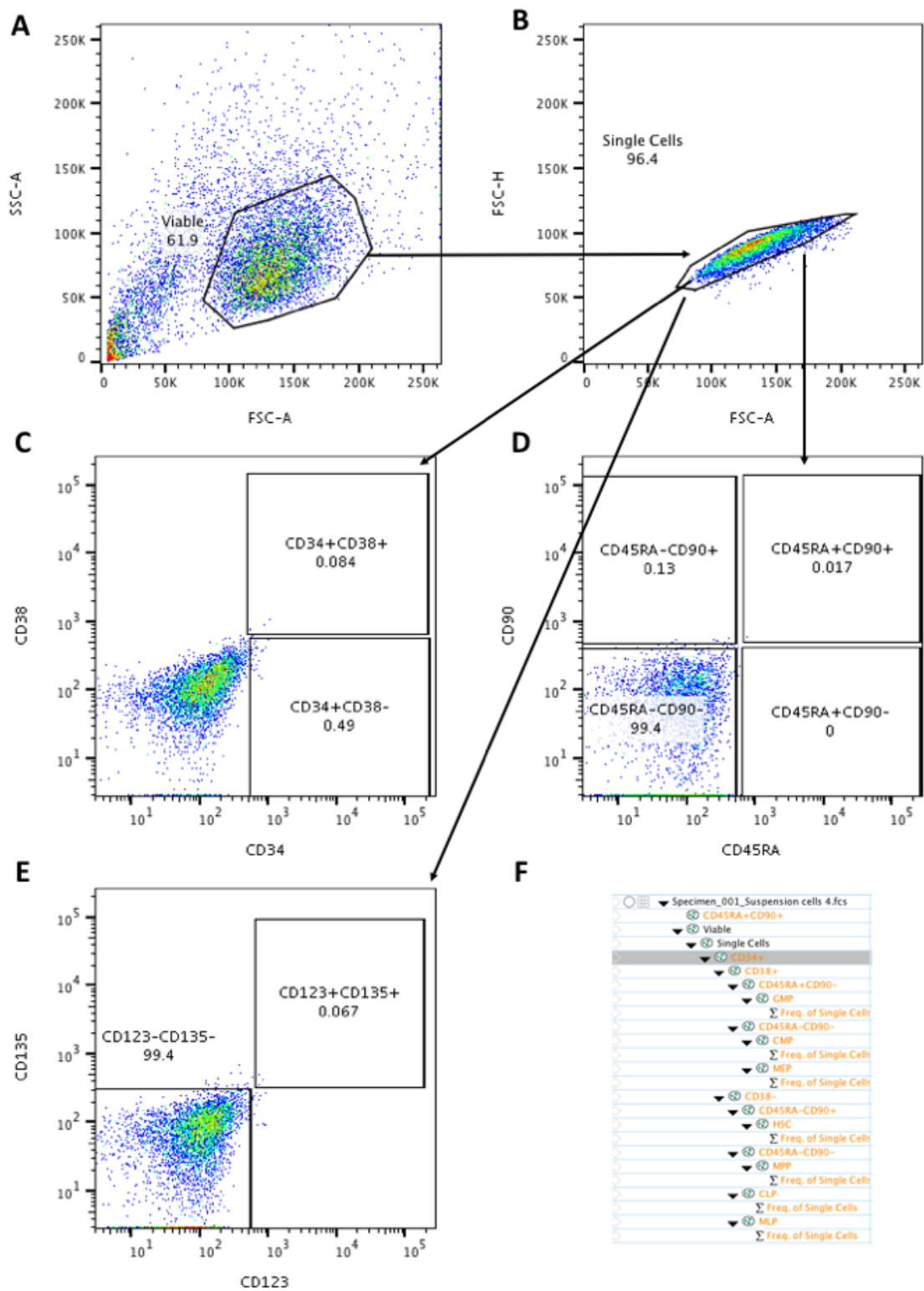
Figure 2.2 Gating strategy used for analysis of data obtained using antibody panel 1.
Sample data is from the isotype control. A, Forward scatter vs. side scatter plot used to identify viable cells; B, Forward scatter (area) vs. forward scatter (height) plot used to identify the population of single cells; C, CD34 vs. CD38 scatter plot; D, CD45RA vs. CD90 scatter plot; E, CD123 vs. CD135 scatter plot; F, diagram of gating strategy used to identify progenitor subsets using combinations of markers.

Progenitor/Marker	CD34	CD38	CD45RA	CD90	CD135	CD123
HSC	+	-	-	+	-	-
MPP	+	-	-	-	-	-
CMP	+	+	-	-	+	+
MEP	+	+	-	-	-	-
GMP	+	+	+	-	+	+
MLP	+	-	+	-		
CLP	+	-/low	+	+		

Table 2.9 Phenotype profiles for haematopoietic progenitor subsets.
HSC, haematopoietic stem cell; MPP, multipotent progenitor; CMP, common myeloid progenitor; MEP, megakaryocyte-erythroid progenitor; GMP, granulocyte-monocyte progenitor; MLP, multi-lymphoid progenitor; CLP, common lymphoid progenitor.

For cell samples stained with antibody panels 2 and 3, subsets were identified from within the single cell fraction individually for each marker. Gates were drawn simply to identify positive and negative cells for each antibody (Figure 2.3 & Figure 2.4), which were then quantified in terms of percentage of single cells.
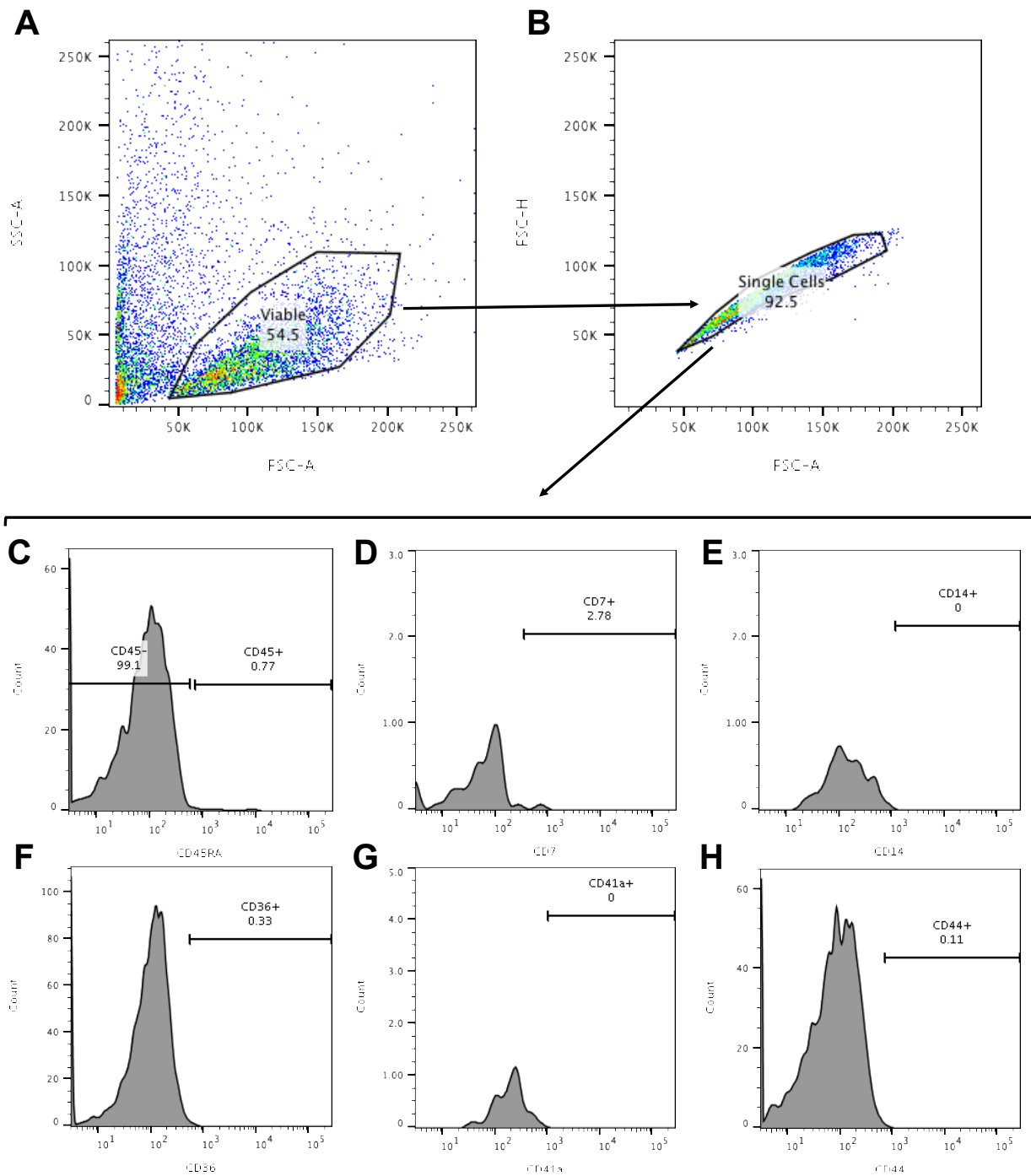
Figure 2.3 Gating strategy used for analysis of data obtained using antibody panel 2.
Sample data is taken from the isotype control. A, Forward scatter vs. side scatter plot used to identify viable cells; B, Forward scatter (area) vs. forward scatter (height) plot used to identify the population of single cells; C-H, gates used for identification of cells positive or negative for CD45, CD7, CD14, CD36, CD41a, and CD44, respectively.
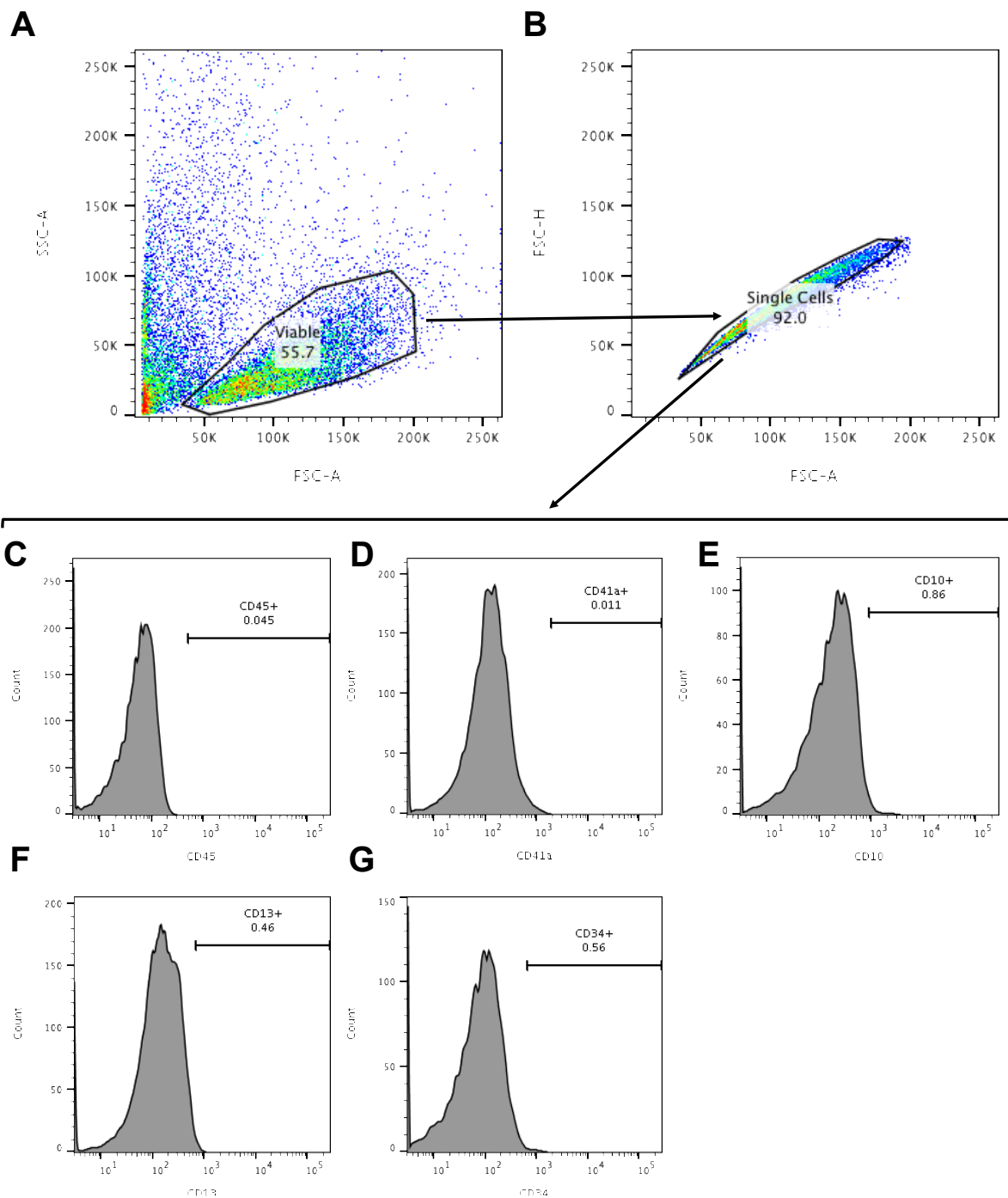
Figure 2.4 Gating strategy used for analysis of data obtained using antibody panel 3.
Sample data is taken from the isotype control. A, Forward scatter vs. side scatter plot used
to identify viable cells; B, Forward scatter (area) vs. forward scatter (height) plot used to
identify the population of single cells; C-G, gates used for identification of cells positive or
negative for CD45, CD41a, CD10, CD13, and CD34, respectively.

2.14 Conclusion

The procedures described above were used to carry out many of the experiments and analyses elaborated on in the following chapters. More detailed information about materials and methods relevant to each chapter are provided if appropriate.

CHAPTER 3

Chapter 3   Model development and optimisation

3.1 Introduction

As previously described, both MSCs and HSCs have great importance in paving the way for regenerative medicine. Both cell types are well studied, and HSCs in particular have been used as a cell therapy for decades (Gratwohl et al. 2015; WBMT 2013). MSC therapies are also beginning to obtain regulatory approval and enter the clinic (Wei et al. 2013). However, culturing them in combination requires the consideration of optimal conditions for each cell type.

MSCs are traditionally cultured as adherent, in medium containing some sort of serum supplement. Common basal media are DMEM, DMEM F-12, or α-MEM supplemented with 10% FBS. Batch variability is often circumvented by using commercial serum supplements, autologous serum, platelet-rich plasma, or serum free media using growth factor supplementation (Bara et al. 2014). However, there is extensive variation between disciplines and even lab groups on the formulation and supplements used. These may also differ depending on the intended application of the cells. For example, fibroblast growth factor and lithium both promote MSC proliferation, and inclusion of synthetic glucocorticoid dexamethasone induces osteogenic differentiation (Both et al. 2007). Furthermore, initial seeding density has an influence on MSC behaviour: at lower seeding densities proliferation is rapid, and slows when the cells reach confluence. Passaging the cells, the process by which cells are removed from the surface of the culture vessel (usually enzymatically) and seeded into a new vessel at a lower density to allow further expansion, also influences multipotency. Higher passage cells can be characterised by lower expression of typical MSC cell surface markers (Both et al. 2007). Nevertheless, maintaining a true naive MSC phenotype may be impossible, as gene expression changes occur immediately after isolation and accumulate throughout prolonged culture (Bara et al. 2014).

Similarly, there is no standard culture method for HSCs/HSPCs[2], and the selected medium may be specific for a particular function or for a particular subset of

---

[2] HSPCs, identified by the presence of the CD34 cell surface marker, are used throughout this project as a proxy for the true HSC population. HSPC is generally used when describing

progenitors. Commonly used basal media are RPMI, α-MEM, and IMDM, which can be supplemented with either serum or cytokines. Culture of HSPCs is proceeding towards serum-free systems to remove the presence of xenogenic compounds that are not appropriate for clinical use, meaning that the media must be supplemented with cytokines. However, this does increase the expense of the system, especially for scale-up (Zainal Ariffin et al. 2016). Cytokines that promote modest HSPC maintenance and proliferation have been identified using functional genomics and proteomics to identify compounds in HSPC supportive cells that are absent in non-supportive cells (Verfaillie 2002). They usually include a combination of EPO, IL-6, Il-3, Flt3L, G-CSF, SCF, GM-CSF, and TPO in various concentrations (Choi et al. 2010; Andrade et al. 2010). However, these cytokines in isolation do not allow cell division without loss of repopulation ability, as the effect of cytokines is modulated by the ECM. Furthermore, direct cell contact through integrins and Notch signalling may be required for synergistic effects of cytokines (Tisdale et al. 1998).

Therefore, MSC and HSPC co-culture in a collagen gel may be able to circumvent the issues encountered with exogenous cytokine application, promoting HSPC proliferation without a loss of repopulation capacity. As described in Chapter 1, several such systems are already in existence. These comprise both simple feeder layer systems and more complex systems that incorporate extracellular matrix and/or organoid structures. This project aims to extend an existing MSC spheroid model (Lewis et al. 2016) to include HSPCs. However, addition of HSPCs into the model requires optimisation of certain aspects of the system. For example, the different cell types require provision of different exogenous substances in the media for culture. Furthermore, analysis of cell populations within the model requires development of a multiple-stage protocol for separation.

---

procedures and results of this study. However, HSC and CD34+ may be used interchangeably when these terms are more appropriate for the context.

3.1.1 Objectives

This chapter aims to extend an existing magnetically-levitated MSC spheroid 3D model developed in the Centre for Cell Engineering (Lewis et al. 2016; Lewis et al. 2017) to include HSPCs, and to develop methods to analyse cell behaviour within the model. This will be achieved by addressing the following issues in turn.

1. Cell culture optimisation: optimisation of cell culture techniques such as freezing and thawing cells will be evaluated.

2. Optimisation of growth media formulations to allow successful co-culture of MSCs and HSPCs.

3. Development of protocols for the 3D co-culture model deconstruction, to allow cell retrieval for downstream analysis of individual cell populations.

3.2 Materials and Methods

3.2.1 Cells and cell culture

HSPCs were isolated from BM and enriched for the CD34 cell surface marker as described in section 2.1.2 C2C12s, MG63s, and h-TERTS were used as a substitute for primary patient MSCs for optimisation of physical aspects of the model. Promocell MSCs were used for MSC functional studies in the model.

3.2.2 Viability staining

Viability staining was performed as described in section 2.3. Viable cells and non-viable cells were counted separately. For some images for which individual cells could not be discerned, percentage green signal area within the cell layer was taken as a proxy for viability. Percentage viability was calculated using the formula: $\frac{number\ of\ viable\ cells}{total\ cell\ number} \times 100$. The average percentage viability from several images was calculated and statistical analyses were performed in GraphPad Prism.

3.2.3 MTT assay

MTT assays were carried out as described in section 2.7. The metabolic activity of MSCs grown in IMDM (HSPC optimal media) was compared to that of MSCs grown in DMEM (MSC optimal media) using an MTT assay. Although an MTT assay evaluates the metabolic activity of cells, it is often used as a proxy for viability or proliferation tests. Samples were analysed at 24, 48, and 72 hours after culture within IMDM or DMEM (control).

3.2.4 BrdU incorporation assay

A BrdU assay was performed as described in section 2.6 to ascertain the level of cell proliferation. MSCs were seeded in DMEM, following which they were cultured in IMDM (or fresh DMEM as a control) for either 24, 48, or 72 hours. Images were collected for each condition and time point and analysed in ImageJ. Data collected was processed in Microsoft Excel.

The binomial test was performed to evaluate whether the number of BrdU-negative cells in IMDM was equal to the number in DMEM. This test was performed

for each time point, taking the DMEM result as the base probability for comparison. The binomial test was performed using the BINOM.DIST function in Excel to evaluate the probability of successes in the control condition compared to the probability in the test condition. Ninety five percent confidence intervals for the proportions were calculated using the Agresti-Coull method, using the online calculator provided by GraphPad[3].

3.2.5 Collagenase digestion

Following culture within a collagen gel, cells were extracted using collagenase at 2 mg ml^{-1} for 90 min. Following this period, the resulting cell suspension was centrifuged at 400 × g to pellet the cells.

3.2.6 Flow cytometry

Flow cytometric analysis was used to characterise the cells extracted from BM, investigate the effectiveness of loading cells with NPs, and for separation of cells following incubation in the model. Following collagenase digestion, cell samples harvested from culture for analysis were washed three times in 2% FBS in PBS by centrifugation at 190 × g for 10 min. Cells were then stained for 30 min in the dark with a 1:100 solution of antibody, if appropriate. Following staining, cells were centrifuged once more with the same parameters. They were then suspended in 2% FBS in PBS containing 1 mM EDTA. Samples containing adherent cells were passed through a filter before being run on the flow cytometer. Antibodies and additional procedures used for phenotyping are listed in Table 2.8 and sections 2.13.2 and 2.13.3.

---

[3] http://www.graphpad.com/quickcalcs/confInterval1/

3.3 Results

3.3.1 Cell culture optimisation

Several methods not yet in use in the Centre for Cell Engineering were optimised for use with HSPCs. The feasibility of banking cell samples for later use once extracted from BM, or once enriched *via* magnetic selection, was tested. This is important because CD34+ cells differentiate and die rapidly in culture, meaning that they have to be used experimentally as soon as possible after isolation. Being able to control the timing of isolation can relieve experimental time pressures.

3.3.1.1 Viability of cells following freeze-thawing

Freezing mononuclear cells (MNCs) after isolation and before sorting can affect percentage viability of the HSPC subpopulation. To investigate this, cell viability was determined in previous frozen cell samples that were (i) isolated and enriched for CD34+ prior to freezing; (ii) isolated, frozen, then enriched for CD34+ post-freezing; and (iii) isolated, frozen, CD34- fraction from enrichment post-freezing (Figure 3.1). The average viability was above 50% for all cell groups. The CD34+ (F/T MNCs) population, enriched post-freezing, had the highest viability with approximately 78% retrieval. This was significantly higher than either the enriched pre-freezing F/T CD34+ or the CD34- (F/T MNCs) populations. Viability was similar in the latter two groups, at approximately 55%.
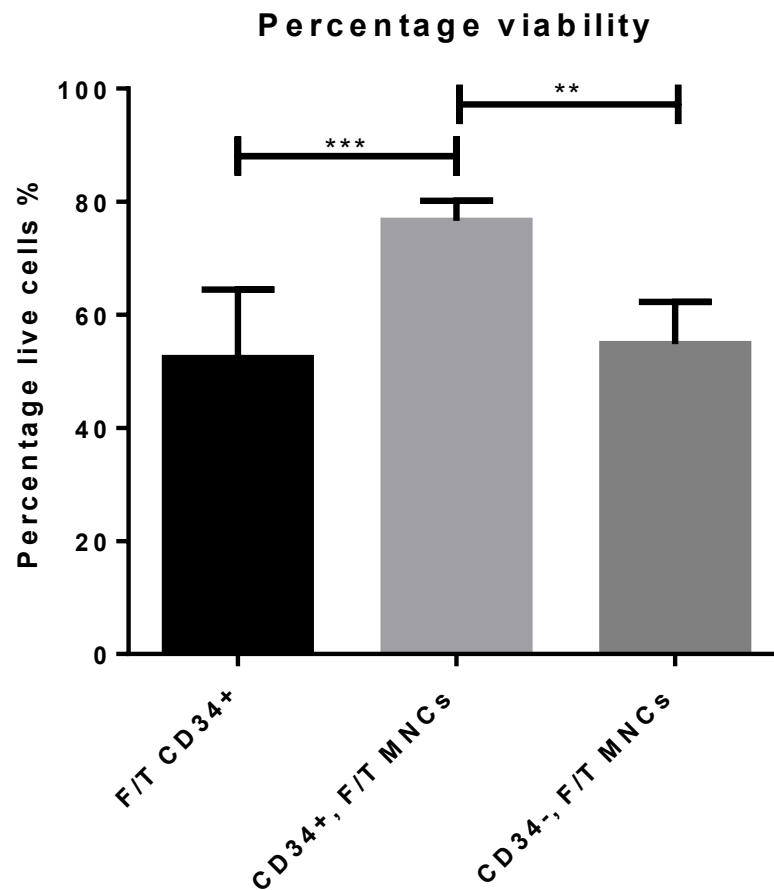
Figure 3.1 Percentage viability of cells following freeze-thawing.
F/T CD34+, freeze-thawed CD34+; CD34+, F/T MNCs, CD34+ population from freeze-thawed
MNCs; CD34-, F/T MNCs, CD34- population from freeze-thawed MNCs. Statistical significance
was tested using one-way ANOVA. **p < 0.01; ***p < 0.001.

Interestingly, the CD34+ enriched pre-freezing sample had a much lower retrieval rate in terms of cell number when compared to the MNC populations, as indicated in Figure 3.2. Collating the cell viability and cell number retrieval following freeze-thawing, it is evident that optimum recovery and viability arose from enriching for CD34 post-freezing from MNCs, rather than from a frozen CD34+ enriched population.
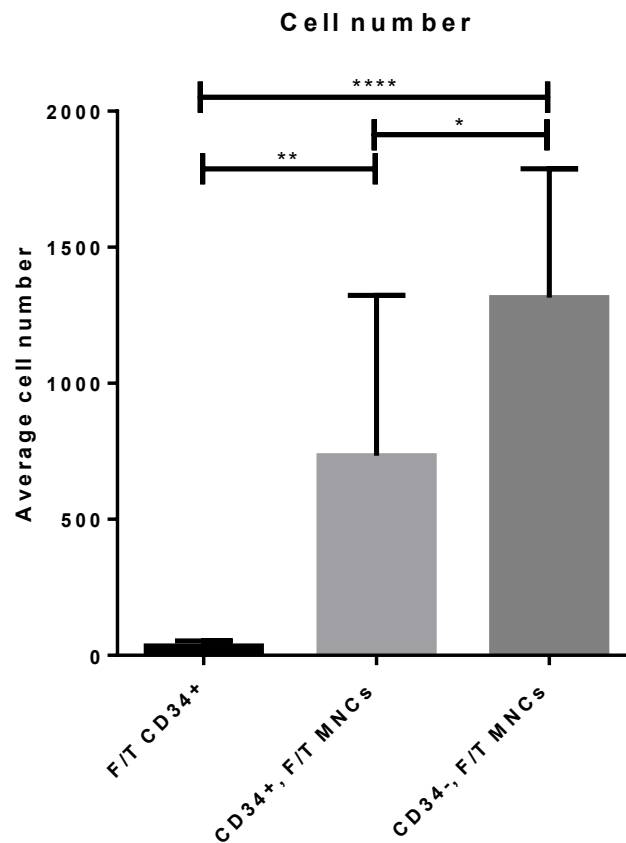
Cell number

Figure 3.2 Average cell number per microscopic field.
F/T CD34+, freeze-thawed CD34+; CD34+, F/T MNCs, CD34+ population from freeze-thawed MNCs; CD34-, F/T MNCs, CD34- population from freeze-thawed MNCs. Statistical significance was tested using one-way ANOVA. *p < 0.05; **p < 0.01; ****p < 0.0001.

3.3.2 Co-culture model development and optimisation

A co-culture system requires the culture conditions to be suitable for all cell types. HSPCs and MSCs are typically cultured very differently, in part due to the fact that the former are non-adherent, and are more susceptible to differentiation and death in culture. The standard method of MSC culture already utilised in the Centre for Cell Engineering is described in section 2.1. For culture of HSPCs, advice was kindly given by Dr Jo Mountford and her lab. The following describes the various methods used to optimise the conditions of the co-culture system to accommodate both cell types.

3.3.2.1 Phenotypic characterisation of the CD34+ population extracted from the bone marrow

Phenotypic analysis was performed to identify the proportions of haematopoietic progenitor subsets present within the HSPC (CD34+) population following isolation

from the BM according to the procedure described in Section 2.1.2. One representative patient sample was used. Following analysis on a flow cytometer, further gating of populations was used to identify progenitor subsets within the viable, single cell population (Figure 2.2). Using antibody panel 1 (Table 2.8), 84% of the cells were identified as CD34+, reflecting the success of the magnetic enrichment technique. The proportion of HSCs within this sample was 7.96%, with the proportion of MPPs at 7.88%, giving a total of approximately 16% (HSCs and MPPs). Presence of lineage progenitors was comparatively low, with CMPs, CLPs, GMPs, and MLPs all at or below 1%. The one exception was for MEPs, which were present at 18.5%.
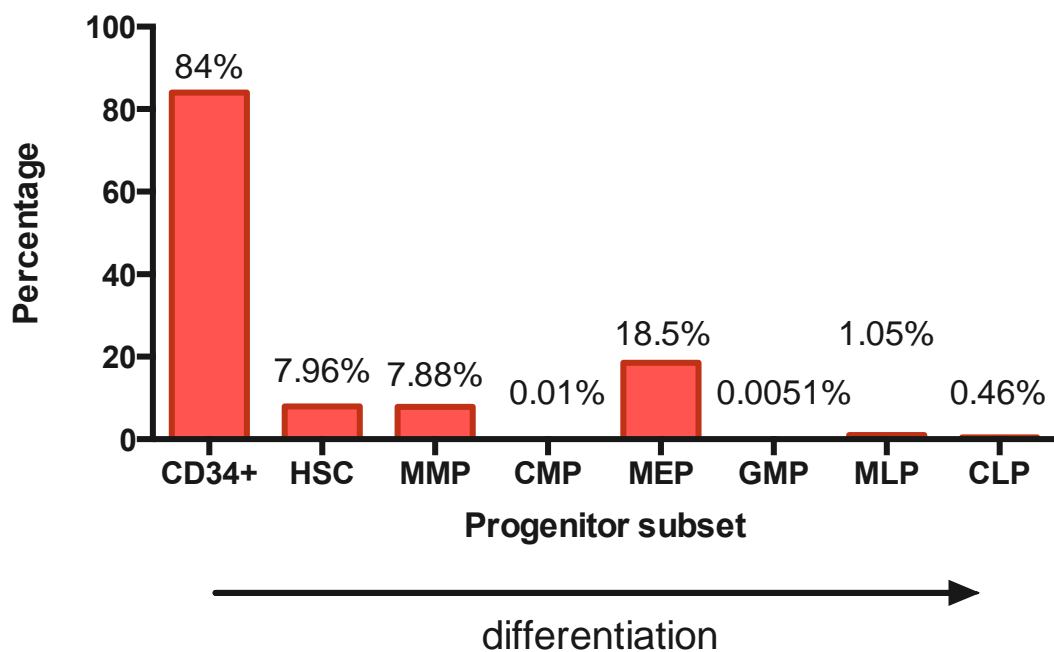
Figure 3.3 Analysis of percentages of progenitor subsets in freshly isolated CD34+ cells. HSC, haematopoietic stem cell; MPP, multipotent progenitor; CMP, common myeloid progenitor; MEP, megakaryocyte-erythroid progenitor; GMP, granulocyte-monocyte progenitor; MLP, multi-lymphoid progenitor; CLP, common lymphoid progenitor.

A separate panel of antibodies was used to identify cells of various haematopoietic lineages within the sample (Figure 2.3, Figure 2.4). Here, the percentage of CD34+ cells (identified using a different antibody), was 96.5%, again reflecting the success of enrichment. The markers CD7, CD14, and CD41a were all expressed by between 2 and 5.2% of cells. CD36, CD10, and CD13 were all expressed on approximately 20-30% of cells.
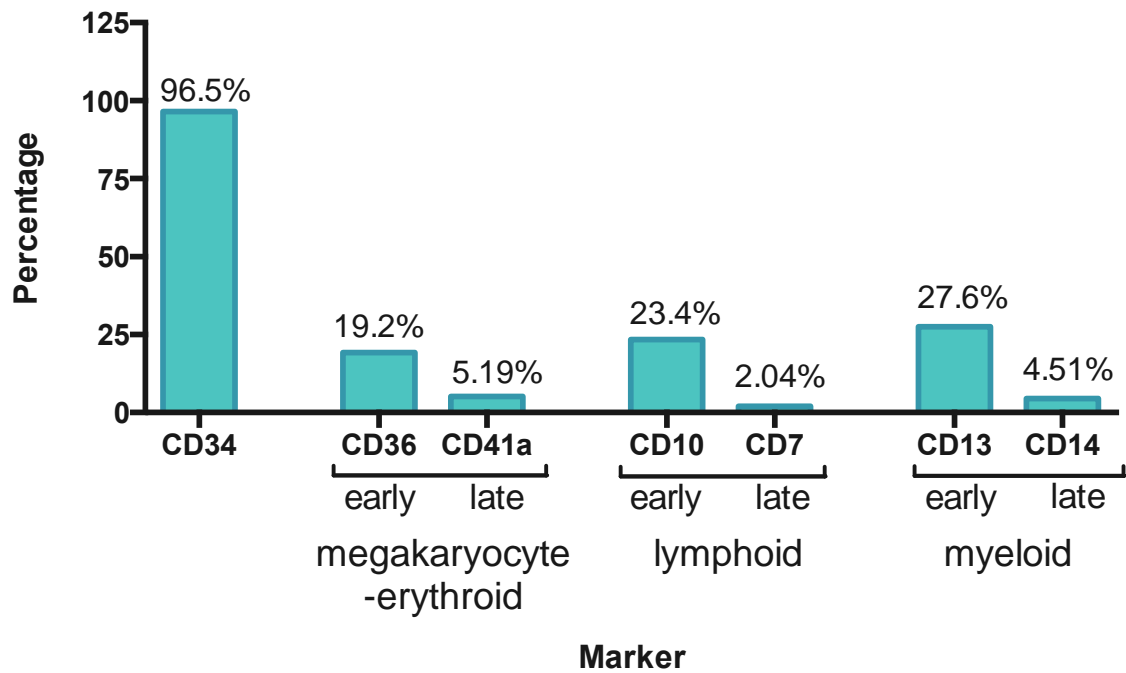
Figure 3.4 Percentages of viable cells expressing haematopoietic lineage markers.

3.3.2.2 Co-culture media survey

To ascertain the appropriate medium for MSC/HSPC co-culture, a literature survey was conducted (Table 3.1). The complexity of this task is highlighted by the fact that, of a survey of 19 co-culture studies, 19 different formulations were used. The most common basal medium was IMDM, followed by RPMI. These were variously supplemented with cytokine cocktails, antibiotics, and human or bovine serum.

Basal medium for co-culture		Author, Date	Title	Supplement(s)	Serum	Comments
Commercial	CellGro SCGM medium (CellGenix, Freiburg, Germany)	Jing et al. 2010	Haematopoietic stem cells in co-culture with mesenchymal stromal cells - modeling the niche compartments *in vitro*	10 % FBS, 15 ng ml^{-1} Flt3-L, 150 ng ml^{-1} SCF, 50 ng ml^{-1} IL-3.	y	In some cultures, HSCs were grown without MSCs but with cytokines.
	HPC Expansion Medium DXF (PromoCell proprietary medium)	Rödling et al. 2017	3D models of the haematopoietic stem cell niche under steady-state and active conditions	Cytokine Mix E (containing TPO, SCF, FLT3L, and IL-3 at unspecified concentrations) and 1% (v/v) penicillin/streptomycin.	n	Perfused system.
	QBSF-60 serum-free medium	Andrade et al. 2010	Systematic delineation of optimal cytokine concentrations to expand hematopoietic stem/progenitor cells in co-culture with mesenchymal stem cells	SCF, Flt-3L, bFGF, TPO, and LIF (leukaemia inhibitory factor protein).	n	Cytokines were tested in different combinations and/or concentrations. For the validation studies (14 day cultures), two controls were performed: (i) without exogenously added cytokines, with a stromal layer (No Cyt), and (ii) without stromal layer, using the most successful cytokine cocktail optimized by the experimental design approach (No Stroma).
	StemSpan	Zhang et al. 2006	Co-culture of Umbilical Cord Blood CD34+ Cells with Human Mesenchymal Stem Cells	40 mg ml^{-1} LDL, 100 ng ml^{-1} SCF, 100 ng ml^{-1} FL, 50 ng ml^{-1} TPO, and 20 ng ml^{-1} IL-3.	n	
	StemSpan (StemCell Technologies proprietary medium)	Alcayaga-Miranda et al. 2015	Characterization of menstrual stem cells: angiogenic effect, migration and hematopoietic stem cell support in comparison with bone marrow mesenchymal stem cells	10 ng ml^{-1} FGF-1, 10 ng ml^{-1} SCF, 20 ng ml^{-1} TPO, 100 ng ml^{-1} IGFBP2, and 100 μg ml^{-1} penicillin/streptomycin.	n	CD34+ HSPCs were co-cultured with, without, and without direct contact (using a Transwell) with menstrual MSCs.

	StemSpan-ACF (StemCell Technologies proprietary medium)	Sieber et al. 2017	Bone marrow-on-a-chip: Long-term culture of human haematopoietic stem cells in a 3D microfluidic environment	25 ng ml^{-1} FLT3-L, 10 ng ml^{-1} TPO, 1% penicillin/streptomycin.	n	Perfused system.
DMEM		de Barros et al. 2010	Osteoblasts and Bone Marrow Mesenchymal Stromal Cells Control Haematopoietic Stem Cell Migration and Proliferation in a 3D *In Vitro* Model	10% FBS and antibiotics	y	
Fischer's medium		Teixido et al. 1992	Role of B1 and B2 Integrins in the Adhesion of Human CD34hI Stem Cells to Bone Marrow Stroma	25% FBS, 0.00005 M hydrocortisone.	y	
IMDM		Kedong et al. 2010	Simultaneous expansion and harvest of hematopoietic stem cells and mesenchymal stem cells derived from umbilical cord blood	SCF 15 ng ml^{-1}, Flt3L 5 ng ml^{-1}, thrombopoietin (TPO) 6 ng ml^{-1}, IL-3 15 ng ml^{-1}, GM-CSF 5 ng ml^{-1}, G-CSF 1 ng ml^{-1}.	y/n	Isolated MSCs cultured in Dulbecco's Modified Eagle's Medium (DMEM, Gibco) with 10 % FBS. Cells were also cultured in induction media to produce chondrocytes, adipocytes, and osteoblasts.
		Wagner et al. 2008	Adhesion of human hematopoietic progenitor cells to mesenchymal stromal cells involves CD44.	20 % FBS, penicillin 1,000 U/ml, and streptomycin 100 U/ml.	y	
		Li et al. 2007	Human mesenchymal stem cells improve *ex vivo* expansion of adult human CD34+ peripheral blood progenitor cells and decrease their allostimulatory capacity	10% FBS and 100 U/mL penicillin, 100 mg ml^{-1} streptomycin, in the presence of SFT or 6-SFT. 10 ng ml^{-1} TPO, 50 ng ml^{-1} FL, 50 ng ml^{-1} SCF, and 10 ng ml^{-1} IL-6.	y	Cytokine cocktails were used in these studies as a combination of 3 factors (SCF, FL, and TPO), named SFT, or 4 factors (IL-6, and SCF), named 6-SFT combination.

		Cheng et al. 2000	Human Mesenchymal Stem Cells Support Megakaryocyte and Pro-Platelet Formation From CD34+ Hematopoietic Progenitor Cells	BIT (10 mg ml^{-1} BSA, 10 µg ml^{-1} human insulin, and 200 µg ml^{-1} human transferrin, final concentration), plus 100 µmol L^{-1} 2-mercaptoethanol and 40 µg ml^{-1} low-density lipoprotein.	n	Cells were cultured for up to 21 days. If CD34+ cells were plated in the absence of hMSCs, few cells (less than 3% of input cells, either adherent or in suspension) survived after 7 days under the previous culture conditions. Most hMSCs were aggregated and were removed by a 30 µm nylon filter; FACS analyses also indicated that most hMSCs were eliminated
		Kedong Song et al. 2011	Co-culture of hematopoietic stem cells and mesenchymal stem cells derived from umbilical cord blood using human autoserum	20% HAS-(Human Autologous Serum) or FBS.	y	HAS compared with FBS in this paper using different concentrations. HAS was isolated from peripheral blood samples using Ficoll-Paque gradients. After growth in test conditions, MSCs were grown in IMDM with 10 % FBS.
		Sharma et al. 2012	Mimicking the functional hematopoietic stem cell niche *in vitro*: recapitulation of marrow physiology by hydrogel-based three-dimensional cultures of mesenchymal stromal cells.	10 % FBS, SCF 50 ng ml^{-1}; IL-6, 50 ng ml^{-1}, and IL-3, 20 ng ml^{-1}.	y	
		Wuchter et al. 2016	Microcavity arrays as an *in vitro* model system of the bone marrow niche for hematopoietic stem cells	12.5% FCS, 12.5% horse serum. 2 mM L-glutamine, 100 U/ml penicillin/streptomycin, 0.05% hydrocortisone 100.	y	Perfused system: HSPCs maintained CD34+ expression.
Mixture	1:1 mix of IMDM and DMEM/F12	Salati et al. 2013	Co-Culture of Hematopoietic Stem/Progenitor Cells with Human Osteblasts Favours Mono/Macrophage Differentiation at the Expense of the Erythroid Lineage	20% FBS, SCF 5 ng ml^{-1}, Flt3 5 ng ml^{-1}, TPO 2 ng ml^{-1}, IL-3 1 ng ml^{-1} and IL-6 1 ng ml^{-1}, streptomycin 100 mg ml^{-1}, penicillin 100 mg ml^{-1}, and L-glutamine 2 mM.	n	In order to assess erythroid and megakaryocytic differentiation, cells were cultured in serum free medium consisting of a 1:1 mix of IMDM and DMEM/F12 supplemented with 20% BIT, growth factors and antibiotics.

Mixture	50:50 mix of EBM-2 and DMEM	Huang et al. 2016	Co-cultured hBMSCs and HUVECs on human bio-derived bone scaffolds provide support for the long-term ex vivo culture of HSC/HPCs	Endothelial basal medium (EBM-2) supplemented with endothelial growth supplement SingleQuots (EGM-2). DMEM supplemented with 10% FBS, 100 U/ml penicillin, 100 µg ml^{-1} streptomycin, 0.29 mg ml^{-1} glutamine and 3 mg ml^{-1} HEPES buffer.	y	Triple co-culture of HUVECs, MSCs, and HSCs.
RPMI		Bug et al. 2002	Rho family small GTPases control migration of hematopoietic progenitor cells into multicellular spheroids of bone marrow stroma cells	10% FCS, IL-3, and GM-CSF; 10 ng ml^{-1} each.	y	Before co-cultivation, cells were washed with medium and subsequently resuspended in IMDM/10% FCS. Co-culture was performed in IMDM.
		Perdomo-Arciniegas & Vernot 2011	Co-culture of hematopoietic stem cells with mesenchymal stem cells increases VCAM-1-dependent migration of primitive hematopoietic stem cells.	SCF, Flt-3L, and TPO cytokines; all used at 50 ng ml^{-1}.	n	Two conditions were used for the experiment: 1. Co-culture with MSC plus cytokines (HMC); 2. MSC-free culture with cytokines (HC). MNCs were enriched and suspended in IMDM supplemented with 10% FBS and 1 mM sodium pyruvate.
		Wagner et al. 2007	Molecular and secretory profiles of human mesenchymal stromal cells and their abilities to maintain primitive hematopoietic progenitors.	10% FBS	y	

Table 3.1 Survey of media used in MSC/HPSC co-culture studies to identify the optimal formulation.

3.3.2.3 Testing cell metabolic activity and proliferation in different media formulations

Firstly, the capacity for the chosen medium formulation to support basic MSC functions in culture compared to standard DMEM was tested. These activities included metabolic activity and viability.

3.3.2.3.1 Metabolic activity of MSCs

An MTT assay was used to assess the metabolic activity of MSCs when cultured in standard DMEM medium compared to the HSPC-optimal IMDM medium. Differences between the groups were analysed using two-way ANOVA. There was no significant difference in metabolic activity between MSCs grown in IMDM or DMEM at any time point ($p > 0.05$). Indeed, contrary to expectations, the cells exhibited higher metabolic activity in IMDM compared to DMEM at all time points.
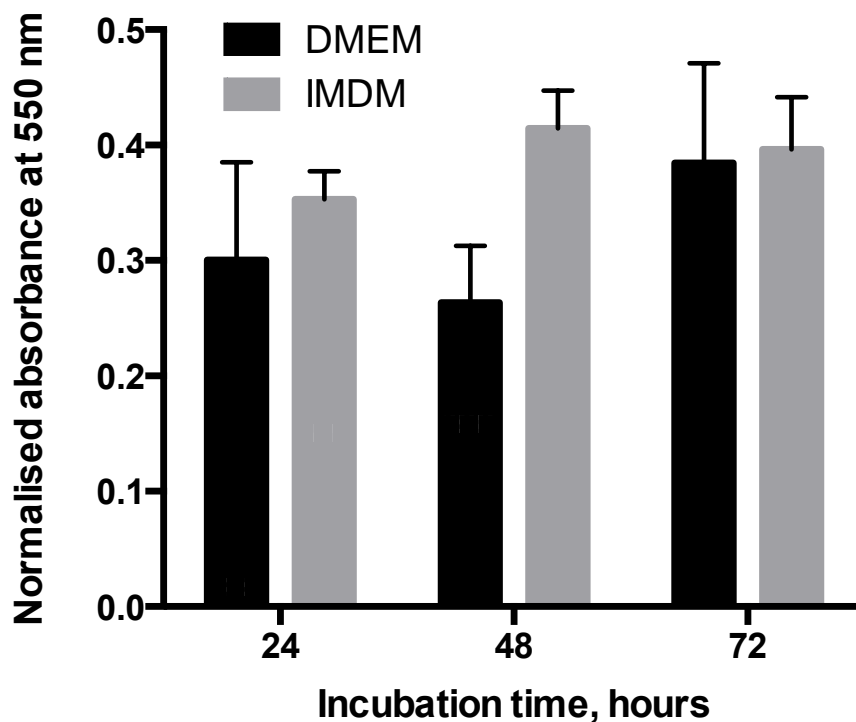
Figure 3.5 Optical density at 550 nm from MTT assay performed on MSCs grown in either DMEM or IMDM media for 24, 48, and 72 hours.
Absorbance expressed as mean ± 95% confidence interval. Two-way ANOVA was used to analyse differences between the groups.

3.3.2.3.2 Proliferation of MSCs

A BrdU assay was used to test whether the reason for the increase in metabolic activity in IMDM was due to increased MSC proliferation. This assay was performed in monolayer culture. The percentage of cells that were non-proliferative (do not exhibit BrdU signal in the nucleus) remained above 90% for all time points in both media conditions (Figure 3.6).
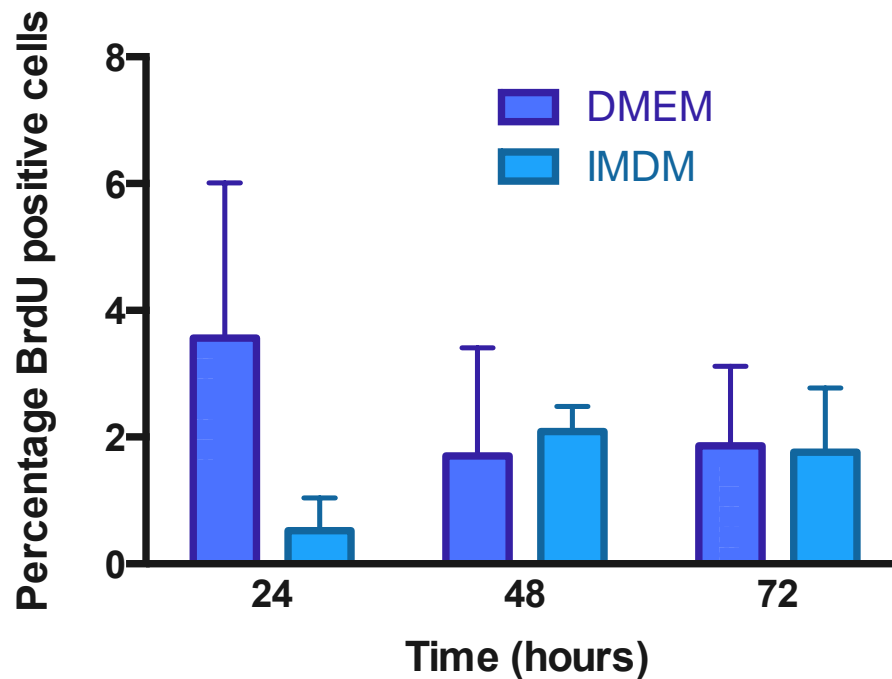
Figure 3.6 Graph of the percentages of BrdU-positive cells after culturing MSCs in DMEM or IMDM for either 24, 48, or 72 hours.
Bars show average percentage of BrdU positive nuclei ± 95% confidence interval of the proportion.

For each time point, $p > 0.05$ (Table 3.2), indicating that there was no significant difference in the number of proliferating MSCs in the two media types at any time point. The slight differences detected in metabolic activity may be due to random fluctuations in cell number, rather than differences in proliferation.

Time (hrs)	24	48	72
p-value (binomial test)	0.997866796	0.366694938	0.551528855

Table 3.2 Table showing the p-values for the binomial tests performed for each time point.
$p > 0.05$ at all time points.

3.3.3 Model Deconstruction

Following a set period of time in the model, cell retrieval from the 3D model for separate downstream analysis of different cell types was necessary. A series of experiments was performed to optimise cell extraction from the model and subsequent cell separation to isolate individual cell populations.

3.3.3.1 Collagenase optimisation

The initial stage of cell retrieval from a 3D type I collagen gel is gel digestion. On Vivek Mudera's recommendation (UCL), lyophilised collagenase D was used for gel digestion, allowing total cell retrieval. Cell populations (ie. MSCs and HSPCs) were subsequently separated *via* flow cytometry. It is essential for the cells to be isolated from the gels without compromising viability. For flow cytometry, obtaining a suspension of single cells is of particular importance to obtain discrete data for each cell, and to prevent damaging the machine during analysis.

Lyophilised collagenase type D (Roche) was reconstituted in PBS to a stock concentration of between 25 and 50 mg ml^{-1}, stored at -20 °C. This was thawed and diluted at point-of use to create working solutions. The volume of collagenase solution used was equal volume to the gel being digested. As collagenase is not inhibited by serum, an equal volume of 10 mM EDTA in PBS was used to quench the reaction after the given incubation time.

3.3.3.1.1 Testing collagenase on cell free gels

To ascertain the range of concentrations and incubation times that could be used for this protocol, digestion of cell-free collagen gels was tested. The manufacturer recommended a working concentration between 0.5-2.5 mg ml^{-1}. Initial trial concentrations of 0.5 mg ml^{-1}, 1 mg ml^{-1}, 2 mg ml^{-1}, and 2.5 mg ml^{-1} were therefore used. To each 500 µl volume of gel, an equal volume of collagenase was added. The incubation times chosen were 15 min, 30 min, and 60 min in accordance with manufacturer recommendations. The same volume of EDTA was added to quench the reaction after the allotted incubation time. The liquid in the digested wells was then removed to a new well plate to observe the extent of fragmentation. From Table 3.3 it is evident that even the highest concentration and incubation time was insufficient to digest the gel. Hence, the lowest concentration was

discarded and the incubation time was increased for subsequent viability tests in 3.3.3.1.2.

Concentration mg ml^{-1}	Time min^{-1}		
	15	30	60
0.5	Gel intact	Gel intact	Gel fragmented but mostly intact
1	Gel visible in removed media	Gel visible in removed media	Gel visible in removed media
2	Gel visible in removed media	Gel visible in removed media	Gel partially intact
2.5	Gel visible in removed media	Gel visible in removed media	Gel intact

Table 3.3 Table showing state of collagen gels after digestion with collagenase of varying concentrations and durations.
Gels that could not be easily removed from the wells are indicated by shaded cells.

3.3.3.1.2 Testing cell viability after collagenase digestion

MG63 cells were seeded as a cell suspension (i.e. not a pre-formed spheroid) into collagen gels at approximately 8×10^4 cells per gel, resulting in a dispersed cell population throughout the gel. Collagenase at concentrations of 1 mg ml^{-1}, 2 mg ml^{-1}, or 2.5 mg ml^{-1} was added to each gel and incubated for 30, 60, or 90 min. 10 mM EDTA was added at the end of the allotted incubation time to quench the reaction. Subsequently, the cells were stained with a calcein AM/ethidium homodimer solution to assess the viability of the cell population after the digestion.

Cells were observed floating in the media after 30 minutes of digestion; the number of floating cells increased with digestion time. At longer incubation times and higher concentrations, cells were observed beginning to adhere to the surface of the well plate, having been freed from the collagen matrix. Viability stained cells were imaged after a 1-hour incubation with the stain. Cells were counted and the percentage viability is indicated in Figure 3.7.
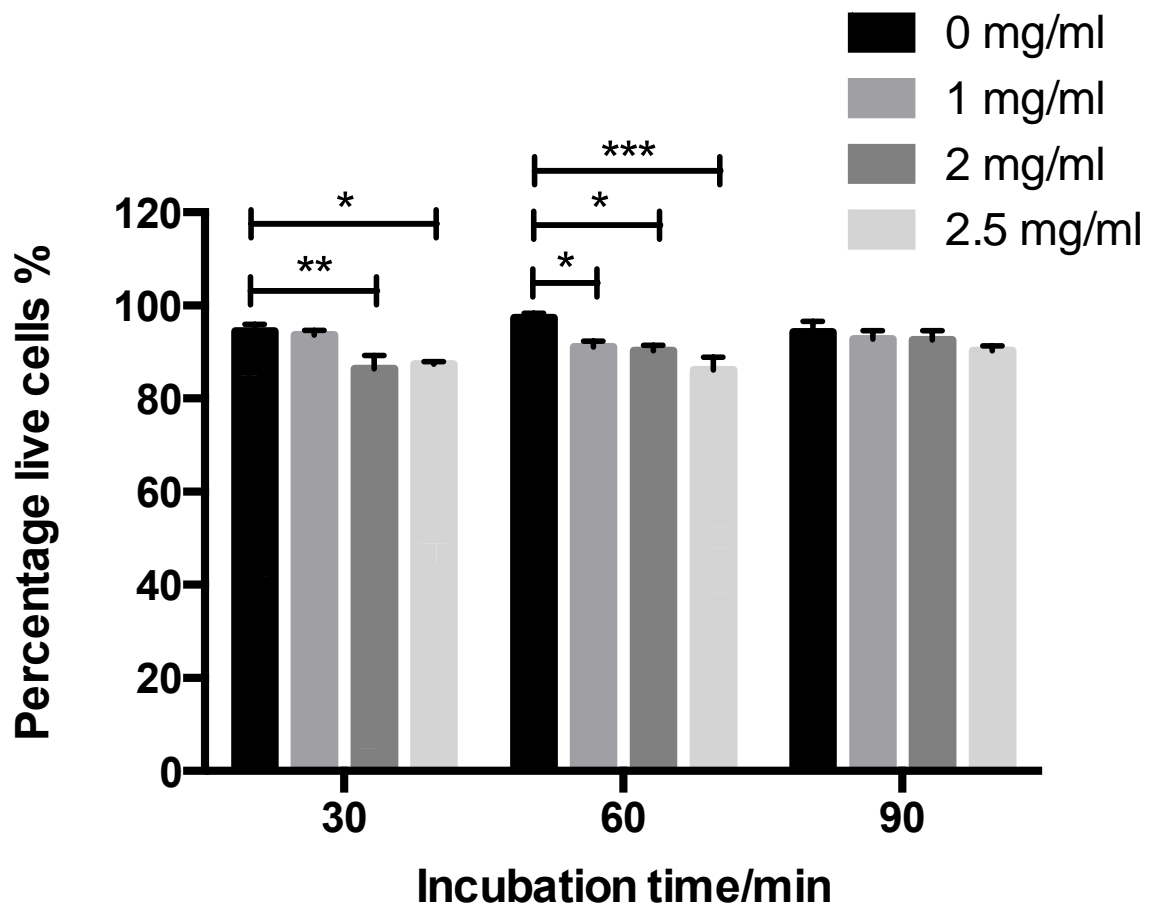
Figure 3.7 MG63 cell viability after digestion of collagen gels with collagenase at different concentrations.
A calcein/ethidium homodimer viability test was performed following digestion and samples were imaged on a fluorescence microscope. The numbers of cells exhibiting green (live) and red (dead) fluorescence were counted, and percentage viability determined for each image. Values are mean percentage viability ± 95 % confidence interval (CI). Mean percentage viability was tested between the concentrations of collagenase at each time point using two-way ANOVA. *p < 0.05; **p < 0.01; ***p < 0.001.

Two-way ANOVA was used to compare the percentage viabilities to the 0 mg ml^{-1} control at each time point. Statistically significant differences from the control were observed for 2 and 2.5 mg ml^{-1} at 30 min and 1, 2, and 2.5 mg ml^{-1} at 60 min. However, at 90 min viability was not significantly different from the control at any concentration. As the viability of cells at all time points and concentrations remained above 80%, this was considered sufficient to obtain a large enough number of cells for RNA extraction and subsequent Fluidigm analysis. A concentration of 2.5 mg ml^{-1} collagenase D and an incubation time of 90 min were therefore used for all subsequent digestions.

3.3.3.1.3 Spheroid dissociation after collagen digestion

As the MSCs were to be cultured as spheroids within the collagen gel, an effective method of dissociating the spheroids post-collagenase digestion was investigated. As cell-cell contacts within the spheroid are not easily dissociated, both enzymatic and mechanical methods were tested. Spheroids were removed from the supernatant following digestion by centrifugation, and then subjected to dissociation. Two methods of mechanical dissociation and incubation with trypsin were tested (Figure 3.8):

1. Needle: spheroids were taken up into a 21-gauge 40 mm needle and vigorously agitated up and down.

2. Pipette tip: spheroids were taken up into a 200 µl pipette tip and vigorously agitated up and down.

3. Trypsin: spheroids were enzymatically digested for either 2 or 5 min.

Following this treatment, the spheroids were seeded into a fresh tissue culture vessel. After 24 hours, they were stained with Coomassie Blue and imaged on a light microscope (Figure 3.8).

needle   pipette tip

trypsin 2 min   trypsin 5 min
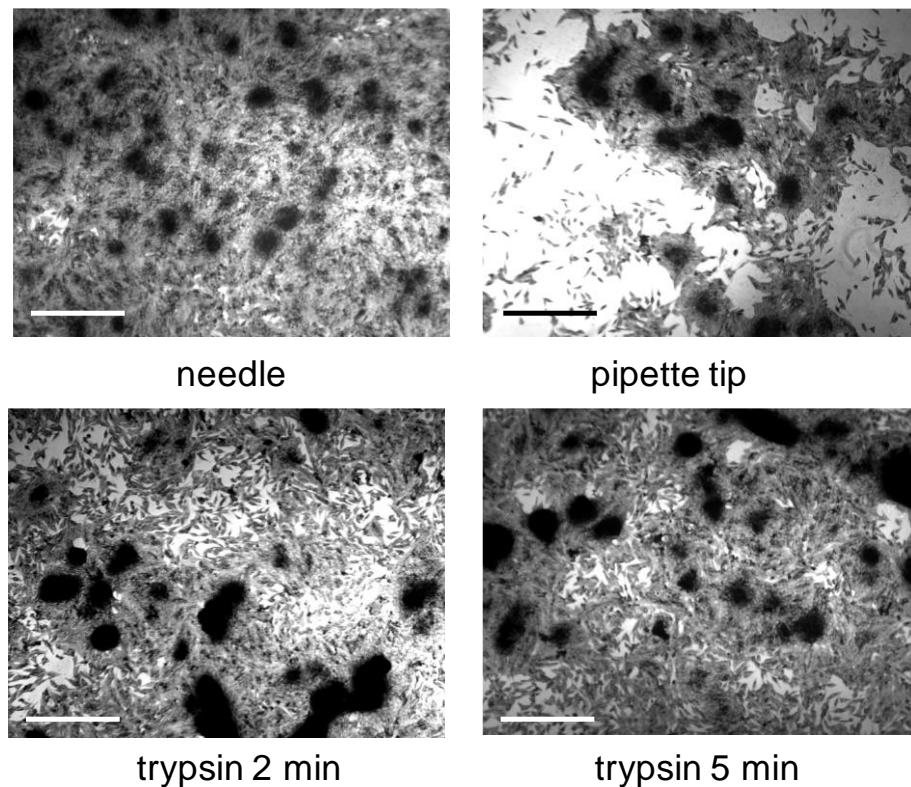
Figure 3.8 Methods for dissociation of spheroids after digestion of collagen gels.
Spheroids were subjected to mechanical or enzymatic dissociation, and the resulting cell suspension was seeded onto a fresh surface. After 24 hours, these were stained with Coomassie Blue. Scale bar = 200 μm.

Successful dissociation was indicted by small size of nanoparticle/cell clumps (dark areas in the images) and confluence of the cell monolayer. The pipette tip method was the least effective, with a disperse cell layer and multiple large cell aggregates. The 2-min trypsin digestion was slightly more effective but also produced large aggregates. No differences were observed between the 5-min trypsin incubation and the needle method: both produced a confluent cell layer, with multiple small aggregates. For the remainder of the project, a needle was used for resuspension, as it does not involve chemical treatment of the cells.

3.3.3.1.4 Investigating the effects of collagenase on a monolayer

For dissociation of the eventual triple co-culture model (Figure 5.2), ensuring that human umbilical vein endothelial cells (HUVECs) or osteoblasts (OBs) can be isolated from the model in addition to MSCs and HSPCs is important, so that they can be analysed separately. If collagenase has no effect on a monolayer beneath a gel, then once the digested gel containing spheroids and HSPCs has been removed, the co-cultured HUVEC/OB monolayer beneath can be extracted using

trypsin. Therefore, the effect of collagenase on a test cell monolayer was assessed.

C2C12 cells were seeded as monolayers onto wells of a 24 well plate at 1×10^4 cells well^{-1}. After the cells had attached to the surface, a collagen gel was overlaid. After 24 hrs of incubation to allow the pH to equilibrate, the gels were digested with 2.5 mg ml^{-1} collagenase for 0, 30, 60, or 90 min, which was quenched with EDTA at the incubation end point. The supernatant containing digested gel was removed from each well, transferred to a fresh well, and stained with a viability kit to determine whether any C2C12 cells were captured during gel digestion, whilst the remaining monolayer was also stained, to ascertain the extent of damage, and whether it remained intact.

The FITC fluorescence area (μm^2) was measured for each image and converted into a percentage of the total image area (measured as 551623.228 μm^2 for each image using ImageJ) as a proxy of monolayer integrity. The percentages were analysed using one-way ANOVA to compare the integrity of the monolayer during each collagenase incubation to that of the control (0 min). No significant differences were observed for any time point ($p > 0.05$). A qualitative analysis of the images is summarised in Table 3.4.
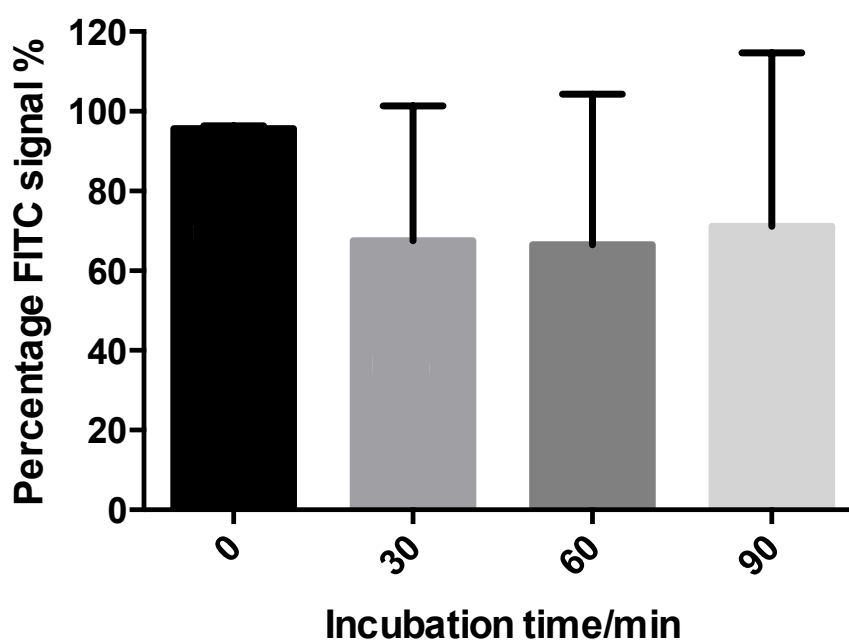
Figure 3.9 Percentage of FITC signal from images taken of monolayers below gels treated with collagenase (0 min, n = 2; 30, 60, and 90 min, n = 4).

Collagenase test using C2C12 monolayers		
Incubation time	Monolayer	Media/gel digest fraction
0 min	Monolayer largely intact, with some peeling from the surface visible. High viability.	Some cell growth from (presumably) transferred cells in suspension. High viability.
30 min	Monolayer largely intact, with some peeling from the surface visible. High viability.	Cell clumps visible, presumably from cells interacting with the collagen. Some cell growth on tissue culture surface. Low viability.
60 min	Monolayer largely intact with a few gaps visible. High viability.	Cells all in clumps, with no growth on the tissue culture surface. Very low viability.
90 min	Monolayer largely intact with a few gaps visible. High viability.	Cells all in clumps, with no growth on the tissue culture surface. Very low viability.

Table 3.4 Qualitative analysis of collagenase digestion.
Analysis used images taken of C2C12 monolayers (beneath collagen gels) following incubation with collagenase, and images of culture media/gel digest supernates containing cells and gel following digestion.

3.3.4 Separation of cell populations using FACS

Isolation of individual cell populations (e.g. MSCs, HSPCs, OBs, and ECs) for downstream analysis following culture within the model is important to elucidate the status and behaviour of the cells. Therefore, a series of experiments was conducted to develop FACS methods to achieve isolation.

3.3.4.1 Loading HSPCs with NPs

As MSCs in the model were labelled with gNPs, the inherent fluorescence can be used to identify the MSC population; similarly, loading CD34+ HSPCs isolated from BM with rNPs was investigated. HSPCs in suspension were incubated for 24 hours with rNPs, added into the cell culture medium. They were then seeded into a collagen gel as described previously, stained with calcein AM after 24 hours of culture (viability stain) and imaged on a fluorescence microscope (Figure 3.10). Co-localisation of green and red signals indicates internalisation or interaction of HSPCs with the NPs; no signal overlap was observed in the sample, and so no interaction was occurring.
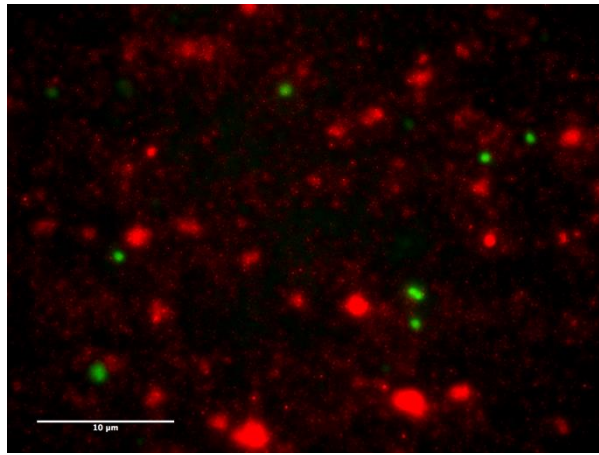
Figure 3.10 Fluorescence image of HSPC incubated with rNPs seeded onto a collagen gel and stained with a calcein viability stain.
Green, live cells; red, nanoparticles. Scale bar = 10 µm.

A separate sample was stained with DAPI and run on a BD FACS Canto II to look at effectiveness of rNP internalisation and the effect on the cells (Figure 3.11). Figure 3.11A shows the total sample loaded into the flow cytometer on a forward-scatter (FSC) versus side-scatter (SSC) plot. Panels B and D show this population on a DAPI (Comp-Pacific Blue) versus SSC plot, with gates drawn identifying the DAPI-positive (79.2%) and DAPI-negative (16.5%), respectively. DAPI-positive cells were considered dead, as internalisation of the dye indicates disruption of cell membranes. Panels C and E show the red (PE) fluorescence of these live and dead cell populations, plotted against SSC, respectively. Both populations are mostly negative for this tag, as emphasised by the histogram in Panel F, which depicts the frequency of red (PE) fluorescent particles in the live and dead populations combined (31.9% positive). The largely negative population indicates that the rNPs were not taken up into the cells.
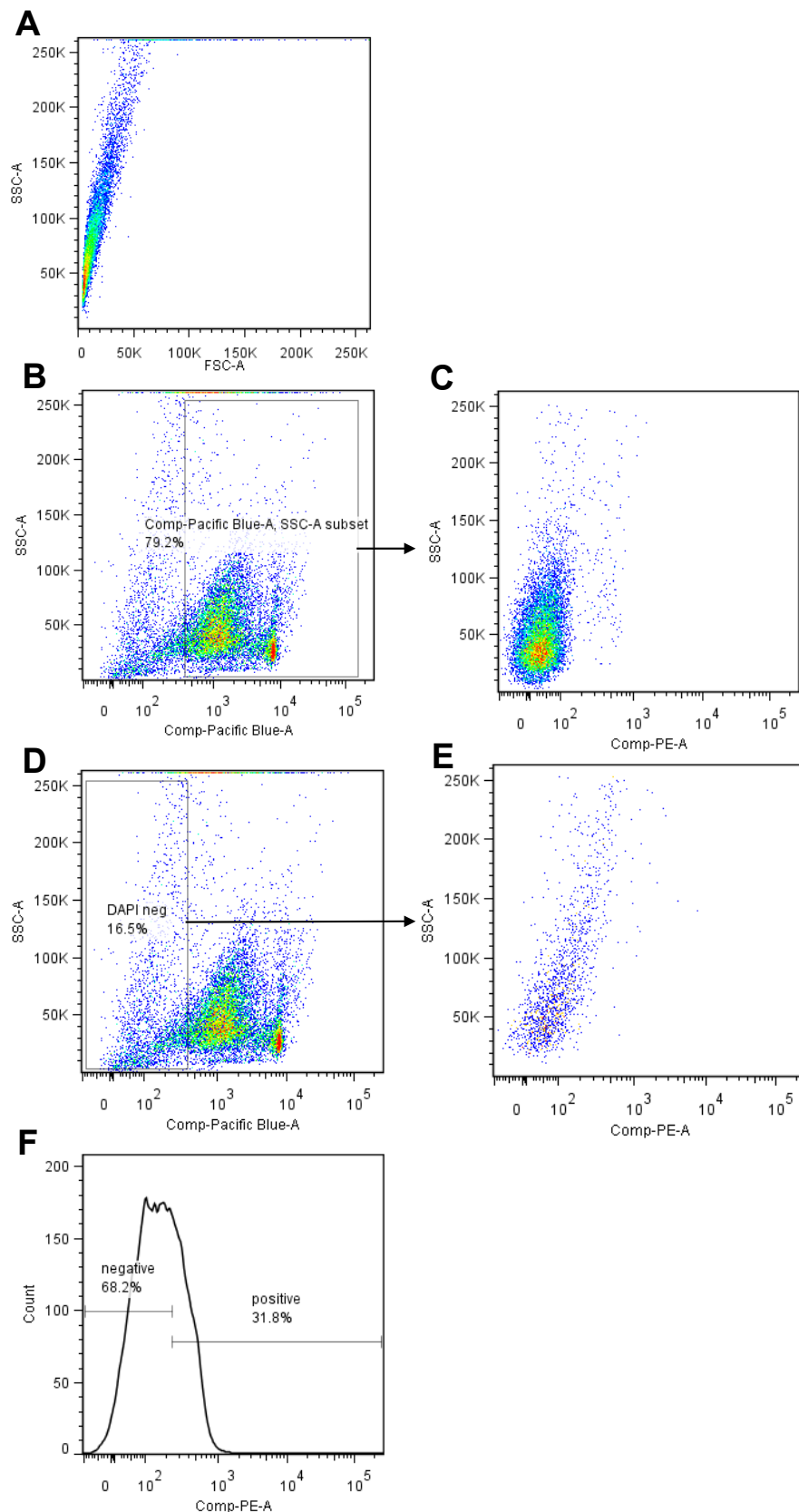
Figure 3.11 Flow cytometric analysis of CD34+ HSPCs incubated with rNPs.
A: Flow cytometric signature of NPs in isolation (FSC vs. SSC). B: Flow cytometric analysis (DAPI vs. SSC) of CD34+ HSPCs incubated with rNPs. Gate represents DAPI positive (dead) cell population. C: Red fluorescence signal in the dead cell population (PE vs. SSC). D: As part (B). Gate represents DAPI negative (live) cell population. E: Red fluorescence signal in the live cell population (PE vs. SSC). F: Histogram depicting frequency of red-positive cells in both live and dead populations combined.

3.3.4.2 Separation of MSCs loaded with gNPs from HSPCs

Following collagenase digestion, the digested gel was removed from the Transwell and all resultant cells (MSCs and HSPCs) were pelleted. They were then separated into population cell types using fluorescence activated cell sorting (FACS) on a BD FACSCalibur flow cytometer. MSCs from spheroids were separated from CD34+ cells based on the inherent green fluorescence of the nanoparticles (Figure 3.12). The cell suspension including both cell types was stained with a CD34 antibody conjugated to allophycocyanin (APC) to extract the HSPC population. Cells remaining on the Transwell membrane surface (ECs or OBs) were trypsinised and pelleted. These were processed by FACS to eliminate any FITC-positive cells (containing nanoparticles).

Figure 3.12 is a representative image of one FACS run following model deconstruction. The gating process below was followed to separate MSCs from HSCs in several samples. Figure 3.12A shows the full population analysed by the flow cytometer, with a gate drawn to isolate cells identified as 'live' by their SSC versus FSC profile (64.3% of particles). Figure 3.12B shows the gate used to identify single cells and exclude doublets using the forward-scatter height (FSC-H) versus forward-scatter area (FSC-A) profile of the cells within the gate drawn in panel A. Figure 3.12C shows the fluorescence in the FITC channel plotted against fluorescence in the APC channel of the cells within the resulting population from panel B. This plot was used to identify a FITC-positive, APC-negative population, i.e. the MSC population containing FITC-fluorescent nanoparticles (49.7%). A separate gate was used to identify cells that were CD34-APC-positive, FITC negative, i.e. HSCs (3.87%). Nanoparticle uptake influences cell granularity, indicated by SSC, meaning that the live cell population is skewed with respect to the expected location of live cells: they appear in a location normally representing dead cells. This was taken into account during the gating process.
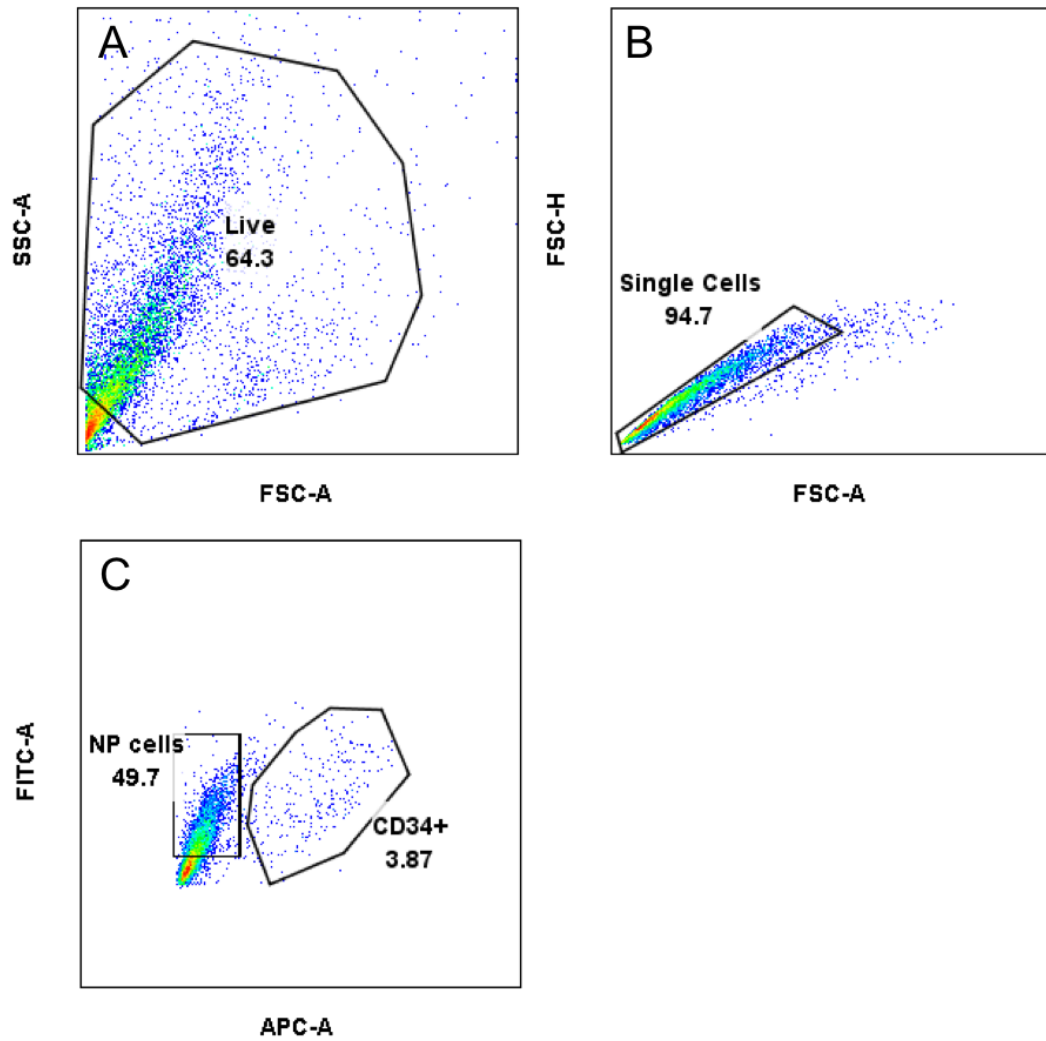
Figure 3.12 Flow cytometry data from FACS sort of MSCs from CD34+ cells after model deconstruction.
MSCs are labelled with green fluorescent NPs (FITC), cell sample is also stained with a CD34+-APC antibody (APC). A: Forward-scatter (FSC) versus side-scatter (SSC) of initial cell population, gated on live cells. B: Single cell population identified from A. C: APC fluorescence versus FITC fluorescence; gates indicate NP-FITC labelled cells and CD34+-APC cells.

3.4 Discussion

3.4.1 Viable CD34+ cell yield is higher when cells are enriched following freezing

Freezing of the whole BM MNC fraction enhances survival of CD34+ cells following thawing (Figure 3.1, Figure 3.2). Enrichment before freezing results in around 50% viability, whereas selection after freezing gives a survival rate of nearly 80%. Viability of the CD34- fraction is also lower. Therefore, to maximise viability of CD34+ cells for experiments, it is optimal to freeze the MNC fraction and perform an enrichment shortly before use in culture. This sequence also vastly increases the total cell yield.

3.4.2 Bone marrow enrichment produces a primitive population highly expressing the CD34 marker

From both Figure 3.3 and Figure 3.4 it is evident that magnetic CD34 enrichment is successful and gives a high purity: the percentages of CD34+ cells is 84% and 96.4% respectively. The difference in these values can be attributed to the differences in antibodies (discussed in more detail in Chapter 5 (page 184)). The population of HSCs is at around 8%, as is the population of MPPs, meaning that around 16% of the population is primitive and CD34+CD38-. MEPs are present at an even higher proportion, at 18.5% of the CD34+ population. In contrast, the remainder of the progenitor subsets are present within the population at very low levels. Hence, this shows that a high proportion of the enriched cells are either HSCs, MPPs, or early MEPs. The lack of progenitors further on in the hierarchy shows that very little differentiation has occurred and few lineage progenitors were isolated in the original sample.

In contrast, expression of some lineage markers was observed in more than 20% of the CD34+ population. Expression of the megakaryocyte-erythroid lineage marker CD41a (Choi et al. 2009), indicates a frequency of around 5% megakaryocytic-erythrocytic cells. However, CD36 expression, which emerges on the earliest MEPs (Ward et al. 2016), is observed on around 20% of cells. This may be evidence that the population are relatively primitive rather than mature erythroid cells (including platelets).

Similarly, there is variation in expression of the two lymphoid markers examined. CD10 is general lymphoid lineage marker (Kohn et al. 2012), which is expressed at 23.4%. CD7, which is expressed on early and mature T cells (Shukla et al. 2017), is expressed by 2.04% of the cells. Again, this may show that a greater number of the cells are primitive and few mature lymphoid cells are present.

Lastly, myeloid lineage cells represented by CD13 (Winnicka et al. 2010) are present at near 30% of the population. CD14 is expressed by cells later in the myeloid differentiation process, i.e. monocytes and macrophages (Monzen et al. 2013) and is expressed by around 5% of the cells. Again, this suggests a higher level of early myeloid cells compared to terminally differentiated cells.

3.4.3 There is no consensus regarding the optimal medium formulation for co-culture of MSCs and HSPCs

An extensive literature survey of existing MSC-HSPC co-culture systems revealed no consensus on an optimal medium to balance MSC and HSPC requirements (Table 3.1). These formulations vary in basal medium, whether they contain serum from human or bovine sources, and the growth factors and supplements used.

The medium used for culture of MSCs and HSPCs separately depends on the purpose of the experiment or culture. For example, the formulation may differ depending on whether the intention is to expand, differentiate, or maintain the cells. Medium for MSCs typically is DMEM supplemented with serum or equivalent, with antibiotic. There are several commercial media formulations available, although the contents of these are not often released. Non-adherent cells including HSPCs are typically cultured in IMDM or RPMI media without serum supplement (BIT or HSA is sometimes used). Growth factor addition is also common.

Within this project, the culture medium used in Prof. Jo Mountford's lab was used for HSPC culture, on her advice. The basal medium is IMDM, supplemented with 20% BIT, 0.02% penicillin/streptomycin, 20 ng ml^{-1} IL-3, 20 ng ml^{-1} IL-6, 20 ng ml^{-1} G-CSF, 100 ng ml^{-1} Flt3L, and 100 ng ml^{-1} SCF. There is some evidence that G-CSF and IL-3 improve the attachment of adherent cells, whereas SCF and Flt3L may depress MSC proliferation, whilst having a positive effect on HSCs (Fan et al.

2009). Before beginning experiments, the effect on MSC viability and activity when they are grown in serum free IMDM (SFM) was assessed using a viability stain and an MTT assay. Relevant results from these tests are summarised below.

3.4.4 MSCs maintain their metabolic activity and proliferation in serum free medium

MTT assay results suggest that MSCs maintain the same or higher levels of metabolic activity in SFM as compared to standard DMEM (Figure 3.5). However, this result could be obtained by a fall in cell number accompanied by an increase in metabolic activity, as previously described by Pieri et al. (2011), resulting in a higher level of proliferation. Nonetheless, results from the BrdU proliferation assay show that most cells grown in either medium formulation are non-proliferative (Figure 3.6). Observed differences are not statistically significant at any time point, and the level is maintained over the duration of the experiment. This demonstrates that media formulation does not have an effect on MSC proliferation.

Results from these two assays (MTT and BrdU) suggest that MSC activity and function are not affected extensively by IMDM. Although this medium does affect production of key niche cytokines (as discussed in section 4.4.8), it was therefore considered appropriate for the model.

3.4.5 Collagenase treatment successfully isolates cells from the gel matrix and does not significantly affect cell viability of spheroids or underlying monolayers

Collagenase D was used to digest the applied collagen ECM and isolate cells. However, as this is a new procedure, optimisation of incubation length and collagenase concentration was required (Table 3.3). The gel was not digested completely and remained partially intact at all concentrations up to 2.5 mg ml^{-1} and incubations up to 60 min. Therefore, all subsequent tests were performed with a maximum time period of 90 min.

Secondly, the concentration and time at which the gel was digested without compromising cell viability was determined. Cell viability of cells suspended within the gel remained above 80% for all concentrations tested (0-2.5 mg ml^{-1},

Figure 3.7). In addition, the integrity of a monolayer beneath the gel following collagenase treatment remained similar regardless of time period or concentration, where viability was maintained above 60% even at the longest incubation duration (Figure 3.9). It was therefore concluded that collagenase digestion did not affect the monolayer to an extent that will compromise the efficacy of cell recovery and separation.

The optimal method for spheroid dissociation following digestion was also investigated. Comparison of mechanical and enzymatic dissociation methods showed minimal differences between using a needle and a 5 min incubation with trypsin (Figure 3.8). As enzymatic treatment is undesirable, the method taken forward was re-suspension using a needle. Prior to analysis on a flow cytometer, the sample was also passed through a filter, further dissociating the cells.

3.4.6 Individual cell populations can be separated following culture within the model by digestion and subsequent FACS

Separation of distinct cell populations from the model is required for downstream analysis (e.g. for Fluidigm qPCR). Therefore, techniques for isolation involving FACS were tested and optimised. Firstly, loading HSPCs with NPs was investigated, due to concern that the abundance of the CD34 surface marker could be compromised by treatment with collagenase, and the cell population may have changed and hence lost the marker in culture. Using NPs provides a stable fluorescent signal and allows tracking of a specific cell population from its introduction to the model.

3.4.6.1 Loading HSPCs with NPs is ineffective and causes high levels of cell death

Several observations can be made from Figure 3.11 to inform the process of separation. Firstly, the NP signature in Part A shows that the NP population has a similar FSC-SSC signature to dead cells (indicating high 'granularity' and small size). This may not have an effect on live cell populations but does have an effect on the voltage required and hence the scatter plots that are produced.

Secondly, approximately 80% of the particles in the sample are DAPI-positive (dead), suggesting that the NPs influence HSPC viability. Dead cells are almost

without exception negative for PE. This suggests that the dead cells have not internalised the NPs, but they have still had an effect on viability externally. Looking at the live cell population, which is 16.5% of the total, these cells are also mostly negative for PE, also indicating that these cells have not internalised the NPs. However, part of the population shows increased granularity, accompanied by a slight increase in PE fluorescence. This subset of cells may have internalised NPs but they are not a large enough population to justify using this technique. Looking at the total number of particles in the sample that are PE-positive gives a percentage of 31.8%, however, this segment probably represents excess NPs that were not included in the live or dead populations.

Analysis of NP uptake by HSPCs shows that the cells have decreased viability and do not take up the particles (Figure 3.10). This is sufficient data to eliminate this method as a procedure for HSPC labelling.

3.4.6.2 Cell populations can be separated from the model using FACS following collagenase digestion

Following the above results (labelling CD34+ cells with rNPs), the CD34+ HSPCs were labelled instead with a fluorescent CD34 antibody for separation. The resulting cell suspension was processed using a FACS machine to produce a CD34+ population and a FITC-positive population (Figure 3.12). Any double positive cells were discarded. Finally, trypsin was used to extract the monolayer cells (HUVECs or OBs) from the model and remove them from the Transwell surface. Purity was ensured by eliminating any FITC-positive cells (MSCs) and small cells (haematopoietic cells).

3.5 Conclusion

In this chapter, several key aspects of the existing model have been optimised, both in terms of set-up and analysis. SFM was determined to be appropriate for A protocol for extraction of separate cell populations from the model for downstream analysis was also optimised.

CHAPTER 4

Chapter 4 The development of an HSC-permissive bone marrow niche model

4.1 Introduction

Chapter 3 described the optimisation of culture methods for the current 3D MSC spheroid bone marrow (BM) niche model with a view to including HSCs. This chapter gives an overview of the characterisation of this MSC spheroid model, firstly in structural and then in biological terms.

As described in Chapter 1, MSCs are increasingly important in tissue engineering and regenerative medicine. Their capacity to differentiate into several cell types, including osteocytes, chondrocytes, and adipocytes (Pittenger et al. 1999), promotes their use for orthopaedics applications in particular. Within the BM, MSCs also act as crucial stromal support to HSCs, where both cell types co-reside in the niche microenvironment. There is a growing understanding of the niche interactions, with several signalling axes being identified as fundamental to MSC/HSC communication and co-support. Such signalling molecules, including soluble growth factors and cytokines, are released from nestin[+] MSCs and are central to HSC homing, maintenance and retention in the BM. The inclusion of nestin[+] MSCs are therefore key in the development of an *in vitro* model aimed at supporting HSCs.

MSCs are typically isolated from BM and are traditionally expanded in culture on tissue culture treated polystyrene in a 2D monolayer. However, major limitations in utilising MSCs *ex vivo* are that they lose their differentiation potential or undergo replicative senescence after a certain number of population doublings (Bonab et al. 2006; Banfi et al. 2000). Therefore, fundamental stem cell properties such as quiescence and multipotency are gradually lost in culture, limiting their usefulness (Lin et al. 2014). There is a growing need to develop MSC culture systems to circumvent these issues.

Multicellular spheroids are one such 3D culture system which has been used to generate embryonic bodies and artificial tumours for cancer studies for decades (Carlsson et al. 1983; Mueller-Klieser 1987; Hirschhaeuser et al. 2010). Spheroids are aggregates of cells, that can self-organise and behave more akin to cells *in*

vivo, replicating tissue organisation and developing concentration gradients of nutrients and cytokines. For example, as spheroids closely mimic tumour architecture, mirroring pathophysiologically relevant cytokine and nutrient gradients, generating 3D ECM features, and promoting secondary central necrosis (Hirschhaeuser et al. 2010), they represent a more reliable test platform for anti-tumour drugs.

Spheroids can be formed *via* several techniques, including spinner flasks (Mueller-Klieser 1987), hanging drops (Banerjee & Bhonde 2006), and culture in low-adherence vessels (Dontu et al. 2003), However, these methods are often costly and time consuming. Magnetic cell levitation (Souza et al. 2010) is a recently developed technique, which offers an alternative method for spheroid generation. During magnetic levitation cells are pre-loaded with magnetic nanoparticles and encouraged to form multicellular spheroids within several hours *via* an external magnetic field. The resultant spheroids are easily manipulated by virtue of their magnetic qualities, and this method also confers benefits in cell tracking and imaging.

The ECM is an important part of the MSC niche (Gattazzo et al. 2014). This network of proteins is comprised of collagen type I, III, and IV, fibronectin, laminin, thrombospondin, haemonectin, and proteoglycans (Gordon 1988; Nilsson et al. 1998). In particular, collagen type I localises to the endosteal surface and endosteal marrow, the proposed stem cell niche site, and is the most abundant type of collagen in the marrow (Nilsson et al. 1998). These ECM molecules present topographical and biological signals to the cells, and allow for enhanced cell adhesion (Chen et al. 2007). The incorporation of these proteins into a 3D culture system may further encourage maintenance of MSC phenotype. In addition, the 3D fibrous network better mimics small molecule diffusion through the bone marrow, an important factor to consider when assessing drug delivery mechanisms.

4.1.1 Objectives

In this chapter, the spheroid culture system in which MSCs are labelled with magnetic nanoparticles, multicellular spheroids are generated, and subsequently implanted into a type I collagen gel with a similar stiffness (modulus of 36 Pa,

Lewis et al. 2016) to the *in vivo* bone marrow microenvironment (modulus of 100 Pa, Metzger et al. 2014; Sobotková et al. 1988) is characterised in terms of physical features and cell phenotype. Aspects explored in this chapter are as follows.

1. Spheroid formation in terms of nanoparticle uptake, morphology, and central necrosis will be investigated using electron microscopy and viability studies.

2. The capacity of MSCs in the model to differentiate into multiple stromal lineages will be evaluated using directed differentiation and histology.

3. Expression of key niche cytokines at the gene and protein levels in monolayer and spheroid culture will be examined using immunohistochemistry and RT-qPCR.

4. The expression of genes involved in cell-cell signalling pathways, niche interactions, stem cell phenotype, and MSC differentiation into stromal lineages will be compared between the two models using RT-qPCR.

5. The effect of spheroid culture on MSC proliferation will be evaluated using a BrdU assay and analysis of cell cycle gene expression.

4.2 Materials and methods

4.2.1 Cell culture

In this chapter, MSCs were cultured in the format described in Section 2.2, i.e. a magnetically levitated spheroid implanted into a collagen gel, unless otherwise stated. MSCs cultured in monolayers were used for the histology assay and as controls for gene expression analysis.

4.2.2 Electron microscopy

Electron microscopy was used to examine the ultrastructure and formation of the spheroids. Samples were prepared for visualisation *via* scanning electron microscopy (SEM) and transmission electron microscopy (TEM) as previously described (section 2.9).

4.2.3 ELISA assays

Enzyme-linked immunosorbent assays (ELISAs) were performed to measure the amounts of particular cytokines secreted by the MSC population. A Human CXCL12 Quantikine ELISA kit (R & D Systems, Minneapolis, USA) was performed according to the manufacturer's instructions, as described previously (section 2.8).

Standards were assayed from 2 technical replicates and experimental samples were assayed from 3 biological replicates. A standard curve was created from the standard absorbance measurements and used to interpolate the concentrations of the experimental samples. Measurements were normalised to the base reading obtained from the respective cell-free sample (DC1 & IC1) to control for the background concentrations in the different media formulations. This is of particular importance as one of the media formulations is serum free.

Duplicate readings from the standard samples were similar, indicating accuracy. Linear regression was used to fit the standard curve to the average standard readings. The equation of the line was $y = 0.4666 + 0.000155x$, indicating high correlation between CXCL12 concentration and absorbance reading, as expected. For some of the biological replicates, no interpolated value was obtained. This is because the absorbance readings were outside the range of the standard curve,

i.e. the readings were below that of the 0 standard. This has decreased the sample size for some of the conditions. n = 3 for all conditions, except for DMEM monolayer day 2 (n = 1), DMEM spheroid day 2 (n = 1), DMEM spheroid day 9 (n = 2), and IMDM spheroid day 2 (n = 2).

4.2.4 Viability staining

Spheroids were stained to assess central necrosis and general survival using calcein/ethidium homodimer staining, as described in section 2.3. Central necrosis was evaluated by taking a cross-section through the spheroid and assessing the intensity of red and green signal indicating dead and live cells, respectively. Cell numbers were also estimated using these signals.

4.2.5 Histology

Histological analysis was used to observe the deposition of terminally differentiated cell products, and hence assess the differentiation potential of MSCs. MSCs were cultured as spheroids, both implanted into collagen gel and maintained in media only. After 7 days, the spheroids in gel were treated with collagenase as described previously (90 min, 2 mg ml^{-1}, equal volume to the gel). All spheroids were then dissociated using resuspension with a needle and re-seeded onto sterilised glass coverslips. The following day, the media was changed to either adipogenic, osteogenic, or chondrogenic induction media (DMEM with 10% FBS and 2% antibiotics, with supplements as listed in Table 4.1), and the cells were grown for 30 days, with media changed twice a week. Cells were fixed and stained with Oil Red O, Alizarin Red, or Safranin O stains respectively. MSCs grown in monolayers for 30 days were used as a control.

Induction media	Supplements
Osteogenic	350 µM ascorbate-2-phosphate, 0.1 µM dexamethasone
Adipogenic	1 µM dexamethasone, 1.7 nM insulin, 200 µM indomethacin, 500 µM isobutylmethylxanthine
Chondrogenic	10 ng ml^{-1} TGFβ1, 100 nM dexamethasone, 6.25 µg ml^{-1} insulin, 50nM ascorbate-2-phosphate, 100 mg L^{-1} sodium pyruvate

Table 4.1 Supplements used for induction media formulations.

4.2.5.1 Oil Red O staining

Oil Red O staining was used to observe the deposition of neutral triglycerides and lipids, indicating adipogenesis. Samples were rinsed in 60% isopropanol and stained in Oil Red O for 15 min. They were then rinsed in isopropanol until colourless, followed by a wash with water. The nuclei were counterstained with Weigert's haematoxylin for 10 min, washed again with water, and mounted onto slides with an aqueous mountant.

4.2.5.2 Alizarin Red staining

Alizarin Red identifies calcium-containing osteocytes in culture. The samples were washed in graded alcohols to water, then stained with Alizarin Red solution for 5 min. The samples were blotted with filter paper, then rinsed in acetone for 30 sec. They were then rinsed in a 1:1 solution of acetone-xylene for 15 sec, followed by a wash with xylene only. They were then mounted onto slides with aqueous mountant.

4.2.5.3 Safranin O staining

Safranin O is an indicator of chondrogenesis. Samples were taken to water through 3 changes of graded alcohols. They were then stained with Weigert's haematoxylin for 10 min, followed by a wash in water for 10 min. they were then stained with 0.001% Fast Green for 5 min, rinsed in 1% acetic acid for 10 sec, and stained with 0.1% Safranin O solution for 7 min. This was followed by a wash with water. The samples were dipped in 1% acetic acid, then dehydrated and mounted onto slides with aqueous mountant.

4.2.6 Quantification of immunohistochemistry

Immunohistochemistry was carried out as described in section 2.5. Images were processed in ImageJ and signals were quantified as follows:

- Cell number was obtained by using a threshold to isolate nuclei in the DAPI channel. Particle analysis, of particles with a size greater than 3 μm, was used to count the number of nuclei.

- Signal in the FITC channel (representing STRO-1, nestin, or CXCL12) was quantified by setting a threshold to isolate areas of green signal. The total area of green signal (μm^2) was obtained using the 'Measure' function in ImageJ.

- The amount of FITC signal per cell nucleus was calculated using the formula: signal per cell = FITC area / total cell number.

- These values were obtained for several cell images for each culture condition at two time points (day 3 and day 7). Significant differences between culture systems at different time points were evaluated using multiple heteroscedastic t-tests.

4.2.7 Gene expression analysis

To examine changes induced in cell behaviour by the spheroid culture system, expression of several genes including those related to cell cycle regulation, MSC differentiation, and signalling pathways was analysed. MSCs were cultured in spheroids or monolayers for 7 days, at which point the cells were harvested and RNA was extracted according to the procedure described in section 2.10. Reverse transcription was performed according to the protocol detailed in section 2.11. Fluidigm analysis was performed according to section 2.12.

Fold change in spheroids compared to monolayers was calculated using the $2^{-\Delta\Delta CT}$ method (Schmittgen & Livak 2008). Briefly, for each technical replicate the values of the housekeeping genes were averaged. These were then subtracted from the value of each test gene. Technical replicates were averaged. The biological replicates for the results obtained from monolayers were averaged and subtracted from each biological replicate for spheroids. These values were converted into fold change by raising 2 to the power of the negative $\Delta\Delta CT$.

The non-parametric Kruskal-Wallis test, followed by Dunn's multiple comparisons test, were performed on the $\Delta\Delta CT$ values to evaluate differences between spheroids and monolayers (n = 3 per gene). $p < 0.05$ was considered statistically significant. Statistical analysis was performed using Microsoft Excel (Microsoft,

Redmond, WA, USA) and GraphPad Prism (GraphPad Software Inc., La Jolla, CA, USA).

4.3 Results

4.3.1 Spheroid morphology and ultrastructure *via* electron microscopy

Transmission and scanning electron microscopy were used to evaluate nanoparticle uptake, spheroid formation, morphology, and ultrastructure at different cell seeding densities. The SEM images indicate that the spheroids, once formed, developed into spherical structures made up of multiple cellular domains (Figure 4.1). This general spheroid shape did not differ between the different seeding densities, although larger aggregates of several spheroid structures were observed at the higher densities. These images confirm that spheroid formation remained constant regardless of cell number. Multiple cellular projections were visible on the cell surface, reflecting cellular interaction with the 3D spheroid environment.

Seeding density (cells/ml)

| 1 x 10⁴ | 5 x 10⁴ | 1 x 10⁵ |
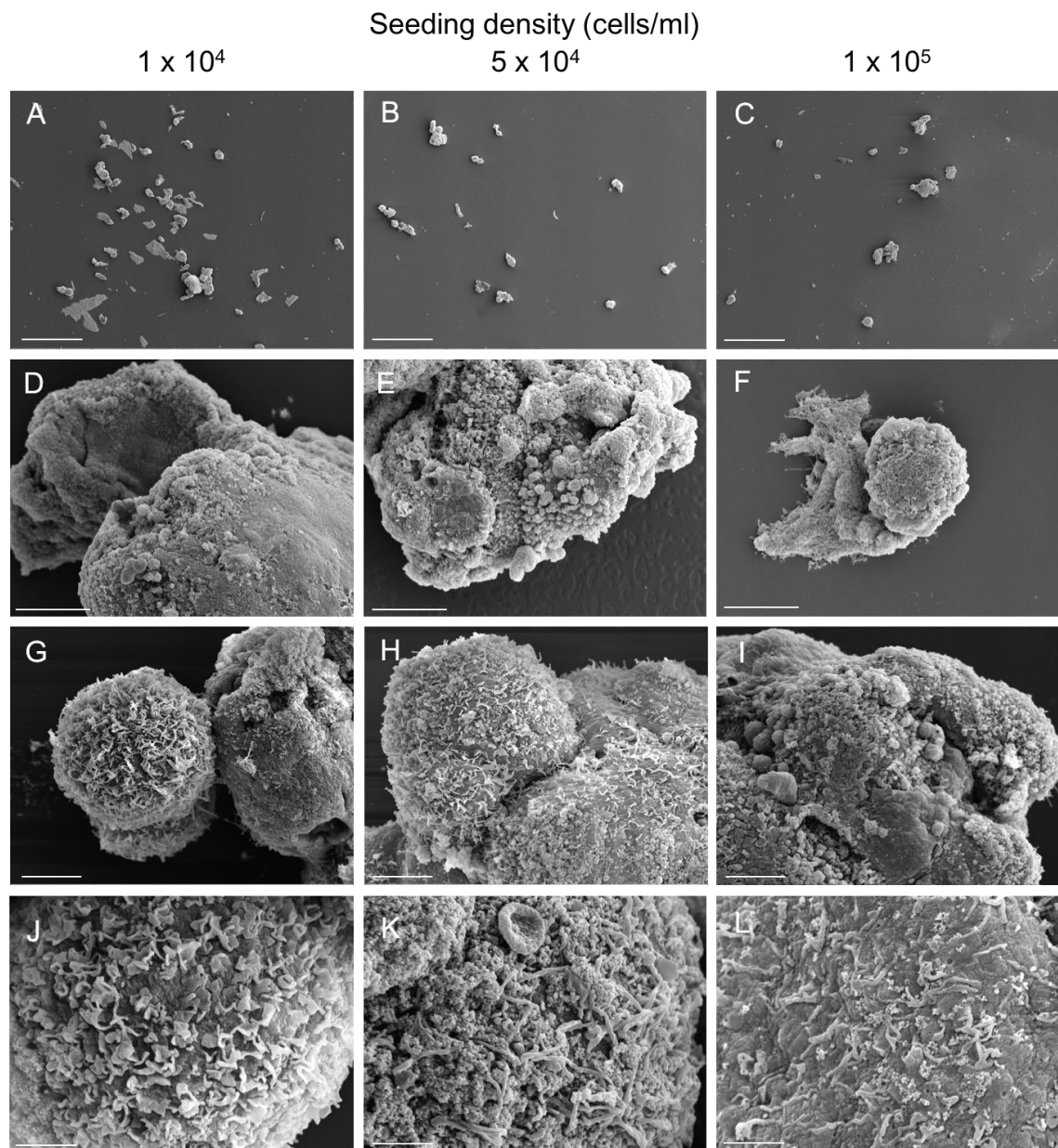
Figure 4.1 Scanning electron micrographs of spheroids formed at different cell seeding densities.
A, B, C, scale bar = 200 μm; D, E, F, scale bar = 10 μm; G, H, I, scale bar = 5 μm; J, K, L, scale bar = 2 μm.

The TEM images clearly show nanoparticle internalisation into the MSCs, located in vesicles within the cytoplasm (Figure 4.2). There was no apparent difference in cellular uptake of nanoparticles between the different seeding densities.
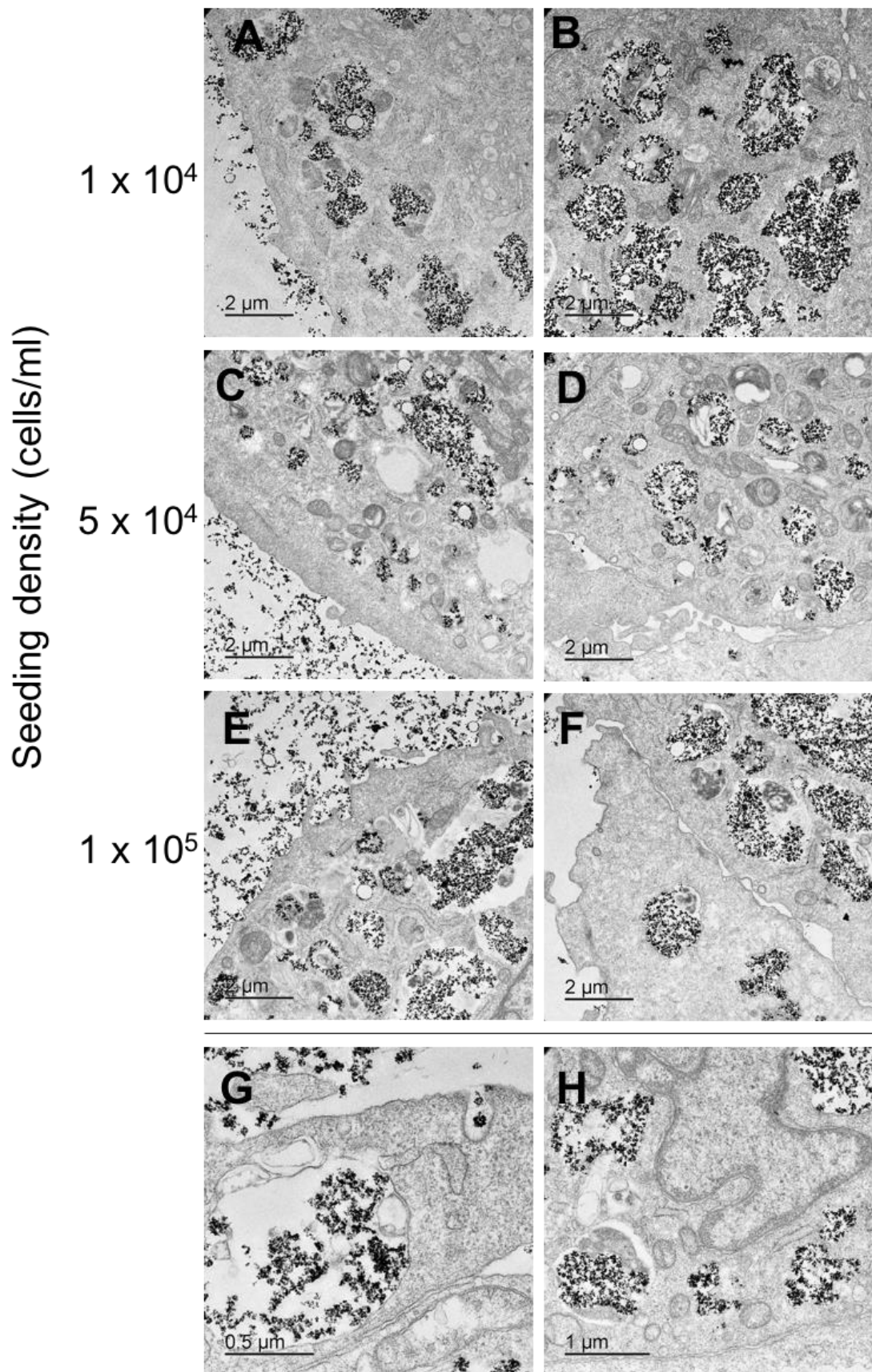
Figure 4.2 Transmission electron micrographs of spheroids formed at different cell seeding densities.
A-F, representative TEM images from spheroids seeded at different initial cell densities. G, H, representative higher magnification images taken of spheroids at the 5 x 10^4 seeding density.

4.3.2 MSC spheroid size

MSC spheroids generated using different seeding densities, stained with a calcein AM/ethidium homodimer viability stain, were measured in terms of their cross-sectional area (CSA) in FIJI (Figure 4.3). The difference in spheroid size at 1×10^4 and 5×10^4 cells ml^{-1} was not statistically significant, however, a large significant increase in size was observed in spheroids seeded at 1×10^5 cells ml^{-1}. The range of sizes at this higher density was varied, with many smaller spheroids apparent, similar to those at the lower seeding densities. When considered with the SEM images in Figure 4.1, this suggests that there may be a limit on spheroid size when formed *via* magnetic levitation, and the larger structures that were observed result from amalgamation of several smaller ones. There was also a strong correlation between spheroid size and cell number (Figure 4.4), with correlation coefficients of 0.98206805, 0.880558, and 0.9755847 for seeding densities 1×10^4, 5×10^4, and 1×10^5 respectively.
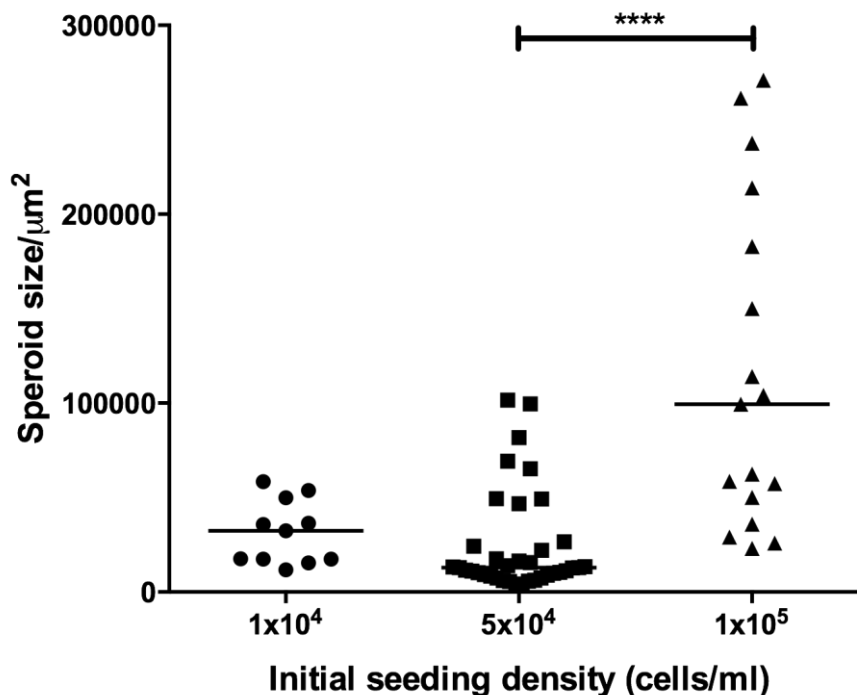
Figure 4.3 Spheroid size variation at different seeding densities.
Spheroid cross-sectional area in µm^2 was measured for all spheroids imaged at each time point: 1×10^4, n = 11; 5×10^4, n = 37; 1×10^5, n = 17. Statistical significance is based on results of the Kruskal-Wallis test followed by Dunn's multiple comparisons test. ****$P < 0.0001$.
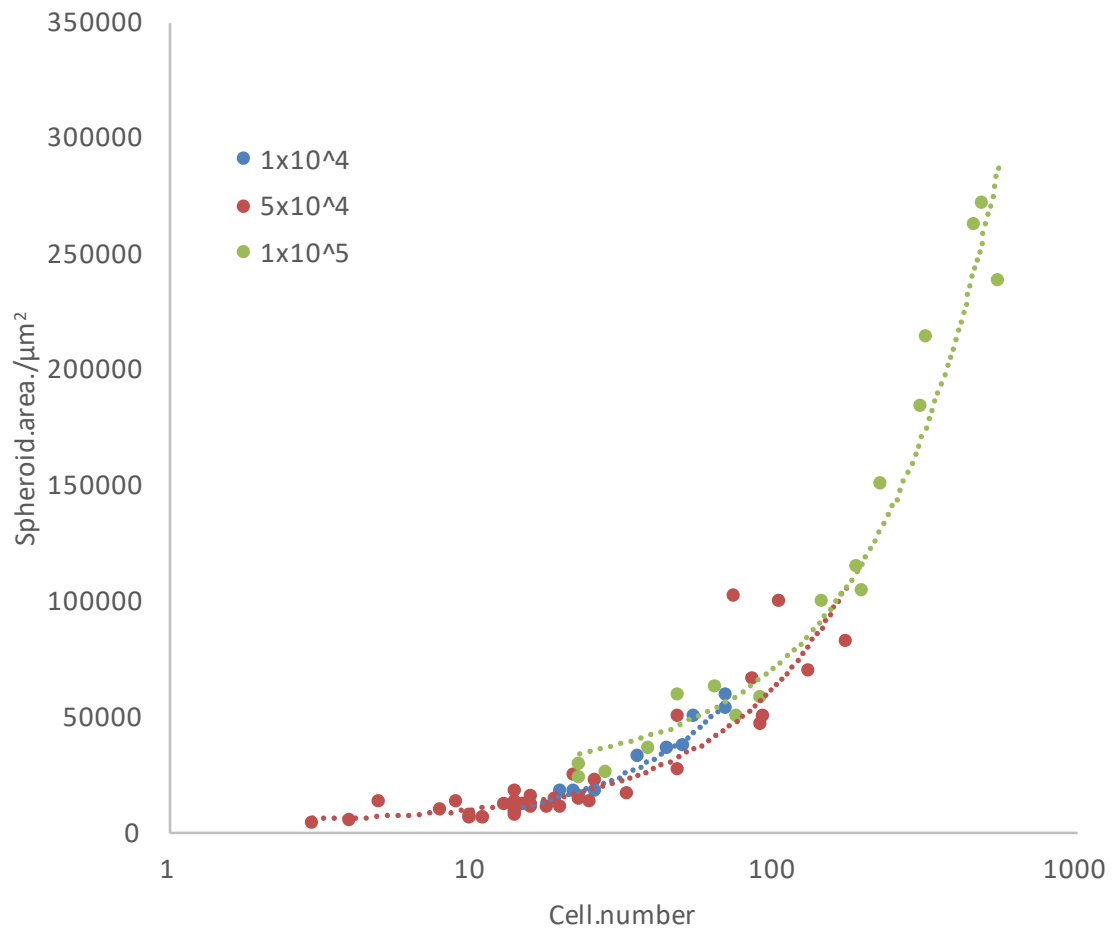
Figure 4.4 Spheroid size increases with increasing cell number.
Spheroids are plotted by cell number against size. The Pearson Product-Moment Correlation Coefficient between spheroid area and cell number was calculated for each seeding density using the CORREL function in Excel: 1×10^4, 0.98206805; 5×10^4, 0.880558; 1×10^5, 0.9755847.

4.3.3 Spheroid viability

MSC viability was determined using a calcein AM/ethidium homodimer viability stain as described in section 4.2.4. The percentage of pixels producing signal above a given threshold in the FITC channel as compared to those producing signal in the TRITC channel was calculated as a proxy for percentage viability for each spheroid. There was no statistically significant difference in percentage viability in spheroids seeded at the different densities (Figure 4.5A). The relationship between percentage viability and spheroid size is shown in Figure 4.5B.
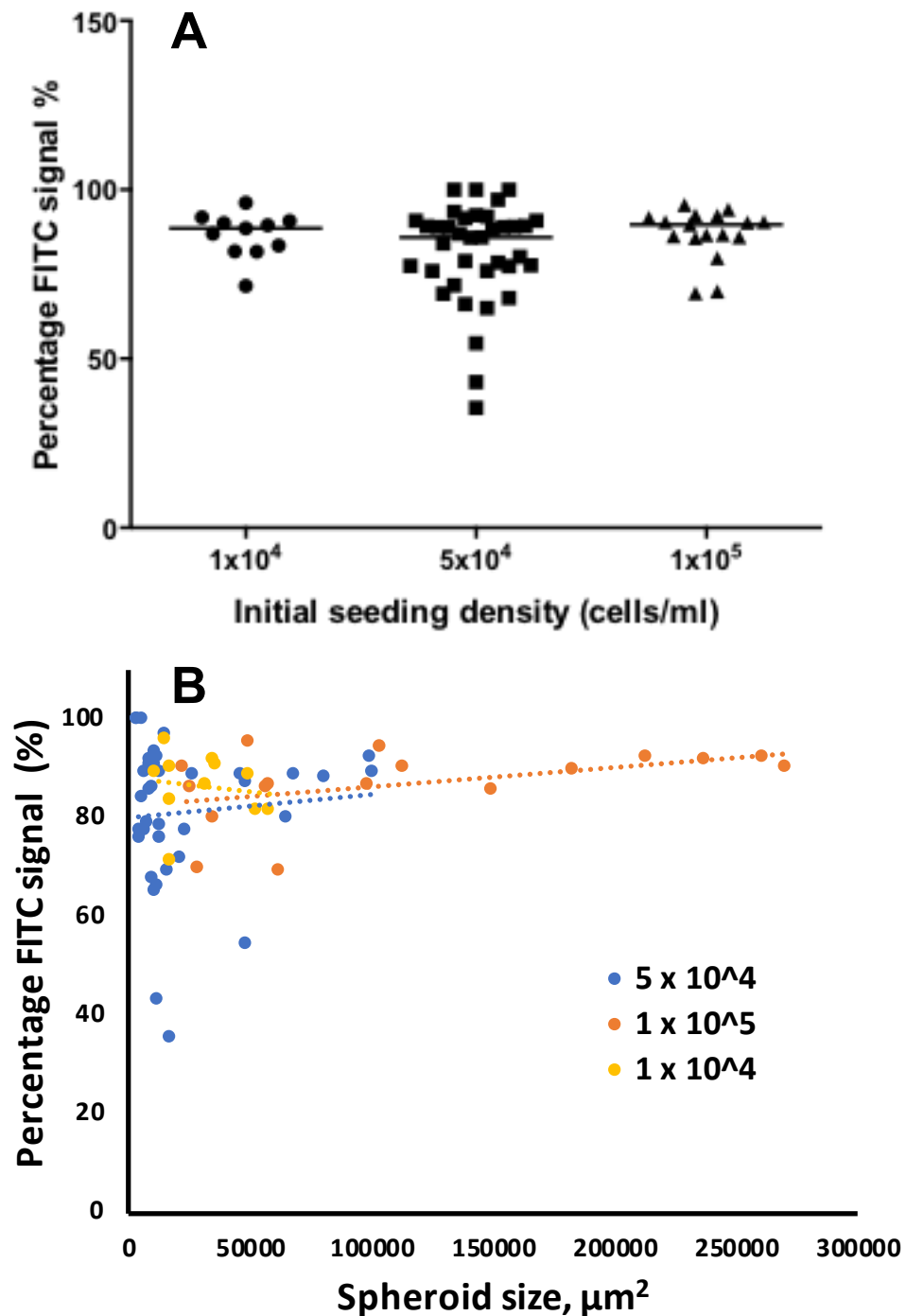
Figure 4.5 MSC spheroid viability varies with initial seeding density and spheroid size.
A: Percentage viability of spheroids seeded at different cell densities. The green signal (FITC channel) indicated calcein stained live cells and red signal (TRITC channel) ethidium homodimer stained dead cells. Percentage FITC signal was calculated to give a proxy for percentage viability. The Kruskal-Wallis test followed by Dunn's multiple comparison test was used to compare the means of all three groups; no statistically significant differences were detected ($p > 0.05$). Mean percentage viability ± 95% confidence interval. B: MSC spheroid viability in relation to spheroid size. Percentage FITC signal detected for each spheroid is plotted against spheroid cross-sectional area in μm^2. The Pearson Product-Moment Correlation Coefficient between spheroid size and percentage viability was calculated for each seeding density using the CORREL function in Excel: 1×10^4, -0.145204; 5×10^4, 0.0885486; 1×10^5, 0.4547947.

Central necrosis in the spheroids was evaluated by taking measurements of FITC and TRITC signal from cross-sections of spheroid images (Figure 4.6). The TRITC signal remained at a lower level than the FITC signal across the spheroid, with a few intermittent peaks indicating dead cells. Basal grey value (as a proxy for fluorescence intensity) for FITC remained at around 4500, and for TRITC around 2000 for all spheroids. The values of the peaks in the FITC channel, indicating live cells, varied depending on strength of absorption of the stain and location in the spheroid. There was a larger number of viable cells compared to dead cells, and a suggestion of central necrosis that increased with spheroid size, as the TRITC signal peaks appeared in the central area of the spheroid.
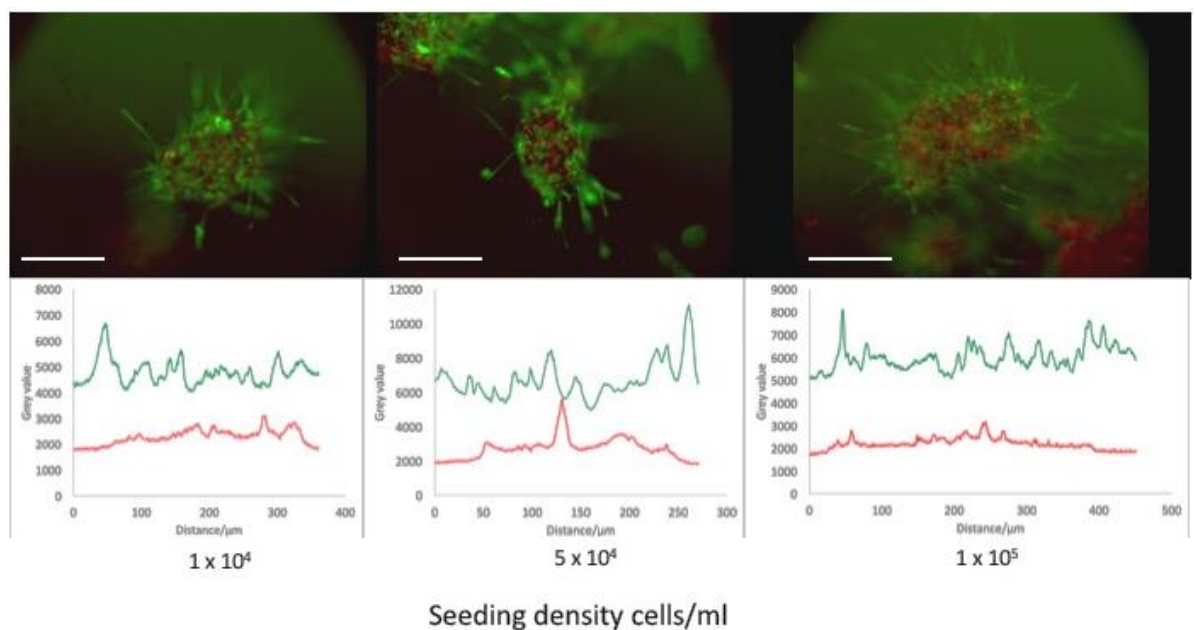
Figure 4.6 MSC spheroid cross-sectional viability via FITC and TRITC signal across spheroids with different cell seeding densities.
Green, FITC; Red, TRITC. Scale bar = 200 µm.

4.3.4 Differentiation capacity of MSCs following spheroid culture

MSC differentiation capacity when cultured as spheroids was evaluated by histological staining (Figure 4.7). Adipogenic differentiation was clearly visible in all three types of cells. Oil Red O stains neutral triglycerides and lipids red, and several cells exhibiting partial or total staining, as well as adipose cell morphology, were visible. However, the staining observed in cells grown in osteogenic and chondrogenic media was more ambiguous, as it was confounded by the presence of nanoparticles, which have a similar colour to the stain. A small

amount of red staining was observed in the corresponding monolayer controls, indicating the presence of calcific deposits and chondrogenic cells, respectively.
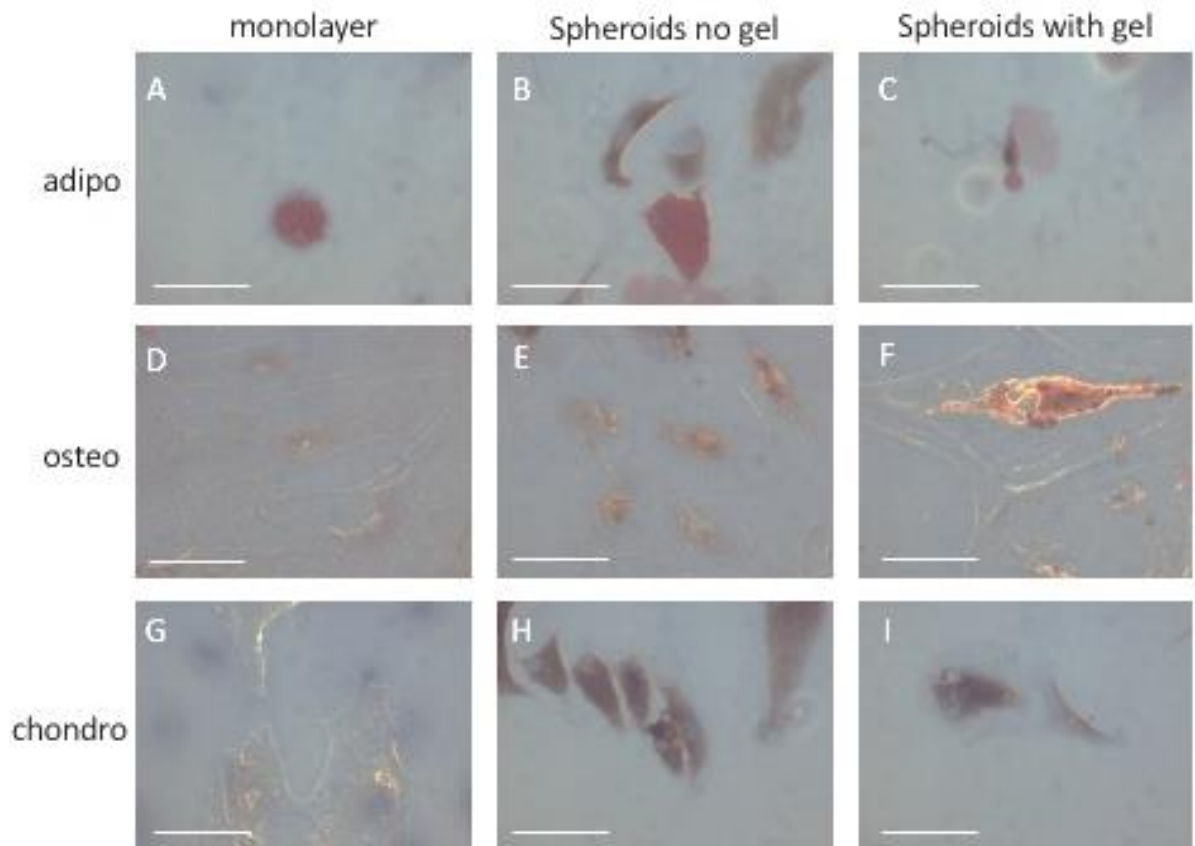
Figure 4.7 Histological analysis of cells grown in adipogenic (A-C), osteogenic (D-F), or chondrogenic (G-I) induction media formulations.
A, D, G, MSCs grown in monolayers; B, E, H, MSCs extracted from spheroids grown in media; C, F, I, MSCs extracted from spheroids grown in collagen type I gel. A-C, stained with Oil Red O; D-F, stained with Alizarin Red; G-I, stained with Safranin O. Scale bar = 100 μm.

4.3.5 Gene expression analysis

Fluidigm high-throughput RT-qPCR was used to evaluate the expression of several gene groups in spheroids compared to monolayers. These included genes involved in the cell cycle, MSC differentiation, niche microenvironment interactions, and cell-cell signalling pathways.

4.3.5.1 Cell cycle genes

The expression of most of the cell cycle genes investigated (Figure 4.8) decreased in spheroids when compared to monolayers. The greatest decreases were observed in p53 and cyclin D2 expression (both approximately 0.31-fold change, $p < 0.05$). The expression of two genes, cyclin D1 and FOS, increased, although neither of

these increases were significant. Cyclin D1 expression increased 2.5-fold, and FOS expression increased 6.2 times in spheroids over monolayers, a significant increase ($p < 0.05$).
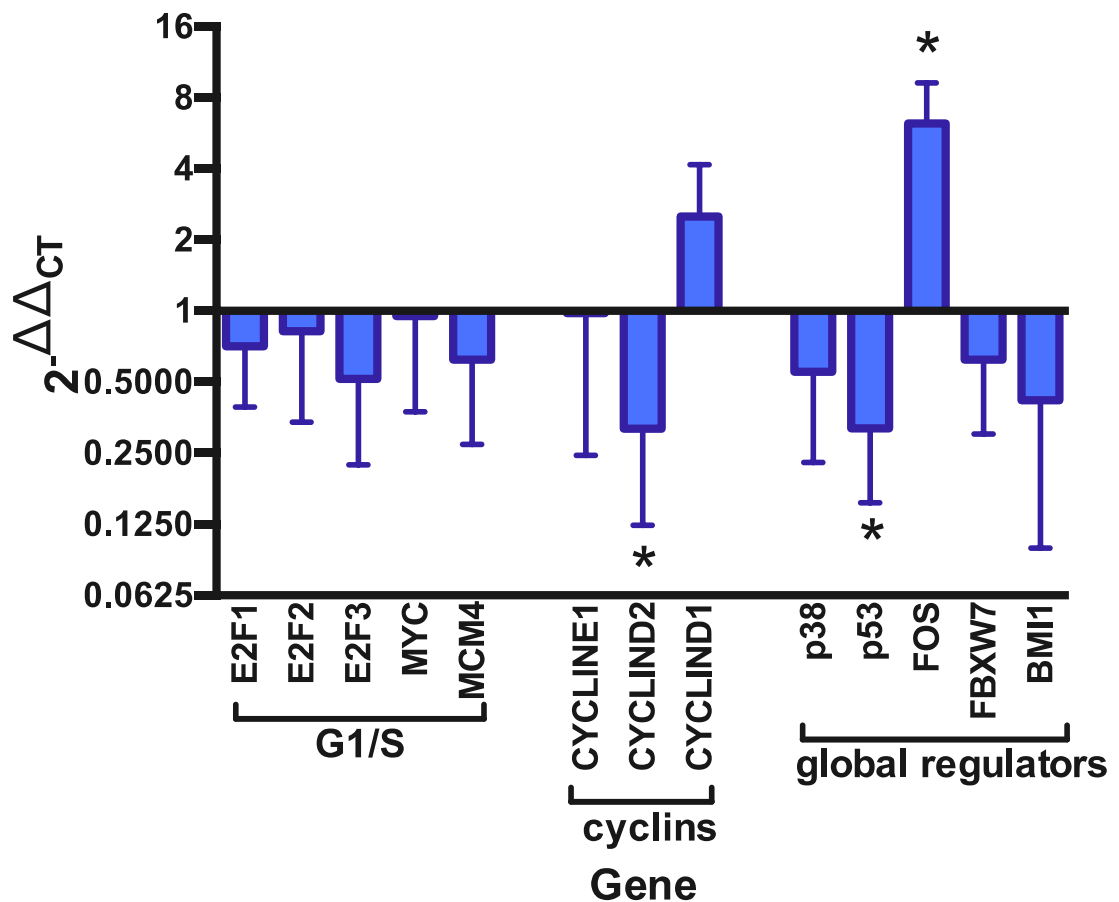
Figure 4.8 Fold-change in expression of genes involved in the cell cycle in MSC spheroids compared to monolayers.
Values presented as mean fold change ± standard error of the mean, n = 3. *p < 0.05.

4.3.5.2 MSC differentiation and phenotype

Several genes were included in the panel that relate to MSC differentiation into bone, fat, and cartilage stromal lineages. They include both early and late indicators of differentiation. Increased expression of osteogenesis related genes osterix, BMP2, and osteopontin was observed in spheroids compared to monolayers (Figure 4.9). The greatest, statistically significant ($p < 0.05$), increase was observed for BMP2, of 55.6 times the amount in monolayers. Osterix and OPN expression were increased 8.8- and 4.9-fold, respectively. GATA2 expression was also increased 4.7-fold ($p < 0.05$). SMAD7 and VEGF were upregulated by 2.2 and 1.7 times, respectively.

Expression of RUNX1 and SMAD7 remained essentially unchanged in spheroids compared to monolayers (expression levels of between 0.8 and 1.0 times that of the monolayer for each). The rest of the genes related to MSC differentiation were downregulated, although not to a degree of magnitude similar to the upregulated genes. TCF3, PML, and RUNX2 expression levels in spheroids were more than half the levels of the monolayer (ranging between 0.63 and 0.7 times the expression). STAT3, TCF4, NFKB1, NFKB2, and LEF1 mRNA levels were lower than half the amount observed in monolayers (range 0.45-0.55 times).
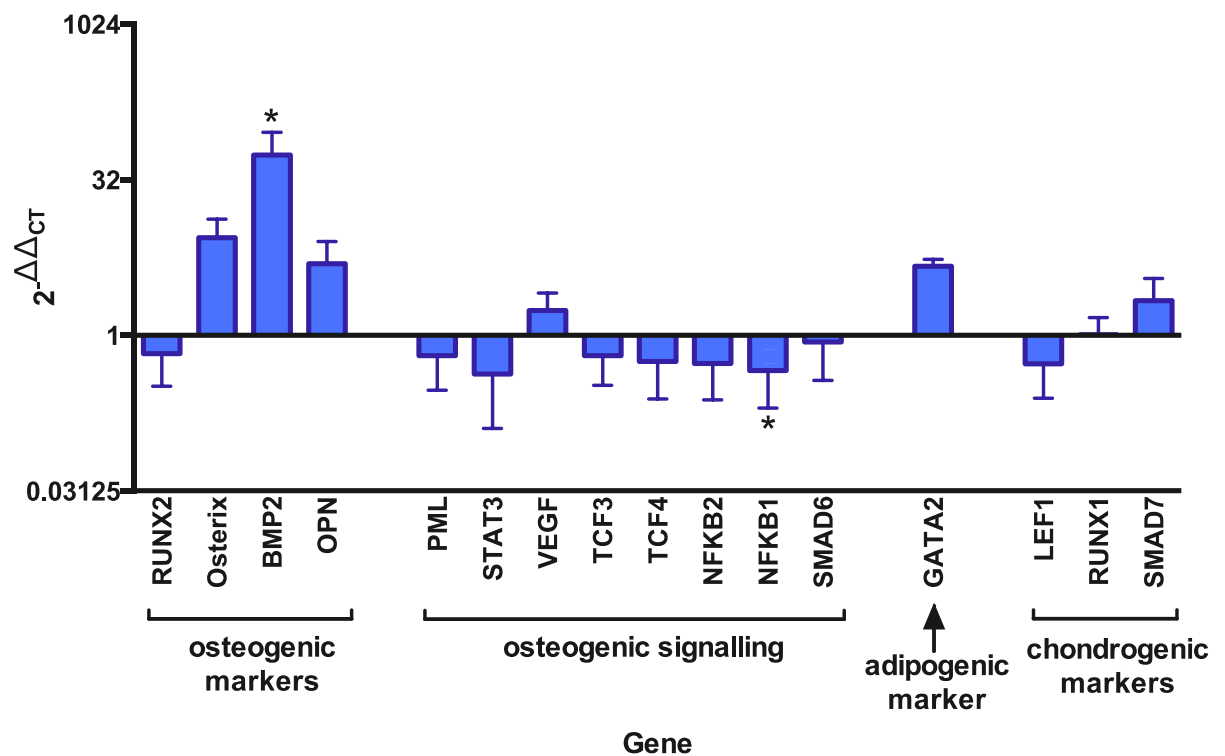
Figure 4.9 Fold-change in expression of genes involved in MSC differentiation in MSC spheroids compared to monolayers.
Values presented as mean fold change ± standard error of the mean, n = 3. *p < 0.05.

Examining the expression of genes involved in MSC phenotype can indicate whether stem cell properties are maintained (Figure 4.10). CD79, MEIS1, and CD63 mRNA abundance were 0.3, 0.4, and 0.5 times the levels observed in monolayers. CD271 and HIF1α levels remained constant. The rest of the MSC markers, CD34, CXCR4, and nestin, were upregulated. Although these changes were not significant, they are of a high magnitude, at 7.9, 9.7, and 31.0 times the levels of the control, respectively.
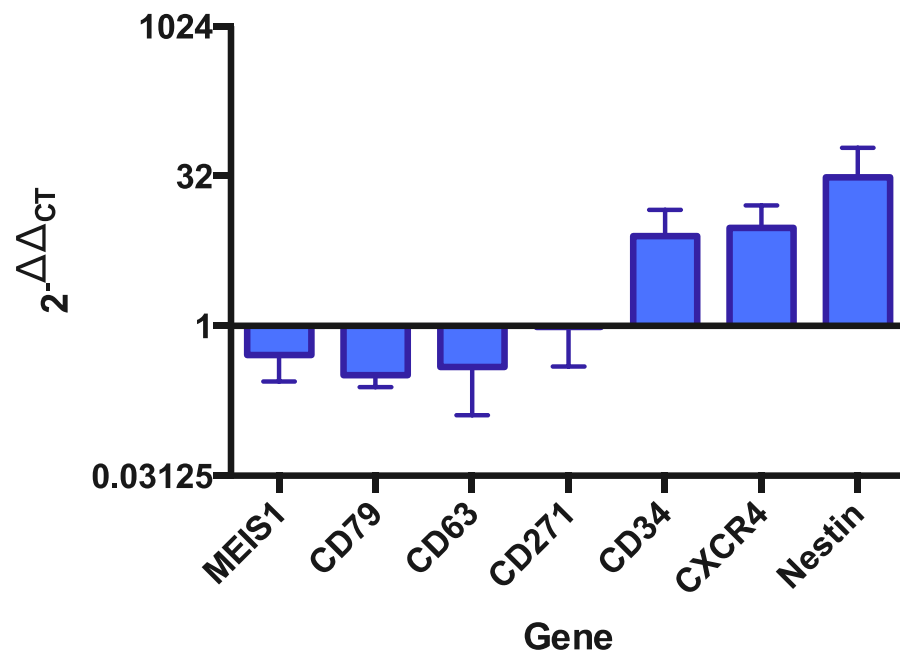
Figure 4.10 Fold-change in expression of genes involved in MSC phenotype in MSC spheroids compared to monolayers.
Values presented as mean fold change ± standard error of the mean, n = 3.

4.3.5.3 Niche microenvironment interactions

Genes involved in cell adhesion and cytokine interactions were examined to evaluate the extent of cell interactions in the model compared to standard culture. All genes involved in direct cell adherence were either downregulated or remained the same in spheroids compared to monolayers (Figure 4.11). In particular, VCAM1 was significantly downregulated (p < 0.05, 0.03 times that of control, equivalent to ~32-fold difference). ALCAM and CD44 expression remained similar to the levels in monolayers, and VLA4, ICAM1, and N-cadherin were all significantly downregulated to approximately 0.25-fold (p < 0.05).
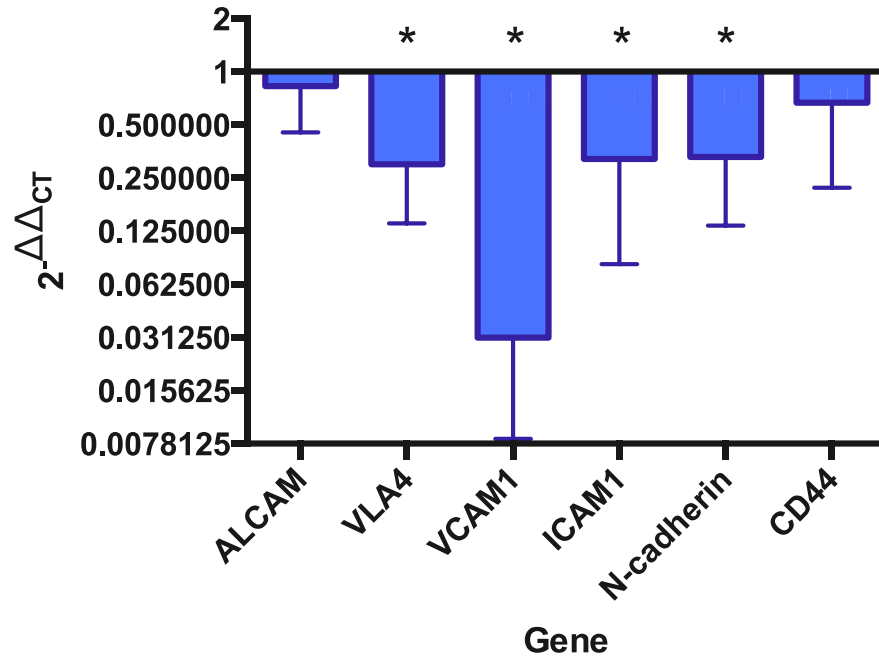
Figure 4.11 Fold-change in expression of genes involved in cell-cell or cell-ECM adhesion in MSC spheroids compared to monolayers.
Values presented as mean fold change ± standard error of the mean, n = 3. *p < 0.05.

One gene (SCF) involved in cytokine interactions was significantly downregulated to 0.15 times the level in spheroids compared to monolayers (p < 0.05). Tie-2 was also downregulated by 0.17 times the level in the control, although this change was not significant. The expression of CXCL12, Ang1, and TPO all remained approximately the same in spheroids compared to monolayers.
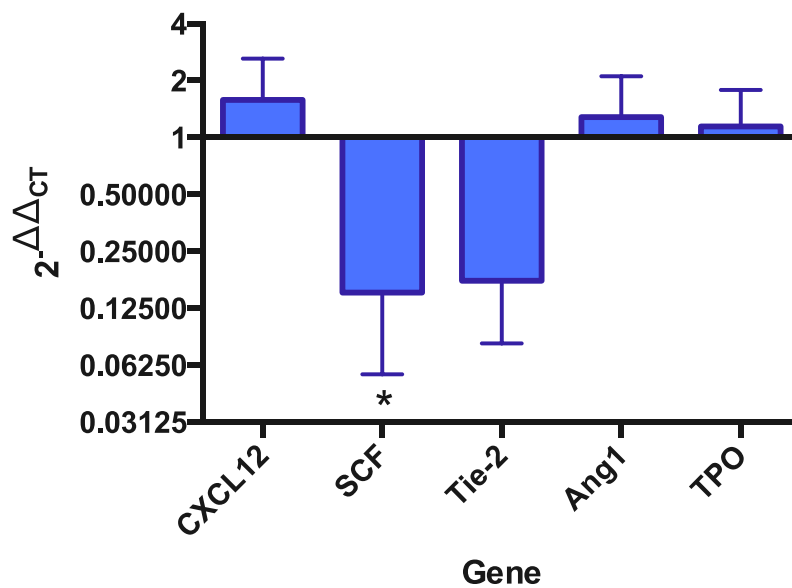
Figure 4.12 Fold-change in expression of cytokines and receptors in MSC spheroids compared to monolayers.

Values presented as mean fold change ± standard error of the mean, n = 3. *p < 0.05.

4.3.5.4 Notch signalling

Notch signalling is both a regulator of osteogenesis and a mediator of HSC-stromal interactions in the niche: the major components of this pathway have been analysed here. HEY2 and Notch4 were significantly downregulated by 0.017-times and 0.26- times (p < 0.05) in spheroids, respectively. All other genes of the Notch pathway have remained relatively constant in spheroids, with the majority exhibiting slight downregulation. DLL4 has increased to the greatest extent, with an 8.28-fold increase.
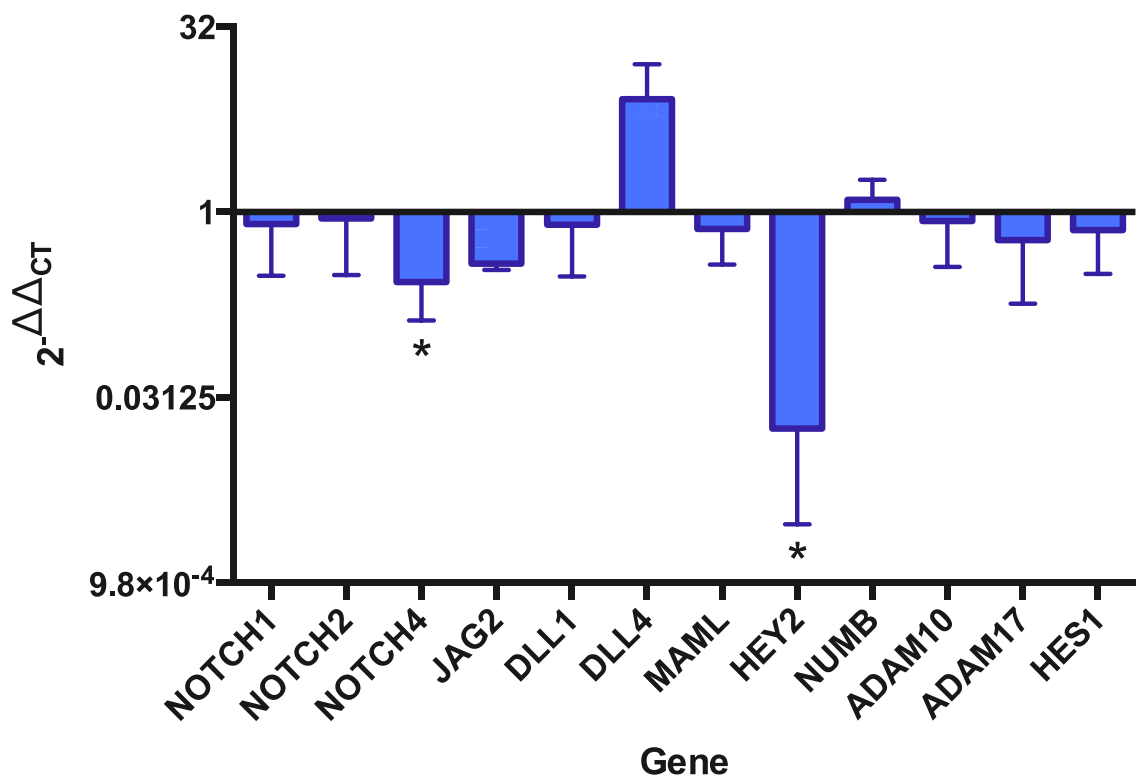
Figure 4.13 Fold-change in expression of genes involved in Notch signalling in MSC spheroids compared to monolayers.
Values presented as mean fold change ± standard error of the mean, n = 3. *p < 0.05.

4.3.5.5 Hedgehog signalling

Hedgehog (HH) signalling is also involved in both differentiation and proliferation of MSCs. All components of the HH signalling pathway decreased in expression or remained constant. GLI1 and 3 exhibited the smallest difference. PTCH2, SMO, and SUFU decreased to around 0.5-times. The significant decrease in PTCH1

expression is slightly greater at 0.32-times the level of that observed in monolayers (p < 0.05).
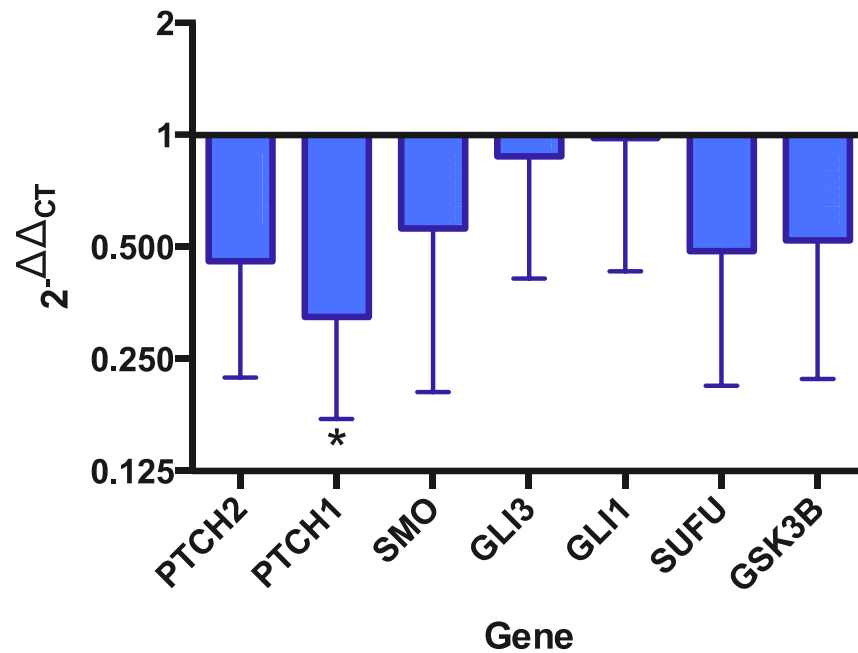
Figure 4.14 Fold-change in expression of genes involved in Hedgehog signalling in MSC spheroids compared to monolayers.
Values presented as mean fold change ± standard error of the mean, n = 3. *p < 0.05.

4.3.6 Protein expression of MSC markers and key cytokines

4.3.6.1 Immunohistochemistry

Immunohistochemistry was used to evaluate the protein levels of the HSC-supportive cytokine CXCL12, and the MSC markers STRO-1 and nestin. Expression of all three gene products was increased in spheroids compared to monolayers, in accordance with the results obtained from genetic analysis.

Expression of STRO-1, indicated by green fluorescent signal, was not evident in cells grown in monolayers at either day 3 or day 7 (Figure 4.15). However, expression was clearly visible in spheroids at both time points, with an increased frequency of cells expressing the marker at day 7. The differences at both time points were statistically significant (day 3, p = 0.032; day 7, p = 0.015).
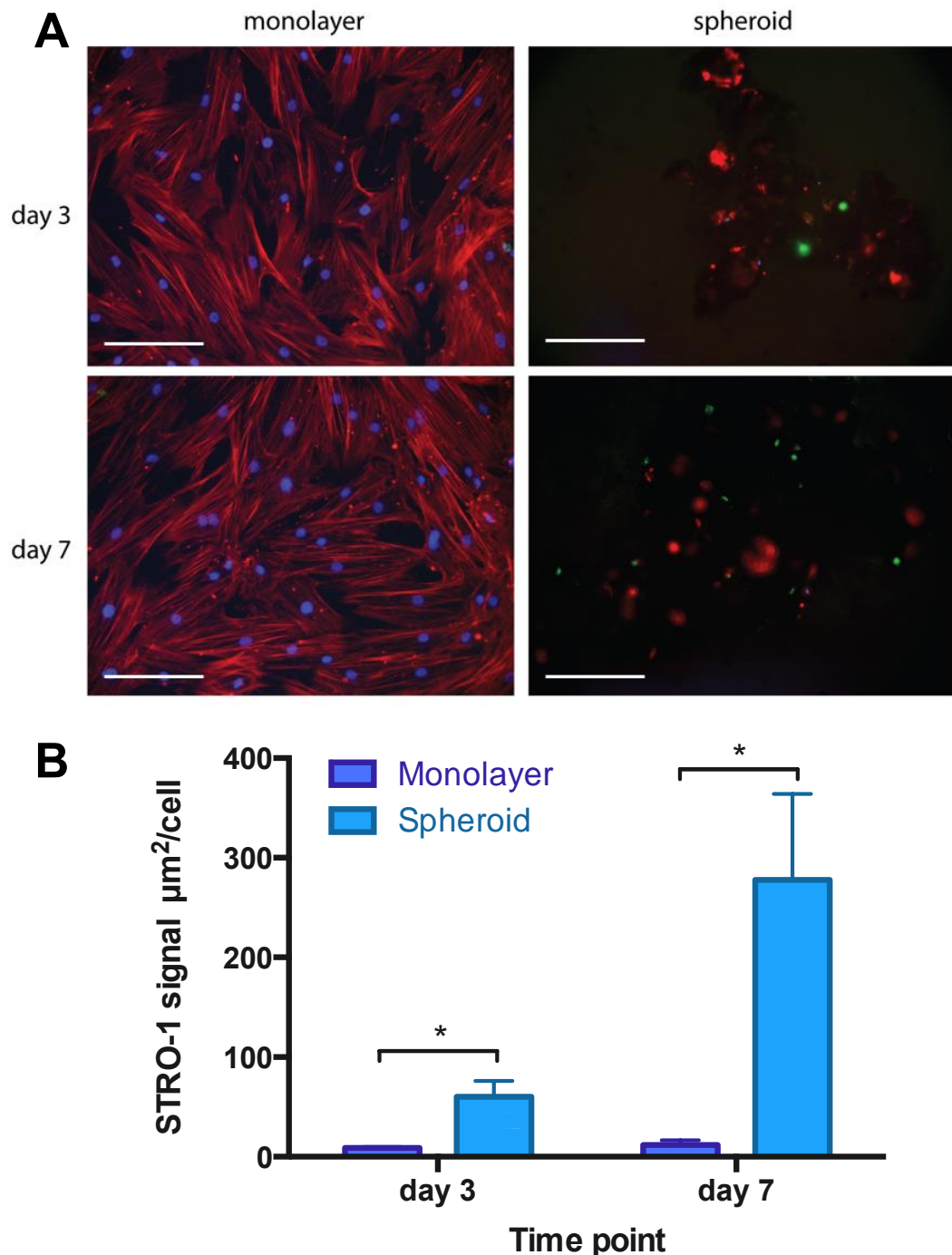
Figure 4.15 STRO-1 staining in MSCs grown in either monolayer or spheroid culture systems for 7 days.
A: Fluorescence microscopy images, DAPI (blue) = DNA/nuclei, TRITC (red) = phalloidin (actin); FITC (green) = STRO-1. Scale bars = 200 µm. B: Average STRO-1 signal (µm^2) in relation to cell number (nucleus number) for each image, mean ± SEM, n ≥ 3, *p < 0.05.

A small amount of expression of CXCL12 was evident in monolayers at day 7 (Figure 4.16). However, none can be seen in monolayers at day 3. In spheroids, there was a small signal at day 3, with no difference observed compared to monolayers (p = 0.51). By day 7, CXCL12 levels increased significantly in spheroids compared to monolayers (p = 0.0093). This indicates that cells in culture do not initially express

CXCL12 and require a conditioning period of time in spheroids before they begin to express this cytokine.
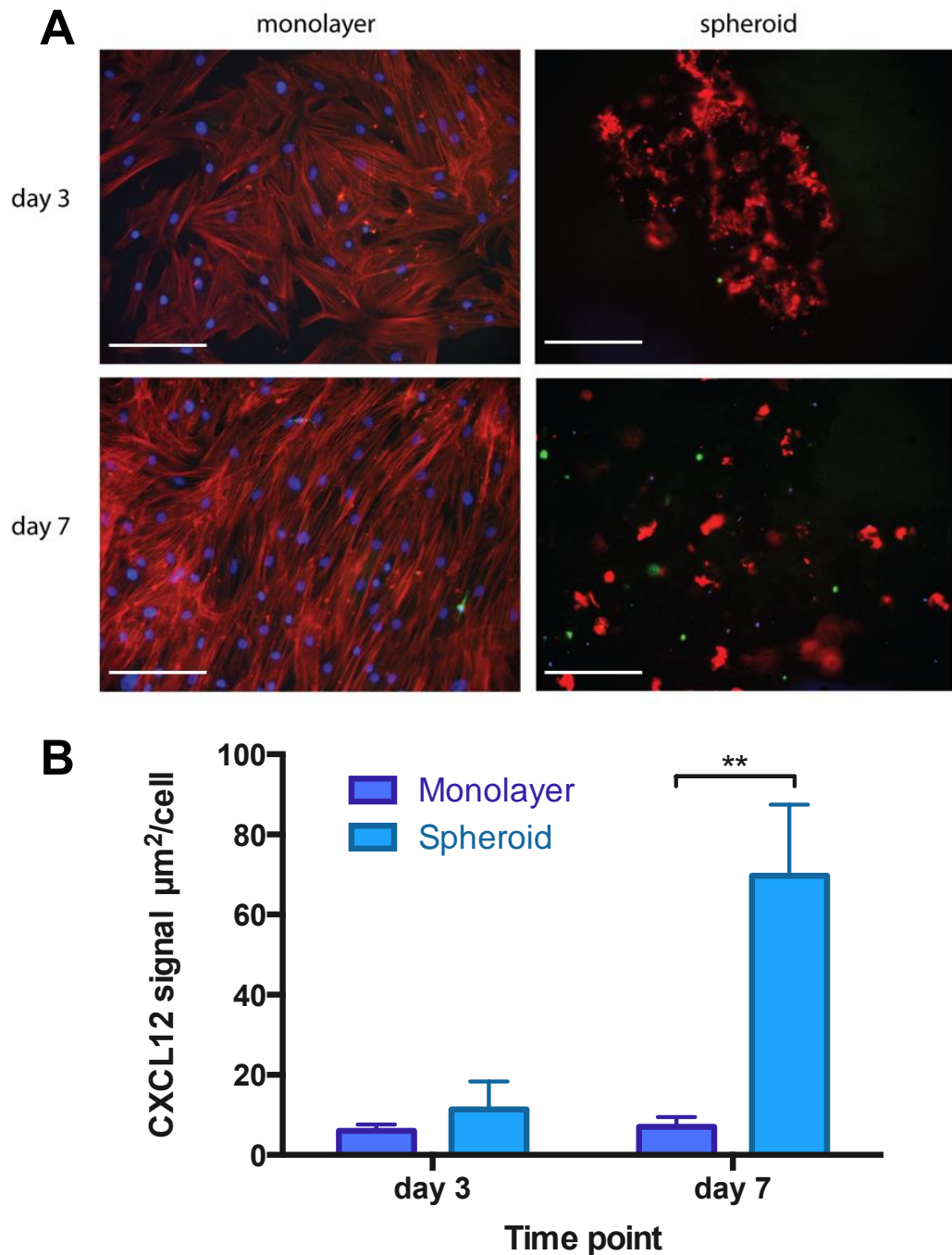
Figure 4.16 CXCL12 staining in MSCs grown in either monolayer or spheroid culture systems for 7 days.
A: Fluorescence microscopy images, DAPI (blue) = DNA/nuclei, TRITC (red) = phalloidin (actin); FITC (green) = CXCL12. Scale bars = 200 µm. B: Average CXCL12 signal (µm^2) in relation to cell number (nucleus number) for each image, mean ± SEM, n ≥ 3, **p < 0.01.

Nestin expression exhibited a difference between the two culture systems at an early time point (Figure 4.17). Green staining was only observed in one cell in

monolayer culture at both time points. However, staining was widely distributed throughout spheroids at both day 3 and day 7, with the protein being almost ubiquitous at day 7. This difference was not significant at day 3 (p = 0.086), but at day 7, nestin was significantly increased in spheroids above the level in monolayers (p = 0.0023).
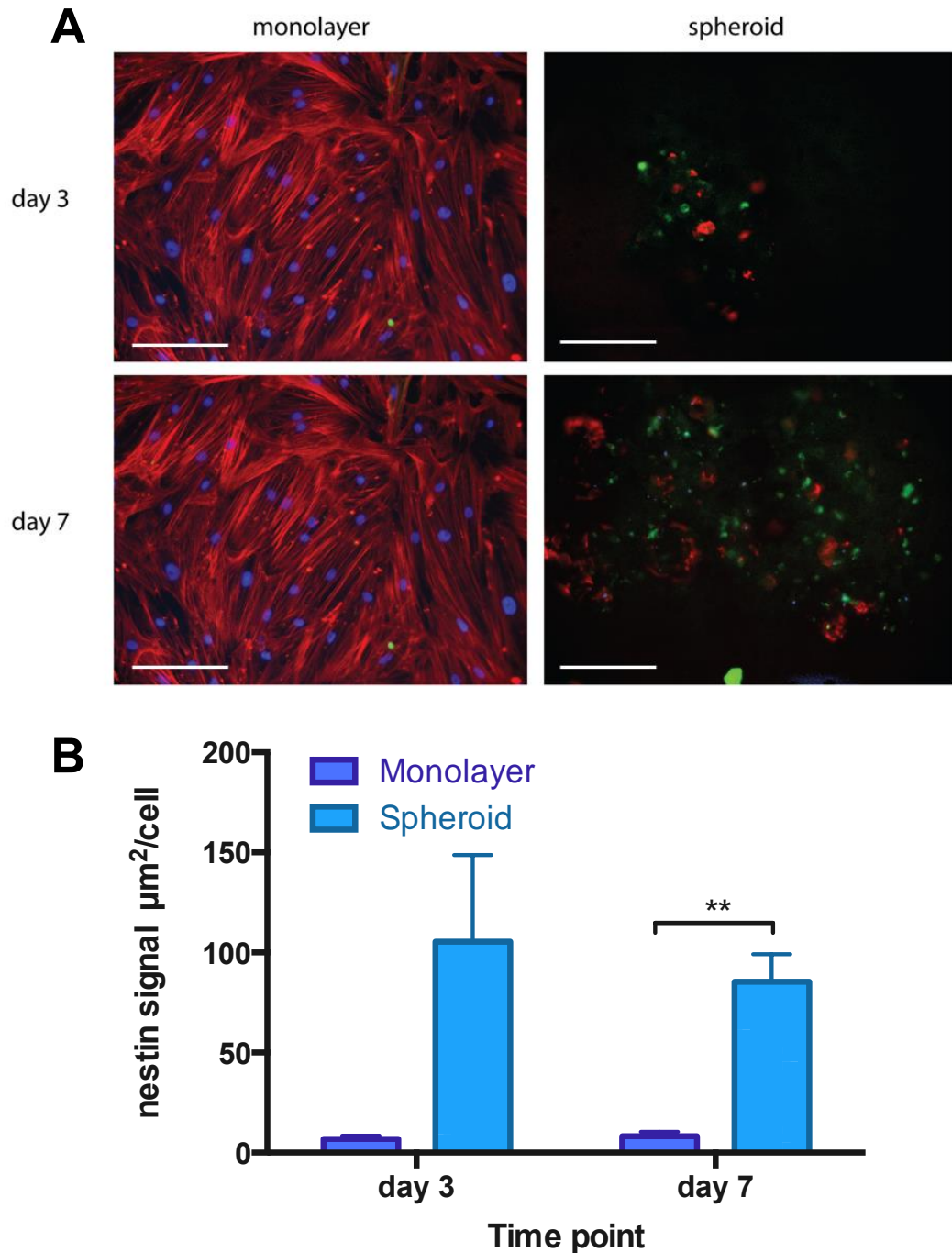
Figure 4.17 Nestin staining in MSCs grown in either monolayer or spheroid culture systems for 7 days.
A: Fluorescence microscopy images, DAPI (blue) = DNA/nuclei, TRITC (red) = phalloidin (actin); FITC (green) = nestin. Scale bars = 200 μm. B: Average nestin signal (μm^2) in relation to cell number (nucleus number) for each image, mean ± SEM, n ≥ 3, **p < 0.01.

4.3.6.2 Quantitative analysis of CXCL12 concentration

Further analysis of CXCL12 was conducted using an ELISA, as it is a secreted cytokine. Two different media formulations were used: standard DMEM containing FBS; and serum-free IMDM suitable for HSCs. In DMEM (Figure 4.18), CXCL12 concentration in the media evidently increased with time, with the highest expression in both monolayers and spheroids at day 14. However, the level in spheroids was significantly lower ($p < 0.01$). In IMDM, the expression increased more quickly, with a higher level at day 1 in both monolayers and spheroids. However, this level was maintained throughout the period of cell culture (14 days). The concentration remained below 100 pg ml^{-1} at every time point, whereas in DMEM the level was above 100 pg ml^{-1} by day 14. There was also no difference between the two culture systems, with spheroids maintaining similar levels at all time points.
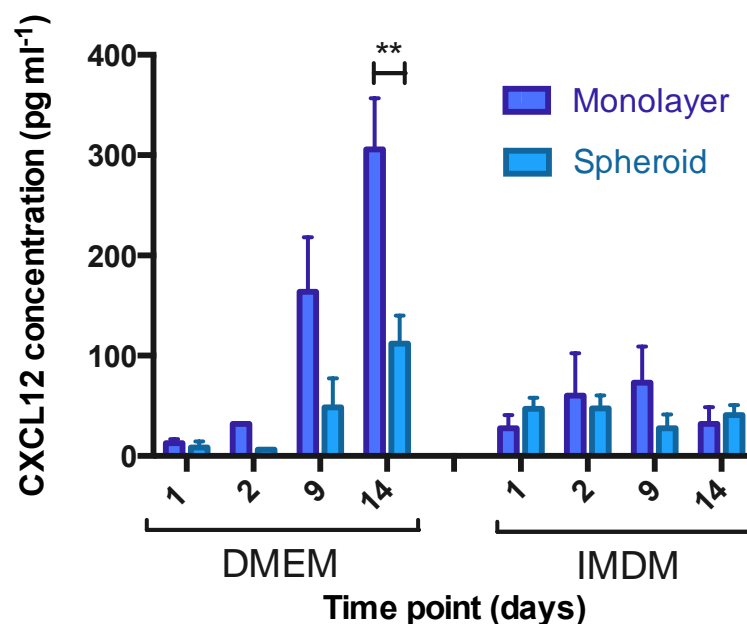
Figure 4.18 CXCL12 concentrations in cell culture supernates from MSCs cultured either in monolayers or spheroids in DMEM or IMDM media formulations.
$**p < 0.01$, n = 3.

4.3.7 Proliferation analysis

A BrdU assay was performed to evaluate MSC proliferation in the two culture systems (Figure 4.19). Proliferating cells are indicated by an overlap of the DAPI stain (blue, nuclei), and the BrdU stain (green, replicating DNA), as the cells integrate the thymine analogue into the DNA strand during replication. Here, this is represented by a turquoise colour. These stains overlapped to a greater extent

in cells in monolayers at day 3. At day 7 the green stain was also more prevalent, but whether these overlapped was more ambiguous. The DAPI stain was less effective in the spheroids; possibly due to the presence of the collagen gel. Hence, elucidating the extent of proliferation is problematic. However, less BrdU was detected in the spheroid samples in general, indicating that it was not integrated into the cell DNA.
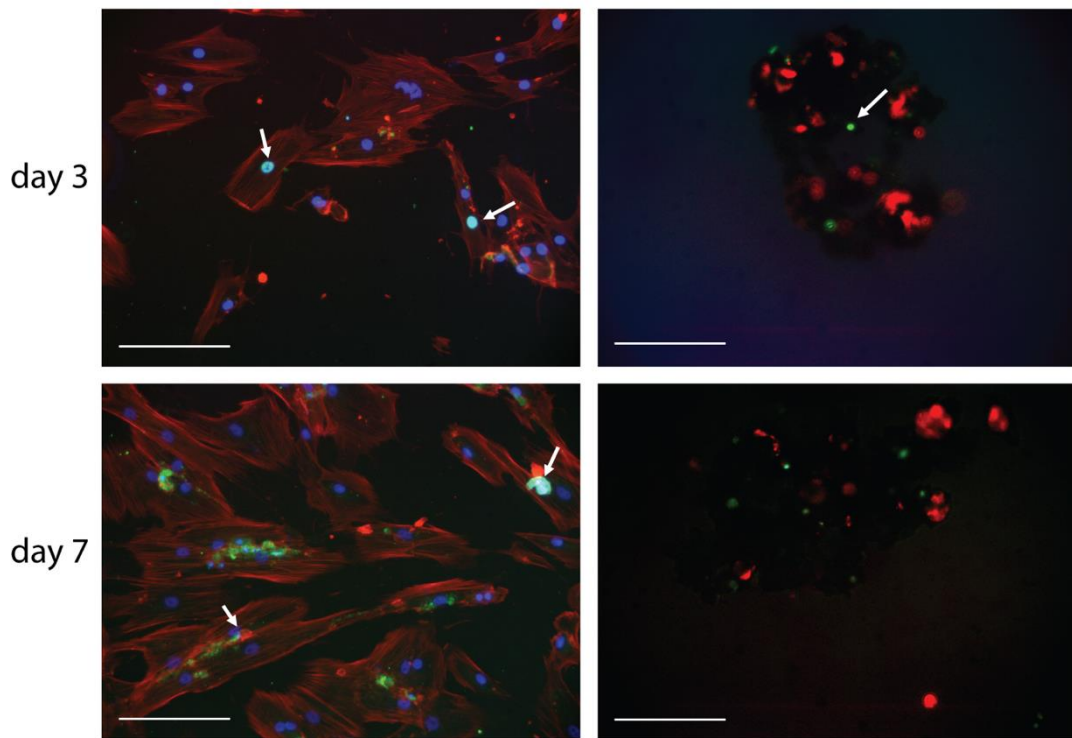
Figure 4.19 MSCs in monolayers and spheroids stained with anti-BrdU antibody following treatment with BrdU.
DAPI (blue) = DNA/nuclei, TRITC (red) = phalloidin (actin); FITC (green) = nestin. Scale bar = 200 μm. Proliferating cells are indicated by overlapping blue and green signals (white arrows).

4.4 Discussion

This chapter aimed to evaluate MSC spheroid formation, and the behaviour of cells grown in the 3D model, in terms of gene expression, protein expression, and cytokine release. Behaviours such as quiescence, differentiation, and expression of HSC-supportive cytokines that are relevant to HSC support were included in the analysis.

4.4.1 Confirmation of nanoparticle uptake and spheroid formation

SEM analysis allows visualisation of gross spheroid morphology and cell surface activity. As evident from high magnification images, spheroid morphology and size vary considerably, although this is not dependent on initial cell seeding density. Looking more closely at the cell surface, excess nanoparticles are clearly visible with a 'grainy' texture above the smoother cell surface, surrounding multiple filopodia. These filopodia may have greater importance for cell spreading dynamics in a 3D environment, compared to a flat environment wherein lamellopodia formation is important (Albuschies & Vogel 2013). The appearance of the abundant projections may be a response to the presence of the NPs, although filopodia have also been observed to a lesser extent in HeLa spheroids formed by the liquid overlay technique (Ma et al. 2012). SEM analysis of these HeLa cell spheroids showed individual spherical cells with distinct junctions, however, this is less clear with the MSC spheroids developed here.

TEM images clearly show NP uptake into endosomes, as has been observed in previous studies (Smith et al. 2010). These endosomes are of varying shapes and sizes, contain varying amounts of NPs, and localise among other organelles. Figure 4.2G also depicts an endosome either fusing with or being formed from the outer cell membrane, confirming that this is a continuing dynamic process even following spheroid formation. Excess NPs are also visible surrounding the cells, and in contact with the filopodia. Here, cellular junctions are more distinctive, demonstrating that cells are in close contact with each other within the spheroid.

4.4.1.1 Magnetic MSC spheroids within collagen gel culture do not exhibit increased cell-cell or cell-ECM adhesion

Cell-cell and cell-ECM adhesion are important during formation of spheroids. Magnetically levitated spheroids are initially generated in culture media over 24 hours, after which time they are cultured within a type I collagen gel, to recapitulate the BM niche microenvironment. It is expected that both integrins (cell-ECM interactions) and cadherins (cell-cell interactions) play a key role. Following the formation of loose aggregates *via* integrin-ECM binding, cadherin expression increases followed by formation of compact spheroids by homophilic cadherin-cadherin interactions (Figure 4.20, Bartosh et al. 2010). In addition, cell-cell interactions are also important for HSC retention *in vivo*. Therefore, the gene expression of a selection of adhesion molecules in MSC spheroids was investigated, although all genes appeared to be either decreased or similar to monolayer controls.

Expression of activated leukocyte-cell adhesion molecule (**ALCAM**)[4], a transmembrane glycoprotein involved in cell-cell adhesion (Nakamura et al. 2010), and CD44, which is involved in cell-cell and ECM adherence (Wagner et al. 2008), both remained unchanged in spheroids compared to monolayers. Although higher expression was expected due to the increased adhesion to the collagen in the model, this may have occurred through separate mechanisms.

Integrins are fundamental components of focal adhesion complexes, which form during cell-ECM and cell-cell adhesion. They interlink ECM proteins with the actin cytoskeleton, transmitting information about the cellular microenvironment to the cytoskeleton and the nucleus, triggering changes in cell gene expression and behaviour. β1 integrins (including α1β1 and α1β2) are the main receptors for collagen binding (Jokinen et al. 2004). The integrins analysed here are very-late antigen 4 (**VLA-4),** an α4β1 integrin, which binds to vascular cell adhesion molecule 1 (VCAM-1); and lymphocyte-associated antigen 1 (**LFA-1**)[5], a β2 integrin normally expressed on leukocytes. Whilst results for LFA-1 were not obtained, the

---

[4] ALCAM is also known as CD166.

[5] An extreme value was obtained for LFA-1 in this analysis, with n=1 due to sample failure. Therefore, it has been removed from the results.

significant decrease in expression of VLA-4 was unexpected, as enhanced cell-cell interactions in spheroids were expected to upregulate integrins.

Aside from cell-ECM interactions, cell-cell interactions are crucial to spheroid formation. In this case, cadherins, a major class of cell-cell adhesion molecule, have been implicated in the latter stages of spheroid compaction. Indeed, MSC spheroid formation from umbilical cord-derived cells clearly requires E-cadherin (Lee et al. 2012). In addition, a paper published after this experiment was conducted (Zhou et al. 2017) showed that spheroid formation is associated with an increase in homotypic cell-cell adhesion via N-cadherin and E-cadherin, rather than through integrin mediated interactions. Although their study did not apply exogenous ECM to hanging drop spheroids, this indicates that cell-cell adhesion, rather than cell-ECM adhesion, is important in spheroid culture. In this magnetically levitated system, however, **N-cadherin** was significantly downregulated, therefore implying that this mechanism is not predominant in this spheroid system.
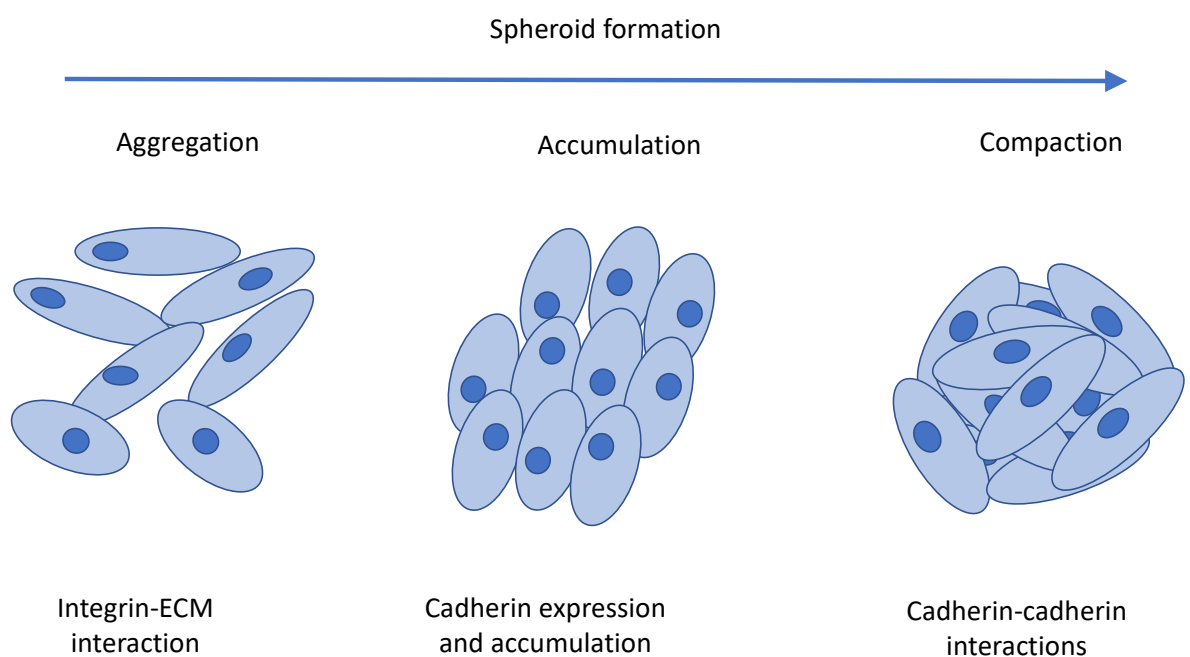
Figure 4.20 Schematic of the stages involved in spheroid formation.

The recent study by Zhou et al. (2017) also noted that 3D spheroid culture was accompanied by an increase in transcription of genes associated with pluripotency, particularly Nanog. Similar phenomena were observed in the gene expression analysis study presented here, with, for example, nestin, CD79, and

CD63. In the previous year, Zhou et al. (2016) investigated the mechanisms for the changes in gene expression in spheroids compared to monolayers, implicating cytoskeletal changes as the causative mechanism. The presence of an F-actin[6] network in the nucleus was observed in spheroid MSCs, which may influence gene expression by regulating chromatin organisation, as Nanog expression is associated with loose chromatin structure (Miyamoto et al. 2011). It is possible that a similar mechanism is acting in the spheroids described here, where actin is reorganised during spheroid formation and throughout culture.

High expression of the VLA-4 ligand **VCAM-1** has been used to identify a self-renewing, rapidly proliferating, and differentiating MSC population (Mabuchi et al. 2013). However, in this study expression of VCAM-1 has been significantly downregulated to a level that equates to a 32-fold decrease. The downregulation may simply reflect that the MSC spheroids are non-proliferating and quiescent.

ICAM-1[7] is also a glycoprotein that binds to integrins, including LFA-1, and is upregulated in BM MSCs upon the addition of nucleated umbilical cord blood (Romanov et al. 2017): rather than participating in MSC-MSC adhesion, ICAM-1 may have a role in facilitating MSC-HSC interactions. Again, ICAM-1 has been significantly downregulated in spheroids compared to monolayers, contrary to expectations.

The adhesion molecules examined in this study are mainly focused on cell-cell adhesion. Further work could examine molecules such as VLA-1 and VLA-2, which are known to interact with collagen specifically. Vimentin expression, another component of focal adhesions, was included in the gene panel, but no results were obtained for this gene.

4.4.2 MSC spheroid size increases relative to cell number

Compared to other MSC spheroid systems generated using different methods, these spheroids are smaller than expected, given the seeding density used. For example, Bartosh et al. 2010 reported MSC spheroids, generated through the

---

[6] F-actin = filamentous actin.

[7] ICAM-1 is also known as CD54.

hanging drop method, of approximately 400 µm diameter, equivalent to a CSA of approximately 0.13 mm^2, when cells were seeded at a density of 10,000 cells per drop. This is compared to a median cross-sectional area (CSA) of around 0.025 mm^2 for magnetically levitated spheroids when seeded with the same number of cells. Similarly, spheroids seeded at 100,000 cells per hanging drop had an approximate CSA of around 0.64 mm^2 (diameter of around 900 µm, Bartosh et al. 2010), compared to 0.2 mm^2 for the magnetically levitated spheroids. Notably, however, the hanging drop method causes formation of numerous small aggregates which gradually coalesce into a single spheroid. This spheroid does not then grow in size but progressively compacts between 48 and 96 hours (Bartosh et al. 2010).

Rossi et al. 2005 used a non-adherent surface to generate MSC spheroids. Similarly, the spheroids from this system were larger than those created through magnetic levitation (50,000 cells produced spheroids of 0.26 mm^2, compared with 0.025 mm^2 in the present study), although they were more comparable to those that were magnetically levitated. This ten-fold difference may be partly due to cell loss during the levitation process, in addition to the formation of several different spheroids.

Zimmermann & Mcdevitt (2014) produced spheroids that were slightly smaller but comparable in size to the magnetically levitated spheroids, using forced aggregation followed by centrifugation. However, given that these were initiated with an order of magnitude fewer cells than with the magnetic levitation method, this again suggests that the latter method produces smaller spheroids than those generated by alternative methods. A possible explanation for these size differences is that in a hanging drop system especially, the cells are forced to aggregate into a single structure. In the magnetic levitation method, cells are forced together, but this results in a collection of smaller aggregates each of under 1000 cells individually (Figure 4.4). These smaller spheroids may be more similar in structure to collections of cells within the BM compared with larger spheroids, as the diameter of BM sinusoids around which MSCs are found is up to 60 µm (Itkin et al. 2016), equivalent to a CSA of 2800 µm^2. Although the smallest spheroids produced through the method described here produced are larger than BM sinusoids, their conformation may be more similar to MSC clusters *in vivo* than the bigger spheroids.

Strong positive correlation was observed between spheroid size and spheroid number at all densities, in accordance with expectations (Figure 4.4). The largest spheroids were made up of over 500 cells individually. It is worth noting that the larger spheroids were less spherical and more cylindrical in shape compared to the smaller ones, due to the non-uniform properties of the magnetic field, as characterised previously in the Centre for Cell Engineering (Dejardin et al. 2011; Smith et al. 2010). A cylindrical shape may contribute to preventing central necrosis by decreasing the distance in one plane from the cells in the centre to the edge of the spheroid, maintaining diffusion of nutrients and oxygen. This may be reflected by the reduced expression of HIF1α in the spheroids.

4.4.3 MSC spheroid viability is maintained with increasing cell density

Many spheroid systems suffer from central necrosis when they reach a certain size threshold, due to increased diffusion distance for vital nutrients and potential internal hypoxia (Hirschhaeuser et al. 2010; Souza et al. 2010; Banerjee & Bhonde 2006). To assess the extent of necrosis in this magnetic MSC spheroid system, cross-sectional signals in the TRITC and FITC channels following viability staining were taken to identify clusters of dead and live cells, respectively. Figure 4.6 displays these cross-sections alongside fluorescence microscope images of spheroids formed from cells seeded at different initial seeding densities. For all densities, the TRITC signal is maintained at a low level with limited elongated peaks, which would indicate clusters of dead cells (central necrosis). On the other hand, the FITC signal is maintained at a high level, indicating consistent high viability across the spheroid.

As best as can be determined, given the often-irregular spheroid shapes generated, the diameter of the spheroids generated from this magnetic levitation method range between 200 μm and 360 μm (median size for the lowest and highest seeding densities, respectively). Areas of central necrosis were not detected in these spheroids. It has been reported that spheroids of diameters greater than 400-600 μm will exhibit central necrosis, at twice the thickness of the viable cell rim (Groebe & Mueller-Klieser 1996). As the magnetically levitated spheroids are below this threshold, they conform to this model, and do not exhibit excessive central necrosis.

4.4.4 MSCs grown in spheroids retain differentiation capacity

One of the defining features of MSCs is the capacity to differentiate into cell types of various lineages. MSCs have been documented as producing cells of the osteoblastic, chondrocytic, fibroblastic, myoblastic, and adipocytic lineages (Caplan & Correa 2011). Hence, MSC capacity for differentiation was assessed following an extended period of growth in spheroids, as shown in Figure 4.7.

Although MSCs grown in spheroids evidently retain adipogenic differentiation capacity, as evidenced by cells clearly stained with Oil Red O, the differentiation results are more ambiguous for chondrogenesis and adipogenesis. Although staining is observed, the nanoparticles contained in the cells confound the red/orange stains that indicate deposition of chondrogenic cells and calcific deposits, respectively. However, previous studies of this model have confirmed the differentiation potential of spheroids grown in media using a combination of histology and immunofluorescence (Lewis et al. 2016).

4.4.5 Spheroid culture maintains MSCs as quiescent

MSC quiescence within the bone marrow is important for retention of niche functionality. Therefore, the expression of certain key cell cycle genes in MSCs and MSC proliferation (via BrdU incorporation) were compared in the monolayer and spheroid culture systems.

With regards to the gene expression study, the results generally show that the cell cycle is downregulated and the MSCs are more quiescent in spheroids compared to monolayers. A large number of these genes are involved in the G1/S phase transition, all of which indicate a downwards trend or have remained similar to controls, suggesting that DNA replication is not triggered. Whilst none of these differences were statistically significant, this trend supports a previous study in the Centre for Cell Engineering, in which genes across different phases of the cell cycle were found to be reduced in spheroid culture (Lewis et al. 2017). There are several differences in the cyclins and main regulators of the cycle. The genes studied are summarised in Figure 4.21, indicating their role in the cell cycle, with further discussion of gene changes compared to monolayer controls below.

TP53 expression has significantly decreased in MSC spheroids compared to monolayers. TP53, also known as p53, is a tumour suppressor gene, which acts through multiple mechanisms to repair DNA and slow the cell cycle at the G1/S checkpoint. Loss of p53 in MSCs increases growth rate (Armesilla-Diaz et al. 2009), promotes senescence, chromosomal instability, and resistance to apoptosis (Velletri et al. 2016). Differentiation into osteogenic lineages is repressed by TP53 expression (Velletri et al. 2016), and both adipogenic and osteogenic differentiation are accelerated by p53 knockdown (Armesilla-Diaz et al. 2009), hence a reduction in p53 may indicate potential to differentiate.
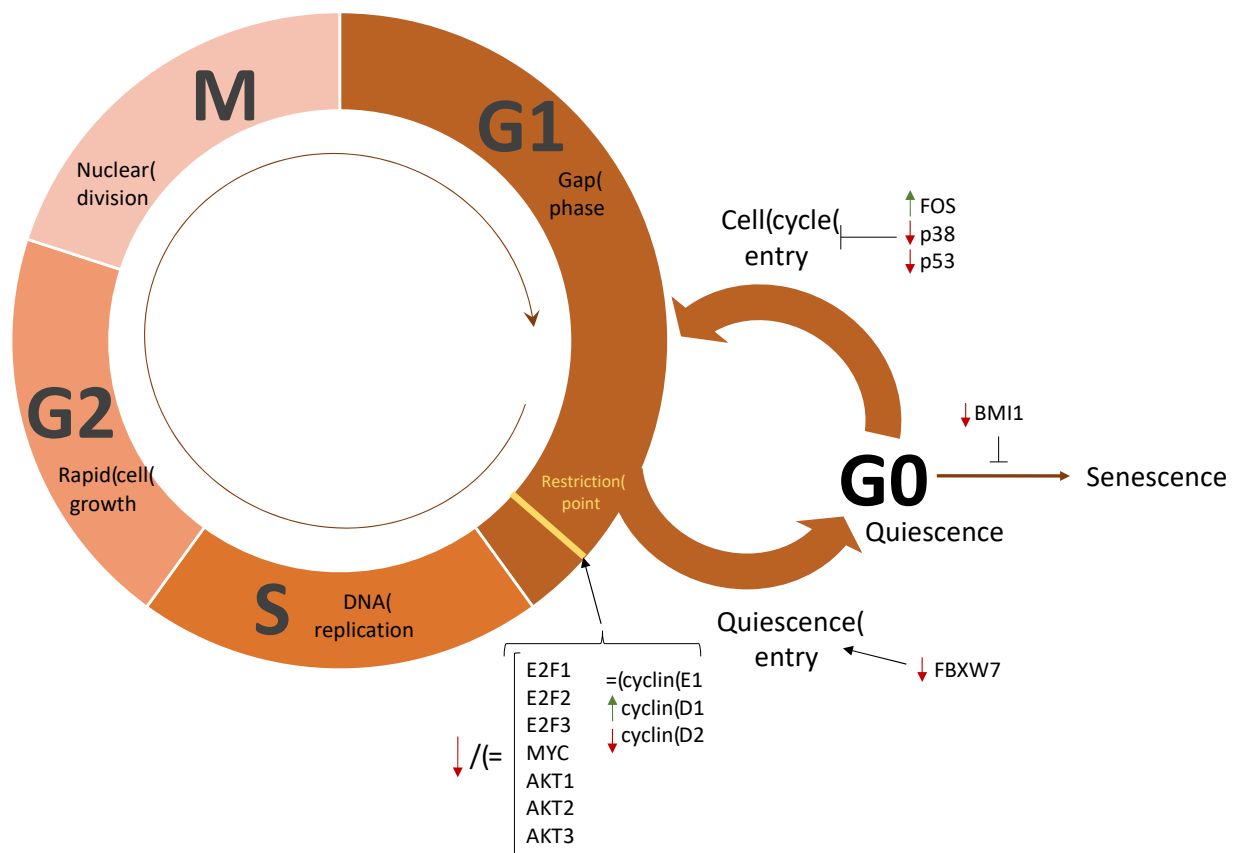
Figure 4.21 Schematic of the cell cycle including changes in gene expression in MSC spheroids identified from this analysis.
Green arrows, increased expression; red arrows, decreased expression.

The D-type cyclins phosphorylate Rb, freeing E2F for cell cycle activation. **Cyclin D2** increases MSC proliferation, and may be a biomarker for MSC transformation (Kono et al. 2013). Cyclin D2 expression has significantly decreased in MSC spheroids compared to monolayers, indicating that cells have decreased proliferation in the model. In contrast, **Cyclin D1** levels increased in spheroids, although this change was not significant.

Significantly increased **FOS** expression in spheroids indicates suppression of cell cycle gene expression, and increased progression to osteoblastic differentiation. FOS is a proto-oncogene and a TF. It forms a heterodimer with c-Jun, forming activator protein 1 (AP-1), a complex that binds DNA to influence gene expression. c-FOS is a negative regulator of cell growth, and prolonged expression suppresses entry into the cell cycle by HSCs. AP1 is a positive regulator of OB differentiation. (Matsumoto et al. 2012; Kushibiki et al. 2015; Liu et al. 2016). The large increase in FOS expression may be related to the increased expression of osteogenic markers observed (Figure 4.9).

As none of the expression changes between cell cycle genes in monolayers and spheroids are significant, it is hard to draw definitive conclusions. However, upregulation of c-FOS, and general downregulation of cyclins and TFs indicates a general trend towards MSC quiescence in spheroid culture. The BrdU assay further supports this conclusion (Figure 4.19), where a higher number of MSCs in monolayer cultures were proliferating compared to MSCs in spheroids. This is again consistent with a reduction in BrdU noted in magnetic MSC spheroids in results obtained from previous studies in the Centre for Cell Engineering (Lewis et al. 2016).

4.4.6 Spheroid culture maintains primitive MSC phenotype

As HSCs are supported by primitive MSCs within the bone marrow niche, maintenance of MSC phenotype is key to the success of generating a HSC permissive BM niche model. The expression of several genes that are key in maintaining MSC state as a regenerative, self-renewing pool of progenitors were therefore examined in both monolayer and spheroid culture. The results were encouraging, with a decrease recorded in **CD79**, which is a qualifying criterion of the identification of true multipotent MSCs (Dominici et al. 2006), and increased trends noted in **nestin**, **CXCR4**, and **CD34,** although none of these changes were significant. In addition, MSCs grown in either monolayers or spheroids for 7 days were analysed using immunohistochemistry to investigate both **STRO-1** and **nestin**, both key MSC features within the BM niche; results indicated increased levels of protein expression in spheroids compared to corresponding monolayer controls.

As previously described, **nestin** is a cytoskeletal component that potentially defines the HSC-supportive subset of MSCs in the BM (Méndez-Ferrer et al. 2010; Pinho et al. 2013). Nestin gene expression has increased 31-fold and demonstrated an increased level of staining in spheroids compared to monolayers. This is encouraging as it indicates that spheroid cultures are more able to support HSCs than monolayers. Whether nestin expression is merely retained to a greater extent in the spheroid culture, or whether this is a case of 'reversal'; i.e. the MSCs are induced by the 3D model conformation to begin expressing nestin following loss in the monolayer culture, is unknown. If expression is due to reversal, this is particularly interesting as it means that MSCs may be able to revert to a more primitive state simply by changing culture system and/or conformation. These results also suggest that MSCs require presence of gel/ECM, 3D culture, and/or intimate cell-cell interactions to express nestin and hence support HSCs. Nestin is an intermediate filament protein, originally observed in primitive cells of the nervous system. MSCs have been shown to express several specific neural proteins prior to differentiation, one of which is nestin (Tondreau et al. 2004), and subsequently nestin^{+} BM cells were shown to possess the fundamental properties of MSCs: self-renewal, trilineage differentiation, and colony-forming unit activity; as well as co-localising with HSCs within the niche (Méndez-Ferrer et al. 2010; Kunisaki et al. 2013). This nestin[+] subset is more quiescent, and although nestin^{+} cells participate in endochondrogenesis during development, in the adult marrow they preferentially contribute to the HSC niche rather than ossification (Isern et al. 2014; Ono et al. 2014).

STRO-1 is a marker used to isolate MSC colony forming units (CFU-C) (Kolf et al. 2007). However, MSCs in standard 2D culture gradually lose STRO-1 expression (Gronthos et al. 2003). The results presented here show that MSCs in spheroid cultures retain high STRO-1 expression for up to 7 days in culture, which increases over time, whereas it is lost in corresponding MSC monolayer cultures. Retention of STRO-1 suggests that the spheroid model system prevents differentiation and maintains the stem cell population.

Overall, the expression of primitive stem cell marker genes suggests that MSCs in spheroids are retaining their undifferentiated, stem cell-like properties to a greater extent compared to monolayers. These results are encouraging, as

maintaining self-renewal capacity is essential for niche formation and preservation and is key to the development of a HSC-permissive niche model.

4.4.7 Whilst maintaining phenotype, spheroid cultures may also induce bone marrow remodelling and differentiation

Many genes are involved in determining MSC fate, maintaining a pool of self-renewing progenitor cells, and thus maintaining HSC support functionality. Therefore, a selection of relevant genes involved in MSC differentiation were investigated. The majority of genes were noted as being similar between monolayers and spheroid culture. However, significantly increased expression of BMP2 (55.6 times higher in spheroids compared to monolayers) and significantly decreased expression of NFκB1 (0.45 times the level of monolayers observed in spheroids). In addition, both osterix and osteopontin (OPN) had large increases in expression.

The increased expression of osteogenic differentiation regulator bone morphogenetic protein 2 (**BMP2**) is interesting. BMP2 stimulates osteogenic differentiation, chondrogenic differentiation, and endochondral ossification in MSCs (Zhou et al. 2016). Other osteogenic genes such as osterix[8] (the 'secondary master regulator' of osteogenesis, Nakashima et al. 2002) are activated by BMP2 signalling, which is reflected in the increased **osterix** expression recorded. In contrast, most of the genes involved in differentiation have either decreased slightly or remained constant. As BMP2 can act in a non-cell autonomous manner, this may indicate that MSCs are secreting signals to remodel the BM niche, as they would *in vivo*, by inducing osteogenesis in surrounding cells.

Osteopontin (**OPN**) is a matrix glycoprotein that is involved in the calcification of bone and is a classic marker of osteoblastic differentiation in MSCs. OPN has slightly increased in the MSC spheroid cultures compared to monolayer. Although this may indicate a number of cells progressing to the osteoblastic lineage, the presence of OPN may also indicate an increase in quiescent HSC-supportive ability in the spheroids: it negatively regulates HSC number *in vivo,* and thrombin-cleaved OPN (tcOPN) is a chemoattractant for HSCs (Stier et al. 2005; Storan et al. 2015).

---

[8] Also known as SP7.

In fact, it has been speculated that the abundant presence of OPN in the endosteum may be the mechanism behind the varying cell cycle status of the HSCs in the different environments within the niche. However, this increase is not significant, and conclusions cannot be drawn.

Despite the gene expression results leaning towards an increase in bone marrow remodelling and osteogenesis, the expression of genes involved in osteogenic signalling are either not changed or slightly decreased in spheroids compared to monolayers. However, NFκB1 has been significantly downregulated. As part of the platelet-derived growth factor (PDGF) pathway, which may be required for osteogenic differentiation, it may have a role in osteogenic signalling (Goff et al. 2008). Therefore, this decrease may indicate a lower level of osteogenic differentiation in the spheroid model.

Several genes linked to chondrogenesis were also analysed, **LEF1** (Paik et al. 2012), **SMAD7** (Iwai et al. 2008), and RUNX1. However, no significant changes were observed in these gees, suggesting that the model environment has little effect on chondrogenic differentiation. This is also the case for GATA2, which can also be a marker of adipogenic differentiation (Kamata et al. 2014).

Analysis of differentiation markers on the whole suggests that MSCs in spheroids culture are retaining MSC phenotype, with a general decrease in differentiation into the chondro and adipo lineages. The increases noted in osterix and osteopontin are likely due to the large significant upregulation of BMP2. As many of the other genes involved in differentiation have not increased, this suggests that MSCs in spheroids are producing BMP2 in order to remodel the niche.

4.4.8 Spheroid culture enhances CXCL12 expression and secretion

The interfaces between cell types in the BM niche are not simply mediated by direct adhesion. Secreted cytokines and chemokines and their ligands also have a large role in facilitating entrance, retention, and maintenance in the microenvironment. **CXCL12** is fundamental to appropriate BM niche function. Expression by early MSCs is required for HSC maintenance (Greenbaum et al. 2013), is involved in HSC homing to the niche, and is necessary for HSC quiescence

(Tzeng et al. 2011). Therefore, expression of this chemokine is very important to evaluate. CXCL12 expression has slightly increased in spheroids compared to monolayers, although not to a large extent at day 3 (Figure 4.16). However, the levels of CXCL12 have dramatically increased at day 7, suggesting that a period of time in culture is required to stimulate production.

The secretion of CXCL12 was further investigated using an ELISA assay, performed in both serum-free IMDM medium and DMEM, to probe the effect of medium formulation on cytokine output. The statistically significant difference in CXCL12 expression between monolayers and spheroids at the 14-day time point could be due in part to (i) the greater proliferative potential of MSCs in monolayers, with an increased signal from an increased number of cells, and/or (ii) a retention of the cytokine within the collagen gel matrix with spheroid culture due to reduced diffusion of chemokines into the culture supernate, resulting in a lower detectable concentration. Therefore, a more helpful measurement to consider in the future would be CXCL12 output per cell.

There was a clear difference in CXCL12 levels secreted in monolayer and spheroid cultures in the different media, with serum containing DMEM stimulating higher secretion values. The maximum concentration measured was around 300 pg ml^{-1} in DMEM, whereas all measurements for IMDM samples were below 150 pg ml^{-1}, implying that CXCL12 is more highly expressed by cells grown in the presence of serum. However, in serum-free medium, spheroids and monolayers produce comparable levels of CXCL12, suggesting that MSCs in spheroids produce large amounts of CXCL12, especially given the diffusion and cell number issues mentioned above. Production by spheroids in both media formulations are also comparable, suggesting that spheroids produce CXCl12 without the presence of serum. There is some evidence to suggest that serum-free media reduces immunoregulatory potential in MSCs (Menard et al. 2013; Zimmermann & Mcdevitt 2014). Therefore, HSC-supportive serum-free media may undermine the supportive capability of MSCs in monolayers but not in spheroids. For cells grown in IMDM, there was no significant difference between the culture methods at any time point. Conversely, SFM may simply reduce the proliferative capacity of MSCs, with the observed differences instead indicating a higher output of CXCL12 from spheroids in comparison to cell number.

This corroborates the results obtained from immunohistochemistry, in which CXCL12 expression is increased in spheroid culture compared to monolayer, and also suggests that a longer time in culture is required for expression (as expression levels were higher at day 7 compared to day 3).

4.4.9 Spheroid culture does not enhance additional cytokine gene expression levels.

As explained with CXCL12 above, secreted cytokines, chemokines, and their ligands play a large role in maintenance of the niche microenvironment. Therefore, the gene expression of several other potentially interesting cytokines in both monolayer and spheroid culture was investigated, including stem cell factor (SCF), Tie-2 (angiopoietin receptor), Ang1 (angiopoietin 1) and TPO (thrombopoietin). Both SCF and Tie-2 were significantly decreased in spheroid culture, whilst Ang1 and TPO remained unchanged.

SCF is expressed by niche cells and has an important role in HSC migration. It is alternatively spliced into transmembrane and soluble forms. The transmembrane form has a role in HSC adherence to the niche (Driessen et al. 2003). SCF expression has been significantly downregulated, unexpectedly. Its receptor is c-kit[9], and c-kit positive MSCs have greater colony forming potential rather than differentiation potential. c-kit/SCF signalling may downregulate lineage specific genes (Suphanantachat et al. 2014), maintaining the MSC undifferentiated state.

Genes involved in niche interactions have, in general, decreased rather than increased as would be expected with enhanced inter-cell interactions and ECM binding. This may reflect that fact that the genes chosen are not in fact involved in spheroid formation, and another mechanism is acting. Furthermore, the cells may require the presence of HSCs and/or other cells to produce niche cytokines via a positive feedback loop.

---

[9] C-kit is aso known as CD117.

4.4.10   Spheroid culture influences major signalling pathways

Major signalling pathways play a role in cell-cell interactions within the niche. Two of these pathways, Notch and Hedgehog, are investigated here to evaluate whether spheroids influence signals between cells.

4.4.10.1   Spheroid culture decreases notch signalling

Notch signalling has a role in bone osteoblastic development and haematological development. It has also been implicated as a potential intermediary in the interaction between HSCs and the osteoblastic niche component, which also requires direct cell-cell interaction. Genes encoding components of the notch pathway are all decreased or unchanged in spheroid culture compared to monolayer controls, except for DLL4. **HEY2**, a downstream regulatory target of Notch, has been significantly downregulated. The effects of notch signalling on osteoblastic differentiation are ambiguous. *In vitro* and *in vivo* studies have produced contradictory results, possibly due to the divergent roles of notch at varying stages of differentiation. Removal of notch from MSCs induces a short term dramatic increase in bone (Hilton et al. 2008), hence, notch signalling may maintain a pool of MSC progenitors by suppressing osteogenesis. This is supported by evidence from Dong et al. (2010), showing that notch is a general repressor of MSC differentiation, without lineage bias.

Notch signalling has also been found to have a role in other stem cell niches, giving a precedent for its activity in the BM niche. Although there is some contradictory evidence, Notch signalling does seem to play a part in HSC maintenance by stromal niche cells (Weber & Calvi 2010). In addition, reduced Notch signalling increases CXCR4 expression, as is also seen in the magnetically levitated spheroids, hence increasing MSC migratory activity towards CXCL12 (Xie et al. 2013).

Notch 1-4 are transmembrane receptors that require direct cell contact for activation. JAG1, JAG2, DLL1, and DLL4 are Notch ligands. Ligand interaction induces Notch cleavage, and hence release of activated Notch intracellular domain (NICD), which translocates into the nucleus. Binding of NICD to CBF1 alters its activity from repressor to an activator, by recruiting coactivators such as

Mastermind-like (MAML). HEY1 and HES1 are downstream signals. A schematic of the Notch signalling pathway is depicted in Figure 1.8.

Notch signalling may inhibit osteoblastic differentiation *via* Hairy and Enhancer of Split (HES) and/or Hairy/enhancer-of-split related with YRPW motif (HEY) proteins, as they directly interact with RUNX2 to decrease its activity (Hilton et al. 2008). **HES1** protects cells from differentiation and senescence (Liu et al. 2015; Sang et al. 2010) and is important for MSC maintenance and suppression of chondrogenesis (Dong et al. 2010). However, levels in MSC spheroids are essentially unchanged from cells in monolayers, indicating no change in notch signalling. Although it has multifactorial effects, the significant **HEY2** expression decrease indicates an decrease in osteoblast related genes (Sharff et al. 2009).

In summary, the evidence from the notch signalling pathway gene expression study indicates that differentiation is decreased in spheroids and it may be increasing expression of HSC-supportive markers. This conclusion is drawn from the significant downregulation of its main target gene HEY2, indicating a general decrease in activity, and the decreased expression of the Notch4 receptor.

4.4.10.2   Spheroid culture does not influence hedgehog signalling

All the genes involved in the HH signalling pathway (**Error! Reference source not found.**) have been minimally downregulated or remain unchanged in spheroids compared to monolayer, save for PTCH1, which has been significantly downregulated. This may indicate decreased progression through the cell cycle, which would corroborate with analysis of the cell cycle genes examined (Figure 4.8), and possibly an increase in osteogenesis, confirmed by increased BMP2 and osterix (Figure 4.9).

Sonic hedgehog (SHH) is the best-studied human homologue of HH. Unfortunately, the qPCR in this study has not generated results for this gene. Therefore, the extent of SHH signalling is unknown. However, the signalling state can be inferred from the other components of the pathway that results have been obtained for. SHH increases ALP expression, osteocalcin expression, and triggers the BMP pathway in rat cells (J. Q. Cai et al. 2012). Applying recombinant SHH to rat BM-MSCs enhances MSC proliferation, as indicated by FACS and MTT assays (J. Q. Cai

et al. 2012). However, contradictory results in human MSCs were obtained by Plaisant et al. (2011), suggesting that the effects of HH signalling on MSCs are species-specific. The Plaisant study also showed that inhibited HH signalling decreases MSC proliferation, *via* arresting the cells in G1/G0 phases of the cell cycle, which is also observed in spheroid cultures (i.e. a decrease in HH signalling and a decrease in MSC proliferation).

PTCH1/2 are transmembrane receptors for HH ligands. They are located in primary cilia on the surface of almost all mammalian cells. When HH ligands bind, PTCH is displaced in the cilium by SMO, which then interacts with downstream elements to activate GLI family members (**Error! Reference source not found.**). T he two PTCH receptors examined here have both been slightly downregulated in spheroids. Alone, this would indicate an increase in HH signalling. However, the concomitant decrease in other pathway constituents suggests a general decrease in HH signalling. Osteoblastic differentiation is associated with a 60% decrease in SMO expression in adipose-derived MSCs, accompanied by a decrease in the number of cells exhibiting primary cilia (Plaisant et al. 2009). SMO expression remains at a similar level in spheroids compared to monolayers, again indicating that HH signalling is decreased and potentially that osteoblastic differentiation is more likely to occur.

Evidence from individual components of the HH pathway is conflicting. However, none of the genes have altered expression greater than four-fold in either direction. Hence, the trend is towards a slight decrease in signalling but with overall minimal change.

4.5 Conclusion

MSC spheroids within a 3D collagen gel culture have been evaluated in terms of structure and size. They express higher levels of stem cell markers at both the gene and protein levels, whilst genetic and BrdU analyses showed that spheroids are more conducive to quiescence than standard monolayer culture. An interesting result also indicates that the MSC spheroids may be progressing towards the osteoblastic lineage, as indicated by upregulation of genes involved in osteoblastogenesis. These results may indicate that they are forming an environment similar to the endosteal niche, which harbours a quiescent OB subset, and to which quiescent HSCs locate.

In the next chapter, this characterised 3D MSC model is extended to include other putative niche cells, OBs and ECs, to model the endosteal and vascular areas of the BM niche, respectively. The model is also used to examine its effect on HSCs and whether proliferation and maturation is affected.

CHAPTER 5

Chapter 5 Study of cell behaviour following co-culture within endosteal and vascular niche environments

5.1 Introduction

The preceding chapters have dealt with the characterisation of a 3D MSC spheroid BM model, and optimisation with a view to introduce HSCs to the culture model. In this chapter, the 3D model has been extended to include additional BM—resident cells in an attempt to model different areas of the BM niche.

As mentioned previously (Chapter 1), there are two niche 'zones' or environments within the BM: the vascular niche, around the BM blood vessels; and the endosteal niche, populated by quiescent osteoblasts on the bone surface. There are various models that have been proposed as to how these environments interact with each other; whether signals from the endosteum are in fact diffusing into a vascular environment, or whether this area independently comprises a distinct niche with a distinct function (Kiel & Morrison 2008, Figure 5.1). In addition to the presence of different cells within this areas, the MSCs present in each location may differ: nestin$^+$ MSCs are perivascular; and CXCL12-abundant reticular (CAR) cells, which are generally considered to include an MSC subset, are located near the endosteum (Morrison & Scadden 2014). To further complicate the issue, the distinction between the vascular niches, i.e. sinusoidal and arteriolar, is unclear and these may themselves serve different niche functions (Kunisaki et al. 2013).

These subsets may have different behaviours and properties which in turn have different influences on haematopoietic cells. For example, the endosteal niche is proposed to house quiescent, long-term HSCs maintained in G_0 for an extended period of time. Injury or other external signals may cause activation and migration to the vascular niche, priming them for differentiation. A separate niche at the endosteum may accommodate cells undergoing self-renewing divisions (Wilson & Trumpp 2006b). Furthermore, these niches feed into haematopoietic differentiation. There is evidence to suggest that the vascular niche biases HSC differentiation into myeloid and megakaryocytic lineages, due to cues originating from BM-ECs (Rafii et al. 1995). In a similar way, early lymphoid progenitors appear to occupy a distinct endosteal niche (Ding & Morrison 2013). In this way,

the niche environments locally control HSC quiescence and multilineage differentiation.
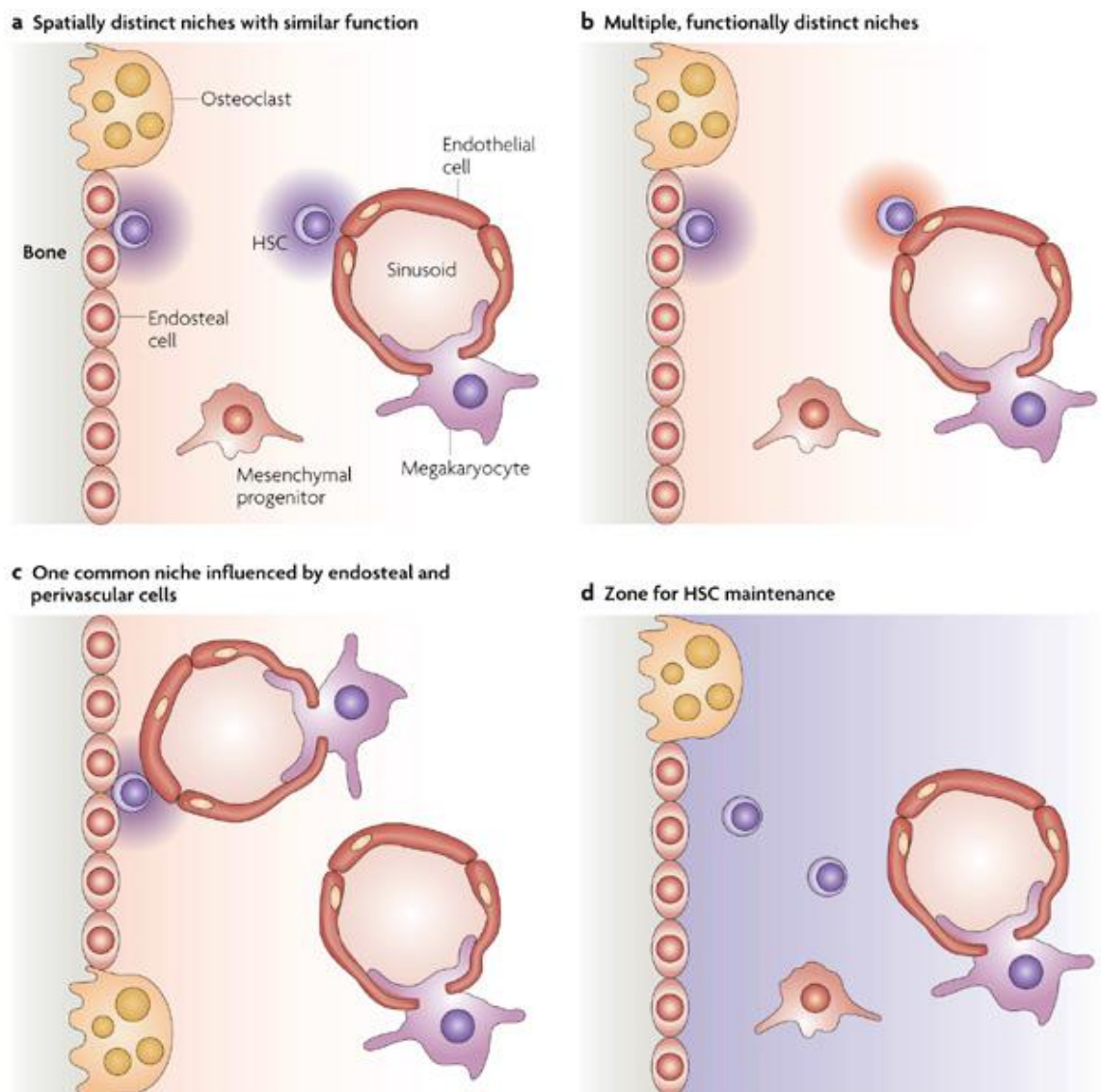
Figure 5.1 from image, with labels: "a Spatially distinct niches with similar function", "b Multiple, functionally distinct niches", "c One common niche influenced by endosteal and perivascular cells", "d Zone for HSC maintenance". Labels within: Osteoclast, Endothelial cell, HSC, Sinusoid, Bone, Endosteal cell, Mesenchymal progenitor, Megakaryocyte. Nature Reviews | Immunology

Figure 5.1 Schematic of possible relationships between endosteal and perivascular niches with in the BM. Taken from (Kiel & Morrison 2008).

5.1.1 Objectives

To evaluate the differences in HSC behaviour when cultured within different environments similar to the endosteal and vascular niches respectively, two triple culture models were developed. The endosteal niche model comprised OBs and an MSC spheroid, and the vascular model comprised ECs and an MSC spheroid. Freshly isolated HSPCs (following a CD34+ selection) were subsequently co-cultured within both environments. Whilst stromal-HSC co-culture is a decades-old concept, efforts to recapitulate these two niche environments by co-culturing HSCs with

additional cell types have been limited. The study described in this chapter aims to evaluate differences in cellular behaviour when cells are cultured in the model compared to when they are cultured in isolation, as follows.

1. The individual cell populations, i.e., MSCs, OBs, endothelial cells, and HSCs will be extracted from the model using methods detailed in earlier chapters.

2. RNA will be extracted from cell samples and expression of genes will be analysed in comparison to cell populations cultured in isolation. Categories of genes that will be examined are as follows:

   - Cell cycle genes, including cyclins, inhibitors, and promoters.

   - Markers of phenotypes, including those of haematopoietic lineages, osteoblastic lineage, endothelial cells, and MSCs.

   - Components of cell-cell signalling pathways including the Notch pathway and the Hedgehog pathway.

   - Genes involved in interactions between cells in the niche, including integrins, cadherins, cytokines, and their receptors.

3. The results of this analysis will be evaluated in the context of the niche environment and hence functionality of the model in replicating the bone marrow.

5.2 Materials and methods

5.2.1 Cell culture

MSCs and HSCs were obtained and cultured as described previously (section 2.1). HUVECs were obtained from Lonza and OBs were obtained from Promocell; cells were separately maintained in their respective optimal medium (EBM and osteogenic DMEM). Following the introduction of HSCs into the model, the resultant triple-cultured models were maintained in SFM (IMDM + 5GFs, section 2.1).

5.2.2 Generation of co-cultured endosteal and vascular bone marrow models

The co-culture models were established using a Transwell tissue culture insert (Figure 5.2, 12-well insert, 0.4 µm pore size, translucent, Greiner Bio-One International GmbH, Stonehouse, UK). ECs or OBs were seeded onto the membrane at 1×10^4 cells membrane^{-1}. MSC spheroids were then formed as previously described (section 2.2). At day 0 of the experiment, spheroids were implanted into a collagen gel within the Transwell insert. This MSC/OB or MSC/HUVEC co-culture was maintained for 7 days, with either OB medium (osteogenic media) or HUVEC medium (EBM) underneath the Transwell, and DMEM above the gel within the Transwell.
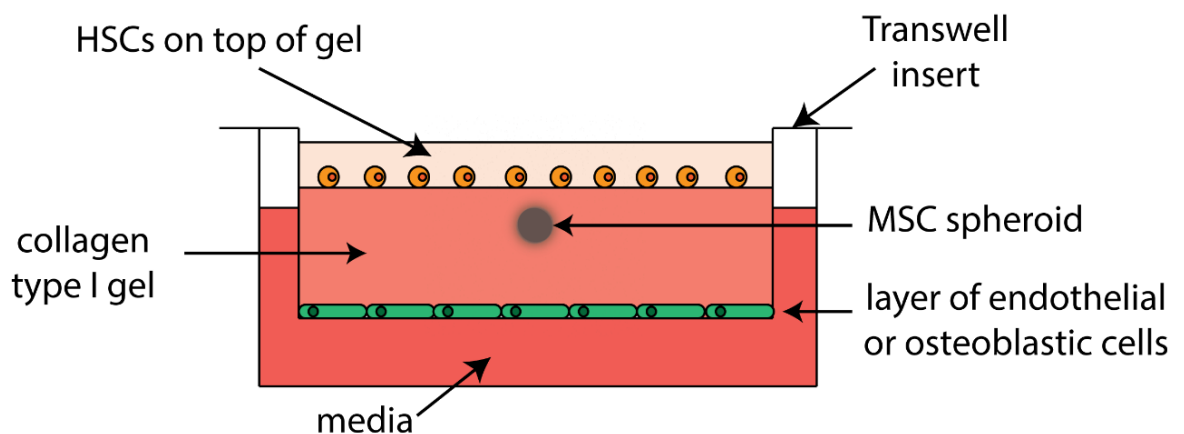
Figure 5.2 Schematic of the triple-culture endosteal and vascular BM models, indicating MSC spheroids cultured within a collagen gel directly above OB/HUVEC monolayers. HSCs are subsequently introduced on top of the gel.

Following 7 days of co-culture, freshly isolated BM CD34+ cells were seeded onto the gel in SFM at a concentration of 15,000 cells well^{-1}. After a further 7 days, the gel was digested with collagenase and the cell populations were extracted for downstream analysis. The timescale for the entire culture period is depicted in Figure 5.3.
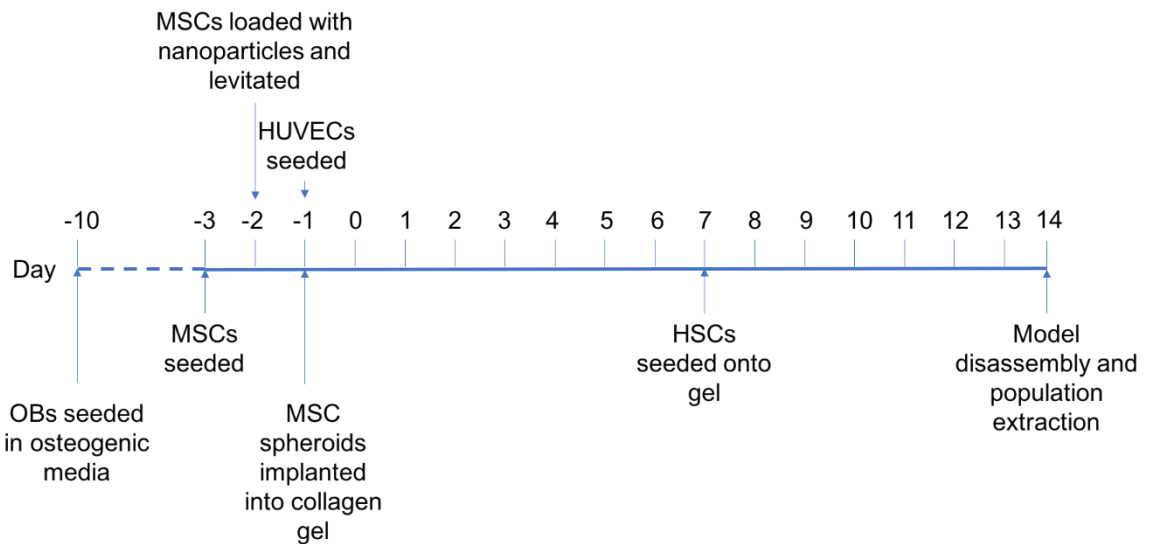
Figure 5.3 Experimental schedule with time points of events indicated.

5.2.3 Cell sample extraction

Suspensions obtained following digestion by collagenase were centrifuged at 400 x *g* to pellet the cells, and washed in PBS twice using the same parameters. If appropriate, cell populations were prepared and separated using FACS as described in section 3.3.4.

5.2.4 Gene expression analysis

Cell pellets were obtained from the endosteal and vascular niche triple-cultures and RNA was extracted and reverse transcribed according to the procedures described in sections 2.10 and 2.11. RNA samples were analysed on a BioMark HD Fluidigm real-time PCR machine, as described previously (section 2.12). Raw data values were normalised by subtracting the average of the 6 housekeeping genes (ENOX2, B2M, UBE, ATP, RNF, and CYC1) from each experimental value. These were specific for each RNA sample. Technical replicates for each biological sample (n = 2 or 3) were then averaged. The averages of the biological control samples

were subtracted from each biological experimental value. These values were input into the equation: fold change = $2^{-\Delta\Delta CT}$. The mean, SD, and CV were calculated from these transformed biological values. Statistical analysis was performed using Microsoft Excel or GraphPad Prism.

5.2.5 Phenotyping

The endosteal and vascular niche models were cultured according to the timeline depicted in Figure 5.3. Freshly isolated BM HSPCs from the sample added to the models at day 7, and following a further 7 days of culture in both models and under various control conditions (see below), HSPCs were subsequently stained and analysed using a flow cytometer according to the procedure described in section 2.13.2. The culture conditions for HSPCs and samples run on the cytometer are as follows:

1. Unstained control sample containing all cell types (HSPCs, MSCs, ECs, OBs).

2. HSPCs cultured in suspension in SFM.

3. HSPCs cultured in suspension in SFM, treated with collagenase on day 7.

4. HSPCs seeded onto a collagen gel, extracted with collagenase.

5. HSPCs cultured in a collagen gel with an MSC spheroid.

6. HSPCs cultured in collagen gel with an MSC spheroid and OBs.

7. HSPCs cultured in collagen gel with an MSC spheroid and ECs.

5.3 Results

5.3.1 Fluidigm

Following retrieval of individual cell populations from the endosteal and vascular models, RNA was extracted and samples were run on a Fluidigm BioMark HD 96x96 RT-PCR chip. Figure 5.4 depicts the heat map of the Fluidigm qPCR chip following the run.

Figure 5.4 Heat map generated from gene expression analysis using Fluidigm qPCR.
The genes are listed along the x-axis and the cell samples are listed along the y-axis. Yellow colours indicate high expression (low Ct value) and blue/purple colours indicate low expression (high Ct value).

#	Model	Cell type	#	Model	Cell type
1	Single sample	OB	21	HUVEC	MSC spheroid
2	Single sample	OB	22	HUVEC	MSC spheroid
3	Single sample	OB	23	Endosteal	HSC
4	Single sample	HUVEC	24	Endosteal	HSC
5	Single sample	HUVEC	25	Endosteal	HSC
6	Single sample	HUVEC	26	Endosteal	HSC
7	Single sample	MSC monolayer	27	Endosteal	HSC
8	Single sample	MSC monolayer	28	Endosteal	HSC
9	Single sample	MSC monolayer	29	Endosteal	MSC spheroid
10	Single sample	MSC spheroid	30	Endosteal	MSC spheroid
11	Single sample	MSC spheroid	31	Endosteal	MSC spheroid
12	Single sample	MSC spheroid	32	Endosteal	MSC spheroid
13	Vascular	HSC	33	Endosteal	OB
14	Vascular	HSC	34	Endosteal	OB
15	Vascular	HSC	35	Endosteal	OB
16	Vascular	HSC	36	Endosteal	OB
17	Vascular	HUVEC	37	Single sample	HSC
18	Vascular	HUVEC	38	Single sample	HSC
19	Vascular	HUVEC	39	Single sample	HSC
20	Vascular	MSC spheroid	40	Non-template control	Non-template control

Table 5.1 Sample identification for the numbers listed on the y-axis of Figure 5.4.

From the heat map, it is evident that the majority of the retrieved cell populations contained sufficient RNA to be successful. The non-template control (expected to fail) is situated at positions 40, 80, and 96, and failed for the majority of the primers used, except B2M in all three and MAML in the sample in inlet 40. As the former is a housekeeping gene and is expected to indicate high expression, and as a signal for MAML only appeared in one of the non-template control samples, the negative control sample was deemed valid. Only one primer failed completely (BMP7, position 95), with no signal generated in any of the cell samples.

Additionally, low Ct values were observed in many of the single culture control samples. This was expected, as these samples were of the highest quality and quantity. These patterns were observed in both the technical and biological replicates, indicating that the results were consistent.

5.3.1.1 MSC spheroid gene expression within the endosteal and vascular niche models

Gene expression in MSC spheroids within the co-culture models, as compared to spheroids cultured alone, was investigated (Figure 5.5). Differences were noted depending on whether the MSCs were cultured within a 'blood vessel' environment (with endothelial HUVEC cells; representing the vascular niche) or within a 'bone' environment (with osteoblasts; representing the endosteal niche). Cells were more quiescent in the endosteal niche model, as expected from the *in vivo* BM environment.

Cell cycle genes (Figure 5.5A) were generally increased in expression in the endothelial HUVEC model but decreased in the OB model. This suggests that the models reflect the vascular (active) and endosteal (quiescent) niches, respectively. The G_1/S transition-related E2F TFs all increased in expression in the HUVEC model, as did MCM4. AKT2 decreased in expression in the HUVEC model, and AKT1, and MYC did not change compared with spheroids in isolation. No results were obtained for cyclin E1, but cyclin D2 increased in expression, although not to the same extent as in the OB model spheroids.

Both environments produced similar levels of MSC **stem cell markers** (Figure 5.5B), except for an increase in the CXCL12 receptor (CXCR4) and nestin in the endosteal model. Conversely, **differentiation markers** (Figure 5.5C) were decreased in the endosteal model (bar one gene), whilst MSCs appeared to be more prone to differentiation in the vascular/sinusoidal model.

MSC spheroids cultured in both bone and vascular environments had generally decreased expression of **cell adhesion molecules** when compared to single culture spheroids (Figure 5.5D). The one exception was ICAM-1, which increased with osteoblast co-culture.

Four key HSC supportive **cytokines and receptor genes** were analysed. Generally, MSCs in the endosteal model demonstrated a decrease in expression. Meanwhile, Tie-2 and TPO were both increased in the vascular model (Tie2 expression increased by around 32-fold).

Finally, **notch pathway** genes were generally decreased in both co-cultures, indicating a decrease in activity of notch signalling. **Hedgehog signalling** remained similar to the control, although HHIP expression increased in both models.
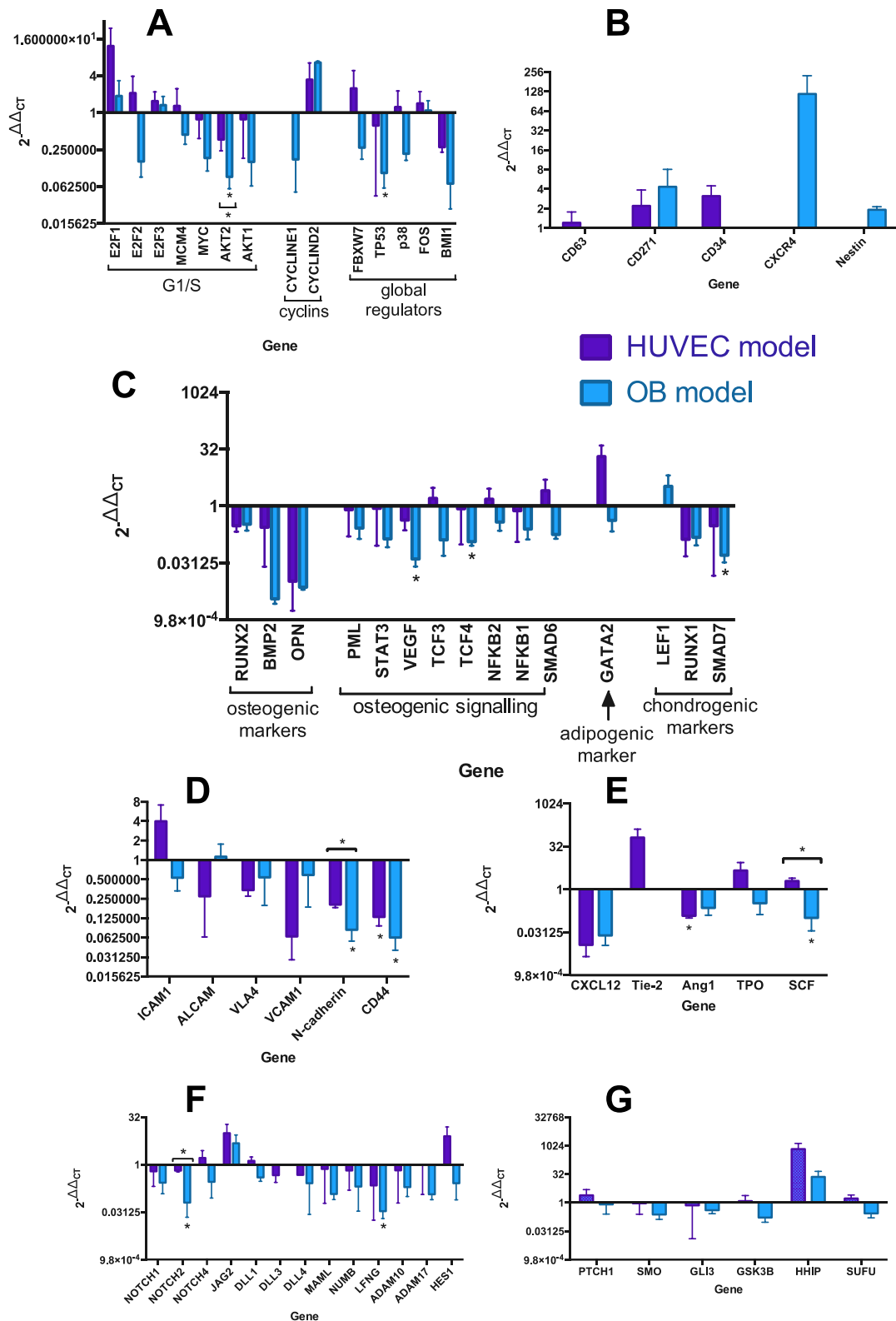
Figure 5.5 Fold-change in expression of genes in MSC spheroids in co-culture models compared to those in isolation.

Values presented as mean fold change ± standard error of the mean, n ≥ 2. A, Cell cycle genes; B, Stem cell markers; C, MSC differentiation markers; D, Adhesion genes; E, Cytokines and receptors; F, Notch signalling genes; G, Hedgehog signalling genes. Statistical significance was evaluated using the Kruskal-Wallis test followed by Dunn's multiple comparisons test (three samples) or the Mann-Whitney U test (two samples), *p < 0.05, **p < 0.01.

5.3.1.2 Endothelial cell gene expression within a triple-culture model

Gene expression in ECs at the 14-day time point, following co-culture is compared here to the control condition (EC monolayer grown in isolation, Figure 5.6). In summary, ECs cultured with the 3D model exhibited decreased proliferation, reduced cell signalling and adhesion, and adopted a mature phenotype.

Expression of genes related to the **cell cycle** generally decreased in ECs in co-culture. The one exception was the cell cycle suppressor FOS, which increased in expression by 16-fold (Figure 5.6A).

A mixed picture is presented by genes related to **angiogenesis**. Positive regulators both increased and decreased in co-culture, as did negative regulators. Genes that are used to define **vascular phenotype** also generally decreased, with a large decrease noted in nestin expression (Figure 5.6B).

Expression of genes involved in niche interactions, both directly *via* **adhesive molecules** and indirectly *via* **cytokines** (Figure 5.6C&D), decreased. In particular, c-kit was downregulated by the equivalent of over 30-fold.

Genes involved in the **Notch signalling pathway** both increased and decreased in expression. However, overall the pathway was slightly upregulated, as evidenced by the increased expression of the downstream components HES1, HEY1, and HEY2 (Figure 5.6E). In contrast, the **Hedgehog signalling pathway** was universally downregulated, with the greatest decrease observed in HHIP expression (Figure 5.6F).
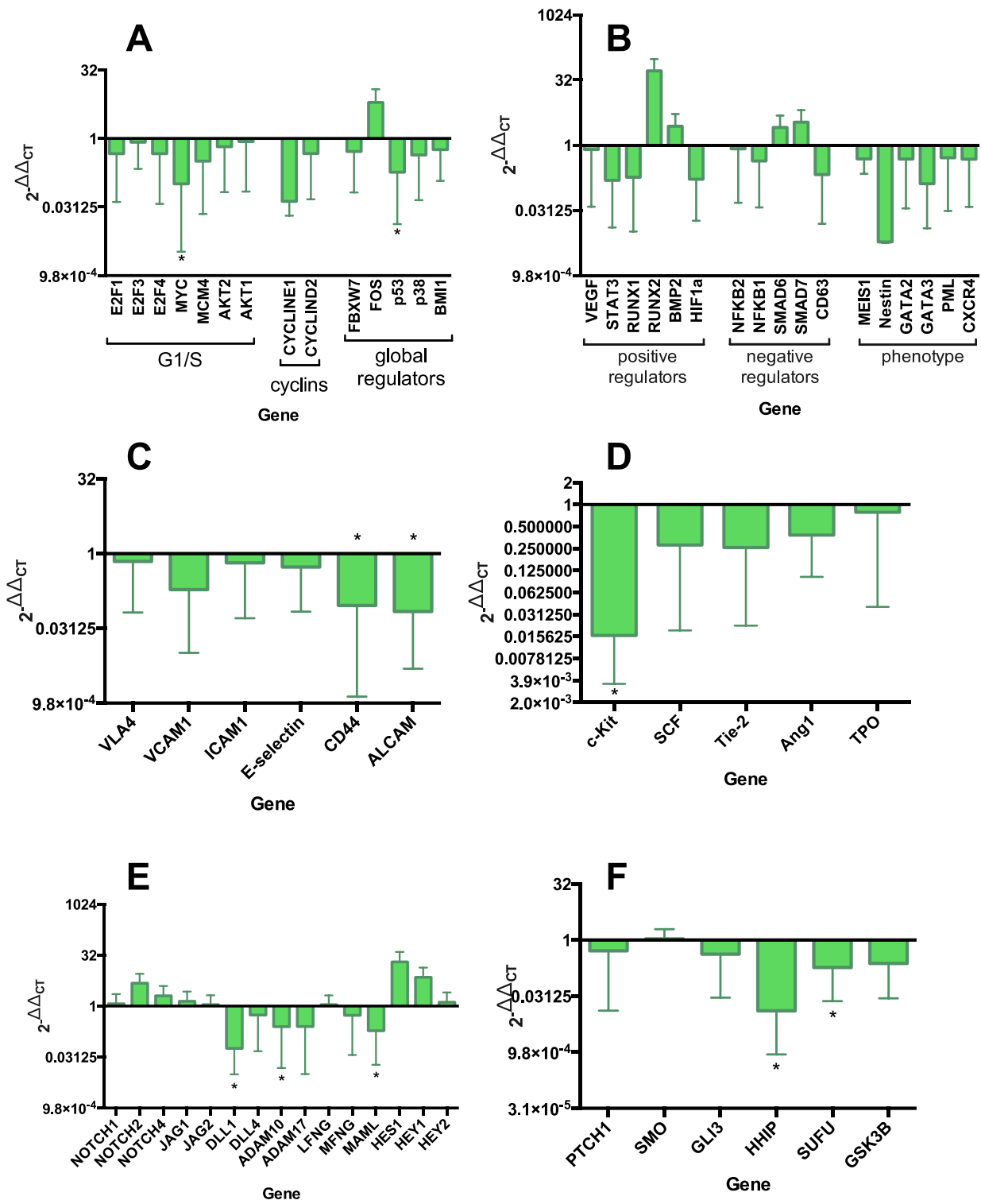
Figure 5.6 Fold-change in expression of genes in endothelial cells in the co-culture model compared to those in isolation.
Values presented as mean fold change ± standard error of the mean, n ≥ 2. A, Cell cycle genes; B, Angiogenesis-related genes; C, adhesion molecules; D, cytokines and receptors; E, Notch signalling genes; F, Hedgehog signalling genes. Statistical significance was evaluated using the Mann-Whitney U test, *p < 0.05.

5.3.1.3 Osteoblast gene expression within a triple-cultured model

Gene expression was analysed in OBs when cultured in the co-culture model for 24 days compared to culture in isolation (Figure 5.7). In summary, OBs cultured with the 3D model slowed their proliferation and exhibited reduced cell signalling and adhesion. With regard to the **cell cycle**, the general trend in expression of genes was very similar to the pattern observed in the MSC spheroids (Figure 5.7A). Downregulation of BMI1, E2F TFs, MYC, and MCM4 indicated a slower progression through the cell cycle, as did upregulation of the cell cycle suppressor FOS. However, the levels of cyclin E1 and cyclin D2 increased or remained the same. Similar to the MSC spheroids, FBXW7 and TP53 decreased, giving a contrary indication.

The expression of **MSC markers** remained similar in the co-culture model compared to spheroids alone, although the general trend was towards decreased expression (Figure 5.7B). Genes related to **differentiation** also remained similar, and generally decreased, saving GATA1, GATA3, and OPN. **Osteogenic markers and signalling** generally decreased compared to monolayers, although osteopontin, found in mature OBs, was increased (Figure 5.7C).

Expression of **niche interaction** genes generally decreased in co-culture. Adhesion gene expression levels remained similar or have decreased, with a significant decrease in VLA-4 levels. However, VCAM1 and ICAM1 levels slightly increased (Figure 5.7D).

Expression of most of the **intercellular signalling** genes related to niche function remained similar in the model compared to monolayer culture. CXCL12 expression increased three-fold, and Ang1 expression decreased to less than a quarter of the level in monolayers (Figure 5.7E). However, large changes in notch signalling and hedgehog signalling were observed: large decreases occurred in many of the pathway components (Figure 5.7F&G).
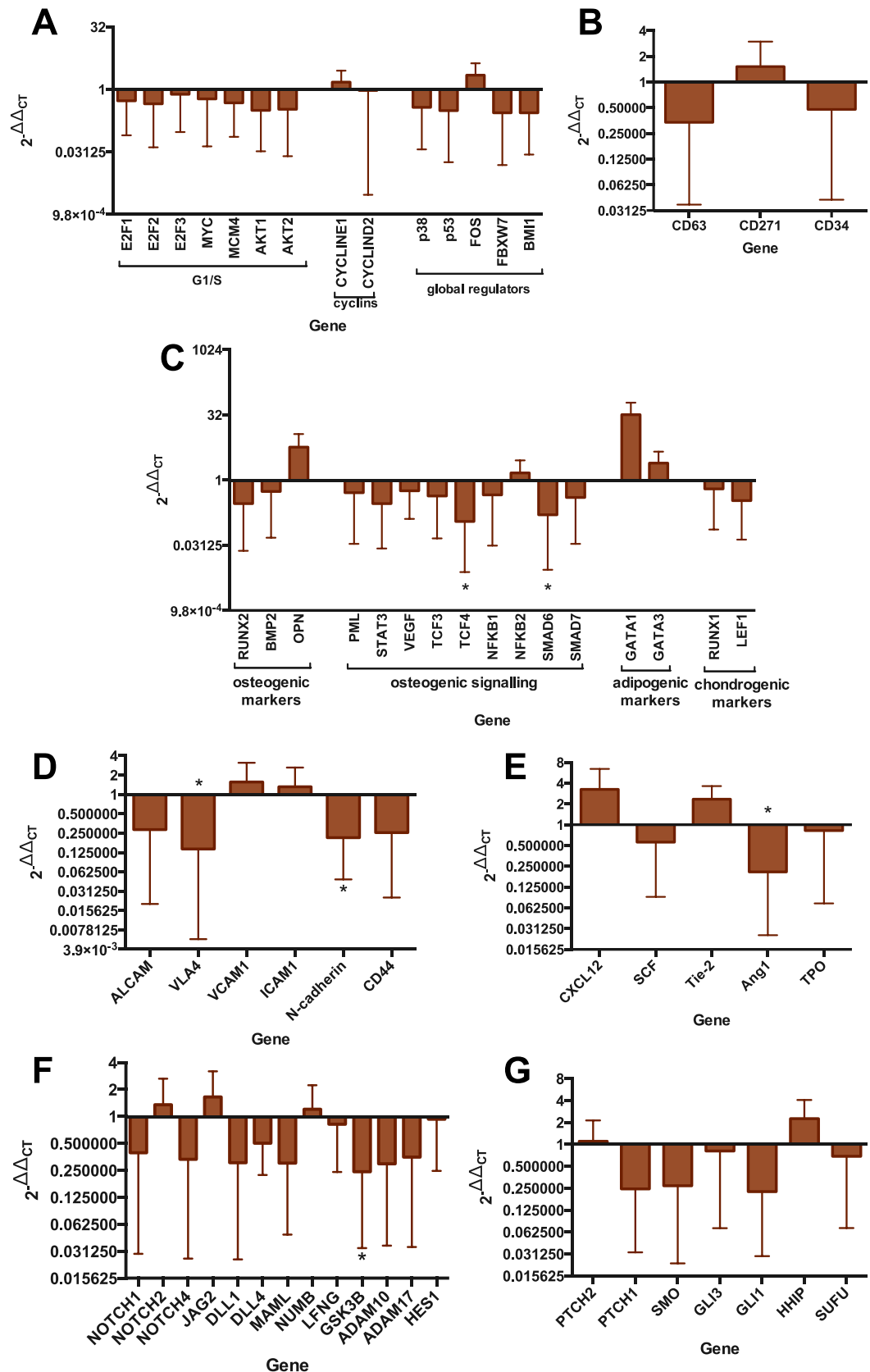
Figure 5.7 Fold-change in expression of genes in osteoblasts in co-culture models compared to those in isolation.
Values presented as mean fold change ± standard error of the mean, n ≥ 2. A, Cell cycle genes; B, Stem cell markers; C, MSC differentiation markers; D, Adhesion genes; E, Cytokines and receptors; F, Notch signalling genes; G, Hedgehog signalling genes. Statistical significance was evaluated using the Mann-Whitney U test, *p < 0.05.

5.3.1.4 Haematopoietic stem cell gene expression within an endosteal and vascular BM niche environment.

Gene expression in HSCs with an MSC spheroid within an endosteal or vascular niche environment for 7 days was compared to expression in HSCs cultured in isolation (in suspension, Figure 5.8). A general increase in gene expression was observed in all gene categories included in the analysis.

Genes involved in G_1/S transition and global regulators of the **cell cycle** were all increased in the niche models compared to isolated culture (Figure 5.8A). This increase was greater in the endosteal model compared to the vascular model for all genes.

All genes involved in the **notch signalling pathway** increased in expression in both models (Figure 5.8B). This increase was greater in the endosteal model, except for DLL3 and HEY1. Results were not obtained for components of the Hedgehog signalling pathway in HSCs.

Expression of genes related to **niche interactions** between cells generally increased, as did all **cytokine** interaction genes in both models (except MPL in the endosteal niche model) (Figure 5.8C). Likewise, **cell adhesion** genes were also increased, in particular in the endosteal model HSCs (Figure 5.8D).

The expression of all genes involved in **differentiation** into different haematopoietic lineages increased (Figure 5.8E). This was true for genes defining progenitor characteristics, those involved in erythroid differentiation, lymphoid differentiation, and myeloid differentiation. In general, the increase was greater in the endosteal model HSCs. With regard to progenitor markers, both models exhibited higher levels of marker expression than the corresponding suspension cultures; in addition, the expression levels appeared higher in the endosteal model as compared to the vascular model. The exceptions within the progenitor related genes were GATA2, which was upregulated to the same level in both models, and CD34, which was increased to a greater extent in the vascular model. For markers of erythroid differentiation, expression in both models was higher than in the control, and expression was higher in the endosteal model than in the vascular model. Expression of lymphoid lineage markers was increased in both models

compared to the corresponding control suspension cultures, with a similar trend, although GATA3 and CD79 were increased to a higher level in the vascular model. A similar pattern was observed in genes related to myeloid differentiation, with general increase in both models, and SMAD7 was the only gene related to myeloid differentiation that is increased to a higher level in the vascular model than the endosteal model.
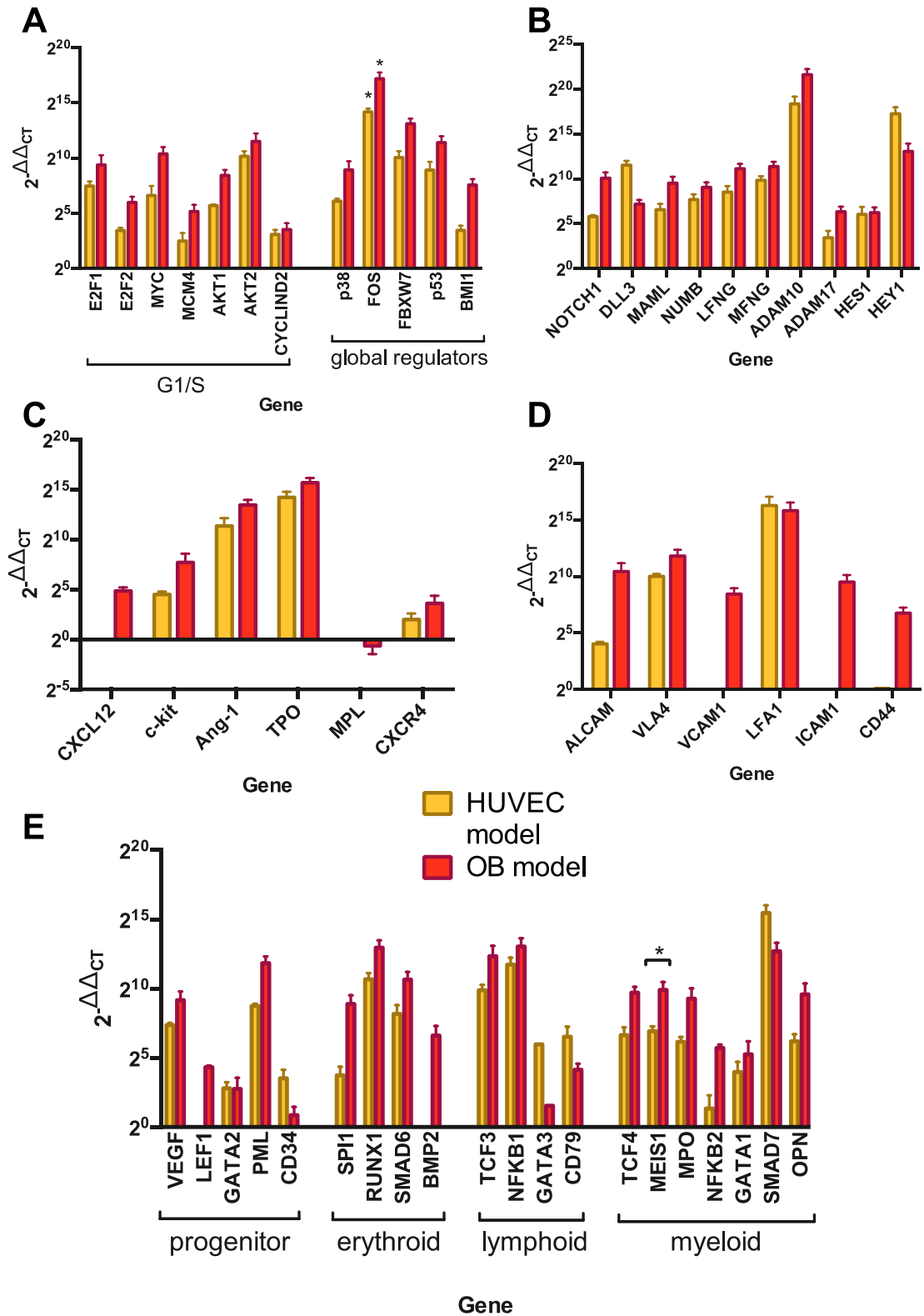
Figure 5.8 Fold-change in expression of genes in HSCs in co-culture models compared to those in isolation.
Values presented as mean fold change ± standard error of the mean, n ≥ 2. A, Cell cycle genes; B, Notch signalling genes; C, cytokine interaction genes; D, adhesion genes; E, haematopoietic differentiation related genes. Statistical significance was evaluated using the Kruskal-Wallis test followed by Dunn's multiple comparisons test (three samples) or the Mann-Whitney U test (two samples), *p < 0.05.

5.3.1.5 Hypoxia (HIF1α) expression in all cell types in the endosteal and vascular niche models

Hypoxia is an important parameter within the BM, as the organ is constitutively hypoxic, despite being highly vascularised (Morikawa & Takubo 2016). Cells in the BM express high levels of hypoxia-inducible factor alpha (HIF1α). The effect of co-culture within the endosteal and vascular models on hypoxia in the different cell types was therefore investigated by looking at expression of HIF1α (Figure 5.9). For MSCs, OBs, and HUVECs, levels remained similar compared to the controls (cells cultured in isolation, the same as in preceding sections). However, large increases in expression were noted in HSCs when cultured in both the endosteal and vascular niche models, compared to when cultured in isolation, with a slightly larger increase in the endosteal model.
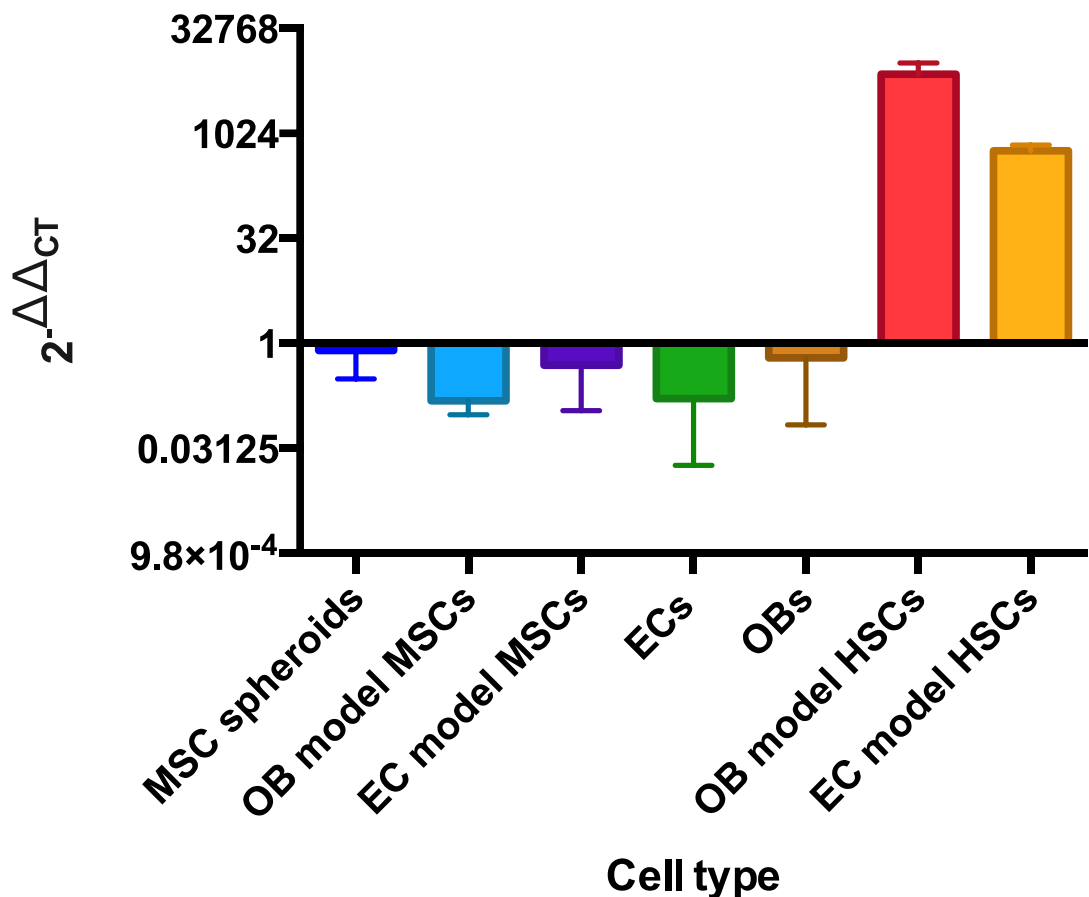
Figure 5.9 Fold-change in expression of hypoxia-inducible factor (HIF1α) in cell types in the endosteal and vascular models compared to the respective controls.
MSC, mesenchymal stem cell; EC, endothelial cell; OB, osteoblast; HSC, haematopoietic stem cell. Statistical significance was evaluated using the Kruskal-Wallis test followed by Dunn's multiple comparisons test (three samples) or the Mann-Whitney U test (two samples).

5.3.2 Phenotype analysis

Following extraction from the model after 7 days of culture, HSCs were analysed in terms of their surface markers to ascertain the extent of differentiation into various haematopoietic lineages.

5.3.2.1 Progenitor subsets

Using expression of several cell surface markers as described in section 2.13.2, populations of individual lineage progenitors were identified after 7 days of culture within the endosteal and vascular models or under various control conditions (Figure 5.10). As a control in the phenotyping experiment, a suspension sample treated with collagenase was included to ascertain the effect that the enzyme has on cell surface markers; as it has been documented to affect some lymphocyte surface markers (Abuzakouk et al. 1996).

Following culture, the percentage of CD34+ cells decreased dramatically in all cell populations (from 84% immediately following isolation). This suggests that the majority of cells in culture were differentiating. HSCs cultured with ECs retained CD34 expression to the greatest extent, followed by cells in suspension (both treated and untreated with collagenase). When looking at the HSC fraction, freshly isolated cells contained approximately 10% HSCs, which was reduced 7 days post-culture; cells in 3D gel culture yielded a higher percentage of HSCs than those in suspension culture and the vascular and endosteal models. Multipotent progenitors (MMPs) decreased in a similar manner, with a decrease from approximately 10% in freshly isolated cells to below 1% in all culture conditions.

With regard to the oligoprogenitor subsets CMPs & GMPs, numbers retrieved post-culture were similar to those of freshly isolated cells, suggesting that these cells were not increased in number following time in culture. However, MEPs were clearly reduced in all culture conditions compared to freshly isolated cells, with small populations remaining particularly in the HSCs in gel and HSCs with a spheroid. Finally, the lymphoid lineage progenitors (MLPs & CLPs) were below 1% in all conditions, but remained at the highest levels in suspension culture.
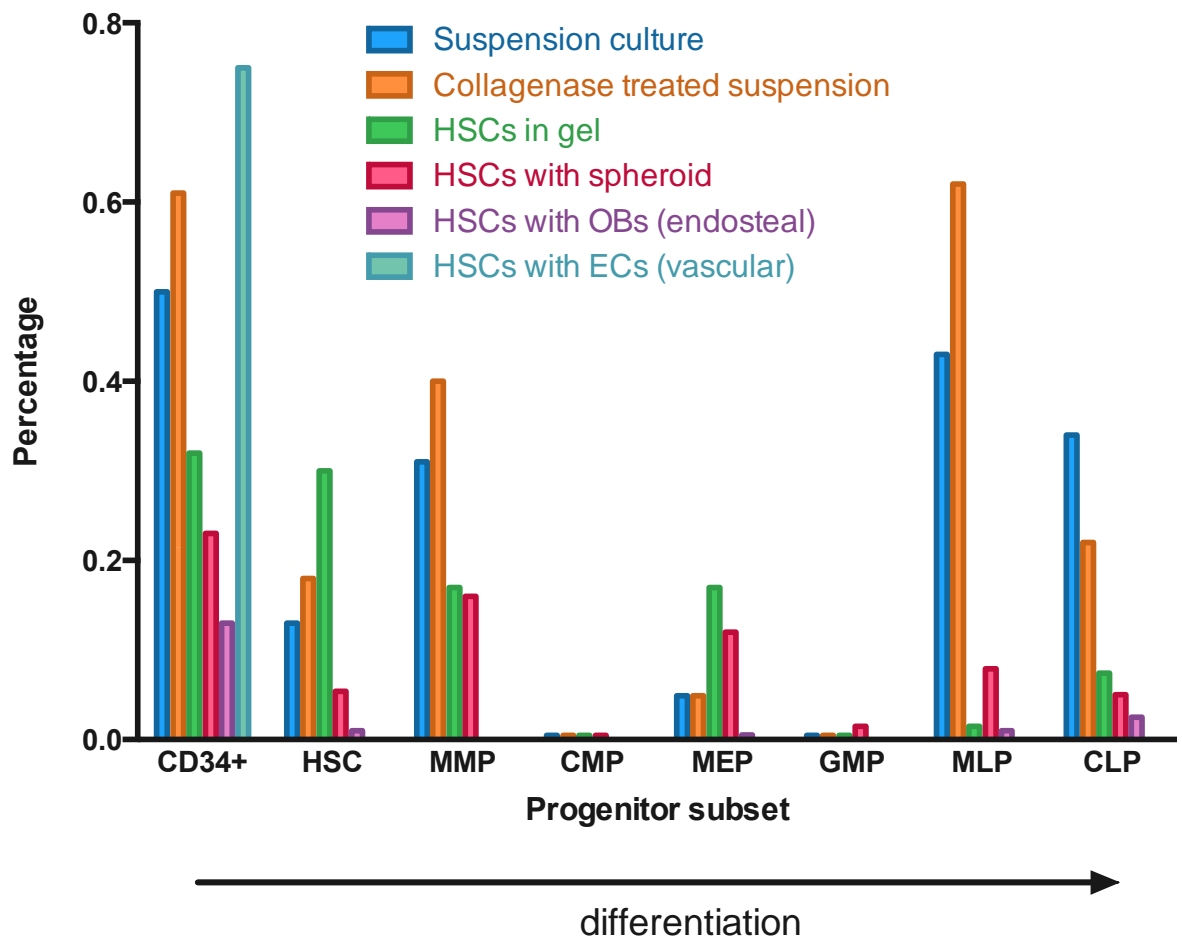
Figure 5.10 Percentage composition of different haematopoietic progenitor subsets following extraction from co-culture models or under various control conditions.
HSC, haematopoietic stem cell; MPP, multipotent progenitor; CMP, common myeloid progenitor; MEP, megakaryocyte-erythroid progenitor; GMP, granulocyte-monocyte progenitor; MLP, multi-lymphoid progenitor; CLP, common lymphoid progenitor.

5.3.2.2 Lineage marker expression

Expression of several lineage markers indicating differentiation into mature haematopoietic cells was investigated (Figure 5.11). CD7 expression was initially low and remained so in all samples at day 7. CD10 was initially expressed in approximately a quarter of cells, but disappeared from the population in all samples by day 7. CD13 was expressed in approximately a quarter of cells in the majority of samples after 7 days of culture. However, this percentage was decreased by about half in the endosteal model, and was slightly increased by culture within a gel. CD14 was essentially absent from all samples at day 7. CD34 was expressed by approximately 20% of cells in all samples, save for HSCs cultured with OBs, in which the marker was essentially absent. The cells cultured with ECs had slightly increased CD34 expression over the suspension cells. CD36 was initially expressed in just above 20% of cells in most samples. In HSCs cultured with OBs,

this proportion was slightly lower. However, in HSCs extracted from the vascular model, there was a large increase in CD36 expression, to over 50% positive. CD41a was initially expressed at a low level, which was maintained in all experimental samples, except for HSPCs from the OB model, in which there was no expression remaining. Overlaid fluorescence profiles for each antibody in each sample are provided in Appendix A (Figure A.1 and Figure A.2) for more information about expression by the populations.

Marker	Cell subset/function
CD34	HSC marker
CD45	Present on all differentiated haematopoietic cells except erythrocyte progenitors and differentiated cells. Not expressed by megakaryocytes
CD44	HA receptor, expressed ubiquitously
CD36	Expressed on monocytes/macrophages, platelets, megakaryocytes, basophils, and erythrocytes
CD41a	Integrin α chain 2b, important for platelet aggregation (fibronectin receptor)
CD10	PreB cells, preT cells; some T cells, B cells, and granulocytes
CD7	Thymocytes and mature T cells
CD13	Aminopeptidase expressed on T cells, monocytes/macrophages, and granulocytes (myeloid antigen).
CD14	Macrophages and neutrophils (to a lesser extent).

Table 5.2 Function of cell surface markers used to identify subsets of haematopoietic cells in experimental samples.
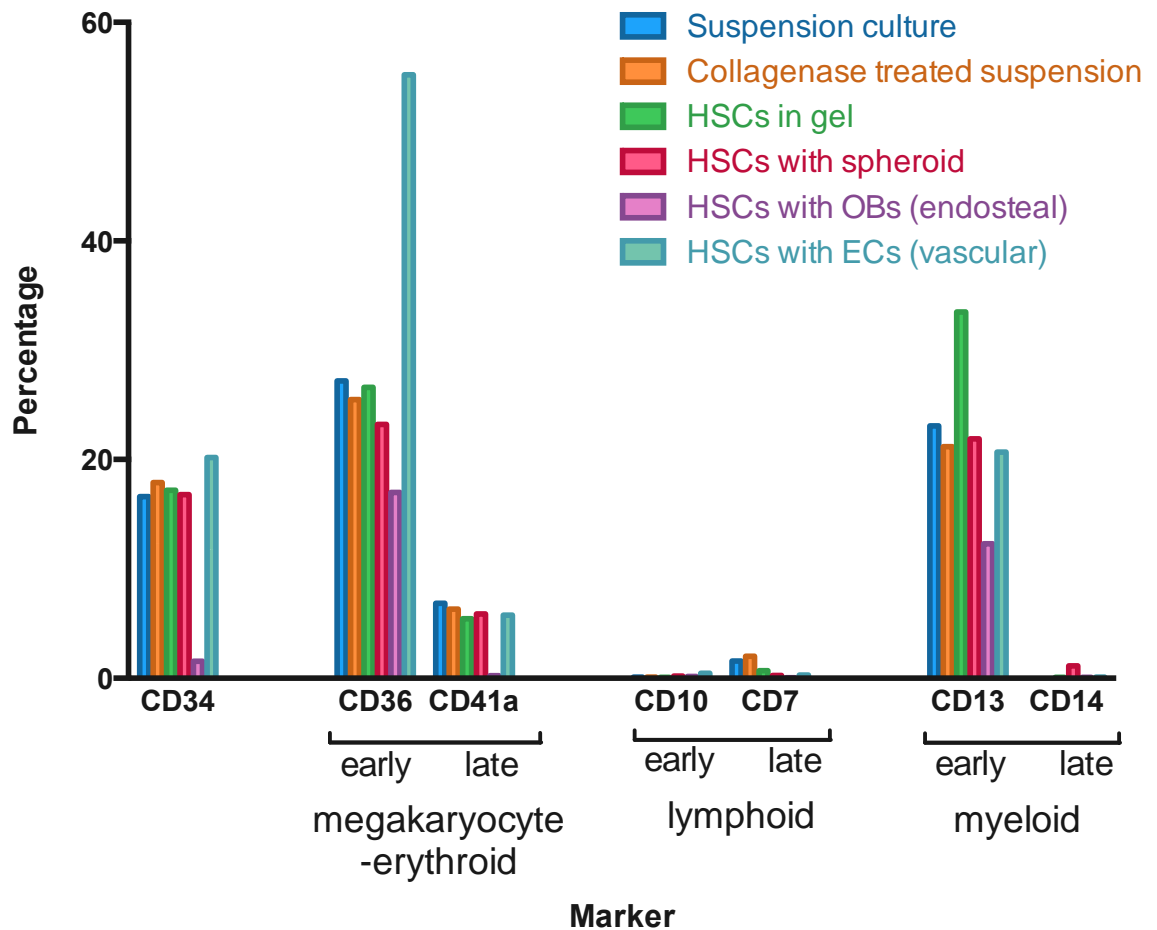
Figure 5.11 Percentage of cell population expressing different haematopoietic lineage markers.

5.3.2.2.1 Collagenase treatment does not affect the success of phenotypic identification

The expression of all markers in the collagenase treated sample compared with the untreated control suspension was similar (Figure 5.10 and Figure 5.11). Therefore, the results obtained from cells extracted from collagen using collagenase are reflective of the true expression levels.

5.3.2.2.2 The proportion of CD34+ cells identified in a sample is dependent on the antibody used

Two separate antibodies against the CD34 marker, each labelled with a different fluorophore, were used for phenotyping for two different panels (Figure 5.10 and Figure 5.11) on the same samples[10] (both freshly isolated cells and those extracted from the model). However, the results produced from the two antibodies were

---

[10] The different antibodies were used in order to increase the range of fluorophores used for each panel.

vastly different, as shown in the profile plots for each antibody organised by sample (Figure 5.12). From this, it is evident that the separation between positive and negative cells was more discernible with the APC antibody. The two populations were less easily defined with the PerCP antibody. As APC is inherently a brighter fluorophore, the results from this channel are probably more reliable, and a better reflection of the true situation. Percentages of CD34+ cells were between 96% and 84% at day 1, using the ACP and PerCP antibodies, respectively. This equates to a difference of around 10%. However, at day 7 this difference increased to around 20%, (under 1% compared with around 20%) although the ratios of CD34+ cells to other cells were similar between samples.

This difference has connotations for the accurate identification of the progenitor subsets in the samples, as the initial step of the gating strategy relies on isolating CD34+ cells, and all subsequent populations are identified from within this population. Hence, the frequency of progenitor subsets may be underestimated (Figure 5.10). To resolve this issue in the future, the lineage marker in the panel, which currently occupies the FITC channel slot, could be replaced with a brighter CD34-FITC antibody.

	SAMPLE
	Unstained sample
	HSPCs cultured in suspension
	Collagenase treated HSPCs
	Endosteal model HSPCs
	Vascular model HSPCs
	HSPCs cultured in gel
	HSPCs cultured in gel with spheroid
	Day 1 sample
	Isotype control sample
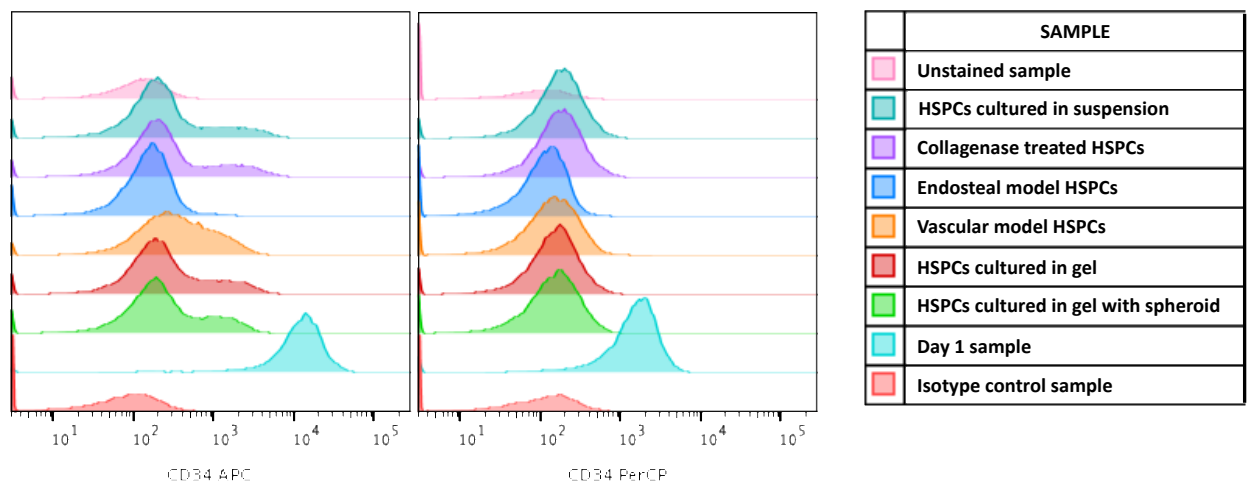
Figure 5.12 Comparison of signals from APC and PerCP CD34 antibodies, both used in different cell phenotypic panels on the same samples (listed).

5.4 Discussion

In this chapter the original MSC spheroid bone marrow niche model has been extended to include both osteoblasts or endothelial cells, generating an endosteal and vascular niche environment respectively. These models were designed to create a HSC-permissive environment, to allow *ex vivo* culture of freshly isolated HSCs. The results from this chapter investigated MSC, osteoblast, endothelial cell, and more specifically HSC behaviour in the two models, in terms of gene expression changes and HSC phenotype. The results for each cell type are then discussed, with comments on the suitability of the two niche models for HSC culture.

5.4.1 MSC spheroids have altered behaviour when co-cultured in endosteal and vascular niche models

As described in Chapter 4, culture of MSCs in a spheroid within a collagen gel rather than as a monolayer has a profound influence on cell behaviour and phenotype. The cells become more quiescent, express higher levels of stem cell markers and nestin, and exhibit decreased inter-cell signalling. Co-culture of MSC spheroids with the two bone marrow niche models further influences the expression of genes involved in cell signalling, the cell cycle, differentiation, stem cell markers, and niche interactions. In order to simplify the results, all changes discussed have been collated into a table for each subset of genes.

5.4.1.1 MSC spheroids are more quiescent in the endosteal model compared to the vascular model

Transcriptome analysis of genes involved in the **cell cycle** in MSC spheroids cultured within the endosteal and vascular niche models has produced interesting results, with MSCs appearing to further down-regulate the cell cycle in the endosteal model, whereas the vascular model appears to be either similar to control (MSC spheroids cultured alone) or re-activating the cell cycle. However, some individual results are conflicting, as shown in Table 5.3. The results are divided into genes involved in G_1/S phase, cyclins, and global regulators of the cell cycle.

Gene	Gene Function	Gene Expression	
		Vascular	Endosteal
G1/S transition genes			
E2F1	Transcription factor (TF) involved in cell cycle regulation and DNA synthesis.	+	+
E2F2	TF involved in cell cycle regulation and DNA synthesis.	+	-
E2F3	TF involved in cell cycle regulation and DNA synthesis.	=	=
MCM4	DNA replication licensing factor	=	-
MYC	TF involved in control of DNA replication	=	-
AKT2	Kinase that promotes growth factor mediated cell survival and can overcome cell cycle arrest	-	-*
AKT1	Kinase that promotes growth factor mediated cell survival and can overcome cell cycle arrest	=	-
Cyclins			
CYCLIN E1	Interacts with cyclin dependent kinase 2, which is required for G1/S transition		-
CYCLIN D2	Interacts with cyclin dependent kinase 4 and 6, which are required for G1/S transition	+	+
Global cell cycle regulators			
FBXW7	Component of a ubiquitin ligase complex targeting cyclins	+	-
TP53	Tumour suppressor, can arrest growth	=	-*
p38	Stress responsive mitogen activated protein kinase	=	-
FOS	Proto-oncogene	=	=
BMI1	Oncogene	-	-

Table 5.3 Summary of changes in expression by MSCs of genes involved in cell cycle regulation.
*p < 0.05. -, decreased expression compared to control; =, similar expression to control; +, increased expression compared to control.

In the endosteal model, downregulation of **MYC**, which is involved in initiating DNA replication, supports reduced proliferation (Sato et al. 2016; Leung et al. 2008). Furthermore, **E2F2** transcription factor expression has decreased in the endosteal model, as has MCM4, as a key component of the pre-replicative complex, which is involved in DNA replication (S phase) (Kuijjer et al. 2008). With regards to the cyclins, a decrease in **cyclin E1** levels supports a conclusion of reduced proliferation. AKT1/2 are also downregulated, as is the global regulator **BMI1**, a regulator of self-renewal (Park et al. 2004).

In contrast, however, with regard to global regulators, **TP53** expression is significantly (p < 0.05) downregulated in the endosteal model compared to control and to the vascular model. This indicates an increase in proliferation and acceleration of differentiation (Velletri et al. 2016; Armesilla-Diaz et al. 2009).

Lower **p38** levels in the endosteal spheroids is also indicative of higher proliferation (Bhandari et al. 2010). Hence, these results suggest that the endosteal model is inducing the MSCs to proliferate and differentiate. In addition, with regard to cyclins, **cyclin D2** expression has increased in both models, which indicates increased proliferation in both environments (Kono et al. 2013).

In the vascular model, during G_1/S phase, the majority of genes are either increased or remain similar to control. Increases in **E2F1** and **E2F2** expression were observed in the EC model compared to controls and the OB model. The liberation of these proteins progresses the cell cycle by activating gene targets such as CDK1, DNA polymerase, cyclin E, and CDK2 (Nevins et al. 1997; Iwanaga et al. 2006; Timmers et al. 2007; Wu et al. 2001). Hence, the changes in expression indicate that vascular model spheroids are proliferative compared to MSC spheroids in isolation. **Cyclin D2** was increased and most global regulators were either unchanged or slightly increased, suggesting an increase in proliferation.

Of the G_1/S phase genes, only **AKT1/2** were reduced in the vascular model compared to control. No cyclins were reduced and only **BMI1** was reduced, suggesting reduced global regulation of self-renewal.

Interestingly, **FOS**, a cell cycle suppressor (Liu et al. 2016), has remained essentially unchanged in both models, when compared to the control and to each other. This is very different to the spheroid/monolayer comparison in Chapter 4, where FOS was highly increased (by 8-fold, Figure 4.8), so the levels are already atypically high in 3D spheroid culture compared to standard culture.

In conclusion, the vascular model (HUVEC-co-cultured MSC spheroids) exhibited fewer changes in gene expression from the control (MSCs in isolation). This may reflect the fact that the OBs have a greater influence on the co-cultured MSC cell cycle, where the general trend is a reduction in cell cycle and potential quiescence.

5.4.1.2 MSCs in the endosteal model are more primitive than in the vascular model

Evidence from genes related to **MSC differentiation** and **MSC markers** suggests that the MSC spheroids cultured with OBs have a more primitive phenotype

compared to both spheroids in isolation and those cultured with HUVECs, with a higher level of potential differentiation within the vascular model. The gene changes are summarised in Table 5.4 and discussed below.

Gene	Gene Function	Gene Expression	
		Vascular	Endosteal
Osteogenic markers			
RUNX2	Transcription factor (TF) associated with OB differentiation	-	-
BMP2	Potent inducer of osteoblastic differentiation	-	-
OPN	Extracellular structural protein with a role in biomineralisation and bone remodelling	-	-
Osteogenic signalling			
PML	Tumour suppressor required for assembly of nuclear bodies	=	-
STAT3	TF mediating cell response to stimuli via JAK-STAT pathway	=	-
VEGF	Growth factor involved in angiogenesis	-	-
TCF3	TF associated with Notch signalling	=	-
TCF4	TF involved in differentiation and apoptosis	=	-
NFKB2	TF involved in cell response to stimuli	=	-
NFKB1	TF involved in cell response to stimuli	=	-
SMAD6	Cell signalling: regulator of TGFß proteins	+	-
Adipogenic marker			
GATA2	TF mainly involved in haematopoiesis	+	-
Chondrogenic markers			
LEF1	TF: transcription enhancer		+
RUNX1	TF involved in haematopoietic differentiation	-	-
SMAD7	Cell signalling: regulator of TGFß proteins	-	-
MSC markers			
CD63	Antigen associated with membranes of intercellular vesicles	=	
CD271	Receptor for neurotrophin also identifying MSCs	+	+
CD34	Cell surface glycoprotein and cell-cell adhesion factor.	+	
CXCR4	Membrane receptor for CXCL12		+
Nestin	Cytoskeletal protein expressed by nerve cells and identifying HSC-supportive MSCs		-

Table 5.4 Summary of changes in expression by MSCs of genes involved in MSC differentiation.
-, decreased expression compared to control; =, similar expression to control; +, increased expression compared to control.

5.4.1.2.1 Osteogenic markers are downregulated in both models

MSC spheroids cultured in both the endosteal and vascular models have reduced levels of osteogenic markers **RUNX2**, **BMP2,** and **OCN**, when compared to controls

(MSC spheroids cultured alone), indicating reduced osteogenic differentiation. The magnitude of the **OPN** reduction is huge; results may indicate reversal of the increase in OB markers observed previously in spheroids when compared to monolayers (Figure 4.10). MSC expression of **BMP2**, another osteogenic differentiation regulator (Zhou et al. 2016), has also decreased in both models, in particular the endosteal model. In this situation, with co-cultured osteoblasts present, BMP2 may no longer be needed, as the surrounding cells are already terminally differentiated. In summary, decreased expression of all osteogenic regulators supports a lower level of osteogenic differentiation in the MSC spheroids when they are in co-culture.

5.4.1.2.2 Osteogenic signalling is decreased in the endosteal model but is maintained in the vascular model

The expression of genes related to **osteogenic signalling** have decreased to a greater extent in MSCs cultured in the endosteal model (with OBs) compared to those cultured in the vascular model (with ECs), further supporting a reduction in osteogenesis in MSCs within the endosteal model.

Osteogenic signalling molecules, **TCF4**, **NFκB1**, and **PML,** have reduced expression in MSC spheroids in the endosteal model; a reduction suggests a decrease in osteogenesis (Almalki & Agrawal 2016; McCarthy & Centrella 2010; Sun et al. 2013). Meanwhile, vascular endothelial growth factor **(VEGF)** may act in a similar way to BMP2 in the vascular model. Expression of this gene decreased in both models, in particular the endosteal model, in which it was significtly ($p < 0.05$). This indicates a reduction in osteogenesis in both niche environments (Mayer et al. 2005), but also that MSCs are not promoting angiogenesis at the 7-day time point when cultured with ECs. Accompanying downregulation of **STAT3** in a corresponding pattern reinforces this conclusion (M. Wang et al. 2007; Nicolaidou et al. 2012).

5.4.1.2.3 Adipogenic differentiation is inhibited to a greater extent in the vascular model

GATA2 expression indicates inhibition of adipogenesis and expression is markedly elevated in the vascular model. This suggests lower levels of adipogenesis in MSC spheroids when they are co-cultured with ECs. There is some evidence in the

literature that angiogenesis and adipogenesis are coupled processes, where angiogenesis promotes the production of fat cells (Cao 2007). Therefore, the fact that ECs have adopted a mature phenotype in the model may be the reason for reduced adipogenesis.

5.4.1.2.4 Chondrogenic differentiation is not affected by co-culture

From the three chondrogenic genes assessed, it appears that chondrogenesis is greater in the endosteal model, both compared to the vascular model and to spheroids in isolation, as demonstrated by a decrease in **SMAD7/RUNX1** and an increase in **LEF1** expression in MSC spheroids (Paik et al. 2012; Iwai et al. 2008; Wang et al. 2005). Therefore, signals originating from OBs may be causing this increased transcription.

5.4.1.2.5 MSCs in both co-culture environments maintain their phenotype

Expression of **MSC marker** genes are generally higher in 3D MSC spheroid culture compared to 2D MSC monolayer culture, as demonstrated in Chapter 4, Figure 4.10. However, when in 3D co-culture, MSC markers are either maintained at this higher level or have increased in both niche environments compared to control MSC spheroids, in particular in the endosteal model. A large increase in expression of **CXCR4**, the receptor for CXCL12, in the endosteal model may reflect the increased cross-talk between OBs and MSCs (note the increase in CXCL12 in the OB data, Figure 5.5E). In addition, **CD271**, a commonly used MSC marker (Quirici et al. 2002), has increased in both models, and to a greater extent in the endosteal model, as has nestin (endosteal model only). Meanwhile, levels of **CD63** are unchanged, indicating a maintenance of stem cell phenotype.

Results from these marker genes show that the original improved MSC state induced by the spheroid culture (section 4.4.6) is maintained, and even enhanced, when additional cell types are introduced into the model.

5.4.1.3 MSC spheroids in the vascular model may have an increased capacity for HSC support

Evidence from expression of genes involved in **niche function** and **interactions** between stromal and haematopoietic cells suggests an increased capacity for HSC support by MSCs within the vascular model, compared to the endosteal model.

Gene	Gene Function	Gene Expression	
		Vascular	**Endosteal**
Adhesion molecules			
ICAM1	Cell surface glycoprotein that binds to integrins	+	-
ALCAM	Immunoglobulin receptor implicated in cell adhesion and migration	-	=
VLA4	Integrin dimer that binds to fibronectin and VCAM1	-	=
VCAM1	Cell surface immunoglobulin receptor, ligand for VLA4	-	=
N-cadherin	Transmembrane protein involved in cell-cell adhesion	-	-*
CD44	Cell surface glycoprotein with multiple ligands, involved in cell adhesion	-	-*
Cytokines and receptors			
CXCL12*	Chemokine expressed by many cell types. Involved in niche homing and retention	-	-
TIE2	Cell surface receptor for Ang1	+	
ANG1	Vascular growth factor mainly involved in angiogenesis	-	-
TPO	Glycoprotein hormone that stimulates production and differentiation of megakaryocytes	+	-

Table 5.5 Summary of changes in expression by MSCs of genes involved in niche interactions. *$p < 0.05$. -, decreased expression compared to control; =, similar expression to control; +, increased expression compared to control.

5.4.1.3.1 MSC spheroids in co-culture express lower levels of adhesion molecules

The results from Chapter 4, Figure 4.11 indicated a reduction in **adhesion-related** genes in MSC spheroid culture compared to monolayer culture. This was surprising, as spheroids are known to employ cell-cell adhesions during spheroid formation (notably cadherins). When the MSC spheroids were subsequently co-cultured in the endosteal and vascular models, a further decrease in the expression of adhesion-related genes was noted (Table 5.5).

N-cadherin and **CD44** have both significantly decreased in expression in both models, especially the endosteal model. The former acts in cell-cell adhesion

(Zhou et al. 2017). Meanwhile, CD44 recognises hyaluronan (HA) and is involved in HSC-MSC adhesion (Wagner et al. 2008). Both of these results are unexpected, as is the reduction in expression of the integrin **VLA4**.

ALCAM expression can be indicative of the ability of stromal cells to maintain a long-term repopulating subset of HSCs (Nakamura et al. 2010). A 0.25-fold change in expression compared to the control in the vascular model indicates a potential reduction in this ability in these spheroids. Expression of **VCAM1**, which can also be used as a marker for a self-renewing and rapidly proliferating MSC population (Mabuchi et al. 2013), has exhibited a decrease equivalent to 16-fold in the vascular model, and was slightly decreased in the endosteal model. This may show that the MSCs are losing some of the stem cell markers when co-cultured with HUVECs, which would correspond with the results in Table 5.4 and support the hypothesis that the vascular niche comprises cells that are less quiescent.

ICAM-1 expression in MSC spheroids, however, has increased nearly 4-fold in the vascular model compared to control spheroids (whereas it has again decreased in the endosteal model). As this glycoprotein has been shown to play a role in HSC-MSC adhesion (Romanov et al. 2017), this may reflect interactions between these cells in the model. Following on from this, it may show that more HSCs are directly interacting with MSCs in the vascular model compared with the endosteal model. However, this change is not significant.

5.4.1.3.2 MSCs express lower levels of cytokines in co-culture

When compared to MSC spheroids cultured alone, several of the key cytokines involved in HSC support and maintenance are decreased in both models. SCF has significantly decreased in the endosteal model, a change which is also significantly different from the small increase observed in the vascular model. This indicates a reduced HSC support function in the endosteal environment. **CXCL12** expression has decreased in both models, although these changes were not significant. However, other cells co-cultured within the model may compensate for this decrease, for example CXCL12 expression has increased in OBs (Figure 5.7E). Similarly, **ANG1** expression has decreased in both models, significantly in the vascular model. In contrast, the expression of the ANG1 receptor **Tie-2** has markedly increased in the vascular model, suggesting that these MSCs may have

an increased capacity to respond to ANG1. **TPO** expression in MSCs has increased in the vascular model and decreased in the endosteal model, suggesting that ECs stimulate production of this cytokine, whereas interaction with OBs suppresses it. In summary, MSCs in the vascular model appear slightly more supportive for HSCs.

5.4.1.3.3 Hedgehog signalling is decreased in both co-culture models

Gene	Gene Function	Gene Expression	
		Vascular	Endosteal
PTCH1	Receptor for sonic hedgehog	+	=
SMO	Transmembrane protein that stimulates HH signal transduction	=	-
GLI3	Zinc finger TF; activates PTCH1 expression	=	=
GSK3B	Serine-threonine kinase involved in multiple signalling pathways	=	-
HHIP	Hedgehog antagonist, interacts with HH ligands	+	+
SUFU	Negative regulator of HH pathway	=	-

Table 5.6 Summary of changes in expression by MSCs of genes involved in hedgehog signalling.
-, decreased expression compared to control; =, similar expression to control; +, increased expression compared to control.

No data has been obtained for the expression of HH ligands, so the activity of the pathway must be inferred from looking at downstream elements. However, evidence from the increase in **HHIP** expression suggests that the pathway may be inhibited in both the endosteal and vascular models (Kobune et al. 2012). Expression of other members of the pathway has not extensively changed compared to the control in either model, with no significant differences (Table 5.6), although the trend suggests a decrease in Hedgehog signalling in the endosteal model and maintenance or small increase in the vascular model.

5.4.1.3.4 Notch signalling is decreased in the endosteal model

Generally, notch signalling is decreased in MSC spheroids cultured in the endosteal model, whereas it remains similar to control levels in the vascular model (Table 5.7).

Gene	Gene Function	Gene Expression

		Vascular	Endosteal
NOTCH1	Notch receptor	=	-
NOTCH2*	Notch receptor	=	-
NOTCH4	Notch receptor	=	-
JAG2	Notch ligand	+	+
DLL1	Notch ligand	=	-
DLL3	Notch ligand	-	
DLL4	Notch ligand	-	-
MAML	Transcriptional co-activator (enhancer) in Notch pathway	=	-
NUMB	Inhibitor of notch signalling	=	-
LFNG	Inhibitor of notch signalling	-	-
ADAM10	Cleavage protein essential for Notch signalling	=	-
ADAM17	Cleavage protein essential for Notch signalling	=	-
HES1	TF induced by Notch signalling	+	-

Table 5.7 Summary of changes in expression by MSCs of genes involved in notch signalling. -, decreased expression compared to control; =, similar expression to control; +, increased expression compared to control.

The expression of **Notch receptors** (Notch 1, 2, and 4) have decreased in the endosteal model, with a significant decrease in Notch2 expression. This contradicts evidence from the differentiation genes, as Notch signalling typically inhibits osteogenesis (noted as reduced in endosteal model spheroids). In addition to the notch receptors, other genes have reduced expression in the endosteal model, including **DLL1**, **MAML**, and **ADAM10/17**. LFNG has significantly decreased in the endosteal model. Collectively, this supports a reduction in notch signalling in the endosteal model.

Conversely, most genes remain unchanged when compared to control spheroids in the vascular model, with some exceptions (notch 4, JAG2, and HES1), which are all increased.

Finally, **HES1** expression (important for MSC maintenance (Dong et al. 2010)), as a target gene of the notch pathway, is different between the two niche models; it is increased in the vascular and decreased in the endosteal. As the main indicator of notch activity, this result is the strongest indication that notch

signalling may be increased in the vascular model, and decreased in the endosteal model.

In conclusion, as depicted in Figure 5.13, the endosteal model is associated with decreased expression of genes involved in the cell cycle, differentiation, signalling, and adhesion, and an increase in MSC phenotype genes. In contrast, the gene expression patterns in MSCs cultured in the vascular model are more similar to the control, with an increase in cell signalling. This corresponds to the hypothesised situation in the BM, wherein the endosteal niche is quiescent and the vascular niche is more active.

ENDOSTEAL

- cell cycle
- adhesion
- differentiation
- signalling
+ MSC phenotype

Osteoblasts

VASCULAR

+/= cell cycle
- adhesion
-/= differentiation
+ signalling
-/= MSC phenotype
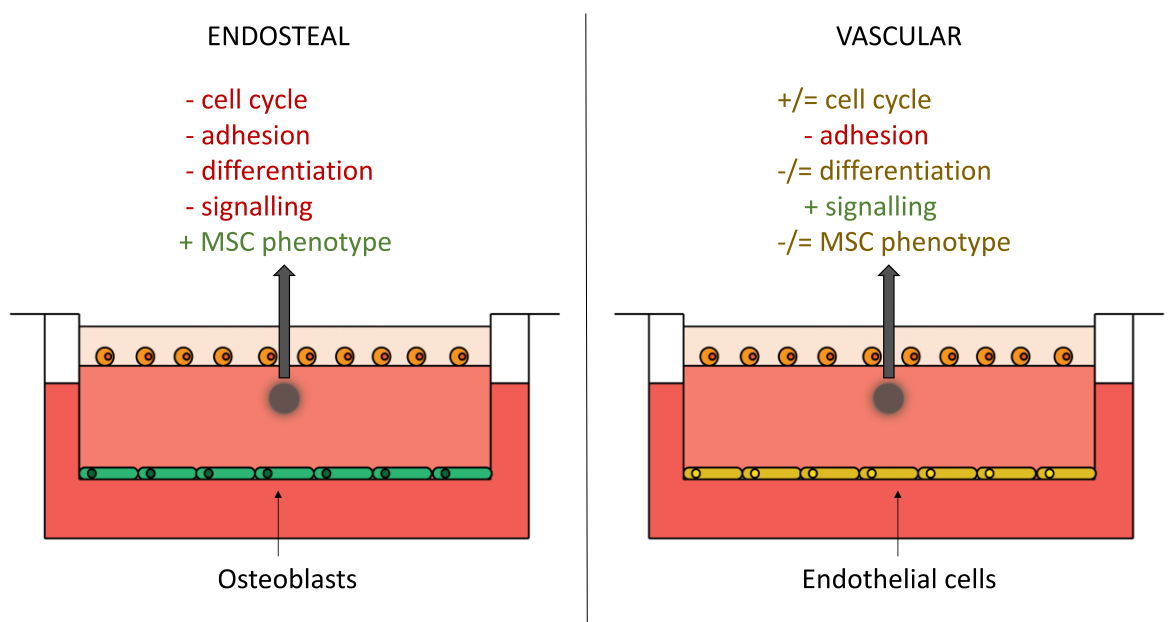
Endothelial cells

Figure 5.13 Summary schematic of changes in gene expression in MSC spheroids cultured in the two niche model environments compared to the control (spheroid alone).

5.4.2 Endothelial cells are more mature in co-culture

ECs have been included in this study as there is strong evidence for them participating in both arteriolar and sinusoidal niches, releasing SCF and CXCL12, as well as directly interacting with haematopoietic cells (Ding et al. 2012). Their inclusion in the 3D model is an attempt to simulate these vascular niches in co-culture. The capacity of ECs to form rudimentary vasculature when cultured in collagen gel *ex vivo* is well documented (Yamamura et al. 2007; Korff & Augustin 1999). Therefore, a secondary aim of this part of the analysis is to investigate

whether the HUVECs are angiogenic in the niche model, which may impact on their ability to support the HSCs directly or indirectly.

5.4.2.1 Endothelial cells in co-culture are more quiescent

A unique property of vascular endothelial cells (ECs) is the 'contact inhibition' they exhibit, i.e. they exit from the cell cycle, ensuring that cells that line the blood vessels are quiescent, protecting against thrombosis and neointima development. Therefore, in the monolayer culture system in which cells are in close contact (which in this study is the control), the cells are expected to be quiescent and non-proliferative. However, evidence here suggests that the HUVECs become even more quiescent in the co-culture model compared to when they are in isolation (Table 5.8).

Gene	Gene expression	Gene	Gene expression
G1/S transition		**Cyclins**	
E2F1	-	CYCLIN E1	-
E2F3	=	CYCLIN D2	-
E2F4	-	**Global cell cycle regulators**	
MYC	-	FBXW7	=
MCM4	-	FOS	+
AKT2	=	p53	-
AKT1	=	p38	-
		BMI1	=

Table 5.8 Summary of changes in expression by ECs of genes involved in cell cycle regulation.
Refer to Table 5.3 for gene functions. -, decreased expression compared to control; =, similar expression to control; +, increased expression compared to control.

The significant downregulation of **MYC** is a strong indicator of cell cycle downregulation, as MYC is essential for maintaining a normal endothelial phenotype (Baudino et al. 2002), and knockdown leads to senescence (Florea et al. 2013).All other G_1/S phase genes analysed either indicate a downwards trend or no change from control ECs, including the E2F TFs, for which repression is well documented in quiescent ECs (Spyridopoulos et al. 1998).

There is also a downregulation trend or no change compared to control ECs noted in the master regulators of the cell cycle in co-culture, aside from **FOS** which has

increased in expression, indicating maintained or improved angiogenesis (Mar et al. 2015). The significant downregulation of p53 suggests an increase in cell cycle progression, but in endothelial cells it has also been shown to have a role in endothelial dysfunction (Kumar et al. 2011), so this decrease may conversely indicate a maintenance of endothelial function.

The evidence from this part of the analysis suggests that the co-culture model is providing signals enhancing quiescence, or increasing the interaction of HUVECs with each other to promote contact inhibition. It has previously been observed that co-culture with stromal cells in a collagen gel inhibits EC proliferation (Stahl et al. 2005). Several of the gene changes are also associated with maintained or enhanced angiogenesis.

5.4.2.2 Endothelial cells adopt a mature bone marrow vasculature phenotype in the model

The angiogenic activities of ECs overlaid with a collagen gel are important, as these structures may be more relevant for HSC niche function than a standard monolayer. Hence, examining the process of angiogenesis, and expression of related genes, is useful for evaluating the model in this regard.

Angiogenesis is the remodelling of existing ECs to form mature vasculature, and proceeds through a series of stages, summarised in Figure 5.14. These can be divided into destabilisation, proliferation, and maturation. One of these early events involves degradation of the vascular basement membrane and ECM remodelling (Tabruyn & Griffioen 2007). Early transcriptional activation of angiogenic factors, such as VEGF and angiopoietins, is required to activate quiescent ECs, causing vessel sprouting and maturation. Proteases digest ECM, allowing the cells to invade and migrate towards the angiogenic factor. They proliferate behind the front of migration. Once lumen formation and sprouting have occurred, the stabilisation phase proceeds; different growth factors are involved in the stabilisation phase such as VEGF (Vailhé et al. 2001).
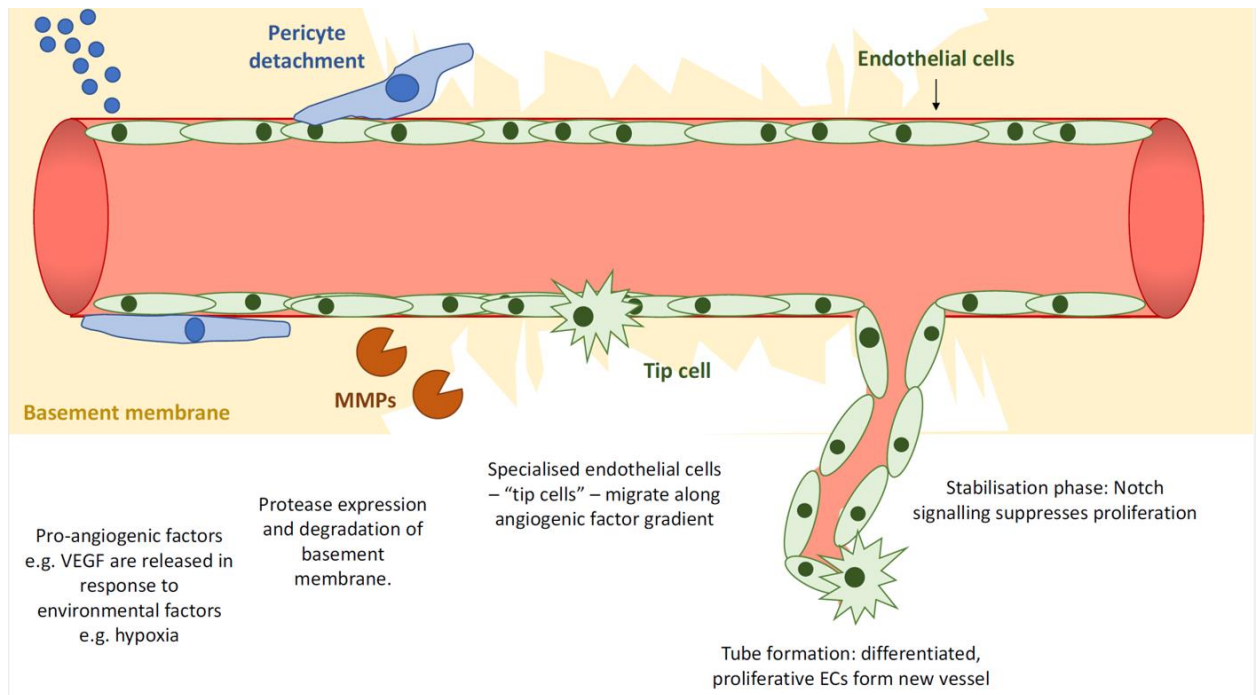
Figure 5.14 Schematic of the processes involved in angiogenesis.
Adapted from (Romero 2015).

With regards to positive regulators of angiogenesis, increases were observed in both RUNX2 and BMP2, with no change or decreases in the other genes compared to control ECs. When analysing negative regulators of angiogenesis, no significant changes were noted compared to control ECs. When considering EC phenotype, the only notable gene change is a decrease in nestin, although this change is not significant. Evidence from several genes discussed here indicate lower angiogenic activity, but a more mature phenotype, similar to that observed in the BM. This may suggest that ECs in the model have entered the stabilisation phase of mature vasculature. However, conclusions cannot be drawn as none of these changes are significant.

Gene	Gene Expression	Gene	Gene Expression
Positive regulators		**Phenotype**	
VEGF	=	MEIS1	-
STAT3	-	Nestin	-
RUNX1	-	GATA2	-
RUNX2	+	GATA3	-
BMP2	+	PML	-
HIF1α	-		
Negative regulators			
NFκB2	=		
NFκB1	-		
SMAD6	+		
SMAD7	+		
CD63	-		

Table 5.9 Summary of changes in expression by ECs of genes involved in angiogenesis.
-, decreased expression compared to control; =, similar expression to control; +, increased expression compared to control.

5.4.2.3 Endothelial notch signalling increases in co-culture

Notch signalling is relevant to niche function in ECs for several reasons. Firstly, expression of notch ligands equates to the ability of ECs to influence HSCs. Secondly, expression of notch and downstream genes indicates the ability of ECs themselves to respond to notch signals from other cells. Notch signalling influences ECs by promoting angiogenesis and/or contact inhibition, depending on the context. Changes in expression of genes involved in the notch pathway are summarised in Table 5.10.

5.4.2.3.1 Notch pathway signalling within endothelial cells may decrease in co-culture

The expression of Notch receptors has remained constant. This suggests that receptiveness to Notch signalling, and hence downstream effects, in ECs has remained similar to the control. The JAG ligands have also remained at similar levels. DLL ligands are inhibitors of endothelial sprouting. The significant downregulation of **DLL1** may therefore indicate a reduction in this inhibition (Benedito et al. 2009), as well as a general decrease in Notch signalling.

Accompanying significant decreases in ADAM10 and MAML also indicate a decrease in the activity of this pathway. Expression of the end products of Notch signalling, **HES1** and **HEY1** has increased, which is an indication of increased Notch signalling. However, this trend is not significant, and so it is more likely that Notch signalling has decreased.

Gene	Gene Expression	Gene	Gene Expression
NOTCH1	=	ADAM17	-
NOTCH2	+	LFNG	=
NOTCH4	+	MFNG	-
JAG1	=	MAML	-
JAG2	=	HES1	+
DLL1	-	HEY1	+
DLL4	=	HEY2	=
ADAM10	-		

Table 5.10 Summary of changes in expression by ECs of genes involved in notch signalling. -, decreased expression compared to control; =, similar expression to control; +, increased expression compared to control.

5.4.2.4 Hedgehog signalling may increase in co-culture

HH signalling has a role in both angiogenesis and vasculogenesis, by targeting both ECs directly, or vessel-supportive cells. The direct effect of HH signalling is to allow tubulogenesis (Byrd & Grabel 2004). Unfortunately, insufficient data was obtained for the HH ligands. The majority of genes analysed indicated no change compared to the control ECs, aside from a decrease in **HHIP** and **SUFU**. HHIP, a natural HH ligand antagonist, is highly expressed in normal ECs (Nagase et al. 2008). The significant decrease of SUFU indicates that HH signalling may be more active in co-culture, as it is a negative regulator of the pathway (Lee et al. 2007).

Gene	Gene Expression
PTCH1	=
SMO	=
GLI3	=
HHIP	-
SUFU	-
GSK3β	-

Table 5.11 Summary of changes in expression by ECs of genes involved in hedgehog signalling.
Refer to Table 5.6 for gene functions. -, decreased expression compared to control; =, similar expression to control; +, increased expression compared to control.

5.4.2.5 Endothelial cells are less supportive towards HSCs in co-culture

Evidence from increased Notch signalling, as well as adhesion molecules and cytokines, suggests that the HUVECs in co-culture do not particularly generate a HSC supportive environment.

5.4.2.5.1 Expression of Notch ligands is decreased in co-culture: endothelial cells have lower direct control of HSCs in co-culture

Expression of Notch ligands is an indication of the ability of ECs to interact with Notch receptors in HSCs/other niche cells and hence trigger signalling within those cells. For the ECs in the co-culture model, the expression of the **DLL ligands** has decreased, and expression of **JAG ligands** has remained constant or decreased, indicating a corresponding reduction in their direct HSC-supportive capacity.

JAG ligands are constitutively expressed by BM ECs, but DLL ligands are generally undetectable; the reduction in **DLL1** observed in EC co-culture may indicate a move towards a more BM-like phenotype (Fernandez et al. 2008). In murine foetal arteries, DLL1 is required for maintenance of arterial identity (Sörensen et al. 2009). A large reduction in expression here may suggest that the ECs are no longer maintaining arterial identity, being more akin to microvasculature.

Expression of DLL and JAG family members enhances the ability to support HSCs *in vitro*: notch activation by these ligands delays myeloid differentiation and increases colony-forming potential of HSCs. JAG2 is specifically expressed by ECs

in the BM (Fernandez et al. 2008). The levels of JAG1 and JAG2 ligands have remained constant, suggesting a maintenance of HSC-supporting ability.

5.4.2.5.2 Endothelial cells in co-culture express similar levels of adhesion molecules compared to control

As mentioned previously, adhesion molecules mediate cell-cell adhesion and cell-ECM interactions. Therefore, they are relevant in both angiogenesis and in niche functionality of ECs. The changes in expression in spheroids compared to monolayers are summarised in Table 5.12.

Gene	Gene Expression	Gene	Gene Expression
Adhesion molecules		**Cytokine molecules**	
VLA4	=	c-kit	-
VCAM1	-	SCF	-
ICAM1	=	TIE2	-
E-selectin	=	ANG1	-
CD44	-	TPO	=
ALCAM	-		

Table 5.12 Summary of changes in expression by ECs of genes involved in niche interactions. Refer to Table 5.5 for gene functions. -, decreased expression compared to control; =, similar expression to control; +, increased expression compared to control.

All genes indicated a downwards trend, in particular **ALCAM**, which has a role in endothelial junction formation and in transendothelial trafficking of leukocytes. It is expressed by several niche cell types, including ECs. It most likely acts through homotypic adhesion to anchor haematopoietic cells (Chitteti et al. 2015). Reduction in the expression of ALCAM in ECs suggests a reduced capacity to retain HSCs or haematopoietic lineage cells in the model. CD44 has also been significantly downregulated. As interaction between CD44 and hyaluronan is involved in tubulogenesis (Olofsson et al. 2014), this downregulation may represent impared tubulogenic behaviour.

5.4.2.5.3 Endothelial cells in co-culture express similar levels of HSC-supportive cytokines compared to control

Expression of all genes involved in cytokine interactions in the niche have been downregulated by at least 0.5-fold in HUVECs, excepting **TPO**, which has

maintained a constant level. This may suggest that the cells are not directly supporting HSCs, at least *via* the mechanisms examined here. However, some angiogenic pathways can also be examined by looking at these genes. The receptor for SCF**, c-kit**, is expressed by mature ECs (Suzuki et al. 2014): the significant decrease in expression noted in co-culture may therefore indicate that the HUVECs have become more mature, supporting previous conclusions. C-kit's downstream signalling pathways promote EC survival, migration, and capillary tube formation; supporting this, SCF dose-dependently promotes these angiogenic features (Matsui et al. 2004).

Results from analysis of cytokine genes cannot determine whether the ECs are more conducive to interaction with HSCs in co-culture, but give some evidence that they are more mature.
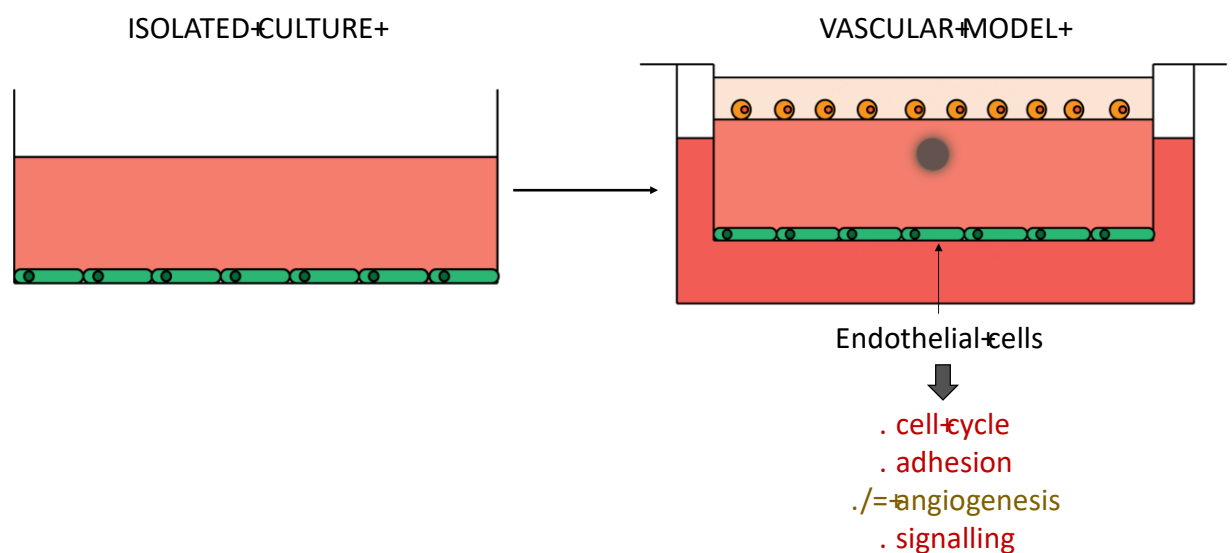
Figure 5.15 Summary diagram of gene expression changes in ECs when in co-culture compared to control.

In summary, evidence from gene expression analysis in ECs shows that they are more quiescent in co-culture, expressing lower levels of signalling related genes and adhesion molecules. Genes related to angiogenesis remain similar or are slightly decreased in co-culture. This evidence suggests that the cells may be adopting a mature vasculature phenotype in the model. However, it would be interesting to further investigate these changes by looking at earlier time points during the experiment.

5.4.2.6 HUVECs may not be optimal for the model

As a final note, the suitability of HUVECs for developing this co-culture method is in question. Firstly, BM-derived ECs compared to HUVECs have a greater ability to support adhesion and migration of HSCs than HUVECs or ECs from other organs (Yun & Jo 2003). Furthermore, the specificity of the pro-angiogenic effect of notch in the BM means that HUVECs may respond differently to BM ECs. Depending on the perspective taken, the increased notch signalling could be taken to indicate either contact inhibition and hence quiescence, or promotion of angiogenesis in the BM-like environment (Fernandez et al. 2008). Although results from transcript analyses suggest that HUVECs are adopting a mature phenotype in the model, these points suggest that using BM-derived ECs in the model may replicate the BM environment more efficiently, and may be more supportive for HSCs.

5.4.3 Osteoblasts adopt an endosteal phenotype in co-culture

OBs are a major component of the BM HSC niche, as components of the endosteum environment. The endosteum comprises a flattened, quiescent OB subset. Results from the RNA analysis show that co-culture within a 3D model influences osteoblast phenotype, encouraging them to adopt these endosteal characteristics.

5.4.3.1 Osteoblasts may be slightly more quiescent in co-culture

Whilst changes are not significant, as shown in Table 5.13, there is a general trend for reduced expression of almost all genes analysed related to the cell cycle although none of these genes have changed significantly from the control

Gene	Gene expression	Gene	Gene expression
G1/S transition		**Cyclins**	
E2F1	-	CYCLIN E1	+
E2F2	-	CYCLIN D2	=
E2F3	-	**Global cell cycle regulators**	
MCM4	-	FBXW7	-
MYC	-	TP53	-
AKT2	-	p38	-
AKT1	-	FOS	+
		BMI1	-

Table 5.13 Summary of changes in expression by OBs of genes involved in cell cycle regulation.
Refer to Table 5.3 for gene functions. -, decreased expression compared to control; =, similar expression to control; +, increased expression compared to control.

5.4.3.2 Osteoblasts are more mature in co-culture

Examining the expression of genes involved in **osteogenic regulation** and **cell markers** suggests that the OBs have a more mature phenotype in the model. This conclusion is based on a general trend for reduced early osteoblast markers with no changes (or a downwards trend) noted in MSC marker genes, as shown in Table 5.14.

Gene	Gene Expression	Gene	Gene Expression
Osteogenic markers		Adipogenic markers	
RUNX2	-	GATA1	+
BMP2	=	GATA3	+
OPN	+		
Osteogenic signalling		Chondrogenic markers	
PML	=	LEF1	=
STAT3	=	RUNX1	-
VEGF	=		
TCF3	=	Stem cell markers	
TCF4	-	CD63	-
NFκB1	=	CD271	=
NFκB2	=	CD34	-
SMAD6	-		
SMAD7	=		

Table 5.14 Summary of changes in expression by OBs of genes involved in osteoblastic differentiation.
Refer to Table 5.4 for gene functions. -, decreased expression compared to control; =, similar expression to control; +, increased expression compared to control.

5.4.3.2.1 Expression of osteogenic regulators and signalling decreases in co-culture

In co-culture, osteoblasts exhibited increased expression of **OPN**, a late osteoblast marker, and decreased expression of early osteogenesis regulator **RUNX2** and **BMP2**. However, these changes are not significant and so the differentiation state of the cells cannot be determined. TCF4, however, activates RUNX2 (McCarthy & Centrella 2010) and was significantly downregulated, which may explain the decrease RUNX2 expression and may correspond to lower levels of osteogenic signalling. SMAD6 is activated by BMP2 (Q. Wang et al. 2007), and so the significant decrease in its expression may reflect lower levels of osteogenic activity.

5.4.3.3 HSC support capacity of osteoblasts remains similar in co-culture

Examination of expression patterns of genes involved in HSC interactions with OBs, both cytokines and adhesion molecules, suggests that support capacity remains similar in the co-culture model as to OBs cultured in monolayer isolation.

5.4.3.3.1 Expression of adhesion molecules slightly decreases in co-culture

Similar to the trend observed with MSCs when cultured within the 3D model, there is a downwards trend in gene expression of adhesion molecules in OBs in co-culture compared to control (Table 5.15). Again, this may be simply because these molecules are in a different conformation in the 3D model compared to standard tissue culture.

The significant decrease in expression of **VLA-4** may reflect the fact that this gene is not typically expressed by OBs and is present at a very low level in both control cells and in the model. N-cadherin has also significantly decreased in expression. **N-cadherin** has been shown to be a negative regulator of OB proliferation and survival (Haÿ et al. 2009). Therefore, the decreased expression may encourage increased survival of OBs in the model compared to in isolation. It is also highly expressed in endosteal lining OBs (Ferrari et al. 2000), suggesting that the OBs in co-culture are not exactly reflecting the nature of the endosteal OB subset.

Gene	Gene Expression	Gene	Gene Expression
Adhesion molecules		Cytokine molecules	
ALCAM	-	CXCL12	+
VLA4	-	TIE2	=
VCAM1	=	ANG1	-
ICAM1	=	TPO	=
N-cadherin	-		
CD44	-		

Table 5.15 Summary of changes in expression in OBs of genes involved in niche intercellular interactions.
Refer to Table 5.5 for gene functions. -, decreased expression compared to control; =, similar expression to control; +, increased expression compared to control.

5.4.3.3.2 Expression of niche cytokines by osteoblasts remains similar in co-culture

Tie-2, CXCL12, SCF, and TPO expression levels remain similar to control OBs. These are key niche molecules, which are required for HSC maintenance, indicating that co-culture has no effect on the capacity of OBs to produce these molecules. **Ang1** is expressed by OBs, although in the co-culture its expression was significantly downregulated. Overexpression of Ang1 increases bone mass and

increases ALP activity, whilst also encouraging angiogenesis, thus the lower levels of Ang1 expression do not support osteogenic activity in co-culture (Suzuki et al. 2007). Overall, very few changes in gene expression were observed, and the changes that are seen are of low magnitude. Therefore, it appears that OB co-culture in the model does not change niche signalling.

5.4.3.4 Notch signalling in osteoblasts remains similar in co-culture

In general, whilst most changes were not significant, a downwards trend was noted in the expression of notch receptors and ligands when compared to control OBs (Figure 5.7F). As notch signalling has a general inhibitory effect on osteoblastogenesis (Canalis 2008), the fact that the pathway is maintained or slightly decreased suggests that osteoblastogenesis is slightly enhanced in co-culture, maintaining OB phenotype. The significant downregulation of GSK3β also suggests that the Notch signalling activity is decreased in co-culture.

5.4.3.5 Hedgehog signalling in osteoblasts decreases in co-culture

HH signalling is required for OB differentiation from progenitors. However, HH signalling progressively decreases during OB maturation, and is constitutively low in mature OBs (Mak et al. 2008). Whilst data has not been obtained for HH ligands, and several other members of the pathway, the trend is again for reduced gene expression (Figure 5.7G).
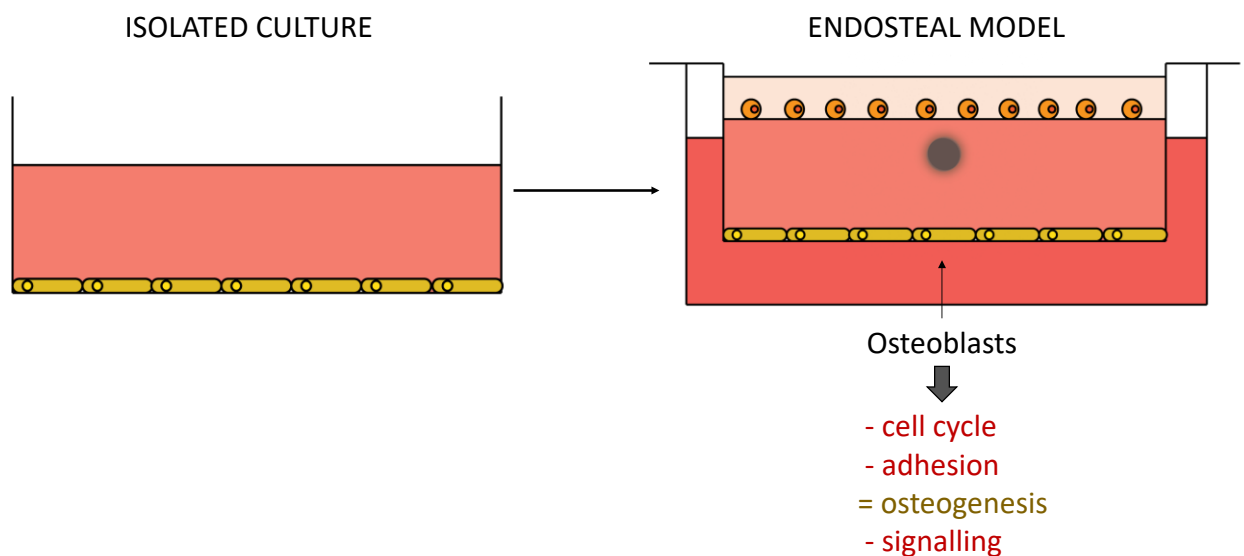
Figure 5.16 Summary of gene expression changes in OBs when in co-culture compared to control.

In summary, changes in gene expression in OBs indicate that they are more quiescent and adopt many characteristics of endosteal OBs in co-culture. This is promising for the success of the model, as they may provide specific signals that are not supplied by the MSC spheroid alone.

5.4.4 Haematopoietic stem cells have altered behaviour when they are cultured in vascular and endosteal niche models

Freshly isolated HSCs were co-cultured in either the endosteal niche model (with MSC spheroids and osteoblasts) or the vascular niche model (with MSC spheroids and endothelial cells). The subsequent analysis of HSC gene expression in both models compared to control HSCs cultured in suspension may provide evidence of their differentiation state, and hence whether the two niche models have different effects on the lineage specification, cell cycle, and cell signalling of HSCs.

5.4.4.1 HSC cell cycle genes have increased in both niche models

The expression of all the analysed genes involved in the cell cycle are shown in Table 5.16. The expression of genes involved in the progression of the cell cycle from G_1 to S phase (**E2F1-2, MYC, MCM4, AKT1-2,** and **cyclin D2**) have increased in both the endosteal and vascular models when compared to control HSCs, indicating increased proliferation. Interestingly, in almost all of these genes, expression is greater in the endosteal model as compared to the vascular model. However, none of these changes are significant.

Gene	Gene Expression		Gene	Gene Expression	
	Vascular	Endosteal		Vascular	Endosteal
G1/S transition			**Global cell cycle regulators**		
E2F1	+	++	p38	+	++
E2F3	+	++	FOS	+	++
MYC	+	++	FBXW7	+	++
MCM4	+	++	p53	+	++
AKT2	+	++	BMI1	+	++
AKT1	+	++			
CYCLIN D2	+	+			

Table 5.16 Summary of changes in expression by HSPCs of genes involved in cell cycle regulation.
Refer to Table 5.3 for gene functions. +, increased compared to control; ++, increased compared to control and other model.

An increase in MYC was noted in both niche models. The role of **MYC** in HSC function is manifold. Exogenous application of MYC to murine HSPCs in culture has been shown to enable proliferation whilst maintaining a progenitor phenotype for

up to 28 days: suggesting that MYC supports HSC self-renewal (Satoh et al. 2004). In progenitors, it is essential for initiating differentiation but in lineage progenitors, its role in cell cycle progression and expansion becomes apparent (Wilson et al. 2004). MYC also has a role in interaction of HSCs with the niche: it represses integrin and N-cadherin expression (both of which are decreased in the niche models) and hence modulates migration and adhesion in the niche.

Expression of several general cell cycle modulators has also increased, although not necessarily in support of proliferation. For example, the increased expression of **p38** indicates that the HSC lifespan is limited in culture, as inactivation of p38 maintains their self-renewal capacity (Ito et al. 2006; Wang et al. 2011). In addition, p38 activation in CD34+ progenitors prevents differentiation (Oeztuerk-Winder & Ventura 2012).

In contrast, **FOS** is a negative regulator of the cell cycle in HSCs, maintaining them in G_1/G_0 phase following prolonged expression (Okada et al. 1999). The large increased fold-change in expression over control in both models suggests a downregulation of the cell cycle, particularly in the endosteal model.

5.4.4.2 Haematopoietic lineage bias depends on culture conditions: comparison of RNA data and phenotypic flow cytometry data

From analysis of the expression of multiple genes involved in haematopoietic lineage determination (Figure 5.8E), it is evident that multiple lineages have arisen within the population, with differentiation into erythroid, lymphoid, and myeloid cells occurring. However, there is also evidence to suggest the continued existence of an early progenitor population. In contrast, evidence from expression of cell surface markers (Figure 5.10 and Figure 5.11) indicates a large decrease, and essentially non-existence of progenitors following a period of culture.

Gene	Gene Expression		Gene	Gene Expression	
	Vascular	Endosteal		Vascular	Endosteal
Progenitor			Lymphoid		
VEGF	+	++	TCF3	+	++
LEF1		+	NFKB1	+	++
GATA2	+	+	GATA3	++	+
PML	+	++	CD79	++	+
CD34	++	+			
Erythroid			Myeloid		
SPI1	+	++	TCF4	+	++
RUNX1	+	++	MEIS1	+	++
SMAD6	+	++	MPO	+	++
BMP2		+	NFKB2	+	++
			GATA1	+	++
			SMAD7	++	+
			OPN	+	++

Table 5.17 Summary of changes in expression by HSPCs of genes involved in HSPC differentiation.
+, increased compared to control; ++, increased compared to control and other model.

5.4.4.2.1 A haematopoietic progenitor population may persist in the niche models

RNA analysis: Firstly, when considering HSC phenotype and characteristics such as quiescence and survival, all genes increased in expression in the co-culture models (Table 5.17).

Flow analysis: In contrast, results from phenotypic analysis (Figure 5.11) indicates a large reduction in the proportion of cells expressing the CD34 marker (under 1%), after 7 days of culture within the niche models. Interestingly, the level of CD34+ cells remains similar whether or not collagen gel or MSCs are present. However, the extent of this decrease is difficult to ascertain due to technical issues, as discussed in section 5.3.2.2.2 (page 184). In particular, the antibody used in detection may be underestimating the frequency of progenitors. Regardless, the percentage of CD34+ cells in the sample has decreased, indicating a loss of both HSCs and progenitor cells, with differentiation in all samples.

In the vascular model, lymphoid progenitor (MLP, CLP) frequency has decreased to a greater extent compared to the endosteal model. However, myeloid progenitors (CMPs) and granulocyte-monocyte progenitors (GMPs) are not present, and erythrocytic progenitors (MEPs) have decreased to a greater extent than the lymphoid progenitors. This may indicate that most haematopoietic cells in the vascular model are terminally differentiated.

Meanwhile, in the endosteal niche model, the percentages of all progenitors are greater than observed in the vascular model. Therefore, there may be less differentiation in this model, as expected considering the *in vivo* role of the endosteum (Acar et al. 2015).

5.4.4.2.2 Erythropoiesis may be increased in the vascular model compared to the endosteal model

RNA analysis: Genes that are involved in erythropoiesis have generally increased in both niche co-culture models. Several of these genes are downregulators of erythropoiesis; hence, evidence from these genes suggests a downregulation of erythropoiesis in comparison to other lineages, despite an increase in BMP2. However, none of these increases are significant changes. As hypoxia is relevant to erythropoiesis (Morikawa & Takubo 2016), culture of the model in a hypoxic incubator may allow replication of physiological proportions of erythroid cells.

Flow analysis: Evidence from cell surface markers also shows that erythrocytic differentiation may be highest in the vascular niche model. In particular, **CD36** is expressed on the earliest megakaryocyte/erythroid progenitors (MEPs, Ward et al. 2016). Its expression is greatly increased in the vascular niche model, showing a strong bias towards these lineages. This is supported by the changes in expression of SPI1. **CD41a** is expressed on progenitors, with persistent expression in MEPs and subsequent mature cells, and is integral to platelet function (Choi et al. 2009). Expression of CD41a in the endosteal model is almost non-existent, compared to the remainder of the experimental samples, in which expression has been maintained at a similar level. This supports the conclusion that the OB model reduces megakaryocytic/erythroid differentiation, whilst the vascular model remains permissive.

5.4.4.2.3 Transcriptomic and phenotypic analyses give conflicting results regarding lymphoid differentiation

RNA analysis: Again, genes involved in production of lymphocytes have been upregulated in the co-culture models. Evidence from lymphoid related genes suggests a bias towards lymphoid development in the vascular niche model compared to the endosteal niche model. This conflicts with *in vivo* evidence from the BM, which suggests that the endosteal BM environment favours lymphoid differentiation (Ding & Morrison 2013). As before, as these changes are not significant, conclusions cannot be drawn from this data.

Flow analysis: The expression profiles of some lymphoid lineage markers suggest a complete lack of these cells in any of the models. **CD10** is a general lymphoid marker that arises at an early stage of development. Progenitor cells that express CD10 tend to be biased towards B-cell production. A high proportion of CD10+ lymphoid lineage progenitors are present in the day 1 samples. However, by day 7, CD10 is not observed in any of the experimental samples, reflecting a lack of both lymphoid progenitors and of mature lymphoid cells. **CD7** is expressed by pro-T cells and mature T cells, therefore being a lymphoid marker (Shukla et al. 2017). CD7 expression is initially low, and remains so after culture for 7 days, with the lowest levels observed in the cells cultured with collagen. Hence, it can be concluded that there are virtually no T-cell lineage cells in any of these samples, and lymphoid differentiation is not occurring, contradicting the RNA analysis.

5.4.4.2.4 Myelopoiesis may be increased to a greater extent in the endosteal model

RNA analysis: The expression of several genes involved in myeloid differentiation was examined, all of which were increased in both niche models. **MEIS1** was the only gene to exhibit a significant difference in expression between the endosteal and vascular models. It is fundamentally linked to several stem cell functions including quiescence and self-renewal, protecting and preserving HSCs in mice (Unnisa et al. 2012) and is also instrumental in erythropoiesis and myelopoiesis (M. Cai et al. 2012; Ariki et al. 2014). The significantly increased expression in the endosteal model compared to the vascular model suggests a bias towards the myelopoiesis lineages.

Flow analysis: Evidence from expression of surface markers suggests a lower level of myeloid differentiation in the endosteal niche model, with about 12% of cells expressing the marker, compared with 20% in the vascular model. **CD13** is expressed by early as well as differentiated myeloid cells (Winnicka et al. 2010). Expression is at around 25% in the baseline sample, and expression is maintained at a slightly lower level in the majority of samples. However, expression has increased in the presence of a collagen gel alone: suggesting that it promotes myeloid differentiation. On the other hand, this effect is offset by the addition of an MSC spheroid. CD13 has decreased to a lower level in the endosteal niche model: again, implying a lower level of myeloid differentiation in this model.

In vivo, the vascular niche is a proposed niche for myeloid progenitors and the early stages of myelopoiesis (Rafii et al. 1995). Although an increase was observed in myeloid-lineage related gene expression in the vascular model, as expected, a greater increase occurred in the endosteal model. This conclusion conflicts with the expectations from looking at the *in vivo* BM environment. In contrast, evidence from cell surface markers shows that there is a slightly higher level of myeloid differentiation in the vascular model. Therefore, no firm conclusions can be drawn as to whether the different cell combinations promote differentiation into different lineages.

5.4.4.3 Expression of genes related to niche cell interactions is increased in co-culture

Genes involved in indirect cytokine interactions and direct cell-cell adhesion in the BM niche were included in the analysis. These genes have increased in expression in both co-culture models, although the increase is slightly greater in the endosteal model.

Gene	Gene Expression		Gene	Gene Expression	
	Vascular	Endosteal		Vascular	Endosteal
Adhesion molecules			Cytokine interaction molecules		
ALCAM	+	++	CXCL12		+
VLA4	+	++	c-KIT	+	++
VCAM1		+	ANG1	+	++
LFA1	+	+	TPO	+	++
ICAM1		+	MPL		-
CD44		+	CXCR4	+	++

Table 5.18 Summary of changes in expression by HSPCs of genes involved in niche interactions.
Refer to Table 5.5 for gene functions. -, decreased compared to control; +, increased compared to control; ++, increased compared to control and other model.

5.4.4.3.1 Cytokine interactions may have increased in co-culture

With regards to cytokine receptors, CXCR4 and c-kit have increased in both models, whereas MPL has decreased in the endosteal model and no results were obtained for the vascular model. The cytokines TPO and Ang-1 have increased in both models and CXCL12 has increased in the endosteal model. These results indicate a general increase In inter-cell communication through cytokines and their receptors, although as none of these results are significant no firm conclusions can be drawn.

5.4.4.3.2 Direct adhesion interactions have increased in co-culture

Unlike the other cell types included in the model, the expression of cellular adhesion genes has increased in HSCs when in co-culture, particularly in the endosteal model. As the HSCs were added to the model in suspension, this may reflect an increase in migration, more so in the endosteal model, as the cells penetrate the collagen gel model and migrate during the 7-day culture period. However, none of these increases are significant.

5.4.4.4 Notch signalling is increased in co-culture

Expression of genes involved in Notch signalling has increased in both the vascular and the endosteal model. Aside from the expression of the notch ligand **DLL3** and the target TF **HEY1**, all genes have increased to a greater extent in the endosteal

model. The increase in expression of the Notch ligand DLL indicates that the HSCs may initiate higher levels of notch signalling in the vascular model. In addition, the increased levels of HEY1 suggest that HSCs have a stronger response to notch signalling in the vascular model. In contrast, the HSCs are more receptive to notch signals in the endosteal model. This aligns with evidence that OBs are a major source of notch signals in the niche (Gu et al. 2016).

Gene	Gene Expression	
	Vascular	Endosteal
NOTCH1	+	++
DLL3	++	+
MAML	+	++
NUMB	+	++
LFNG	+	++
MFNG	+	++
ADAM10	+	++
ADAM17	+	++
HES1	+	+
HEY1	++	+

Table 5.19 Summary of changes in expression by HSPCs of genes involved in notch signalling.
Refer to Table 5.7 for gene functions. +, increased compared to control; ++, increased compared to control and other model.

As discussed previously, notch signals from stromal niche cells, particularly OBs, promote proliferation, self-renewal, and maintenance of haematopoiesis (Gu et al. 2016). The general increase in components of the pathway indicates increased signalling and hence increased stem cell function.

VASCULAR   ENDOSTEAL

+ cell cycle   ++ cell cycle
+ myeloid differentiation   ++ myeloid differentiation
+ erythroid differentiation   ++ erythroid differentiation
+ lymphoid differentiation   + lymphoid differentiation
+ niche interactions   ++ niche interactions
+ cell signalling   ++ cell signalling

Endothelial cells   Osteoblasts
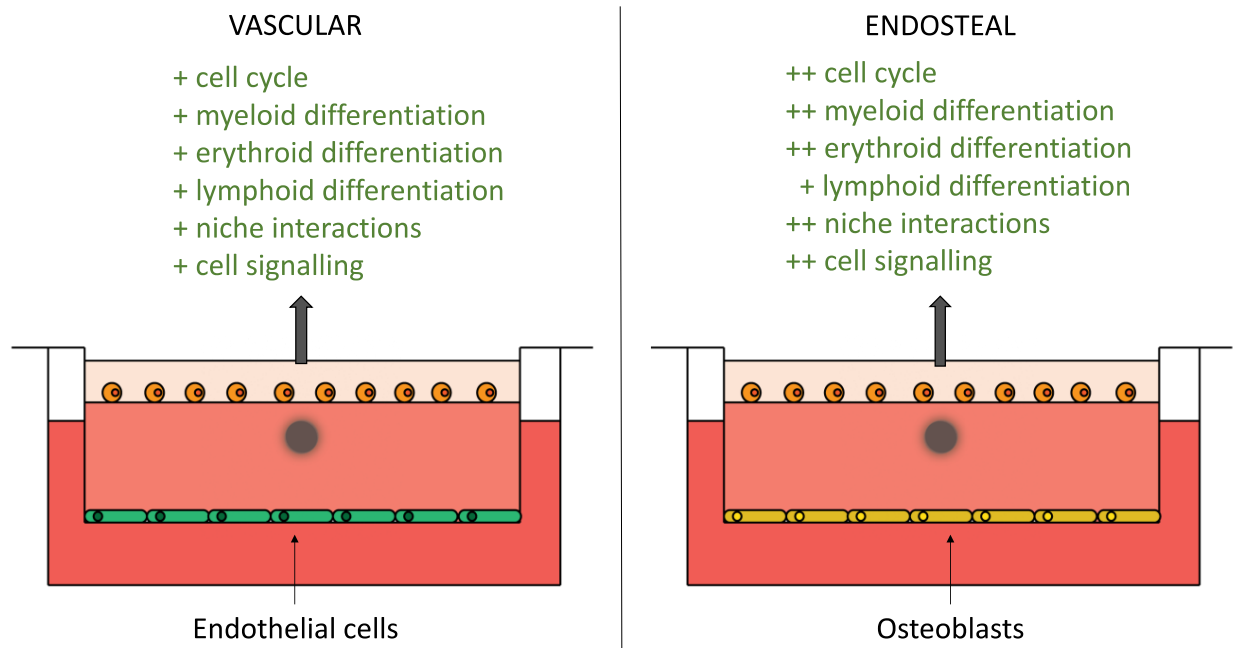
Figure 5.17 Summary of gene expression changes in HSCs when in co-culture compared to control.

In summary, HSPCs cultured in the endosteal model appear to be more active than those cultured in the vascular model. Conflicting results from flow cytometry and RNA analysis make drawing conclusions complicated, but a primitive population seems to be preserved within both models, whilst differentiation is occurring.

5.4.5 Co-culture in 3D collagen gels has differential effects on hypoxia depending on cell type

Hypoxia is a major regulator of the HSC niche. The BM is physiologically hypoxic, despite being highly vascularised. This is because the anatomical structure limits the abundance of afferent arterioles and haematopoietic cells actively consume oxygen (Morikawa & Takubo 2016). In the 3D collagen gel, the diffusion of oxygen may be limited and hence it may be a hypoxic environment. This was investigated by looking at the expression of HIF1α in the different cell types.

HSCs: HIF1α is highly expressed in HSCs following activity of the TF MEIS1. It mediates hypoxia responses that maintain HSC quiescence. Its presence also enhances mobilisation and dynamics of HSCs (Morikawa & Takubo 2016). HIF1α expression has markedly increased in HSCs cultured in both the vascular and endosteal BM models, reflecting their hypoxic status. Hence, stem cell properties such as quiescence are expected to increase in HSCs. The HSCs in the endosteal

model are more hypoxic than those from the vascular model, which is accordance with the expectation that the endosteum is more hypoxic. However, it should be noted that as the model does not simulate blood flow, this difference is due to inherent differences in the support cells themselves, rather than a difference in oxygenation between the cultures. The increase in HIF1α expression observed in HSCs extracted from both co-culture models may also induce the increased VEGF expression, which also promotes HSC survival and function (Gerber et al. 2002).

MSC spheroids: HIF1α expression in MSCs is also relevant to the maintenance of a stem cell phenotype, as it is a transcriptional repressor of RUNX2, which initiates osteogenesis. It also encourages expression of niche factors including CXCL12 and SCF, hence, hypoxia regulates the niche function of MSCs. However, HIF1α expression in MSC spheroids is maintained at a similar level to MSC monolayers. In fact, a very slight decrease in hypoxia was noted in the endosteal model spheroids; this is contrary to the hypothesis that the endosteum environment is more hypoxic than the vascular area, and also conflicts with the hypoxia status in the HSCs from the two models.

HUVECs: Evidence as to whether HIF1α expression is relevant to EC niche function in the BM is limited, but it may influence the expression of HSC maintenance factors in a similar manner to MSCs (Morikawa & Takubo 2016). HIF1α levels have decreased to a greater extent in ECs compared to the other cell types when in co-culture. This is consistent with the vascular area of the niche being less hypoxic.

OBs: HIF1α levels have not changed extensively between control and co-cultured cells. Increased HIF levels in OBs regulates erythropoiesis and HSC population size *in vivo* (Morikawa & Takubo 2016). However, the co-culture has little effect on this function.

Evidence from analysis of expression of HIF1α in all cell types suggests that the endosteal model may induce a more hypoxic phenotype in HSCs, consistent with the *in vivo* physiological BM. However, the other model cell types are all less hypoxic in the 3D model compared to the control.

5.5 Conclusion

This chapter developed an endosteal 3D model (comprising MSC spheroids and monolayer osteoblasts) and a 3D vascular model (comprising MSC spheroids and monolayer endothelial cells) to assess whether either provided a HSC-permissive environment for HSC culture *ex vivo*. Detailed RNA analysis of the multiple cell types following co-culture within the 3D niche models identified some differences compared to the same cell type cultured in isolation, in particular:

- Endosteal and vascular niche models affect MSC spheroid phenotype in a manner that reflects the *in vivo* characteristics of these niche environments: i.e. quiescence at the endosteum and higher activity at the vasculature.

- ECs adopt a mature, quiescent phenotype in the co-culture model, akin to mature vasculature.

- Similarly, OBs have adopted a mature, quiescent phenotype, which may be similar to the phenotype of endosteal OBs *in vivo*.

- Analysis of HSPCs is harder to draw conclusions from as RNA and cell surface markers give conflicting profiles. However, in general extensive differentiation and an increase of cell-cell interactions, supporting HSPC migration, is observed.

It is evident that the stromal cell types within the model are behaving as hypothesised based on the *in vivo* niche. However, conditions for the HSCs may require further optimisation, for example optimising cell number. As this model is being developed with a view towards the co-cultured cells providing an environment which encourages HSPC migration and retention, this may negate the need for the addition of cytokines and GFs to the media, reducing cost. Therefore, adjusting and reducing the concentrations and GF cocktail used in the media may have effects on HSPC behaviour that enhance the model functionality.

CHAPTER 6

Chapter 6   Discussion

6.1 Project summary

As outlined in Chapter 1, this project aimed to recreate the BM niche environment in a way that allows maintenance of an HSC population in a stem cell-like state. There is a clear research and clinical need for such a system, and this study has made progress towards making this goal a reality. Key achievements are described below:

- HSC cell source: in order to carry out the project, a reliable cell source of freshly isolated HSPCs needed to be established; this was *via* a clinical collaboration with a local hospital, who donated bone marrow samples from which HSPCs were isolated. Following this, BM samples were evaluated and determined to be an appropriate HSPC source.

- Media optimisation: as the model involves a co-culture system, comprising MSCs, OBs, and ECs as support cells for the HSCs, the optimisation and characterisation of culture conditions capable of maintaining all cell types is important. An appropriate media formulation for co-culture, which adequately maintained the MSCs and HSCs was idenitifed.

- Cell retrieval from the 3D model: a procedure for extraction of cell populations for downstream analysis was developed and optimised, involving collagenase treatment of the type I collagen gel and subsequent cell population isolation via flow cytometry.

- MSC spheroid model characterisation: extensive characterisation of an existing MSC spheroid model within a collagen gel was carried out. MSCs were shown to be more quiescent, express greater levels of HSC niche-relevant cytokines, and retain key stem cell characteristics when cultured as magnetically labelled spheroids. Hence, this was considered an appropriate starting point to introduce further elements of the BM microenvironments and support HSCs.

- Finally, two further niche cell types (OBs and ECs) were introduced to basic MSC spheroid model, to mimic the endosteal and vascular environments of the niche respectively. HSCs were subseqeuenlty introduced to the co-culture niche models. All cell types were cultured for 7 days, retrieved, separated, and RNA was isolated to analyse key differences in cell cycle, cell markers (self-renewal/differentiation), and cell signalling (cytokine, notch and hedgehog). Results indicated that OBs and ECs adopted mature, quiescent phenotypes akin to those observed in the BM. Similarly, MSC spheroids behaved as expected when separately co-cultured with the cells (i.e. quiescent with OBs and active with ECs). HSPCs cultured within these two models proliferated and a pool of CD34+ cells was retained, although differentiation into more mature cells was observed in both models.

Therefore, in conclusion, endosteal and vascular BM niche models, capable of maintaining MSCs and HSCs in co-culture for up to 7 days, have been developed. Both the niche models do contribute key characteristics to allow for an HSC permissive environment, although further work is needed in order to produce a functional BM model that is able to maintain HSCs in a primitive state for longer periods of time.

6.2 Prospective applications of a bone marrow niche model

A BM niche model has multiple potential applications in investigation of haematopoietic processes, pharmaceutical development, modelling disease, and providing cells for clinical use. Some of these applications are summarised in the following text.

6.2.1 Probing haematopoiesis

Although HSCs remain the most studied and clinically relevant adult stem cell, the relative lack of success in maintaining them *ex vivo* means that a deeper understanding of their biology is required to improve these processes. Many of the signals that cause changes in HSC behaviour have been identified, and are discussed in earlier chapters. However, many still remain to be elucidated (Figure 6.1). The opportunities for studying HSC biology in humans are limited, and using

a murine model may not always produce appropriate results, especially given differences between the murine and human immune systems. An *in vitro* HSC culture system, such as the one developed in this project, may allow identification of such signals, by elimination or subtraction, and hence the development of novel methods to control these behaviours.

For example, the importance of a signal before, during, and after events such as self-renewing division, differentiation, and migration can be investigated. One such microfluidics system has already been used to show that SCF is not important during a first HSC division, but is required for survival afterwards (Choi & Harley 2016). Another possibility is to set up spatial gradients of cells and growth factors in the ECM. This could be used to investigate the importance of gradients for migration and locations of progenitor niches. For example, studies have been performed using opposing gradients of osteoblasts and HSCs (Mahadik et al. 2014), and gradients of SCF covalently linked to a hydrogel (Mahadik et al. 2015).
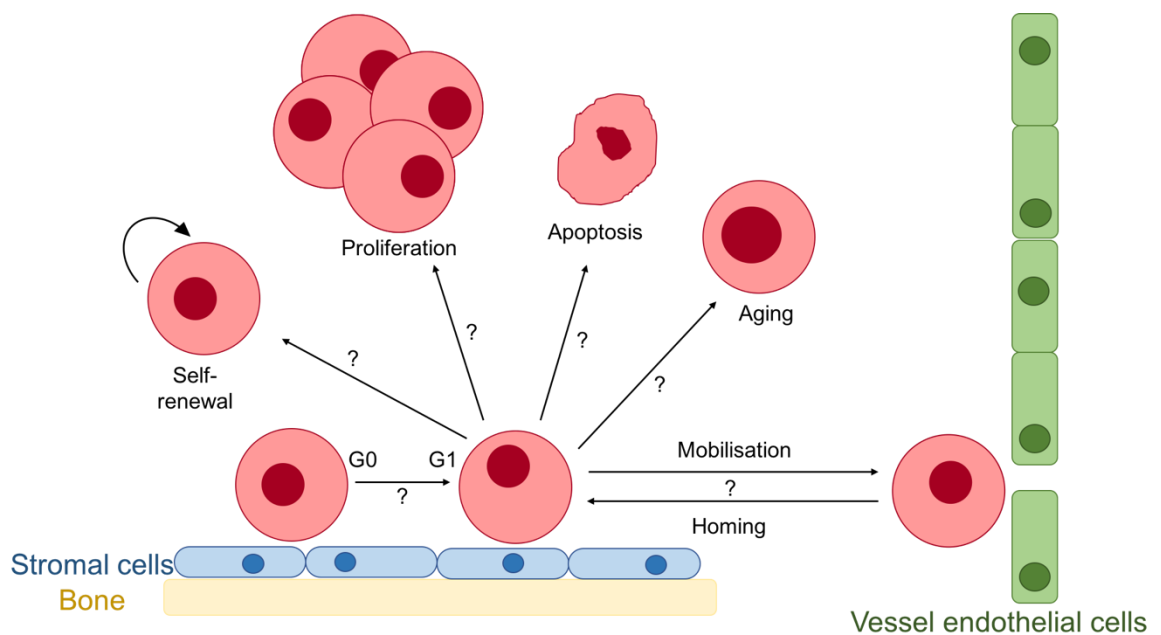
Figure 6.1 Schematic of HSC behaviours that could be investigated using an *in vitro* culture platform.

6.2.2 Modelling disease

In vitro BM models also allow modelling of disease niche states. Many haematological disorders involve HSCs: for example, in leukaemias, stem or progenitor cells can become damaged so that they overproduce one type of white

blood cell, fundamentally changing the cellular composition of the bone marrow (Bonnet 2005, Figure 6.2). Leukaemic stem cells can migrate into the BM and remodel the niche environment to favour themselves at the expense of HSCs (Lane et al. 2009). In turn, an abnormal niche microenvironment can alter the behaviour of HSCs. As LSCs share quiescent and self-renewing properties with HSCs, and are protected from external clinical treatments by the niche environment (Tabe & Konopleva 2014), developing treatments that target only LSCs is difficult. An *in vitro* model could therefore be used to study how these interactions occur and identify therapeutic targets. Furthermore, as these malignancies are heterogeneous in terms of the original mutation and in terms of phenotypic changes, an *in vitro* model can provide a platform to identify the most appropriate therapeutic for an individual patient, whilst also taking into account the microenvironmental conditions. A co-culture system has already been used to identify personalised treatment for multiple myeloma using patient cell samples (MSCs and HSCs) (Pak et al. 2015). A new PhD project in CCE, in collaboration with the Paul O'Gorman Leukaemia Research Centre, is investigating how LSCs migrate into the niche and how they subsequently interact with the resident MSCs and HSCs using the system developed here.
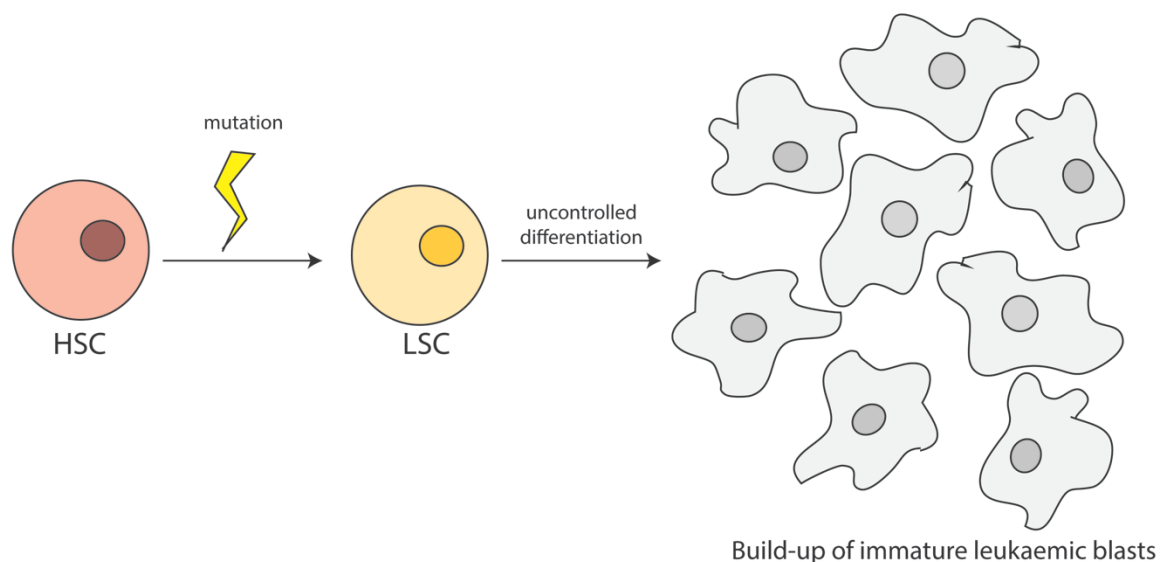
Figure 6.2 Schematic of leukaemia development from HSCs.

6.2.3 Modelling the aging niche

A further opportunity is to study how aging of both HSCs and the niche affects their function. Aged HSCs have lower potential and the prevalence of

haematological disorders increases with age (Sharpless & DePinho 2007). This may not simply be a cell-intrinsic effect, but may also arise due to aging of niche cells. Studies comparing young and aged HSCs have shown that properties such as mobilisation ability are dependent on niche age rather than HSC age (Nakamura-Ishizu & Suda 2014). The mechanisms relating to the aging of HSCs and their niche are currently not well understood. They may involve changes in expression of adhesion molecules, which reduces with age, as aged HSCs are less adherent to stromal cells in culture (Geiger et al. 2007). Metabolic state may also play a role: for example, MSC ROS levels increase with age, along with senescence. An *in vitro* model provides a system to study the effects of introducing an aged cell to a young system and *vice versa*. It could also provide a way to analyse specific cell behaviours and outputs such as metabolites. This has clinical relevance for evaluating and improving transplant procedures between individuals of different ages.

6.2.4 *Ex vivo* pharmaceutical screening

Given the importance of HSCs, studying their behaviour and function requires them to be studied both *in vivo* and *in vitro*. To increase the length of time they can be studied, this means co-culture systems and animal models are usually used to probe HSC biology. However, these systems often have low applicability to humans, due to interspecies differences in immune systems and the lack of support in tissue culture. This contributes to the high attrition rate of experimental treatments in phases I and II of clinical trials. They are also time consuming and expensive. An emerging alternative is developing *in vitro* model systems in a multiwell plate format that suitably mimic organs of the body. These systems can be fully humanised with primary human cells. Individual organs and combinations of organs have the potential to be much more predictive than traditional animal and 2D monolayer cell culture systems. Multiple combinations of drugs and personalised therapeutics can also be tested (Dehne et al. 2017). However, mimicking organs *ex vivo* is complicated, models need to combine ECM molecules, multiple cell types, and appropriate mechanical and biochemical stresses. Nevertheless, there are several examples of organ systems that have been developed successfully and are in use (Marx et al. 2016).

Incorporation of physiological conditions such as shear stress and perfusion by using a microfluidic system may enhance the functionality and properties of niche models. It would also allow precise temporal and spatial control of growth factors, cytokines, and ECM. In particular, the pharmaceutical industry is beginning to move towards these systems in a bid to increase the efficiency of pre-clinical screening, and reduce failure rate.

	Animal models	Artificial organ models
Positives	+ Well established systems	+ Potential for standardisation and high throughput
	+ Systemic effects can be examined	+ Humanised system
		+ Include increased numbers of experimental variables
Negatives	- Time consuming	- Difficult to recapitulate systemic physiology
	- Expensive	- Early stages of development
	- Low predictability of success in later trial stages	
	- Ethical issues	

Table 6.1 Comparison of positive and negative aspects of using animal models versus artificial organ models for pharmaceutical screening.

Only 10 substances out of every 100 that enter clinical trials will be approved for market access (DiMasi et al. 2016). The high attrition rate of experimental treatments between pre-clinical studies and Phase I/II clinical trials can be at least partially attributed to the insufficient predictability of the former. Hence, if *in vitro* models are more predictive than animal models, they have the potential to save the pharmaceutical industry millions of pounds on wasted trials, and also bring back into contention previously discarded candidates. High throughput models would also allow large scale screening of treatments with increased numbers of experimental variables, including evaluation of combination therapies. Therefore, developing such a system would be economically valuable and has the potential to revolutionise the pharmaceutical industry.

6.2.5 Cell source for research and the clinic

A major application of this technology is the potential to supply large numbers of high-quality cells for both research and for use as cell therapies. Currently, HSCs are stored as frozen and thawed at point-of-use. This process, though relatively

successful, involves high levels of necrosis and apoptosis (approximately 40% loss in umbilical cord blood CD34+ cell samples), and reduces functionailty (Hodgkinson et al. 2017; Duchez et al. 2013). A system that can maintain HSCs for an extended period of time, and allows expansion of the population on demand, could overcome these limitations. In a related way, such a system could be used to produce large autologous grafts from a small sample of a patient's own cells. A patient's cells could be extracted, and then maintained or expanded while the patient undergoes myeloablative therapy. This may enable a higher yield and negate the need for a donor, avoiding issues of graft-versus-host disease and the need to find an HLA match. *In vitro* organ models may allow this expansion or retention.

6.2.6 Gene editing platform

Combination of gene editing with artificial organ models provide an ideal vehicle for gene therapy strategies (Bredenoord et al. 2017). For example, intestinal stem cell organoids have been used as proof of principle for gene correction using homologous recombination in primary adult stem cells from patients with cystic fibrosis (Schwank et al. 2013). HSCs are particularly a prime target for gene editing for experimental therapies, due to their primitive nature and involvement in many haematological indications. Gene editing is an area of intensive clinical investigation and is expected to grow rapidly in the next decade. If this model allows gene editing of HSCs, and subsequent retrieval for use *in vivo*, its potential would be tremendous.

6.2.7 Personalised medicine

Incorporating specific patients' cells into a model could pave the way for personalised treatments. This could include engineering disease models using induced pluripotent stem cells from a donor. Any treatment screened on such a platform would then be tailored to the patient's specific genetic profile. As mentioned previously, a co-culture system using patient cells has already been used to screen treatment for multiple myeloma (Pak et al. 2015).

6.3 Limitations of the model

Although the model system presented here has included a greater number of niche components than many other bone marrow models, several key parameters have not been included. There remain many challenges to creating a truly functional bone marrow model. Firstly, there are many types of cells that reside in the bone marrow and feed into the HSC support and regulation network, including megakaryocytes and components of the sympathetic nervous system. Omitting some of these cell types may compromise the functionality of the system and its ability to maintain HSCs. Using multiple cell types with different requirements in traditional cell culture requires extensive optimisation of the system, balancing conflicting priorities. Furthermore, replicating the complex architecture of the bone marrow, including vessels, bone, and trabecular structures has not yet been achieved. With the help of advanced scaffold technologies this may be possible in the future. In particular, this study has only included collagen in the ECM; the addition of molecules such as fibronectin could increase the relevance of the system.

6.5 Conclusion

In this project, an HSC-permissive BM niche model has been optimised, developed, and characterised. The stromal cell types, MSCs, ECs, and OBs adopt phenotypes akin to those observed *in vivo*. HSCs proliferate in co-culture and a pool of CD34+ progenitors is maintained, although the results do not align exactly with behaviour in the BM. Therefore, further optimisation of the model is required before it can be taken forward for applications discussed in this chapter.

6.5.1 Recommendations for future work

- Increase the number of biological replicates for phenotypic characterisation to investigate repeatability of results.

- Optimise cell numbers for the model, particularly for HSCs. At present, the HSC cell numbers were limited by BM availability, however freezing techniques (section 3.3.1.1) have been developed that allow for good retrieval levels. This allows us to bank down cells for future use.

- Characterise the levels of growth factors and cytokines released by spheroids (I identified CXCL12 levels, but need to look at TPO and other key GFs/cytokines involved in HSC maintenance).

- Remove growth factors from the media formulation to ascertain whether they are redundant for HSC support functions.

- Examine gene expression at the protein level (proteomics), as a follow up to the changes noted in the RNA study.

- Investigate cell signalling, quiescence, and differentiation when cultured for longer time points.

- As a long-term goal, introduce LSCs into the model to investigate remodelling of the niche in a disease environment; a study which is currently underway.

Appendix A

Figure A.1 and Figure A.2 show overlapping signal profiles for the different markers used in phenotyping experiments described in section 2.13.2 and 2.13.3, organised by antibody. This gives an overview of the separation of the positive and negative populations present in the different samples: for some of the markers this distinction is not obvious. For several of the markers, however, there is a clear difference in the number of cells expressing the marker at day 1, compared to all the other samples.
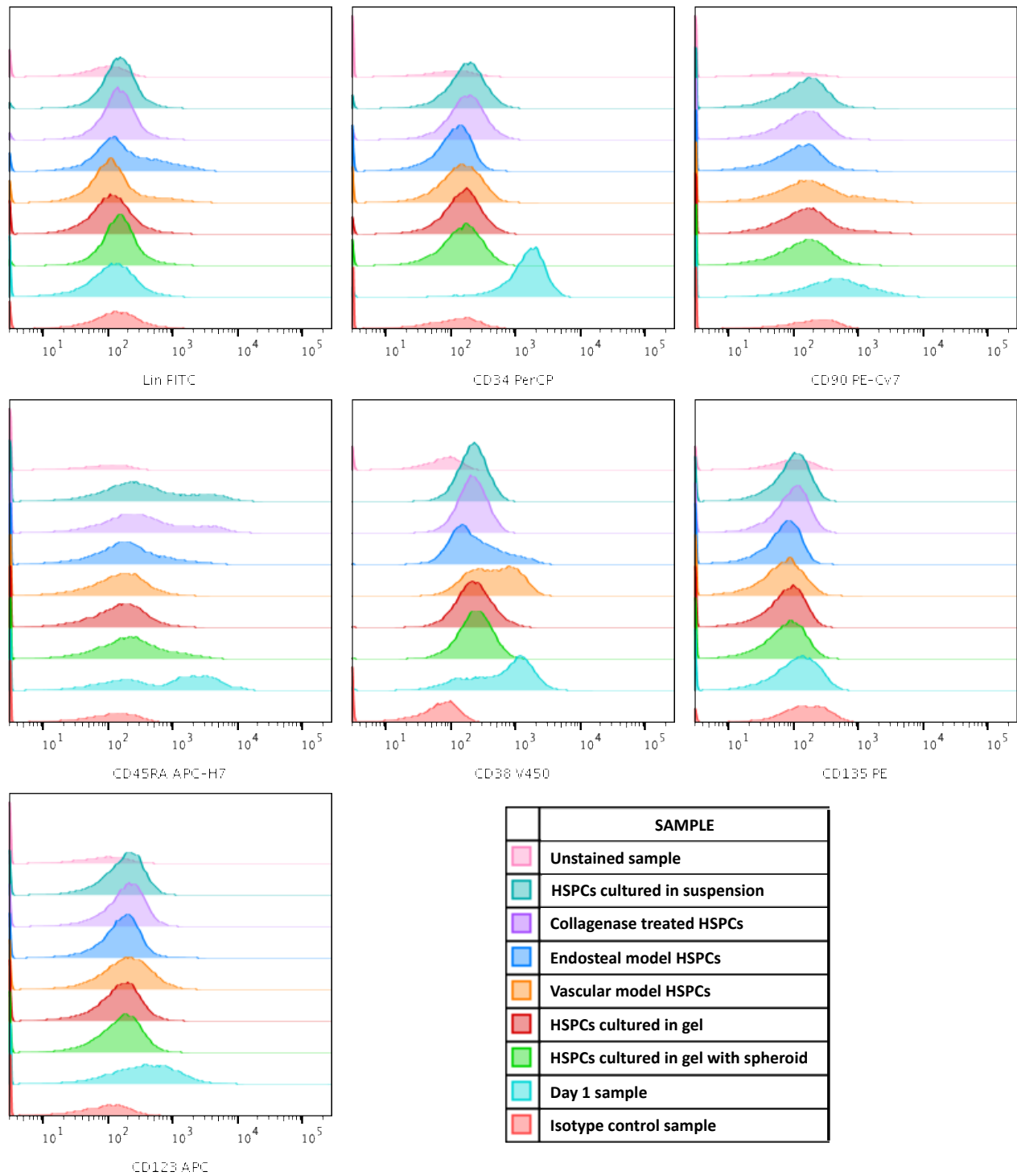
Figure A.1 Overlaid profiles of signals from lineage markers used to identify progenitor subsets in different samples.
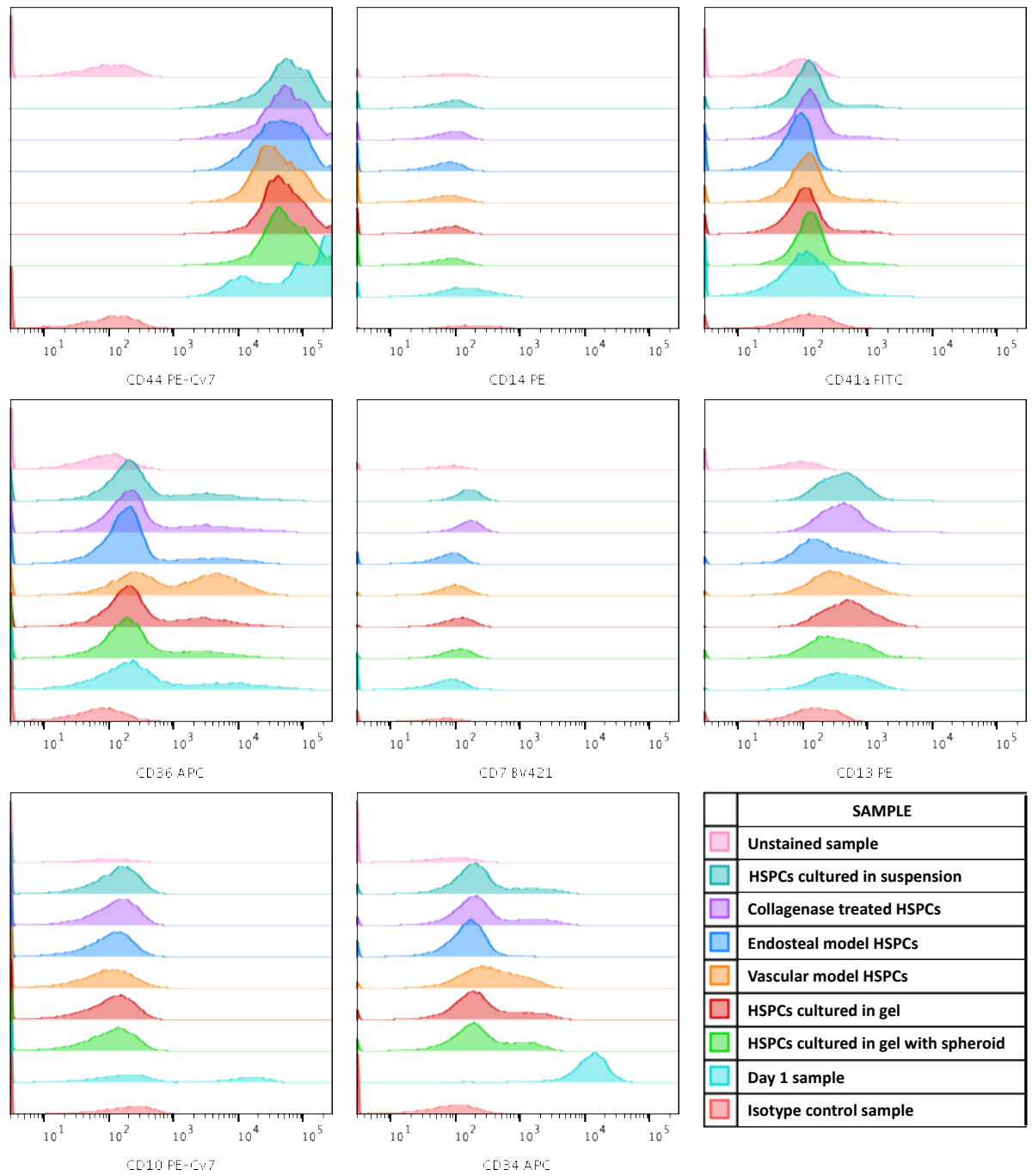
Figure A.2 Overlaid profiles of signals from lineage markers in different samples.

List of References

Abuzakouk, M., Feighery, C. & O'Farrelly, C., 1996. Collagenase and Dispase enzymes disrupt lymphocyte surface molecules. *Journal of Immunological Methods*, 194(2), pp.211–216.

Acar, M. et al., 2015. Stem Cells Are Mainly Perisinusoidal.

Alberts, B., Johnson, A. & Lewis, J., 2002. *Molecular Biology of the Cell*, New York, NY: Garland Science. Available at: https://www.ncbi.nlm.nih.gov/books/NBK26848/.

Albuschies, J. & Vogel, V., 2013. The role of filopodia in the recognition of nanotopographies. *Scientific Reports*, 1658(3), pp.1–9. Available at: http://www.pubmedcentral.nih.gov/articlerender.fcgi?artid=3625890&tool=pmcentrez&rendertype=abstract%5Cnhttp://www.nature.com/doifinder/10.1038/srep01658.

Alcayaga-Miranda, F. et al., 2015. Characterization of menstrual stem cells: angiogenic effect, migration and hematopoietic stem cell support in comparison with bone marrow mesenchymal stem cells. *Stem Cell Research & Therapy*, 6(32), pp.1–14. Available at: ???

Alimperti, S. et al., 2014. Serum-free spheroid suspension culture maintains mesenchymal stem cell proliferation and differentiation potential. *Biotechnology Progress*, 30(4), pp.974–983.

Almalki, S.G. & Agrawal, D.K., 2016. Key transcription factors in the differentiation of mesenchymal stem cells. *Differentiation*, 92(1–2), pp.41–51. Available at: http://dx.doi.org/10.1016/j.diff.2016.02.005.

Almeida-Porada, G. & Ascensao, J.L., 1996. Isolation, characterization, and biologic features of bone marrow endothelial cells. *The Journal of laboratory and clinical medicine*, 128(4), pp.399–407.

Álvarez-Viejo, M., Menendez-Menendez, Y. & Otero-Hernandez, J., 2015. CD271 as a marker to identify mesenchymal stem cells from diverse sources before culture. *World Journal of Stem Cells*, 7(2), pp.470–476. Available at: http://www.wjgnet.com/1948-0210/full/v7/i2/470.htm.

Andrade, P.Z. et al., 2010. Systematic delineation of optimal cytokine concentrations to expand hematopoietic stem/progenitor cells in co-culture with mesenchymal stem cells. *Molecular BioSystems*, 6(7), pp.1207–1215. Available at: http://xlink.rsc.org/?DOI=b922637k.

Antin, J.H. & Raley, D.Y., 2013. *Manual of Stem Cell and Bone Marrow Transplantation* 2nd ed., Cambridge, UK: Cambridge University Press.

Arai, F. et al., 2004. Tie2/angiopoietin-1 signaling regulates hematopoietic stem cell quiescence in the bone marrow niche. *Cell*, 118(2), pp.149–61. Available at: http://www.ncbi.nlm.nih.gov/pubmed/15260986.

Ariki, R. et al., 2014. Homeodomain transcription factor Meis1 is a critical regulator of adult bone marrow hematopoiesis. *PLoS ONE*, 9(2), pp.1–11.

Armesilla-Diaz, A., Elvira, G. & Silva, A., 2009. P53 Regulates the Proliferation, Differentiation and Spontaneous Transformation of Mesenchymal Stem Cells. *Experimental Cell Research*, 315(20), pp.3598–3610. Available at: http://dx.doi.org/10.1016/j.yexcr.2009.08.004.

Arufe, M.C. et al., 2009. Differentiation of synovial CD-105+ human mesenchymal stem cells into chondrocyte-like cells through spheroid formation. *Journal of Cellular Biochemistry*, 108(1), pp.145–155.

Ashman, L.K., 1999. The biology of stem cell factor and its receptor C-kit. *The International Journal of Biochemistry & Cell Biology*, 31(10), pp.1037–51.

Available at: http://www.ncbi.nlm.nih.gov/pubmed/10582338.

Askmyr, M. et al., 2009. What is the true nature of the osteoblastic hematopoietic stem cell niche? *Trends in endocrinology and metabolism: TEM*, 20(6), pp.303–9. Available at: http://www.ncbi.nlm.nih.gov/pubmed/19595609 [Accessed May 26, 2014].

Avecilla, S.T. et al., 2004. Chemokine-mediated interaction of hematopoietic progenitors with the bone marrow vascular niche is required for thrombopoiesis. *Nature medicine*, 10(1), pp.64–71.

Bai, L.Y. et al., 2008. Differential expression of Sonic hedgehog and Gli1 in hematological malignancies. *Leukemia*, 22(1), pp.226–228. Available at: http://www.ncbi.nlm.nih.gov/pubmed/17928882.

Baldari, S. et al., 2017. Challenges and strategies for improving the regenerative effects of mesenchymal stromal cell-based therapies. *International Journal of Molecular Sciences*, 18(10).

Banerjee, M. & Bhonde, R.R., 2006. Application of hanging drop technique for stem cell differentiation and cytotoxicity studies. *Cytotechnology*, 51(1), pp.1–5. Available at: http://www.pubmedcentral.nih.gov/articlerender.fcgi?artid=3449481&tool=pmcentrez&rendertype=abstract [Accessed May 7, 2014].

Banfi, A. et al., 2000. Proliferation kinetics and differentiation potential of ex vivo expanded human bone marrow stromal cells. *Experimental Hematology*, 28(6), pp.707–715. Available at: http://www.sciencedirect.com/science/article/pii/S0301472X00001600.

Bara, J.J. et al., 2014. Concise review: bone marrow-derived mesenchymal stem cells change phenotype following in vitro culture: implications for basic research and the clinic. *Stem cells (Dayton, Ohio)*, 32(7), pp.1713–23. Available at: http://www.ncbi.nlm.nih.gov/pubmed/24449458.

Baraniak, P.R. & McDevitt, T.C., 2012. Scaffold-free culture of mesenchymal stem cell spheroids in suspension preserves multilineage potential. *Cell and Tissue Research*, 347(3), pp.701–711.

de Barros, A.P.D.N. et al., 2010. Osteoblasts and bone marrow mesenchymal stromal cells control hematopoietic stem cell migration and proliferation in 3D in vitro model. *PloS one*, 5(2), p.e9093. Available at: http://www.pubmedcentral.nih.gov/articlerender.fcgi?artid=2816998&tool=pmcentrez&rendertype=abstract [Accessed May 7, 2014].

Bartosh, T.J. et al., 2010. Aggregation of human mesenchymal stromal cells (MSCs) into 3D spheroids enhances their anti-inflammatory properties. *PNAS*, 107(31), pp.13724–13729.

Baudino, T.A. et al., 2002. c-Myc is essential for vasculogenesis and angiogenesis during development and tumor progression. *Genes and Development*, 16(19), pp.2530–2543.

Benedito, R. et al., 2009. The Notch Ligands Dll4 and Jagged1 Have Opposing Effects on Angiogenesis. *Cell*, 137(6), pp.1124–1135. Available at: http://dx.doi.org/10.1016/j.cell.2009.03.025.

Bhandari, D.R. et al., 2010. REX-1 expression and p38 MAPK activation status can determine proliferation/differentiation fates in human mesenchymal stem cells. *PloS one*, 5(5), p.e10493. Available at: http://www.pubmedcentral.nih.gov/articlerender.fcgi?artid=2864743&tool=pmcentrez&rendertype=abstract.

Bhang, S.H. et al., 2012. Transplantation of Cord Blood Mesenchymal Stem Cells as Spheroids Enhances Vascularization. *Tissue Engineering Part A*, 18(19–20),

pp.2138–2147. Available at: http://online.liebertpub.com/doi/abs/10.1089/ten.tea.2011.0640.

Bianco, P., 2011. Bone and the hematopoietic niche: a tale of two stem cells. *Blood*, 117(20), pp.5281–8. Available at: http://www.ncbi.nlm.nih.gov/pubmed/21406722 [Accessed January 21, 2014].

Bigas, A., Robert-Moreno, A. & Espinosa, L., 2010. The Notch pathway in the developing hematopoietic system. *The International journal of developmental biology*, 54(6–7), pp.1175–88. Available at: http://www.ncbi.nlm.nih.gov/pubmed/20711994 [Accessed June 12, 2014].

Bonab, M.M. et al., 2006. Aging of mesenchymal stem cell in vitro. *BMC cell biology*, 7, p.14. Available at: http://www.pubmedcentral.nih.gov/articlerender.fcgi?artid=1435883&tool=pmcentrez&rendertype=abstract.

Bonnet, D., 2005. Normal and leukaemic stem cells. *British Journal of Haematology*, 130(4), pp.469–479.

Both, S.K. et al., 2007. A rapid and efficient method for expansion of human mesenchymal stem cells. *Tissue Eng*, 13(1), pp.3–9.

Bredenoord, A.L., Clevers, H. & Knoblich, J.A., 2017. Human tissues in a dish: The research and ethical implications of organoid technology. *Science*, 355(260).

Brizzi, M.F., Tarone, G. & Defilippi, P., 2012. Extracellular matrix, integrins, and growth factors as tailors of the stem cell niche. *Current opinion in cell biology*, 24(5), pp.645–51. Available at: http://www.ncbi.nlm.nih.gov/pubmed/22898530 [Accessed July 9, 2014].

Bug, G. et al., 2002. Rho family small GTPases control migration of hematopoietic progenitor cells into multicellular spheroids of bone marrow stroma cells. *Journal of Leukocyte Biology*, 72(October), pp.837–845.

Byrd, N. & Grabel, L., 2004. Hedgehog signaling in murine vasculogenesis and angiogenesis. *Trends in Cardiovascular Medicine*, 14(8), pp.308–313.

Cai, J.Q. et al., 2012. Sonic hedgehog enhances the proliferation and osteogenic differentiation of bone marrow-derived mesenchymal stem cells. *Cell Biol Int*, 36(4), pp.349–355. Available at: http://www.ncbi.nlm.nih.gov/entrez/query.fcgi?cmd=Retrieve&db=PubMed&dopt=Citation&list_uids=22149964.

Cai, M. et al., 2012. Dual actions of Meis1 inhibit erythroid progenitor development and sustain general hematopoietic cell proliferation. *Blood*, 120(2), pp.335–346.

Callaway, E., 2016. Embryo editing gets green light. *Nature*, 530, pp.18–19.

Canalis, E., 2008. Notch signaling in osteoblasts. *Science signaling*, 1(17), p.pe17. Available at: http://www.ncbi.nlm.nih.gov/pubmed/18445833.

Cao, Y., 2007. Angiogenesis modulates adipogenesis and obesity. *Journal of Clinical Investigation*, 117(9), pp.2362–2368.

Caplan, A.I. & Correa, D., 2011. The MSC: an injury drugstore. *Cell stem cell*, 9(1), pp.11–5. Available at: http://www.pubmedcentral.nih.gov/articlerender.fcgi?artid=3144500&tool=pmcentrez&rendertype=abstract [Accessed July 16, 2014].

Carlsson, J. et al., 1983. Formation and growth of multicellular spheroids of human origin. *International journal of cancer.*, 31(5), pp.523–33. Available at: http://www.ncbi.nlm.nih.gov/pubmed/6852971.

Celebi, B., Mantovani, D. & Pineault, N., 2011. Effects of extracellular matrix

proteins on the growth of haematopoietic progenitor cells. *Biomedical materials*, 6(5), p.11. Available at: http://www.ncbi.nlm.nih.gov/pubmed/21931196 [Accessed June 13, 2014].

Cesarz, Z. & Tamama, K., 2016. Spheroid Culture of Mesenchymal Stem Cells. *Stem Cells International*, 2016.

Chen, X.-D. et al., 2007. Extracellular Matrix Made by Bone Marrow Cells Facilitates Expansion of Marrow-Derived Mesenchymal Progenitor Cells and Prevents Their Differentiation Into Osteoblasts. *J Bone Miner Res*, 22(12), pp.1943–1956.

Cheng, L. et al., 2003. Human Adult Marrow Cells Support Prolonged Expansion of Human Embryonic Stem Cells in Culture. *Stem Cells*, 21, pp.131–142.

Cheng, L. et al., 2000. Human mesenchymal stem cells support megakaryocyte and pro-platelet formation from CD34(+) hematopoietic progenitor cells. *Journal of cellular physiology*, 184(1), pp.58–69. Available at: http://www.ncbi.nlm.nih.gov/pubmed/10825234.

Cheng, N.C., Wang, S. & Young, T.H., 2012. The influence of spheroid formation of human adipose-derived stem cells on chitosan films on stemness and differentiation capabilities. *Biomaterials*, 33(6), pp.1748–1758. Available at: http://dx.doi.org/10.1016/j.biomaterials.2011.11.049.

Chitteti, B.R. et al., 2015. CD166 regulates human and murine hematopoietic stem cells and the hematopoietic niche. *Blood*, 124(4), pp.519–530.

Choi, J.S. & Harley, B.A.C., 2016. Challenges and Opportunities to Harnessing the (Hematopoietic) Stem Cell Niche. *Current Stem Cell Reports*, 2(1), pp.85–94.

Choi, K.-D. et al., 2009. Hematopoietic and Endothelial Differentiation of Human Induced Pluripotent Stem Cells. *Stem Cells*, 27(3), pp.559–567. Available at: http://doi.wiley.com/10.1634/stemcells.2008-0922.

Choi, Y.S. et al., 2010. Optimization of ex vivo hematopoietic stem cell expansion in intermittent dynamic cultures. *Biotechnology Letters*, 32(12), pp.1969–1975.

Christophis, C. et al., 2011. Shear stress regulates adhesion and rolling of CD44+ leukemic and hematopoietic progenitor cells on hyaluronan. *Biophysical journal*, 101(3), pp.585–93.

Clarke, B., 2008. Normal bone anatomy and physiology. *Clinical Journal of the American Society of Nephrology: CJASN*, 3(Suppl 3), pp.S131–S139.

Copelan, E. a, 2006. Hematopoietic stem-cell transplantation. *The New England journal of medicine*, 354(17), pp.1813–26. Available at: http://www.ncbi.nlm.nih.gov/pubmed/16641398.

Corselli, M. et al., 2013. Perivascular support of human hematopoietic stem / progenitor cells. *Blood*, 121(15), pp.2891–2901.

Crane, G.M., Jeffery, E. & Morrison, S.J., 2017. Adult haematopoietic stem cell niches. *Nature Reviews Immunology*. Available at: http://www.nature.com/doifinder/10.1038/nri.2017.53.

Dalby, M.J. et al., 2007. The control of human mesenchymal cell differentiation using nanoscale symmetry and disorder. *Nature materials*, 6(12), pp.997–1003. Available at: http://www.ncbi.nlm.nih.gov/pubmed/17891143 [Accessed January 9, 2014].

Dehne, E.-M., Hasenberg, T. & Marx, U., 2017. The ascendance of microphysiological systems to solve the drug testing dilemma. *Future Science OA*, p.FSO185. Available at: http://www.future-science.com/doi/10.4155/fsoa-2017-0002.

Dejardin, T. et al., 2011. Influence of both a static magnetic field and penetratin on magnetic nanoparticle delivery into fibroblasts. *Nanomedicine*, 3(10), pp.1719–1731.

DiMasi, J.A., Grabowski, H.G. & Hansen, R.W., 2016. Innovation in the pharmaceutical industry: New estimates of R&D costs. *Journal of Health Economics*, 47, pp.20–33. Available at: http://dx.doi.org/10.1016/j.jhealeco.2016.01.012.

Ding, L. et al., 2012. Endothelial and perivascular cells maintain haematopoietic stem cells. *Nature*, 481(7382), pp.457–62. Available at: http://www.pubmedcentral.nih.gov/articlerender.fcgi?artid=3270376&tool=pmcentrez&rendertype=abstract [Accessed March 22, 2014].

Ding, L. & Morrison, S.J., 2013. Haematopoietic stem cells and early lymphoid progenitors occupy distinct bone marrow niches. *Nature*, 495(7440), pp.231–5. Available at: http://www.pubmedcentral.nih.gov/articlerender.fcgi?artid=3600153&tool=pmcentrez&rendertype=abstract [Accessed March 26, 2014].

Dominici, M. et al., 2006. Minimal criteria for defining multipotent mesenchymal stromal cells. The International Society for Cellular Therapy position statement. *Cytotherapy*, 8(4), pp.315–7. Available at: http://www.sciencedirect.com/science/article/pii/S1465324906708817.

Dong, J. et al., 2009. Response of mesenchymal stem cells to shear stress in tissue-engineered vascular grafts. *Acta pharmacologica Sinica*, 30(5), pp.530–6. Available at: http://www.ncbi.nlm.nih.gov/pubmed/19417732 [Accessed August 13, 2014].

Dong, Y. et al., 2010. RBPjkappa-dependent Notch signaling regulates mesenchymal progenitor cell proliferation and differentiation during skeletal development. *Development*, 137(9), pp.1461–1471.

Dontu, G. et al., 2003. In vitro propagation and transcriptional profiling of human mammary stem / progenitor cells. *Genes & Development*, 17(10), pp.1253–1270.

Driessen, R.L., Johnston, H.M. & Nilsson, S.K., 2003. Membrane-bound stem cell factor is a key regulator in the initial lodgment of stem cells within the endosteal marrow region. *Experimental hematology*, 31(12), pp.1284–91. Available at: http://www.ncbi.nlm.nih.gov/pubmed/14662336.

Drüeke, T.B., 2006. Haematopoietic stem cells--role of calcium-sensing receptor in bone marrow homing. *Nephrology Dialysis Transplantation*, 21(8), pp.2072–4. Available at: http://www.ncbi.nlm.nih.gov/pubmed/16702207 [Accessed August 12, 2014].

Duchez, P. et al., 2013. Cryopreservation of hematopoietic stem and progenitor cells amplified ex vivo from cord blood CD34+ cells. *Transfusion*, 53(9), pp.2012–2019.

Ehninger, A. & Trumpp, A., 2011. The bone marrow stem cell niche grows up: mesenchymal stem cells and macrophages move in. *The Journal of experimental medicine*, 208(3), pp.421–8. Available at: http://www.pubmedcentral.nih.gov/articlerender.fcgi?artid=3058583&tool=pmcentrez&rendertype=abstract [Accessed April 28, 2014].

Elefteriou, F., Campbell, P. & Ma, Y., 2014. Control of bone remodeling by the peripheral sympathetic nervous system. *Calcified Tissue International*, 94(1), pp.140–151.

Ellis, S.L. et al., 2011. The relationship between bone, hemopoietic stem cells, and vasculature. *Blood*, 118, pp.1516–1524.

Eltoukhy, H.S. et al., 2016. CXCL12-Abundant Reticular Cells (CAR) Cells : A Review of the Literature with Relevance to Cancer Stem Cell Survival. *Journal of Cancer Stem Cell Research*, 4(e1004), pp.1–7.

Engler, A.J. et al., 2006. Matrix elasticity directs stem cell lineage specification. *Cell*, 126(4), pp.677–89. Available at: http://www.ncbi.nlm.nih.gov/pubmed/16923388 [Accessed January 20, 2014].

Fan, X. et al., 2009. Optimization of Primary Culture Condition for Mesenchymal Stem Cells Derived from Umbilical Cord Blood with Factorial Design. *Biotechnology Progress*, 25(2), pp.499–507.

Fernandez, L. et al., 2008. Tumor necrosis factor-alpha and endothelial cells modulate Notch signaling in the bone marrow microenvironment during inflammation. *Experimental hematology*, 36(5), pp.545–558. Available at: http://www.pubmedcentral.nih.gov/articlerender.fcgi?artid=3437760&tool=pmcentrez&rendertype=abstract.

Ferrari, S.L. et al., 2000. A role for N-cadherin in the development of the differentiated osteoblastic phenotype. *Journal of Bone and Mineral Research*, 15(2), pp.198–208.

Ferreira, M.S.V. et al., 2012. Cord blood-hematopoietic stem cell expansion in 3D fibrin scaffolds with stromal support. *Biomaterials*, 33(29), pp.6987–97. Available at: http://www.ncbi.nlm.nih.gov/pubmed/22800538 [Accessed June 24, 2014].

Fleming, W.H. et al., 1993. Functional Heterogeneity Is Associated with the Cell Cycle Status of Murine Hematopoietic Stem Cells. *Journal of cell biology*, 122(4), pp.897–902.

Florea, V. et al., 2013. c-Myc Is Essential to Prevent Endothelial Pro-Inflammatory Senescent Phenotype. *PLoS ONE*, 8(9), pp.1–12.

Fontaine, C. et al., 2008. Hedgehog Signaling Alters Adipocyte Maturation of Human Mesenchymal Stem Cells. *Stem Cells*, 26, pp.1037–1046.

Frenette, P.S. et al., 2013. Mesenchymal stem cell: keystone of the hematopoietic stem cell niche and a stepping-stone for regenerative medicine. *Annual Review of Immunology*, 31, pp.285–316. Available at: http://www.ncbi.nlm.nih.gov/pubmed/23298209 [Accessed February 5, 2014].

Galipeau, J. et al., 2015. International Society for Cellular Therapy perspective on immune functional assays for mesenchymal stromal cells as potency release criterion for advanced phase clinical trials. *Cytotherapy*, 18(2), pp.151–159. Available at: http://dx.doi.org/10.1016/j.jcyt.2015.11.008.

Gao, J. et al., 2009. Hedgehog Signaling Is Dispensable for Adult Hematopoietic Stem Cell Function. *Cell Stem Cell*, 4(6), pp.548–558. Available at: http://dx.doi.org/10.1016/j.stem.2009.03.015.

Gattazzo, F., Urciuolo, A. & Bonaldo, P., 2014. Extracellular matrix: A dynamic microenvironment for stem cell niche. *Biochimica et Biophysica Acta*, 1840(8), pp.2506–2519. Available at: http://dx.doi.org/10.1016/j.bbagen.2014.01.010.

Geiger, H., Koehler, A. & Gunzer, M., 2007. Stem cells, aging, niche, adhesion and Cdc42: A model for changes in cell-cell interactions and hematopoietic stem cell aging. *Cell Cycle*, 6(8), pp.884–887.

Genovese, P. et al., 2014. Targeted genome editing in human repopulating haematopoietic stem cells. *Nature*, 510(7504), pp.235–40. Available at: http://www.nature.com/doifinder/10.1038/nature13420%5Cnhttp://dx.doi.

org/10.1038/nature13420%5Cnhttp://www.pubmedcentral.nih.gov/articlere
nder.fcgi?artid=4082311&tool=pmcentrez&rendertype=abstract.

Gerber, H.-P. et al., 2002. VEGF regulates haematopoietic stem cell survival by
an internal autocrine loop mechanism. *Nature*, 417(6892), pp.954–8.
Available at: http://www.ncbi.nlm.nih.gov/pubmed/12087404.

Goff, L.A. et al., 2008. Differentiating Human Multipotent Mesenchymal Stromal
Cells Regulate microRNAs: Prediction of microRNA Regulation by PDGF
During Osteogenesis. *Experimental Hematology*, 36(10), pp.1354-1369.

Gordon, M., 1988. Extracellular Matrix of the Marrow Microenvironment. *British
journal of haematology*, 70, pp.1–4. Available at:
http://onlinelibrary.wiley.com/doi/10.1111/j.1365-
2141.1988.tb02425.x/abstract.

Gratwohl, A. et al., 2015. One million haemopoietic stem-cell transplants: a
retrospective observational study. *The Lancet Haematology*, 2(3), pp.e91–
e100. Available at:
http://www.thelancet.com/article/S2352302615000289/fulltext%5Cnhttp://
/linkinghub.elsevier.com/retrieve/pii/S2352302615000289%5Cnhttp://www.
sciencedirect.com/science/article/pii/S2352302615000289.

Greenbaum, A. et al., 2013. CXCL12 in early mesenchymal progenitors is
required for haematopoietic stem-cell maintenance. *Nature*, 495(7440),
pp.227–30. Available at:
http://www.pubmedcentral.nih.gov/articlerender.fcgi?artid=3600148&tool=
pmcentrez&rendertype=abstract [Accessed January 22, 2014].

Groebe, K. & Mueller-Klieser, W., 1996. On the relation between size of necrosis
and diameter of tumor spheroids. *Int. J Radiation Oncology Biol. Phys.*,
34(2), pp.395-401.

Gronthos, S. et al., 2003. Molecular and cellular characterisation of highly
purified stromal stem cells derived from human bone marrow. *Journal of
Cell Science*, 116(Pt 9), pp.1827–1835.

Gu, Y., Masiero, M. & Banham, A.H., 2016. Notch signaling: its roles and
therapeutic potential in hematological malignancies. *Oncotarget*, 7(20),
pp.29804-29823.

Guarnerio, J. et al., 2014. Bone Marrow Endosteal Mesenchymal Progenitors
Depend on HIF Factors for Maintenance and Regulation of Hematopoiesis.
Stem cell reports, 2(6), pp.794–809. Available at:
http://www.pubmedcentral.nih.gov/articlerender.fcgi?artid=4050345&tool=
pmcentrez&rendertype=abstract [Accessed June 19, 2014].

Gundry, M.C. et al., 2016. Highly efficient genome editing of murine and human
hematopoietic progenitor cells by CRISPR/Cas9. *Cell Reports*, 17(5),
pp.1453-1461.

Guo, L., Zhou, Y., et al., 2014. Epigenetic changes of mesenchymal stem cells in
three-dimensional (3D) spheroids. *Journal of Cellular and Molecular
Medicine*, 18(10), pp.2009-2019.

Guo, L., Ge, J., et al., 2014. Three-Dimensional Spheroid-Cultured Mesenchymal
Stem Cells Devoid of Embolism Attenuate Brain Stroke Injury After Intra-
Arterial Injection. *Stem Cells and Development*, 23(9), pp.978–989.
Available at: http://online.liebertpub.com/doi/abs/10.1089/scd.2013.0338.

Haÿ, E., Nouraud, A. & Marie, P.J., 2009. N-cadherin negatively regulates
osteoblast proliferation and survival by antagonizing Wnt, ERK and PI3K/Akt
signalling. *PLoS ONE*, 4(12).

Heazlewood, S.Y. et al., 2014. Analyzing hematopoietic stem cell homing,

lodgment, and engraftment to better understand the bone marrow niche. *Annals of the New York Academy of Sciences*, 1310(1), pp.119–28. Available at: http://www.ncbi.nlm.nih.gov/pubmed/24428368 [Accessed May 23, 2014].

Heazlewood, S.Y. et al., 2013. Megakaryocytes co-localise with hemopoietic stem cells and release cytokines that up-regulate stem cell proliferation. *Stem cell research*, 11(2), pp.782–92. Available at: http://www.ncbi.nlm.nih.gov/pubmed/23792434 [Accessed May 26, 2014].

Hilton, M.J. et al., 2008. Notch signaling maintains bone marrow mesenchymal progenitors by suppressing osteoblast differentiation. *Nature medicine*, 14(3), pp.306–14. Available at: http://www.pubmedcentral.nih.gov/articlerender.fcgi?artid=2740725&tool=pmcentrez&rendertype=abstract.

Hirschhaeuser, F. et al., 2010. Multicellular tumor spheroids: An underestimated tool is catching up again. *Journal of Biotechnology*, 148(1), pp.3–15. Available at: http://dx.doi.org/10.1016/j.jbiotec.2010.01.012.

Hodgkinson, K.M. et al., 2017. Intersecting Worlds of Transfusion and Transplantation Medicine: An International Symposium Organized by the Canadian Blood Services Centre for Innovation. *Transfusion Medicine Reviews*, 31(3), pp.183–192.

Hooper, A.T. et al., 2009. Engraftment and Reconstitution of Hematopoiesis Is Dependent on VEGFR2-Mediated Regeneration of Sinusoidal Endothelial Cells. *Cell Stem Cell*, 4(3), pp.263–274. Available at: http://dx.doi.org/10.1016/j.stem.2009.01.006.

Hosokawa, K. et al., 2010. Cadherin-based adhesion is a potential target for niche manipulation to protect hematopoietic stem cells in adult bone marrow. *Cell stem cell*, 6(3), pp.194–8. Available at: http://www.ncbi.nlm.nih.gov/pubmed/20207221 [Accessed July 9, 2014].

Hsu, S. et al., 2014. Substrate-dependent modulation of 3D spheroid morphology self-assembled in mesenchymal stem cell-endothelial progenitor cell coculture. *Biomaterials*, 35(26), pp.7295–7307. Available at: http://dx.doi.org/10.1016/j.biomaterials.2014.05.033.

Huang, X. et al., 2016. Co-cultured hBMSCs and HUVECs on human bio-derived bone scaffolds provide support for the long-term ex vivo culture of HSC/HPCs. *Journal of Biomedical Materials Research - Part A*, 104(5), pp.1221–1230.

Imanirad, P. & Dzierzak, E., 2013. Hypoxia and HIFs in regulating the development of the hematopoietic system. *Blood Cells, Molecules, and Diseases*, 51(4), pp.256–263. Available at: http://dx.doi.org/10.1016/j.bcmd.2013.08.005.

Isern, J. et al., 2013. Self-renewing human bone marrow mensenspheres promote hematopoietic stem cell expansion. *Cell reports*, 3(5), pp.1714–24. Available at: http://www.ncbi.nlm.nih.gov/pubmed/23623496 [Accessed February 20, 2014].

Isern, J. et al., 2014. The neural crest is a source of mesenchymal stem cells with specialized hematopoietic stem cell niche function. *eLife*, 3, pp.1–28.

Itkin, T. et al., 2016. Distinct bone marrow blood vessels differentially regulate haematopoiesis. *Nature*, pp.1–19. Available at: http://www.nature.com/doifinder/10.1038/nature17624.

Ito, K. et al., 2006. Reactive oxygen species act through p38 MAPK to limit the lifespan of hematopoietic stem cells. *Nature medicine*, 12(4), pp.446–451.

Iwai, T. et al., 2008. Smad7 inhibits chondrocyte differentiation at multiple steps during endochondral bone formation and down-regulates p38 MAPK pathways. *Journal of Biological Chemistry*, 283(40), pp.27154-27164.

Iwanaga, R. et al., 2006. Identification of novel E2F1 target genes regulated in cell cycle-dependent and independent manners. *Oncogene*, 25(12), pp.1786–1798.

Janeczek, A.A. et al., 2015. Skeletal Stem Cell Niche of the Bone Marrow. In *Tissue Specific Stem Cell Niche*. pp. 245–279. Available at: http://link.springer.com/10.1007/978-3-319-21705-5.

Jiang, Y., Prosper, F. & Verfaillie, C.M., 2000. Opposing effects of engagement of integrins and stimulation of cytokine receptors on cell cycle progression of normal human hematopoietic progenitors. *Blood*, 95(3), pp.846–854.

Jie Sun, Shan Fu, Weijun Zhong, H.H., 2013. PML overexpression inhibits proliferation and promotes the osteogenic differentiation of human mesenchymal stem cells. *Oncology Reports*, 30(6), pp.2785–2794.

Jing, D. et al., 2010. Hematopoietic stem cells in co-culture with mesenchymal stromal cells--modeling the niche compartments in vitro. *Haematologica*, 95(4), pp.542–50. Available at: http://www.pubmedcentral.nih.gov/articlerender.fcgi?artid=2857183&tool=pmcentrez&rendertype=abstract [Accessed May 7, 2014].

Jokinen, J. et al., 2004. Integrin-mediated cell adhesion to type I collagen fibrils. *Journal of Biological Chemistry*, 279(30), pp.31956–31963.

Kamata, M. et al., 2014. GATA2 regulates differentiation of bone marrow-derived mesenchymal stem cells. *Haematologica*, 99(11), pp.1686–1696.

Kedong, S. et al., 2011. Co-culture of hematopoietic stem cells and mesenchymal stem cells derived from umbilical cord blood using human autoserum. In *2011 International Symposium on Advanced Control of Industrial Processes (ADCONIP)*. pp. 258–261.

Kedong, S. et al., 2010. Simultaneous expansion and harvest of hematopoietic stem cells and mesenchymal stem cells derived from umbilical cord blood. *Journal of materials science. Materials in medicine*, 21(12), pp.3183-3193.

Kiel, M.J. et al., 2009. Hematopoietic stem cells do not depend on N-cadherin to regulate their maintenance. *Cell stem cell*, 4(2), pp.170–9. Available at: http://www.pubmedcentral.nih.gov/articlerender.fcgi?artid=2681089&tool=pmcentrez&rendertype=abstract [Accessed June 16, 2014].

Kiel, M.J. et al., 2005. SLAM family receptors distinguish hematopoietic stem and progenitor cells and reveal endothelial niches for stem cells. *Cell*, 121(7), pp.1109–21. Available at: http://www.ncbi.nlm.nih.gov/pubmed/15989959 [Accessed January 23, 2014].

Kiel, M.J. & Morrison, S.J., 2008. Uncertainty in the niches that maintain haematopoietic stem cells. *Nature reviews. Immunology*, 8(4), pp.290–301. Available at: http://www.ncbi.nlm.nih.gov/pubmed/18323850 [Accessed May 30, 2014].

Kiel, M.J., Radice, G.L. & Morrison, S.J., 2007. Lack of evidence that hematopoietic stem cells depend on N-cadherin-mediated adhesion to osteoblasts for their maintenance. *Cell stem cell*, 1(2), pp.204-17. Available at: http://www.ncbi.nlm.nih.gov/pubmed/18371351 [Accessed June 10, 2014].

Kilian, K. a et al., 2010. Geometric cues for directing the differentiation of mesenchymal stem cells. *Proceedings of the National Academy of Sciences*

of the United States of America, 107(11), pp.4872–7. Available at: http://www.pubmedcentral.nih.gov/articlerender.fcgi?artid=2841932&tool= pmcentrez&rendertype=abstract [Accessed January 23, 2014].

Kim, J. & Ma, T., 2013. Endogenous extracellular matrices enhance human mesenchymal stem cell aggregate formation and survival. *Biotechnology Progress*, 29(2), pp.441–451.

Kobune, M. et al., 2012. Stromal cells expressing hedgehog-interacting protein regulate the proliferation of myeloid neoplasms. *Blood Cancer Journal*, 2(9), p.e87. Available at: http://dx.doi.org/10.1038/bcj.2012.36.

Kohn, L.A. et al., 2012. Lymphoid priming in human bone marrow begins before expression of CD10 with upregulation of L-selectin. *Nature Immunology*, 13(10), pp.963–971. Available at: http://www.nature.com/doifinder/10.1038/ni.2405.

Kolf, C.M., Cho, E. & Tuan, R.S., 2007. Mesenchymal stromal cells. Biology of adult mesenchymal stem cells: regulation of niche, self-renewal and differentiation. *Arthritis research & therapy*, 9(1), p.204.

Kono, K., Niimi, S. & Rumi Sawada, 2013. Cyclin D2 Promotes the Proliferation of Human Mesenchymal Stem Cells. *Journal of Bone Marrow Research*, 2(1), pp.1–8. Available at: http://www.esciencecentral.org/journals/cyclin-d-promotes-the-proliferation-of-human-mesenchymal-stem-cells-2329-8820-2-136.php?aid=22209.

Korff, T. & Augustin, H.G., 1999. Tensional forces in fibrillar extracellular matrices control directional capillary sprouting. *Journal of Cell Science*, 112(1), pp.3249–3258.

Krause, D., 2002. Regulation of hematopoietic stem cell fate. *Oncogene*, 21(11), pp.3262–3269.

Kuijjer, M.L. et al., 2008. Identification of Osteosarcoma Driver Genes by Integrative Analysis of Copy Number and Gene Expression Data. *Genes, Chromosomes & Cancer*, 47(April), pp.238–246.

Kumar, A. et al., 2011. P53 Impairs endothelial function by transcriptionally repressing kruppel-Like factor 2. *Arteriosclerosis, Thrombosis, and Vascular Biology*, 31(1), pp.133–141.

Kunisaki, Y. et al., 2013. Arteriolar niches maintain haematopoietic stem cell quiescence. *Nature*, 502(7473), pp.637–43. Available at: http://www.pubmedcentral.nih.gov/articlerender.fcgi?artid=3821873&tool= pmcentrez&rendertype=abstract [Accessed May 24, 2014].

Kushibiki, T. et al., 2015. Photodynamic activation as a molecular switch to promote osteoblast cell differentiation via AP-1 activation. *Scientific Reports*, 5(April), p.13114. Available at: http://www.nature.com/doifinder/10.1038/srep13114.

Kyu Hong, J. et al., 2015. Three-Dimensional Culture of Mesenchymal Stem Cells. *Tissue Engineering and Regenerative Medicine*, 12(4), pp.211–221. Available at: http://dx.doi.org/10.1007/s13770-015-0005-7.

Lam, B.S., Cunningham, C. & Adams, G.B., 2010. Pharmacologic modulation of the calcium-sensing receptor enhances hematopoietic stem cell lodgment in the adult bone marrow. *Blood*, 117(4), pp.1167–1175.

Lane, S.W. et al., 2011. Differential niche and Wnt requirements during acute myeloid leukemia progression Differential niche and Wnt requirements during acute myeloid leukemia progression. , 118(10), pp.2849–2856.

Lane, S.W. et al., 2009. The leukemic stem cell niche: current concepts and therapeutic opportunities. *Blood*, 114(6), p.1150. Available at:

http://bloodjournal.hematologylibrary.org/cgi/content/abstract/114/6/1150.

Lapidot, T. & Petit, I., 2002. Current understanding of stem cell mobilization: the roles of chemokines, proteolytic enzymes, adhesion molecules, cytokines, and stromal cells. *Experimental hematology*, 30(9), pp.973–81. Available at: http://www.ncbi.nlm.nih.gov/pubmed/12225788.

Laschke, M.W. et al., 2013. Three-dimensional spheroids of adipose-derived mesenchymal stem cells are potent initiators of blood vessel formation in porous polyurethane scaffolds. *Acta Biomaterialia*, 9(6), pp.6876–6884. Available at: http://dx.doi.org/10.1016/j.actbio.2013.02.013.

Lee, D.Y. et al., 2007. MicroRNA-378 promotes cell survival, tumor growth, and angiogenesis by targeting SuFu and Fus-1 expression. *Proceedings of the National Academy of Sciences of the United States of America*, 104(51), pp.20350–5. Available at: http://www.pubmedcentral.nih.gov/articlerender.fcgi?artid=2154434&tool=pmcentrez&rendertype=abstract.

Lee, E.J. et al., 2012. Spherical bullet formation via E-cadherin promotes therapeutic potency of mesenchymal stem cells derived from human umbilical cord blood for myocardial infarction. *Molecular Therapy*, 20(7), pp.1424–33. Available at: http://dx.doi.org/10.1038/mt.2012.58.

Leisten, I. et al., 2012. 3D co-culture of hematopoietic stem and progenitor cells and mesenchymal stem cells in collagen scaffolds as a model of the hematopoietic niche. *Biomaterials*, 33(6), pp.1736–47. Available at: http://www.ncbi.nlm.nih.gov/pubmed/22136713 [Accessed June 2, 2014].

Leung, J.Y. et al., 2008. A role for Myc in facilitating transcription activation by E2F1. *Oncogene*, 27, pp.4172–4179.

Lewis, E.E.L. et al., 2016. A Quiescent, Regeneration-Responsive Tissue Engineered Mesenchymal Stem Cell Bone Marrow Niche Model via Magnetic Levitation. *ACS Nano*, 10, pp.8346–8354. Available at: http://www.ncbi.nlm.nih.gov/pubmed/27602872.

Lewis, N.S. et al., 2017. Magnetically levitated mesenchymal stem cell spheroids cultured with a collagen gel maintain phenotype and quiescence. *Journal of Tissue Engineering*, 8, pp.1–11. Available at: http://journals.sagepub.com/doi/10.1177/2041731417704428.

Li, N. et al., 2007. Human mesenchymal stem cells improve ex vivo expansion of adult human CD34+ peripheral blood progenitor cells and decrease their allostimulatory capacity. *Experimental hematology*, 35(3), pp.507–15. Available at: http://www.ncbi.nlm.nih.gov/pubmed/17309831 [Accessed June 24, 2014].

Li, P. & Zon, L.I., 2010. Resolving the controversy about N-cadherin and hematopoietic stem cells. *Cell stem cell*, 6(3), pp.199–202. Available at: http://www.ncbi.nlm.nih.gov/pubmed/20207222 [Accessed July 25, 2014].

Lin, S.P. et al., 2014. RB maintains quiescence and prevents premature senescence through upregulation of DNMT1 in mesenchymal stromal cells. *Stem Cell Reports*, 3(6), pp.975–986. Available at: http://dx.doi.org/10.1016/j.stemcr.2014.10.002.

Liu, Y.-Q. et al., 2016. Wedelolactone enhances osteoblastogenesis by regulating Wnt/ß-catenin signaling pathway but suppresses osteoclastogenesis by NF-κB/c-fos/NFATc1 pathway. *Scientific Reports*, 6(1), p.32260. Available at: http://www.nature.com/articles/srep32260.

Liu, Z.H., Dai, X.M. & Du, B., 2015. Hes1: A key role in stemness, metastasis and

multidrug resistance. *Cancer Biology and Therapy*, 16(3), pp.353–359.

Lord, B.I., 1990. The architecture of bone marrow cell populations. *International Journal of Cell Cloning*, 8(5), pp.317–331.

Lv, F.-J. et al., 2014. Concise Review: The Surface Markers and Identity of Human Mesenchymal Stem Cells. *Stem Cells*, 32(6), pp.1408–1419. Available at: http://www.ncbi.nlm.nih.gov/pubmed/24578244%5Cnhttp://doi.wiley.com /10.1002/stem.1681.

Ma, H.L. et al., 2012. Multicellular tumor spheroids as an in vivo-like tumor model for three-dimensional imaging of chemotherapeutic and nano material cellular penetration. *Molecular Imaging*, 11(6), pp.487–498.

Mabuchi, Y. et al., 2013. LNGFR+THY-1+VCAM-1hi+ Cells Reveal Functionally Distinct Subpopulations in Mesenchymal Stem Cells. *Stem Cell Reports*, 1(August), pp.152–165.

Mahadik, B.P. et al., 2014. Microfluidic generation of gradient hydrogels to modulate hematopoietic stem cell culture environment. *Advanced healthcare materials*, 3(3), pp.449–58. Available at: http://www.ncbi.nlm.nih.gov/pubmed/23997020 [Accessed September 5, 2017].

Mahadik, B.P. et al., 2015. The use of covalently immobilized stem cell factor to selectively affect hematopoietic stem cell activity within a gelatin hydrogel. *Biomaterials*, 67, pp.297–307. Available at: http://linkinghub.elsevier.com/retrieve/pii/S0142961215006249.

Mak, K.K. et al., 2008. Hedgehog Signaling in Mature Osteoblasts Regulates Bone Formation and Resorption by Controlling PTHrP and RANKL Expression. *Developmental Cell*, 14(5), pp.674–688.

Mar, A.C. et al., 2015. Interleukin-1 receptor type 2 acts with c-Fos to enhance the expression of interleukin-6 and vascular endothelial growth factor A in colon cancer cells and induce angiogenesis. *Journal of Biological Chemistry*, 290(36), pp.22212–22224.

Marx, U. et al., 2016. Biology-inspired microphysiological system approaches to solve the prediction dilemma of substance testing. *Altex*, 33(3), pp.272–321.

Matsui, J. et al., 2004. Stem Cell Factor/c-kit Signaling Promotes the Survival, Migration, and Capillary Tube Formation of Human Umbilical Vein Endothelial Cells. *Journal of Biological Chemistry*, 279(18), pp.18600–18607.

Matsumoto, T. et al., 2012. Regulation of osteoblast differentiation by interleukin-11 via AP-1 and Smad signaling. *Endocr J*, 59(2), pp.91–101. Available at: http://www.ncbi.nlm.nih.gov/pubmed/21931225%5Cnhttps://www.jstage.j st.go.jp/article/endocrj/59/2/59_EJ11-0219/_pdf.

Mayer, H. et al., 2005. Vascular endothelial growth factor (VEGF-A) expression in human mesenchymal stem cells: Autocrine and paracrine role on osteoblastic and endothelial differentiation. *Journal of Cellular Biochemistry*, 95(4), pp.827–839.

McBeath, R. et al., 2004. Cell shape, cytoskeletal tension, and RhoA regulate stem cell lineage commitment. *Developmental cell*, 6(4), pp.483–95. Available at: http://www.ncbi.nlm.nih.gov/pubmed/15068789.

McCarthy, T.L. & Centrella, M., 2010. Novel links among Wnt and TGF-beta signaling and Runx2. *Molecular Endocrinology*, 24(3), pp.587–97. Available at: http://www.pubmedcentral.nih.gov/articlerender.fcgi?artid=2840811&tool=

pmcentrez&rendertype=abstract.

McNiece, I. et al., 2004. Ex vivo expansion of cord blood mononuclear cells on mesenchymal stem cells. *Cytotherapy*, 6(4), pp.311–317. Available at: http://dx.doi.org/10.1080/14653240410004871.

Menard, C. et al., 2013. Clinical-grade mesenchymal stromal cells produced under various good manufacturing practice processes differ in their immunomodulatory properties: standardization of immune quality controls. *Stem cells and development*, 22(12), pp.1789–801. Available at: http://www.pubmedcentral.nih.gov/articlerender.fcgi?artid=3668498&tool= pmcentrez&rendertype=abstract.

Méndez-Ferrer, S. et al., 2009. Circadian rhythms influence hematopoietic stem cells. *Current opinion in hematology*, 16(4), pp.235–42. Available at: http://www.pubmedcentral.nih.gov/articlerender.fcgi?artid=4117204&tool= pmcentrez&rendertype=abstract [Accessed October 21, 2014].

Méndez-Ferrer, S. et al., 2010. Mesenchymal and haematopoietic stem cells form a unique bone marrow niche. *Nature*, 466(7308), pp.829–834.

Metzger, T.A. et al., 2014. Rheological behavior of fresh bone marrow and the effects of storage. *Journal of the Mechanical Behavior of Biomedical Materials*, 40, pp.307–313.

Miyamoto, K. et al., 2011. Nuclear actin polymerization is required for transcriptional reprogramming of Oct4 by oocytes. *Genes and Development*, 25(9), pp.946–958.

Mo, M. et al., 2016. Mesenchymal stem cell subpopulations: phenotype, property and therapeutic potential. *Cellular and Molecular Life Sciences*, 73(17), pp.3311–3321. Available at: http://link.springer.com/10.1007/s00018-016-2229-7.

Monzen, S. et al., 2013. Characteristics of Myeloid Differentiation and Maturation Pathway Derived from Human Hematopoietic Stem Cells Exposed to Different Linear Energy Transfer Radiation Types. *PLoS ONE*, 8(3), p.e59385.

Moore, M. a S., 2012. Waking up HSCs: a new role for E-selectin. *Nature medicine*, 18(11), pp.1613–4. Available at: http://www.ncbi.nlm.nih.gov/pubmed/23135509 [Accessed August 12, 2014].

Morikawa, T. & Takubo, K., 2016. Hypoxia regulates the hematopoietic stem cell niche. *Pflügers Archiv - European Journal of Physiology*, 468, pp.13–22. Available at: http://link.springer.com/10.1007/s00424-015-1743-z.

Morrison, S.J. & Scadden, D.T., 2014. The bone marrow niche for haematopoietic stem cells. *Nature*, 505, pp.327–34.

Mueller-Klieser, W., 1987. Multicellular spheroids - A review on cellular aggregates in cancer research. *Journal of Cancer Research and Clinical Oncology*, 113(2), pp.101–122.

Muraro, P.A. et al., 2017. Long-term outcomes following stem cell transplant for multiple sclerosis. *JAMA Neurology*, 74(4), pp.459–469.

Murphy, K.C., Fang, S.Y. & Leach, J.K., 2014. Human mesenchymal stem cell spheroids in fibrin hydrogels exhibit improved cell survival and potential for bone healing. *Cell and Tissue Research*, 357(1), pp.91–99.

Nagase, T. et al., 2008. Hedgehog signalling in vascular development. *Angiogenesis*, 11(1), pp.71–77.

Nakamura-Ishizu, A. & Suda, T., 2014. Aging of the hematopoietic stem cells niche. *International Journal of Hematology*, 100(4), pp.317–325.

Nakamura, Y. et al., 2010. Isolation and characterization of endosteal niche cell populations that regulate hematopoietic stem cells. *Blood*, 116(9), pp.1422–1432.

Nakashima, K. et al., 2002. The novel zinc finger-containing transcription factor Osterix is required for osteoblast differentiation and bone formation. *Cell*, 108(1), pp.17–29.

Nevins, J.R. et al., 1997. Role of the Rb/E2F pathway in cell growth control. *Journal of cellular physiology*, 173(2), pp.233–6. Available at: http://www.ncbi.nlm.nih.gov/pubmed/9365528.

Nicolaidou, V. et al., 2012. Monocytes induce STAT3 activation in human mesenchymal stem cells to promote osteoblast formation. *PLoS ONE*, 7(7), p.e39871.

Nilsson, S.K. et al., 2003. Hyaluronan is synthesized by primitive hemopoietic cells, participates in their lodgment at the endosteum following transplantation, and is involved in the regulation of their proliferation and differentiation in vitro. *Blood*, 101(3), pp.856–862.

Nilsson, S.K. et al., 1998. Immunofluorescence Characterization of Key Extracellular Matrix Proteins in Murine Bone Marrow In Situ. *The Journal of Histochemistry & Cytochemistry*, 46(3), pp.371–377. Available at: http://jhc.sagepub.com/lookup/doi/10.1177/002215549804600311 [Accessed May 27, 2014].

Nilsson, S.K. et al., 2005. Osteopontin, a key component of the hematopoietic stem cell niche and regulator of primitive hematopoietic progenitor cells. *Blood*, 106(4), pp.1232–1239. Available at: http://www.ncbi.nlm.nih.gov/pubmed/15845900 [Accessed June 13, 2014].

Nombela-Arrieta, C. et al., 2013. Quantitative imaging of haematopoietic stem and progenitor cell localization and hypoxic status in the bone marrow microenvironment. *Nature cell biology*, 15(5), pp.533–43. Available at: http://www.ncbi.nlm.nih.gov/pubmed/23624405 [Accessed May 23, 2014].

Occhetta, P. et al., 2015. High-Throughput Microfluidic Platform for 3D Cultures of Mesenchymal Stem Cells, Towards Engineering Developmental Processes. *Scientific Reports*, 5(April), p.10288. Available at: http://www.nature.com/doifinder/10.1038/srep10288.

Oeztuerk-Winder, F. & Ventura, J.-J., 2012. The many faces of p38 mitogen-activated protein kinase in progenitor/stem cell differentiation. *The Biochemical journal*, 445(1), pp.1–10. Available at: http://www.ncbi.nlm.nih.gov/pubmed/22702973.

Okada, S. et al., 1999. Prolonged expression of c-fos suppresses cell cycle entry of dormant hematopoietic stem cells. *Blood*, 93(3), pp.816–825.

Olofsson, B., Porsch, H. & Heldin, P., 2014. Knock-down of CD44 regulates endothelial cell differentiation via NFκB-mediated chemokine production. *PLoS ONE*, 9(3).

Ono, N. et al., 2014. Vasculature-associated cells expressing nestin in developing bones encompass early cells in the osteoblast and endothelial lineage. *Developmental Cell*, 29(3), pp.330–339. Available at: http://dx.doi.org/10.1016/j.devcel.2014.03.014.

Oswald, J. et al., 2006. Gene-expression profiling of CD34+ hematopoietic cells expanded in a collagen I matrix. *Stem Cells*, 24(3), pp.494–500. Available at: http://www.ncbi.nlm.nih.gov/pubmed/16166251 [Accessed June 24, 2014].

Paik, S. et al., 2012. miR-449a regulates the chondrogenesis of human mesenchymal stem cells through direct targeting of lymphoid enhancer-

binding factor-1. *Stem cells and development*, 21(18), pp.3298–308. Available at: http://www.pubmedcentral.nih.gov/articlerender.fcgi?artid=3516419&tool=pmcentrez&rendertype=abstract.

Pak, C. et al., 2015. MicroC3: an ex vivo microfluidic cis-coculture assay to test chemosensitivity and resistance of patient multiple myeloma cells. *Integrative Biology*, 7(6), pp.643–654. Available at: http://xlink.rsc.org/?DOI=C5IB00071H.

Papayannopoulou, T., 2003. Bone marrow homing: the players, the playfield, and their evolving roles. *Current opinion in hematology*, 10(3), pp.214-9. Available at: http://www.ncbi.nlm.nih.gov/pubmed/12690289.

Park, I.K., Morrison, S.J. & Clarke, M.F., 2004. Bmi1, stem cells, and senescence regulation. *Journal of Clinical Investigation*, 113(2), pp.175–179.

Perdomo-Arciniegas, A.-M. & Vernot, J.-P., 2011. Co-culture of hematopoietic stem cells with mesenchymal stem cells increases VCAM-1-dependent migration of primitive hematopoietic stem cells. *International journal of hematology*, 94(6), pp.525–32. Available at: http://www.ncbi.nlm.nih.gov/pubmed/22127557 [Accessed July 8, 2014].

Perucca, S. et al., 2017. Mesenchymal stromal cells (MSCs) induce ex vivo proliferation and erythroid commitment of cord blood haematopoietic stem cells (CB-CD34+ cells). *PloS one*, 12(2), p.e0172430. Available at: http://dx.plos.org/10.1371/journal.pone.0172430%0Ahttp://www.ncbi.nlm.nih.gov/pubmed/28231331.

Petit, I. et al., 2002. G-CSF induces stem cell mobilization by decreasing bone marrow SDF-1 and up-regulating CXCR4. *Nature immunology*, 3(7), pp.687–94. Available at: http://www.ncbi.nlm.nih.gov/pubmed/12068293 [Accessed June 2, 2014].

Pieri, L. et al., 2011. Human mesenchymal stromal cells preserve their stem features better when cultured in the Dulbecco's modified Eagle medium. *Cytotherapy*, 13(5), pp.539–548. Available at: http://dx.doi.org/10.3109/14653249.2010.542459.

Pinho, S. et al., 2013. PDGFRα and CD51 mark human nestin+ sphere-forming mesenchymal stem cells capable of hematopoietic progenitor cell expansion. *The Journal of experimental medicine*, 210(7), pp.1351-67. Available at: http://www.pubmedcentral.nih.gov/articlerender.fcgi?artid=3698522&tool=pmcentrez&rendertype=abstract [Accessed February 24, 2014].

Pittenger, M.F. et al., 1999. Multilineage Potential of Adult Human Mesenchymal Stem Cells. *Science*, 284(April), pp.143–147.

Plaisant, M. et al., 2009. Activation of hedgehog signaling inhibits osteoblast differentiation of human mesenchymal stem cells. *Stem cells*, 27(3), pp.703–713.

Plaisant, M. et al., 2011. Inhibition of hedgehog signaling decreases proliferation and clonogenicity of human mesenchymal stem cells. *PLoS ONE*, 6(2).

Quirici, N. et al., 2002. Isolation of bone marrow mesenchymal stem cells by anti-nerve growth factor receptor antibodies. *Experimental Hematology*, 30(7), pp.783–791.

Rafii, S. et al., 1995. Human bone marrow microvascular endothelial cells support long-term proliferation and differentiation of myeloid and megakaryocytic progenitors. *Blood*, 86(9), pp.3353–63. Available at: http://www.bloodjournal.org/content/86/9/3353.abstract.

Rettinger, C.L. et al., 2014. In vitro characterization of scaffold-free three-dimensional mesenchymal stem cell aggregates. *Cell and Tissue Research*, 358(2), pp.395–405.

Reya, T. et al., 2003. A role for Wnt signalling in self-renewal of haematopoietic stem cells. *Nature*, 423(6938), pp.409–14. Available at: http://www.ncbi.nlm.nih.gov/pubmed/12717450.

Rödling, L. et al., 2017. 3D models of the hematopoietic stem cell niche under steady-state and active conditions. *Scientific Reports*, 7(1), p.4625. Available at: http://www.nature.com/articles/s41598-017-04808-0.

Romanov, Y.A. et al., 2017. Expression of Surface Molecules in Human Mesenchymal Stromal Cells Co-Cultured with Nucleated Umbilical Cord Blood Cells. *Bulletin of Experimental Biology and Medicine*, (4), pp.578–582. Available at: http://www.ncbi.nlm.nih.gov/pubmed/28239788.

Romero, M.B., 2015. Cancer Research. *Product Guide (Tocris)*, p.28.

Rossi, M.I.D. et al., 2005. Multicellular spheroids of bone marrow stromal cells: a three-dimensional in vitro culture system for the study of hematopoietic cell migration. *Brazilian Journal of Medical and Biological Research*, 38(10), pp.1455–62. Available at: http://www.ncbi.nlm.nih.gov/pubmed/16172738.

Salati, S. et al., 2013. Co-Culture of Hematopoietic Stem/Progenitor Cells with Human Osteblasts Favours Mono/Macrophage Differentiation at the Expense of the Erythroid Lineage. *PLoS ONE*, 8(1), p.e53496.

Sanchez, S., Tafforeau, P. & Ahlberg, P.E., 2014. The humerus of Eusthenopteron: a puzzling organization presaging the establishment of tetrapod limb bone marrow. *Proceedings of the Royal Society B*, 281(1782), p.20140299. Available at: http://www.ncbi.nlm.nih.gov/pubmed/24648231.

Sang, L., Roberts, J.M. & Coller, H.A., 2010. Hijacking HES1: how tumors co-opt the anti-differentiation strategies of quiescent cells. *Trends in Molecular Medicine*, 16(1), pp.17–26.

Sato, Y. et al., 2016. Notch2 signaling regulates the proliferation of murine bone marrow-derived mesenchymal stem/stromal cells via c-Myc expression. *PLoS ONE*, 11(11), pp.1–14.

Satoh, Y. et al., 2004. Roles for c-Myc in self-renewal of hematopoietic stem cells. *Journal of Biological Chemistry*, 279(24), pp.24986–24993.

Schmittgen, T.D. & Livak, K.J., 2008. Analyzing real-time PCR data by the comparative CT method. *Nature Protocols*, 3(6), pp.1101–1108. Available at: http://www.nature.com/doifinder/10.1038/nprot.2008.73.

Schofield, R., 1978. The relationship between the spleen colony-forming cell and the haemopoietic stem cell. *Blood cells*, 4(1-2), pp.7–25. Available at: http://europepmc.org/abstract/MED/747780 [Accessed May 26, 2014].

Schwank, G. et al., 2013. Functional repair of CFTR by CRISPR/Cas9 in intestinal stem cell organoids of cystic fibrosis patients. *Cell Stem Cell*, 13(6), pp.653–658. Available at: http://dx.doi.org/10.1016/j.stem.2013.11.002.

Sharff, K.A. et al., 2009. Hey1 basic helix-loop-helix protein plays an important role in mediating BMP9-induced osteogenic differentiation of mesenchymal progenitor cells. *Journal of Biological Chemistry*, 284(1), pp.649-659.

Sharma, M.B., Limaye, L.S. & Kale, V.P., 2012. Mimicking the functional hematopoietic stem cell niche in vitro: recapitulation of marrow physiology by hydrogel-based three-dimensional cultures of mesenchymal stromal cells. *Haematologica*, 97(5), pp.651–60. Available at: http://www.pubmedcentral.nih.gov/articlerender.fcgi?artid=3342965&tool=pmcentrez&rendertype=abstract [Accessed January 21, 2014].

Sharpless, N.E. & DePinho, R. a, 2007. How stem cells age and why this makes us grow old. *Nature reviews. Molecular cell biology*, 8(9), pp.703–13. Available at: http://www.ncbi.nlm.nih.gov/pubmed/17717515 [Accessed September 23, 2014].

Shin, J.-W. et al., 2014. Contractile forces sustain and polarize hematopoiesis from stem and progenitor cells. *Cell stem cell*, 14(1), pp.81–93. Available at: http://www.ncbi.nlm.nih.gov/pubmed/24268694 [Accessed May 28, 2014].

Shukla, S. et al., 2017. Progenitor T-cell differentiation from hematopoietic stem cells using Delta-Like 4 and VCAM-1. *Nature Methods*, 14, pp.531–538. Available at: http://dx.doi.org/10.1038/nmeth.4258.

Sieber, S., Rosowski, M. & Lauster, R., 2017. Bone marrow-on-a-chip: Long-term culture of human hematopoietic stem cells in a 3D microfluidic environment. *Journal of Tissue Engineering and Regenerative Medicine*.

Simmons, P.J. et al., 1992. Vascular cell adhesion molecule-1 expressed by bone marrow stromal cells mediates the binding of hematopoietic progenitor cells. *Blood*, 80(2), pp.388–95. Available at: http://www.ncbi.nlm.nih.gov/pubmed/1378318.

Smith, C.A.M. et al., 2010. The effect of static magnetic fields and tat peptides on cellular and nuclear uptake of magnetic nanoparticles. *Biomaterials*, 31(15), pp.4392–4400. Available at: http://dx.doi.org/10.1016/j.biomaterials.2010.01.096.

Sobotková, E. et al., 1988. Rheological behaviour of bone marrow. In H. Giesekus & M. F. Hibberd, eds. *Progress and Trends in Rheology II: Proceedings of the Second Conference of European Rheologists*. Heidelberg: Steinkopff, pp. 467–469. Available at: http://dx.doi.org/10.1007/978-3-642-49337-9_165.

Sörensen, I., Adams, R.H. & Gossler, A., 2009. DLL1-mediated Notch activation regulates endothelial identity in mouse fetal arteries. *Blood*, 113(22), pp.5680–5688.

Souza, G.R. et al., 2010. Three-dimensional tissue culture based on magnetic cell levitation. *Nature nanotechnology*, 5(4), pp.291–296. Available at: http://www.ncbi.nlm.nih.gov/pubmed/20228788 [Accessed May 7, 2014].

Spyridopoulos, I. et al., 1998. Restoration of E2F Expression Rescues Vascular Endothelial Cells From Tumor Necrosis Factor-alpha–Induced Apoptosis. *Circulation*, 98(25), pp.2883–2891.

Staal, F.J.T. & Luis, T.C., 2010. Wnt signaling in hematopoiesis: crucial factors for self-renewal, proliferation, and cell fate decisions. *Journal of cellular biochemistry*, 109(5), pp.844–9. Available at: http://www.ncbi.nlm.nih.gov/pubmed/20069555 [Accessed August 13, 2014].

Stahl, A. et al., 2005. Endothelial progenitor cell sprouting in spheroid cultures is resistant to inhibition by osteoblasts: A model for bone replacement grafts. *FEBS Letters*, 579(24), pp.5338–5342.

Stier, S. et al., 2005. Osteopontin is a hematopoietic stem cell niche component that negatively regulates stem cell pool size. *The Journal of experimental medicine*, 201(11), pp.1781–91. Available at: http://www.pubmedcentral.nih.gov/articlerender.fcgi?artid=2213260&tool=pmcentrez&rendertype=abstract [Accessed June 5, 2014].

Storan, M.J. et al., 2015. Brief Report : Factors Released by Megakaryocytes Thrombin Cleave Osteopontin to Negatively Regulate Hematopoietic Stem Cells. *Stem Cells*, 33, pp.2351–2357.

Suárez-Álvarez, B., López-Vázquez, A. & López-Larrea, C., 2012. Mobilization and homing of hematopoietic stem cells. *Advances in experimental medicine and biology*, 741, pp.152–70. Available at: http://www.ncbi.nlm.nih.gov/pubmed/22457109.

Sugimura, R. et al., 2012. Noncanonical Wnt signaling maintains hematopoietic stem cells in the niche. *Cell*, 150(2), pp.351–65. Available at: http://www.ncbi.nlm.nih.gov/pubmed/22817897 [Accessed June 5, 2014].

Sugiyama, T. et al., 2006. Maintenance of the hematopoietic stem cell pool by CXCL12-CXCR4 chemokine signaling in bone marrow stromal cell niches. *Immunity*, 25(6), pp.977–88. Available at: http://www.ncbi.nlm.nih.gov/pubmed/17174120 [Accessed May 24, 2014].

Suphanantachat, S. et al., 2014. A role for c-Kit in the maintenance of undifferentiated human mesenchymal stromal cells. *Biomaterials*, 35(11), pp.3618–3626. Available at: http://dx.doi.org/10.1016/j.biomaterials.2014.01.031.

Suzuki, T. et al., 2014. c-Kit immunoexpression delineates a putative endothelial progenitor cell population in developing human lungs. *American journal of physiology. Lung cellular and molecular physiology*, 306(9), pp.L855-65. Available at: http://www.ncbi.nlm.nih.gov/pubmed/24583878.

Suzuki, T. et al., 2007. Osteoblast-specific Angiopoietin 1 overexpression increases bone mass. *Biochemical and Biophysical Research Communications*, 362(4), pp.1019–1025.

Tabe, Y. & Konopleva, M., 2014. Advances in understanding the leukaemia microenvironment. *British Journal of Haematology*, 164(6), pp.767–778.

Tabruyn, S.P. & Griffioen, A.W., 2007. A new role for NF-κB in angiogenesis inhibition. *Cell Death and Differentiation*, 14(8), pp.1393–1397. Available at: http://www.nature.com/doifinder/10.1038/sj.cdd.4402156.

Teixido, J. et al., 1992. Role of B1, and B2 Integrins in the Adhesion of Human CD34hI Stem Cells to Bone Marrow Stroma. *Journal of Clinical Investigation*, 90(August), pp.358–367.

Timmers, C. et al., 2007. E2f1, E2f2, and E2f3 control E2F target expression and cellular proliferation via a p53-dependent negative feedback loop. *Molecular and cellular biology*, 27(1), pp.65–78.

Tisdale, J.F. et al., 1998. Ex Vivo Expansion of Genetically Marked Rhesus Peripheral Blood Progenitor Cells Results in Diminished Long-Term Repopulating Ability. *Blood*, 92(4), pp.1131–1142.

Tondreau, T. et al., 2004. Bone marrow-derived mesenchymal stem cells already express specific neural proteins before any differentiation. *Differentiation; research in biological diversity*, 72(7), pp.319–326.

Torikai, H. et al., 2016. Genetic editing of HLA expression in hematopoietic stem cells to broaden their human application. *Scientific Reports*, 6, p.21757. Available at: http://www.nature.com/articles/srep21757%255Cnhttp://www.ncbi.nlm.nih.gov/pubmed/26902653%255Cnhttp://www.pubmedcentral.nih.gov/articlerender.fcgi?artid=PMC4763194.

Torisawa, Y. et al., 2014. Bone marrow-on-a-chip replicates hematopoietic niche physiology in vitro. *Nature methods*, 11(6), pp.663–9. Available at: http://www.ncbi.nlm.nih.gov/pubmed/24793454.

Trowbridge, J.J., Scott, M.P. & Bhatia, M., 2006. Hedgehog modulates cell cycle regulators in stem cells to control hematopoietic regeneration. *Proceedings of the National Academy of Sciences of the United States of America*, 103,

pp.14134–14139.

Tsai, A.-C. et al., 2015. Compaction, fusion, and functional activation of three-dimensional human mesenchymal stem cell aggregate. *Tissue engineering. Part A*, 21(9-10), pp.1705–19. Available at: http://online.liebertpub.com.globalproxy.cvt.dk/doi/abs/10.1089/ten.tea.2014.0314?journalCode=tea%5Cnhttp://www.ncbi.nlm.nih.gov/pubmed/25661745%5Cnhttp://www.pubmedcentral.nih.gov/articlerender.fcgi?artid=PMC4426301.

Tzeng, Y.S. et al., 2011. Loss of Cxcl12/Sdf-1 in adult mice decreases the quiescent state of hematopoietic stem/progenitor cells and alters the pattern of hematopoietic regeneration after myelosuppression. *Blood*, 117(2), pp.429–439.

Ugarte, F. & Forsberg, E.C., 2013. Haematopoietic stem cell niches: new insights inspire new questions. *The EMBO journal*, 32(19), pp.2535–47. Available at: http://www.ncbi.nlm.nih.gov/pubmed/24022369 [Accessed May 28, 2014].

Unnisa, Z. et al., 2012. Meis1 preserves hematopoietic stem cells in mice by limiting oxidative stress. *Blood*, 120(25), pp.4973–4981.

Vaidya, A. & Kale, V.P., 2015. TGF-β signaling and its role in the regulation of hematopoietic stem cells. *Systems and synthetic biology*, 9(1-2), pp.1–10. Available at: http://www.ncbi.nlm.nih.gov/pubmed/25972984.

Vailhé, B., Vittet, D. & Feige, J.J., 2001. In vitro models of vasculogenesis and angiogenesis. *Laboratory investigation; a journal of technical methods and pathology*, 81(4), pp.439–452.

Velletri, T. et al., 2016. P53 functional abnormality in mesenchymal stem cells promotes osteosarcoma development. *Cell death & disease*, 7(1), p.e2015. Available at: http://www.nature.com/doifinder/10.1038/cddis.2015.367%5Cnhttp://www.ncbi.nlm.nih.gov/pubmed/26775693.

Verfaillie, C.M., 2002. Hematopoietic stem cells for transplantation. *Nature immunology*, 3(4), pp.314–317.

Wagner, W., Wein, F., et al., 2007. Adhesion of hematopoietic progenitor cells to human mesenchymal stem cells as a model for cell-cell interaction. *Experimental hematology*, 35(2), pp.314–25. Available at: http://www.ncbi.nlm.nih.gov/pubmed/17258080 [Accessed July 9, 2014].

Wagner, W. et al., 2008. Adhesion of human hematopoietic progenitor cells to mesenchymal stromal cells involves CD44. *Cells, tissues, organs*, 188(1-2), pp.160–9. Available at: http://www.ncbi.nlm.nih.gov/pubmed/18160820 [Accessed July 10, 2014].

Wagner, W., Roderburg, C., et al., 2007. Molecular and secretory profiles of human mesenchymal stromal cells and their abilities to maintain primitive hematopoietic progenitors. *Stem cells (Dayton, Ohio)*, 25(10), pp.2638–47. Available at: http://www.ncbi.nlm.nih.gov/pubmed/17615262 [Accessed May 27, 2014].

Wang, L.D. & Wagers, A.J., 2011. Dynamic niches in the origination and differentiation of haematopoietic stem cells. *Nature reviews. Molecular cell biology*, 12(10), pp.643–55. Available at: http://www.pubmedcentral.nih.gov/articlerender.fcgi?artid=4040463&tool=pmcentrez&rendertype=abstract [Accessed June 10, 2014].

Wang, M. et al., 2007. STAT3 mediates bone marrow mesenchymal stem cell VEGF production. *Journal of Molecular and Cellular Cardiology*, 42(6), pp.1009–1015.

Wang, Q. et al., 2007. Bone morphogenetic protein 2 activates Smad6 gene transcription through bone-specific transcription factor Runx2. *Journal of Biological Chemistry*, 282(14), pp.10742–10748.

Wang, W. et al., 2009. 3D spheroid culture system on micropatterned substrates for improved differentiation efficiency of multipotent mesenchymal stem cells. *Biomaterials*, 30(14), pp.2705–2715. Available at: http://dx.doi.org/10.1016/j.biomaterials.2009.01.030.

Wang, Y. et al., 2011. Inhibition of p38 mitogen-activated protein kinase promotes ex vivo hematopoietic stem cell expansion. *Stem cells and development*, 20(7), pp.1143–52. Available at: http://www.ncbi.nlm.nih.gov/pubmed/21198398%5Cnhttp://www.pubmedcentral.nih.gov/articlerender.fcgi?artid=PMC3121934.

Wang, Y. et al., 2005. Runx1/AML1/Cbfa2 mediates onset of mesenchymal cell differentiation toward chondrogenesis. *Journal of bone and mineral research : the official journal of the American Society for Bone and Mineral Research*, 20(9), pp.1624–36. Available at: http://www.ncbi.nlm.nih.gov/pubmed/16059634.

Ward, D. et al., 2016. Mathematical modeling reveals differential effects of erythropoietin on proliferation and lineage commitment of human hematopoietic progenitors in early erythroid culture. *Haematologica*, 101(3), pp.286–296.

WBMT, 2013. 1 Millionth Blood Stem Cell Transplant Marks Major Medical Milestone. *www.wbmt.org*. Available at: http://www.wbmt.org/fileadmin/pdf/01_General/Press_release_final.pdf.

Weber, J.M. & Calvi, L.M., 2010. Notch signaling and the bone marrow hematopoietic stem cell niche. *Bone*, 46(2), pp.281–285. Available at: http://dx.doi.org/10.1016/j.bone.2009.08.007.

Wei, X. et al., 2013. Mesenchymal stem cells: a new trend for cell therapy. *Acta pharmacologica Sinica*, 34(6), pp.747–54. Available at: http://www.ncbi.nlm.nih.gov/pubmed/23736003.

Wein, F. et al., 2010. N-cadherin is expressed on human hematopoietic progenitor cells and mediates interaction with human mesenchymal stromal cells. *Stem cell research*, 4(2), pp.129-39. Available at: http://www.ncbi.nlm.nih.gov/pubmed/20116358 [Accessed July 9, 2014].

WHO, 2013. WHO | Stem cells are daily circulating around the World. *WHO*. Available at: http://www.who.int/transplantation/stem_cells/en/ [Accessed April 26, 2017].

Whoriskey, S.K., Schofield, M.A. & Miller, J.H., 1994. Isolation and Characterization of Human Bone Marrow Microvascular Endothelial Cells: Hematopoietic Progenitor Cell Adhesion. *Blood*, 84(1), pp.10–19.

Wilson, A. et al., 2004. c-Myc controls the balance between hematopoietic stem cell self-renewal and differentiation. *Genes & development*, 18(22), pp.2747–63. Available at: http://www.pubmedcentral.nih.gov/articlerender.fcgi?artid=528895&tool=pmcentrez&rendertype=abstract [Accessed May 30, 2014].

Wilson, A. & Trumpp, A., 2006a. Bone-marrow haematopoietic-stem-cell niches. *Nature Reviews Immunology*, 6(2), pp.93–106.

Wilson, A. & Trumpp, A., 2006b. Bone-marrow haematopoietic-stem-cell niches. *Nature Reviews Immunology*, 6(2), pp.93–106. Available at: http://www.nature.com/doifinder/10.1038/nri1779.

Winkler, I.G. et al., 2012. Vascular niche E-selectin regulates hematopoietic

stem cell dormancy, self renewal and chemoresistance. *Nature medicine*, 18(11), pp.1651–7. Available at: http://www.ncbi.nlm.nih.gov/pubmed/23086476 [Accessed August 12, 2014].

Winnicka, B. et al., 2010. CD13 is dispensable for normal hematopoiesis and myeloid cell functions in the mouse. *Journal of leukocyte biology*, 88(2), pp.347–359.

Wu, L. et al., 2001. The E2F1-3 transcription factors are essential for cellular proliferation. *Nature*, 414(6862), pp.457–462.

Wuchter, P. et al., 2016. Microcavity arrays as an in vitro model system of the bone marrow niche for hematopoietic stem cells. *Cell and Tissue Research*, 364, pp.573–584. Available at: http://link.springer.com/10.1007/s00441-015-2348-8.

Xie, J. et al., 2013. Notch signaling regulates CXCR4 expression and the migration of mesenchymal stem cells. *Cell Immunol*, 281(1), pp.68–75. Available at: http://www.ncbi.nlm.nih.gov/pubmed/23474530.

Yamamura, N. et al., 2007. Effects of the Mechanical Properties of Collagen Gel on the *In Vitro* Formation of Microvessel Networks by Endothelial Cells. *Tissue Engineering*, 13(7), pp.1443–1453. Available at: http://www.liebertonline.com/doi/abs/10.1089/ten.2006.0333.

Yamazaki, S. et al., 2009. TGF-beta as a candidate bone marrow niche signal to induce hematopoietic stem cell hibernation. *Blood*, 113(6), pp.1250–1256.

Yeh, H.-Y. et al., 2014. Substrate-dependent gene regulation of self-assembled human MSC spheroids on chitosan membranes. *BMC Genomics*, 15(1), p.10. Available at: http://bmcgenomics.biomedcentral.com/articles/10.1186/1471-2164-15-10.

Ylöstalo, J.H. et al., 2012. Human mesenchymal stem/stromal cells cultured as spheroids are self-activated to produce prostaglandin E2 that directs stimulated macrophages into an anti-inflammatory phenotype. *Stem Cells*, 30(10), pp.2283–2296.

Yoshihara, H. et al., 2007. Thrombopoietin/MPL signaling regulates hematopoietic stem cell quiescence and interaction with the osteoblastic niche. *Cell stem cell*, 1(6), pp.685–97. Available at: http://www.ncbi.nlm.nih.gov/pubmed/18371409 [Accessed June 5, 2014].

Yoshimi, A. et al., 2016. Global Use of Peripheral Blood vs Bone Marrow as Source of Stem Cells for Allogeneic Transplantation in Patients With Bone Marrow Failure. *Journal of the American Medical Association*, 315(2), pp.19–200.

Yourek, G. et al., 2010. Shear stress induces osteogenic differentiation of human mesenchymal stem cells. *Regen Med*, 5(5), pp.713–724.

Yun, H.J. & Jo, D.Y., 2003. Production of Stromal Cell-Derived Factor-1 (SDF-1) and Expression of CXCR4 in Human Bone Marrow Endothelial Cells. *Journal of Korean Medical Science*, 18(5), pp.679–685.

Zainal Ariffin, S.H. et al., 2016. Analyses of basal media and serum for in vitro expansion of suspension peripheral blood mononucleated stem cell. *Cytotechnology*, 68(4), pp.675–686.

Zhang, Y. et al., 2006. Co-culture of Umbilical Cord Blood CD34+ Cells with Human Mesenchymal Stem Cells. *Tissue Engineering*, 12(8), pp.2161–2170.

Zhou, N. et al., 2016. BMP2 induces chondrogenic differentiation, osteogenic differentiation and endochondral ossification in stem cells. *Cell and Tissue*

Research, 366(1), pp.101–111.

Zhou, Y. et al., 2017. 3D culture increases pluripotent gene expression in mesenchymal stem cells through relaxation of cytoskeleton tension. *Journal of Cellular and Molecular Medicine*, XX(X), pp.1–12. Available at: http://doi.wiley.com/10.1111/jcmm.12946.

Zimmermann, J.A. & Mcdevitt, T.C., 2014. Pre-conditioning mesenchymal stromal cell spheroids for immunomodulatory paracrine factor secretion. *Cytotherapy*, 16(3), pp.331–345. Available at: http://dx.doi.org/10.1016/j.jcyt.2013.09.004.

Zöller, M., 2011. CD44: can a cancer-initiating cell profit from an abundantly expressed molecule? *Nature reviews. Cancer*, 11(4), pp.254–67. Available at: http://www.ncbi.nlm.nih.gov/pubmed/21390059 [Accessed July 10, 2014].